Neurocognitive networks in higher-level visual perception

Mark A. Postans

A Thesis submitted for the degree of Doctor of Philosophy (2015)

Cardiff University

School of Psychology

Table of Contents

Acknowledgements

I'd like to begin by thanking my supervisor, Professor Kim Graham. I will always be grateful to Kim for taking a chance with me and giving me the opportunity to work in this fascinating field of academia. I think that Kim knows of my admiration for her so to spare her any potential embarrassment, I'll just say here that it has been a privilege!

I would also like to thank my colleagues within the Graham/Lawrence lab groups – Dr Hodgetts, Dr Umla-Runge, and Dr Muhlert in particular - for the friendship and professional support that they have extended to me throughout the duration of my PhD.

I also owe my thanks to my colleagues at CUBRIC for all of the technical assistance that they have provided. I am especially grateful to Greg Parker who provided the Matlab code that was used to correct diffusion MR images for free water contamination in Chapters 3-5.

I would also like to thank Dr Mariam Aly at the Princeton Neuroscience Institute for being generous with her advice on how to analyse perception receiver operating characteristics.

On a more personal level, I am deeply grateful to my girlfriend Samantha for supporting my academic ambitions for what has been a protracted period of time. I know that it has been difficult at times but I can at least promise that I will not undertake another PhD!

Finally, I could not have pursued my interests and ambitions without the support of my family. All of the things that my parents have done for me have not gone unnoticed and I hope to continue to make them proud. The same goes for the various matriarchs/patriarchs of our family: Barbara, Evelyn, Ralph and Sidney.

Chapter 1: Introduction

The ability to accurately perceive and respond to our visual environment is critical for optimising primate behaviour. A number of related cognitive functions, such as visual learning and longer-term memory, also depend upon an accurate percept of objects and their location within the visual environment. Understanding how the healthy brain supports higher-order visual perception is, therefore, a key goal for cognitive neuroscientists. A substantial body of research involving both humans and nonhuman primates has consistently demonstrated a role for regions within the extrastriate visual cortex (EVC) in visual perception, with many of these regions apparently exhibiting a high degree of functional specialisation for the processing of particular categories of complex stimuli (e.g. faces versus scenes). More recently, studies have also found that patients with selective damage to structures within the medial temporal lobe (MTL), such as the hippocampus (HC) and perirhinal cortex (PRC), present with not only the significant memory impairments associated with MTL amnesia (Squire et al., 2004), but also with category-sensitive impairments in visual perception, which seem to underpin category-sensitive deficits in visual memory. More specifically, damage to the PRC has been linked to impairments in perception for complex object-like stimuli such as faces, whereas HC damage has been linked to impairments in perception for visual scenes (Lee et al., 2005a). Such research has produced important insights into how *multiple* regions distributed across both the EVC and the MTL may make individual category-sensitive contributions to visual perception, but it remains unclear how these spatially distinct brain regions interact with one another, and to what extent their ability to interact underpins successful visual perception in humans.

These issues are addressed here via a series of novel experiments involving the use of a combination of behavioural paradigms and magnetic resonance imaging (MRI) techniques in healthy human participants. These experiments aim to: a) investigate the distinct patterns of functional and structural connections that support the category-sensitive contributions of the PRC and HC to higher-level visual perception, and b) demonstrate that inter-individual variation in the structural properties of white matter pathways providing inputs/outputs to the PRC or HC is an important factor underpinning the contributions of these MTL regions to successful higher-level perception. These experiments are summarised briefly at the end of this Chapter, and are described in detail in Chapters 2-5. In Chapter 6, the findings of these experiments will be discussed in the context of representational accounts of perception, which,

briefly, propose that multiple regions throughout the EVC and MTL construct and store perceptual representations of complex visual stimuli, and that the nature of the functional specialisation that exists across these regions is best described in terms of the type of representations that are instantiated within them, rather than the cognitive 'processes' that they support (Graham et al., 2010; Saksida and Bussey, 2010). Such models have provoked debate about MTL function and its role in perception, in particular, because most other contemporary accounts of MTL function consider this region to be specialised for supporting long-term declarative memory processes (Aggleton and Brown, 1999; Squire et al., 2004), and make limited, if any, claims about an additional role in high-level perception. They also make few predictions about how and why different categories of visual stimuli may differentially engage different sub-structures within the MTL.

Overview of Chapter 1

This Introductory Chapter seeks to frame the experimental work in the context of contemporary accounts of how the brain supports memory and perception in humans and nonhuman primates. Section 1.1 will introduce the reader to some basic EVC and MTL anatomy, including discussion of the prominent white matter pathways that support communication between some of these regions. Section 1.2 will then review lesion and neuroimaging studies that indicate a critical role for regions within the EVC in visual perception. Section 1.3 will discuss evidence for a specialised role for MTL substructures in memory, and consider how this has informed contemporary models of human memory. Section 1.4 will review recent studies that challenge the view that perception and memory are distinct 'modular' entities, in particular highlighting findings that regions within the MTL contribute to visual perception as well as memory. Section 1.5 introduces representational accounts of memory and perception, and explains how such models may be able to integrate many seemingly contradictory findings in the literature into a single coherent framework. Section 1.6 concludes the Introduction by: a) extending these representational models in order to make specific predictions about the distinct functional/structural connections that may support PRC/HC contributions to successful perception, and b) summarising how the experiments reported here are designed to investigate key predictions from this account.

1.1: Basic Anatomy of the EVC and MTL

1.1.1. An overview of the anatomy of early visual processing regions in EVC

Visual processing in the primate brain begins in primary visual cortex, which sits within the calcarine fissure of the occipital lobe (Fig 1.1). The primary visual cortex is also sometimes referred to as the striate cortex, or 'area V1', and contains neurons that demonstrate a high degree of selectivity to specific low-level attributes of visual stimuli, including line-orientation, spatial frequency, shape, motion, colour, and depth (Orban, 2008). From area V1, information about these low-level stimulus attributes is passed along to regions throughout the occipital, inferior temporal, and posterior parietal lobes, which are often referred to collectively as the 'extrastriate visual cortex' (EVC). Neurons in EVC sub-regions respond preferentially to higher order aspects of a visual image that do not appear to be processed in V1, such as speed gradients in an area called MT/V5, curvature in area V4, and global shape in area TE of the infero-temporal cortex (IT) (Orban, 2008). Indeed, the EVC has been differentiated into more than 30 distinct sub-regions based on the combination of the anatomical, physiological, and behavioural differences between them (Van Essen et al., 1992).

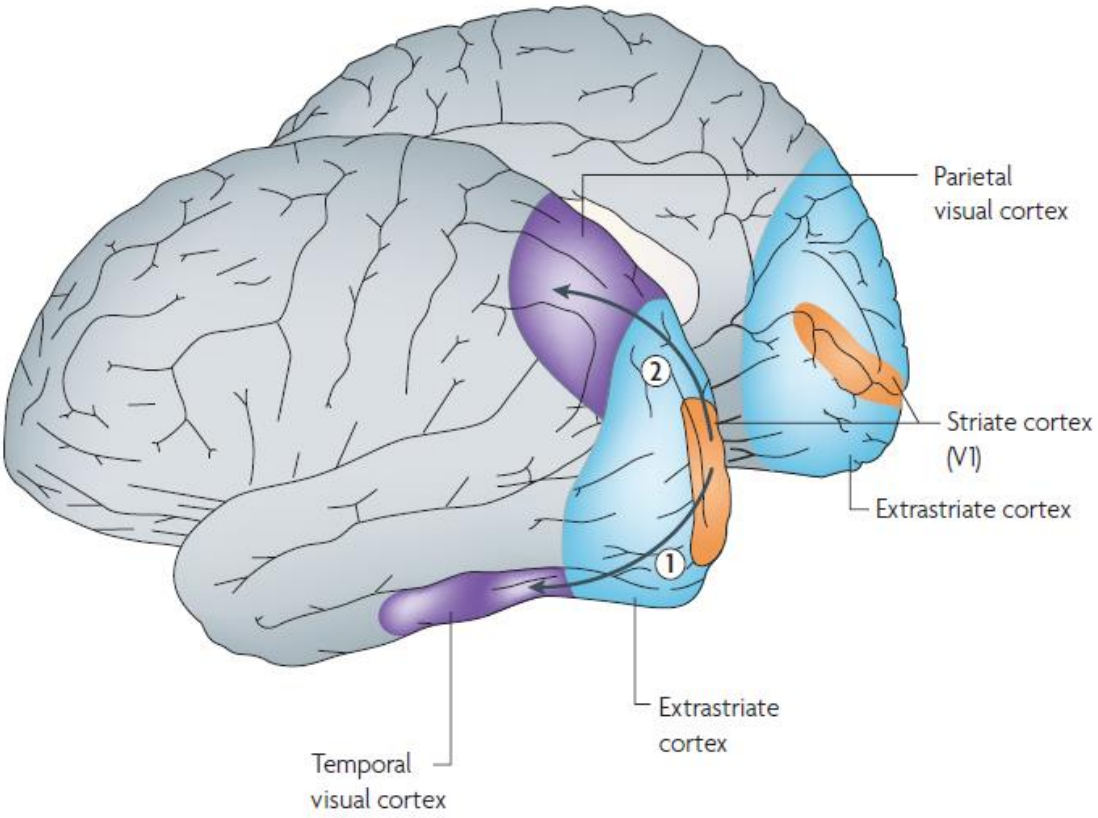

Fig 1.1. A lateral and medial-surface view of the core visual processing system of the human brain. Lower and upper arrows indicate the ventral (1) and dorsal (2) visual processing streams, respectively. Figure adapted from Op de Beeck et al., (2008).

It is worth highlighting several basic functional characteristics of the EVC here, though they will be further elaborated in section 1.2:

1) It is generally accepted that visual processing occurs along two parallel, though partly interconnected streams; a ventral or occipito-temporal "what" stream, involved in the processing of object-like stimuli (i.e. the ventral visual stream; VVS), and a dorsal or occipito-parietal "where" stream involved in spatial perception and visually guided action (see Fig 1). The specialisation and segregation of these two streams is relative rather than absolute (Zachariou et al., 2013), but functional, physiological, and pathway tracer studies have revealed that this basic organisational principle of the visual processing system is conserved across multiple species, including rodents (Wang et al., 2012), monkeys (Mishkin et al., 1983), and humans (Ungerleider and Haxby, 1994).

2) These streams are organised hierarchically, so that as visual information is gradually relayed in an anterior direction (i.e. towards the temporal pole), it passes to regions with increasingly complex neuronal response properties. For example, area TE of the IT cortex is located at the anterior extreme of the classic VVS (Fig 1.2), and is consequently involved in the processing of more complex properties of object stimuli relative to more posterior visual regions, such as area V4.
3) Some EVC regions can be identified non-invasively using behavioural paradigms in conjunction with *in vivo* brain imaging techniques, such as functional magnetic resonance imaging (fMRI), because they respond preferentially to stimuli from particular visual categories, such as faces, objects, and scenes (Op de Beeck et al., 2008). For example, the parahippocampal place area (PPA) and the fusiform face area (FFA) are two extensively-studied functionally-defined EVC regions that respond preferentially to scene and face stimuli, respectively, compared to other visual categories (Epstein and Kanwisher, 1998; Kanwisher et al., 1997). Other category-sensitive EVC regions include the lateral occipital complex (LOC; Grill-Spector et al., 2001a), the occipital face area (OFA; Gauthier et al., 2000), and the scene-sensitive transverse occipital sulcus (TOS; Tootell et al., 1997). I will describe these EVC regions in more detail in subsequent sections of this chapter because they are, indeed, defined functionally, rather than anatomically, in both the existing literature and the present experimental work.

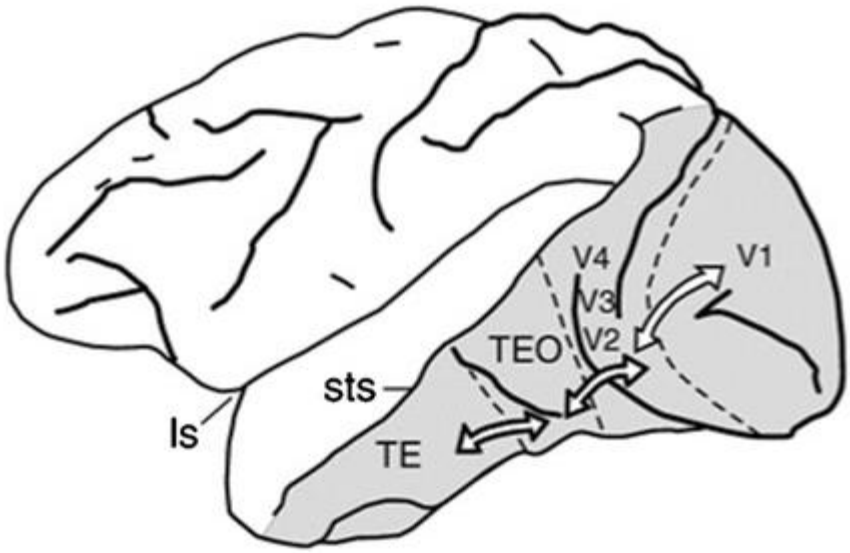

Fig 1.2. Lateral view of the macaque cerebral cortex, highlighting the VVS (grey) and the anatomical connections between some VVS sub-regions. Abbreviations: ls = lateral sulcus; sts = superior temporal sulcus; V1-V4, TEO and TE = visual cortical areas. Figure adapted from Murray et al., (2007).

1.1.2. An overview of the anatomy of the MTL

The term 'MTL' refers to a region of the brain that comprises a number of anatomically and cytoarchitectonically distinguishable substructures that are spatially distributed in a comparable fashion across many different species. One such structure is the hippocampus (HC), which can be further subdivided into HC subfields CA1-4, the dentate gyrus (DG), and the subicular cortices (Sb). The brain imaging protocols described in the current Thesis do not offer the spatial resolution required to accurately distinguish between these HC subfields, so, consistent with other fMRI studies of HC function (Mundy et al., 2013; Mundy et al., 2012; Lee et al., 2008), I do not investigate the functions of these subregions separately. I do, however, distinguish between the posterior and the anterior portions of the HC, particularly in Chapters 2 and 3, because previous fMRI studies in humans have consistently demonstrated increased activity in the posterior, but not the anterior HC during the kind of scene perception tasks reported in the present Thesis (Aly et al., 2013; Mundy et al., 2012; Lee and Rudebeck, 2010; Lee et al., 2008), and previous studies in rodents have shown that lesions to the dorsal but not the ventral HC consistently result in significant maze-learning impairments (Moser and Moser, 1998) (see also Poppenk et al., 2013). The MTL also contains the entorhinal, perirhinal and parahippocampal cortices (ERC, PRC, and PHC,

respectively), which sit alongside the inferior aspect of the HC and are sometimes referred to collectively as the 'parahippocampal region' (Fig 1.3). As with the HC, the PRC can be further subdivided into Brodmann's areas 35 and 36, and the PHC can be subdivided into areas TH and TF. Again, I will not differentiate between these distinct PRC/PHC sub-regions for the remainder of this Thesis, consistent with previous fMRI investigations of PRC/PHC function (Mundy et al., 2012; Devlin and Price, 2007; Epstein and Kanwisher, 1998). The MTL also contains the amygdala; the experiments reported here do not address the functions of the amygdala, but it too is introduced here for completeness.

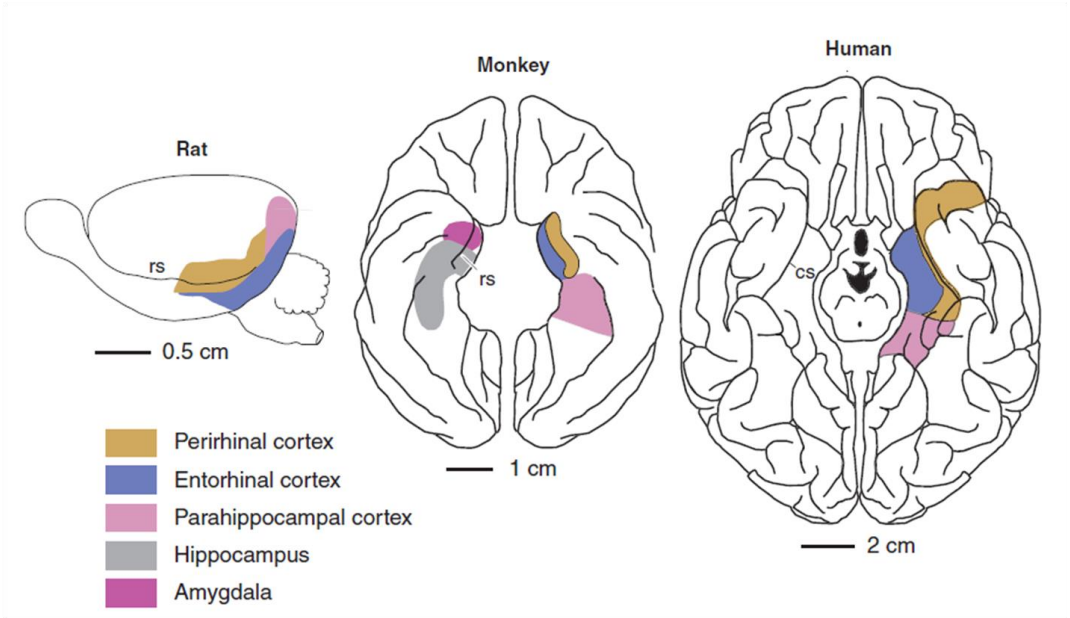

Fig 1.3. Key sub-regions of the MTL highlighted on the lateral surface of the brain in the rat (left), and the ventral surface in both the monkey (middle) and the human (right). cs = collateral sulcus. rs = rhinal sulcus. Figure from Murray et al., (2007).

These MTL sub-structures are highly, though differentially, interconnected, both with one another, and with more posterior visual processing regions in the EVC (Fig 1.4). The ERC is thought to act as the main 'hub' through which information flows to the hippocampus from other areas within the MTL. Interestingly, the ERC-HC connections that mediate this flow of information possess gradual anterior-posterior topography; the anterior HC is preferentially connected with tissue in the anteromedial ERC, whereas the posterior HC is preferentially connected with posterolateral ERC (Aggleton, 2012). The anterior and posterior ERC in turn receive inputs from the PRC and PHC, respectively. Though there is also a degree of cross-talk between these two latter

regions, they each receive highly distinct cortical afferents. PRC primarily receives inputs from visual association areas in the temporal lobe, such as areas TE and TEO of the VVS, whereas the PHC primarily receives inputs from more dorsal visual areas involved in visuospatial processing, such as posterior parietal cortex, posterior cingulate cortex, and retrosplenial cortex (Burwell, 2000). As well as their indirect connections with the HC via the ERC, the PRC and PHC are also known to have some direct connections with the anterior/posterior HC, respectively (Aggleton, 2012; Suzuki and Amaral, 1994). This differential pattern of connectivity suggests that, in the MTL, there may be relative segregation of item and visuospatial information, similar to that achieved by the two visual 'streams' of the EVC.

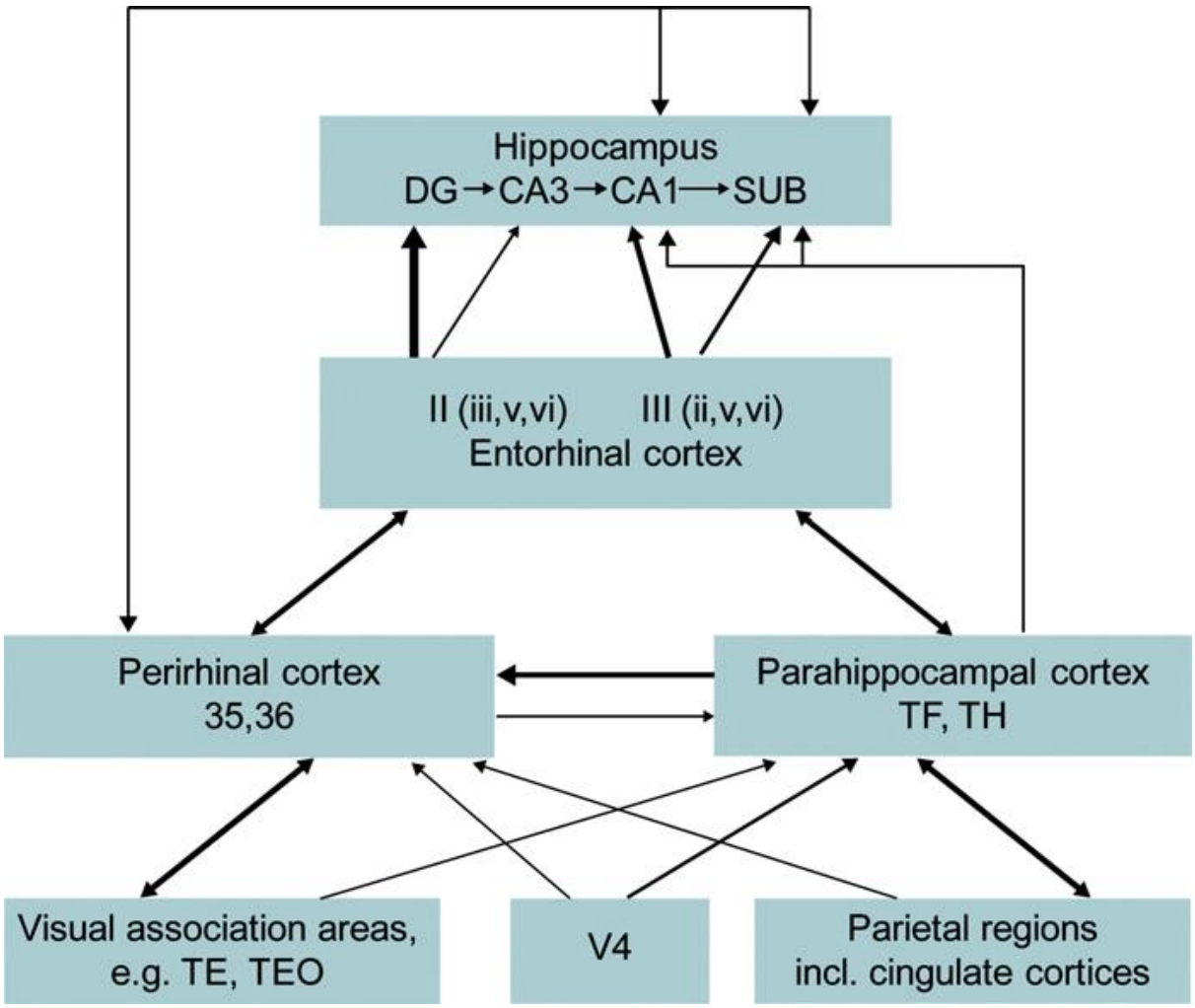

Fig 1.4. Proposed interconnections between MTL substructures and striate/extrastriate regions involved in visual processing in monkeys and humans. Arrow thickness is reflective of the strength of the connections between regions. Figure from Aggleton (2012).

1.1.3. An overview of medial diencephalon anatomy

Although the substructures of the medial diencephalon do not fall within the immediate purview of the current Thesis, it is also worth briefly noting some anatomy of this brain region. The diencephalon is a region that is composed of the thalamus, hypothalamus, epithalamus, and subthalamus. The *medial* diencephalon includes the mammillary bodies (MB's) and the anterior thalamic nuclei (ATN), and these two structures are of interest because they both receive dense inputs from the HC via a white matter pathway called the fornix (see below). Indeed, they are sometimes referred to as individual components of an extended HC-fornix-ATN-MB network, which contributes to important aspects of cognition (Gaffan, 1994; Aggleton & Brown, 1999). Aggleton and Brown (1999). For example, it is proposed that together with the HC, the fornix and medial diencephalon form a circuit that is specialised for 'recollection'; a long-term memory process that affords the recall of specific contextual details associated with a pre-studied stimulus (Fig 1.5). This model of MTL function will be discussed further in section 1.3.

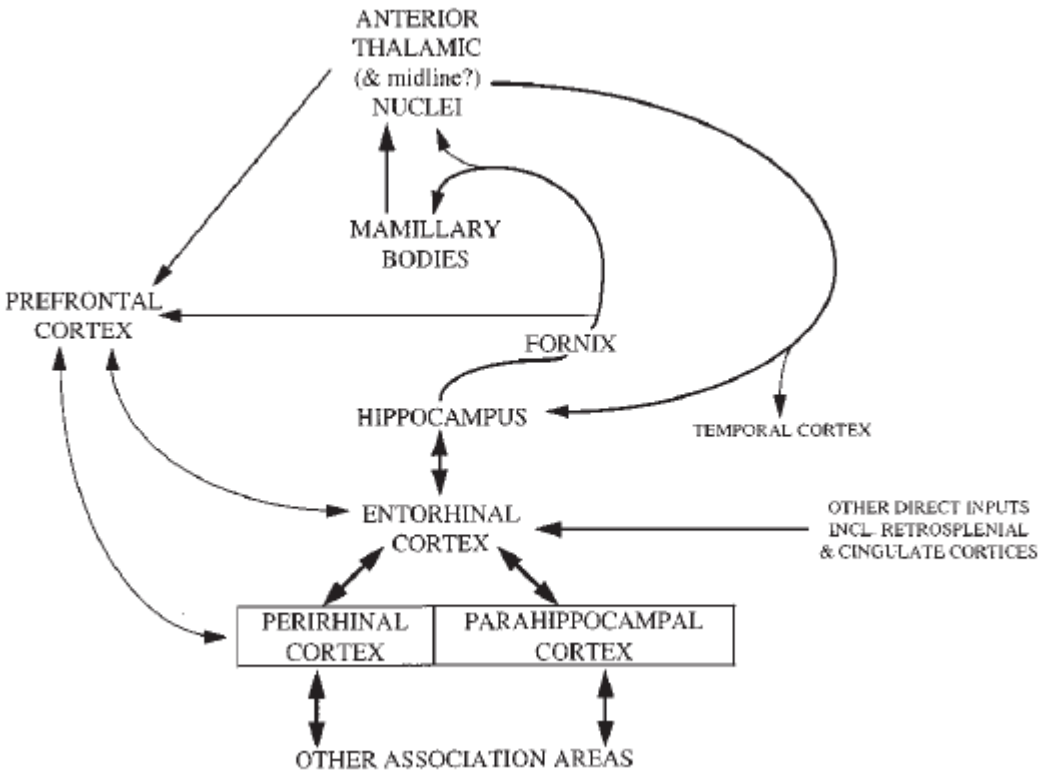

Fig 1.5. Schematic diagram of the structures and pathways that support recollection-based recognition memory according to Aggleton & Brown (1999). Line thickness reflects the putative importance of the connections for recollection, as understood at that time.

1.1.4. White matter connections facilitating communication between spatially distinct brain regions

Whilst the perceptual processing of visual stimuli is conducted in the gray matter regions of the EVC/MTL, the current Thesis aims to show that successful perception also depends on the ability of these spatially distinct regions to relay information to one another effectively. In this section, therefore, I introduce the reader to two prominent white matter bundles that may support communication between regions involved in processing similar categories of visual stimuli; the fornix and the inferior longitudinal fasciculus (ILF). The contributions of these pathways to perception for distinct visual categories is investigated in Chapters 3-5.

1.1.4.1. The Fornix

The fornix is a prominent c-shaped white matter tract that is comprised of approximately 500,000 fibers in each hemisphere of the monkey brain (Simpson, 1952), and around 2,700,000 individual fibers in the human brain (Daitz, 1953) (Fig 1.6). The fimbria of the fornix emerge from the hippocampus to form the crus in each hemisphere. The fornix crus of both hemispheres then gradually converge to form the body of the fornix at the sagittal midline of the brain. The body of the fornix then descends towards the medial diencephalon, approximately at the level of the anterior commissure, which bisects the fornix into posterior and anterior columns. These columns subsequently provide the hippocampus with connections to a number of sub-cortical (e.g. the ATN and MBs) and cortical (e.g. prefrontal cortex) brain regions (Saunders and Aggleton, 2007). Studies in animals demonstrate that fornix transection, which functionally lesions the HC by disconnecting it from these other functionally related structures, produces deficits in spatial learning and memory tasks that are also sensitive to HC lesions (e.g., object-in-scene memory tasks; Gaffan, 1994). As with the MBs and ATN, the fornix is, therefore, often referred to as a component of an ‘extended HC network’ of regions involved in similar aspects of cognition (e.g. Aggleton and Brown, 1999).

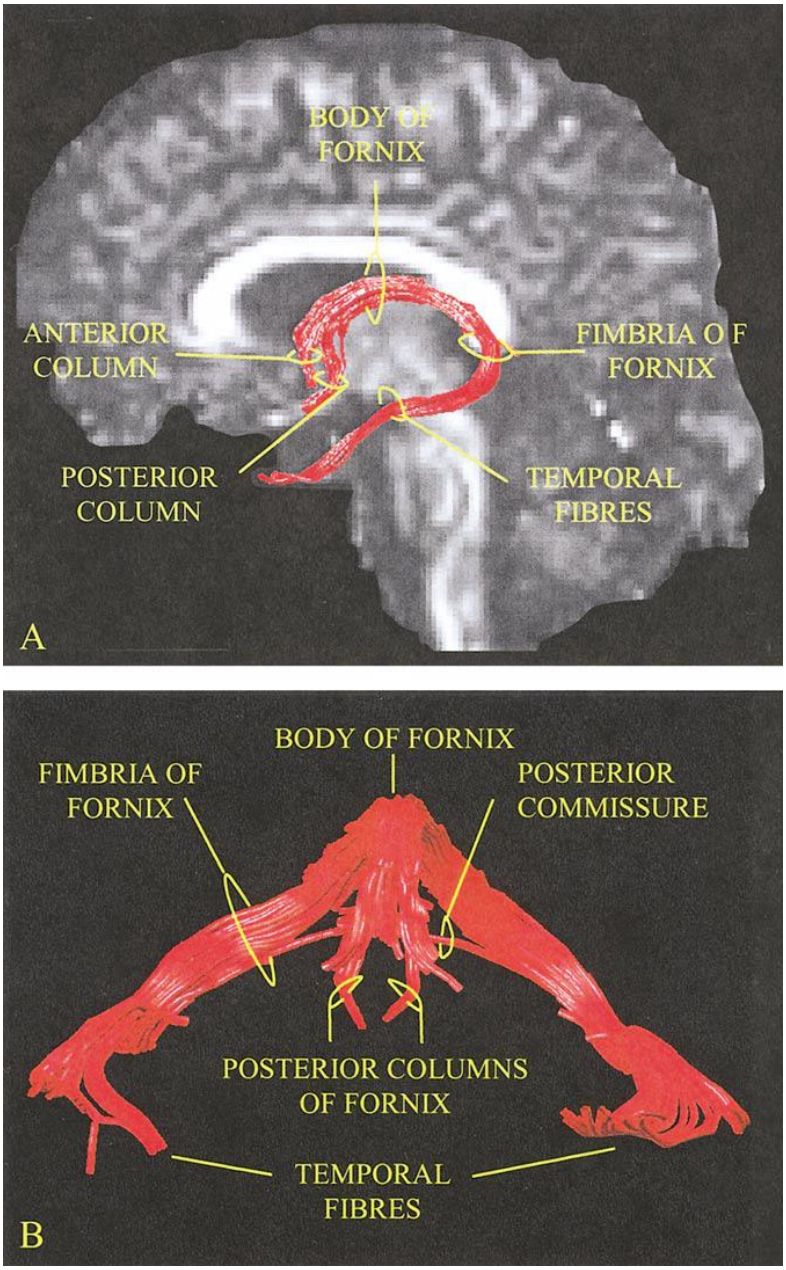

Fig 1.6. (**A**) A left-lateral view of the human fornix, which has been reconstructed using diffusion-weighted MR imaging and a white matter tractography protocol; (**B**) An anterior view of the coronal projection of the fornix. Figure from Catani et al., (2002).

Studies that have used retrograde tracers to investigate the origin of the fibers that comprise the fornix have confirmed that, of the efferent fibers that project *from* the temporal lobe, the vast majority originated in subfield CA3, and the subicular cortices of the HC (Fig 1.7). Although cells in other regions of the MTL, such as the PRC, contributed some fibers to the fornix, these comprised less than 3% of the total number of cells that were successfully labelled in the MTL. It is, therefore, not surprising that

whilst fornix damage/transection often produces significant behavioural impairments consistent with those observed following HC lesions, it typically spares those aspects of learning and memory that are thought to be supported by PRC, such as spontaneous object-recognition in animals, and familiarity-based recognition in humans (Bussey et al., 2000; Vann et al., 2008). This implies that: a) the fornix plays a role in HC function, which can be disrupted by damage, and b) normal functioning in other MTL areas is not dependent upon the integrity of the fornix.

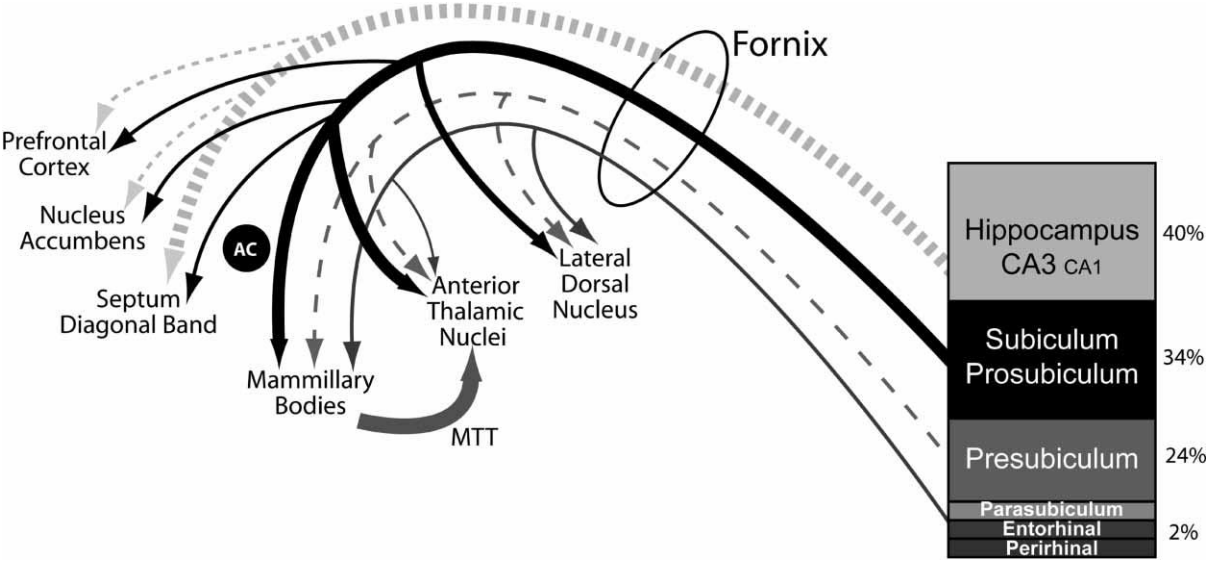

Fig 1.7. The percentage of fornix fibres that originate in the various sub-regions of the macaque MTL. Abbreviations: MTT = mammillothalamic tract; AC = Anterior commissure. Data from Saunders and Aggleton (2007); Figure from Aggleton (2008).

1.1.4.2 The Inferior Longitudinal Fasciculus (ILF)

The ILF is a prominent associational white matter pathway that is comprised of both long and short-range association fibres in humans, and connects the occipital pole to the temporal pole (Fig 1.8). In nonhuman primates, the ILF has been found to be predominantly composed of short-range U-shaped associational fibres, and is sometimes referred to as the occipito-temporal projection system (Catani et al., 2002; Tusa and Ungerleider, 1985). In humans, the ILF contains fibres that arise in multiple regions including the cuneus, lateral occipital cortex, and the occipital pole, which project to the superior, middle, and inferior temporal and fusiform gyri (Catani et al., 2002; Gschwind et al., 2012). Given that this pathway effectively traverses the VVS,

the ILF may play an important role in visual perception by relaying information between this hierarchically organised set of brain regions. For example, the ILF possesses highly reproducible connections with a number of core face processing regions along the VVS, including the fusiform face area (FFA) and the occipital face area (OFA) and anterior temporal lobe (Pyles et al., 2013; Gschwind et al., 2012). Furthermore, congenital prosopagnosia (CP) - a rare condition characterised by impairments in face perception and recognition - has been associated with lower fractional anisotropy (FA; a well-established diffusion-MRI measure of white matter microstructure) in the ILF (Thomas et al., 2009). Reductions in FA have also been reported in the ILF in a group of children with object recognition deficits, relative to a group of typically developing children (Ortibus et al., 2011). ILF damage may therefore impair some aspects of face/object perception and recognition by disrupting or preventing the relay of information between visual processing regions along the VVS.

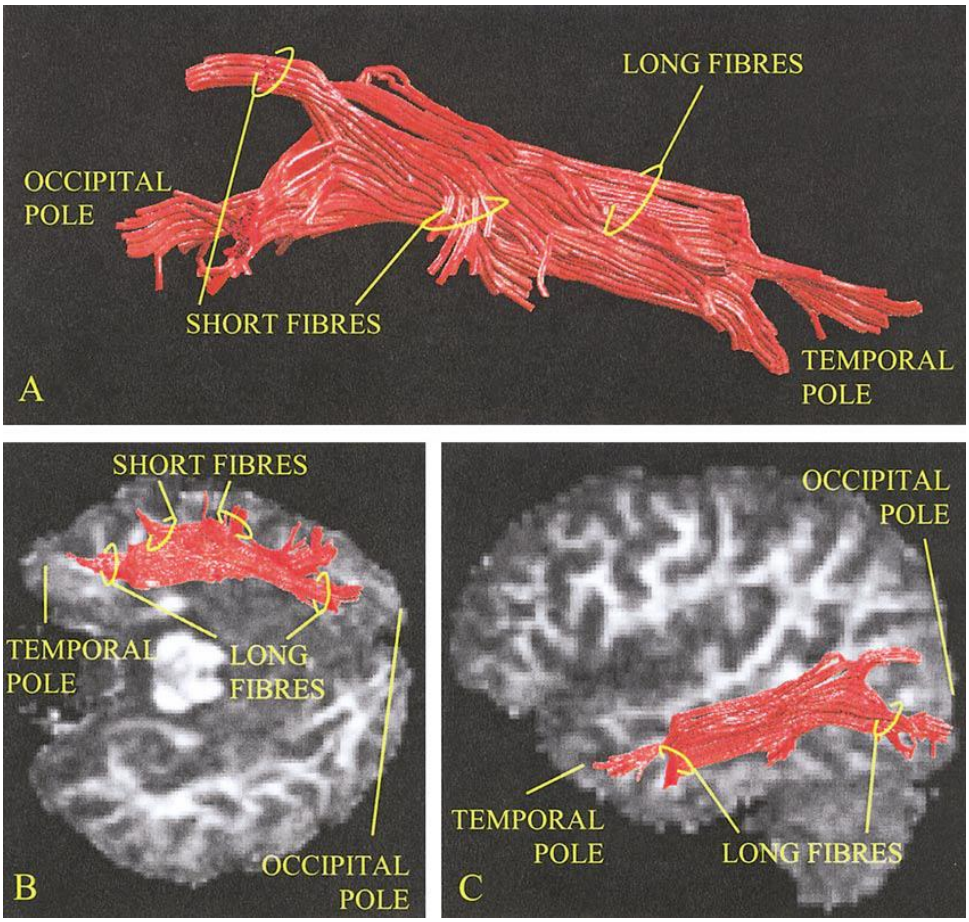

Fig 1.8. (**A**) Right-lateral, (**B**) superior, and (**C**) medial views of the human ILF in the right hemisphere. Figure from Catani et al., (2002).

1.1.5 Cross-species anatomical consistency affords translational research

The anatomical, and cytoarchitectonic similarities of these gray and white matter regions across species are highly suggestive of cross-species *functional* homology (Burwell, 2000; Ungerleider and Haxby, 1994). In discussing models of how the brain supports memory and perception, therefore, I will draw support for my arguments from studies of animal models of cognitive impairment, as well as neuropsychological and brain imaging studies in humans.

1.2: The role of the EVC in visual perception

As noted in section 1.1., visual processing for object and visuospatial information occurs along a ventral and dorsal processing stream, respectively (see also Goodale and Milner, 1992). This basic characterisation of the organisation of the visual system is supported by numerous studies from human neuropsychology. For example, Karnath et al., (2009) reported patient J.S., who presented with a lesion of the medial aspect of the ventral occipito-temporal cortex as a result of an ischemic stroke. Consistent with the two streams conception of visual processing, J.S. demonstrated significant impairments in object discrimination and recognition relative to healthy controls (a condition known as visual agnosia), but relatively preserved visuomotor and navigation abilities. By contrast, patients with bilateral damage to the cortex at the occipito-parietal junction typically present with severe impairments in spatial and visuomotor processing; a condition known as Balint's syndrome (Rafal, 2001). Balint's syndrome is characterised by numerous symptoms including simultaneous agnosia (an inability to perceive and attend to more than one object at a time), spatial disorientation, impaired depth perception, and optic-ataxia (impaired visual object-reaching behaviour). The differential impact that damage to ventral versus dorsal visual regions has upon cognition is strong support for the two streams hypothesis about how visual processing is organised in the healthy brain.

In section 1.1, it was noted that visual processing occurs sequentially (i.e. hierarchically) along these two streams, with anterior regions involved in processing more complex stimulus properties than their posterior counterparts. This concept of hierarchical processing was highlighted by a now-classic study in which researchers

took extracellular single-cell electrode recordings of cells along the inferior temporal (IT) cortex of immobilized anaesthetized macaque monkeys while they were presented with a variety of simple and complex visual stimuli, ranging from slits and spots of various colours, to faces and animal-imitation objects (Tanaka et al., 1991). Importantly, the complex stimuli to which a given cell might respond preferentially were gradually simplified in order to identify the 'critical' features required to prompt a response from the cell. The authors were then able to classify cells as Primary, Texture, Elaborate, Others, Weak, or Unresponsive on the basis of their response properties. Of particular interest were the Primary cells, which could be activated by a variety of simple stimuli such as spots, slits, squares and ellipses, simply by changing the orientation, size and/or colour of these shapes appropriately. By contrast, Elaborate cells responded preferentially to *specific* shapes, or a conjunction of a specific shape with a specific colour or texture. It was found that these Primary and Elaborate cells were distributed differentially across IT, with Primary cells disproportionately concentrated in the posterior third of IT, and Elaborate cells disproportionately concentrated in the anterior two-thirds of IT. Cells located in the anterior VVS are therefore involved in the processing of more complex 'critical' features, or conjunctions of stimulus features, relative to their more posterior counterparts.

In section 1.1, it was also noted that researchers have identified EVC regions that are consistently activated bilaterally across multiple subjects and show a disproportionate functional response to particular categories of visual stimuli. Using functional Magnetic Resonance Imaging (fMRI), where blood-oxygen level dependent (BOLD) MR signal is measured throughout the brain whilst a task is taking place and compared to when the subject is at rest (or compared to another baseline condition), researchers have identified EVC regions that consistently respond preferentially to particular visual categories.

One previously reported category-sensitive region is the lateral occipital complex (LOC), which is located on the lateral bank of the fusiform gyrus of the occipito-temporal cortex and responds preferentially to images of intact objects relative to scrambled images of objects and textures, suggesting this region is involved in processing of the shape and structure of intact objects (Grill-Spector et al., 2001a; Malach et al., 1995). The LOC response gradually diminishes with repeated presentation of identical images of the same object stimulus – a process known as repetition-suppression – but it does not diminish in response to repeated presentation of pictures of the same object presented from different viewpoints (Grill-Spector and Malach, 2001b). This suggests that the LOC supports viewpoint-specific

representations of visual objects, and that it treats different-view images of the same object as images of multiple distinct objects. This finding suggests that flexible view-invariant object representations must be supported outside the LOC.

Kanwisher et al., (1997) described another category-sensitive cluster of voxels in the fusiform gyrus of the occipitotemporal cortex, which responded preferentially to face stimuli with great consistency across participants. The so-called 'fusiform face area' (FFA) has since been extensively studied in the face perception/recognition field. This region actually responds to a variety of non-face stimuli, including images of bodies, mammals, cars, chairs, tools, and scenes, though it responds maximally to face stimuli (Downing et al., 2006). Furthermore, studies in patients with acquired prosopagnosia (a condition characterised by face processing impairments in the context of relatively spared perception/recognition for other object-like stimuli) have confirmed that this rare condition is often associated with lesions to the putative FFA (Barton et al., 2002). Some authors have, however, noted that the focus on the role of the FFA in face-perception has led to a neglect of other nearby cortical regions that are also preferentially engaged by face stimuli (Rossion, 2008).

One such relatively neglected region is located in, or near, the inferior occipital gyrus, and is commonly referred to as the 'occipital face area' (OFA; Gauthier et al., 2000). The OFA is displaced from the FFA, in a posterior direction, by a mere 2cm (Pitcher et al., 2007), and as with the FFA, damage to this region is often associated with acquired prosopagnosia (Bouvier and Engel, 2006). What distinguishes the face representations/processes supported by the OFA and the FFA? Consistent with the hierarchical organisation of the visual system in general, the OFA has been described as the first face-selective cortical region within a distributed face processing network along the ventral visual stream, which also incorporates the FFA and areas within the anteromedial temporal lobe (Pitcher et al., 2011; Haxby et al., 2000; see also Fig 1.9). According to this framework, the OFA rapidly processes the low-level properties or parts of faces, which are subsequently combined at higher levels of the processing hierarchy to form increasingly complex face representations. Whilst these higher-level face representations may be needed in order to support complex face processing operations such as view-invariant person-identification, the lower level representations/operations supported by the OFA may be sufficient to support lower-level face part processing. Indeed, transcranial magnetic stimulation (TMS) of the right OFA as early as 60-100ms post stimulus-onset impairs the discrimination of individual face parts, but not the ability to discriminate the spacing between them (Pitcher et al.,

2007), and PET studies show that the right FFA, but not the right OFA, is more active in response to whole faces relative to face-part stimuli (Rossion et al., 2000).

Analogous to the hierarchically-organised face processing regions along the ventral visual stream, there are also a number of functionally-definable scene processing regions, distributed throughout the dorsal-medial visual stream (Fig 1.9). One frequently-studied scene-sensitive EVC region is known as the parahippocampal place area (PPA) (Epstein and Kanwisher, 1998). In humans, the PPA is typically centred on the lips of the collateral sulcus where it joins the medial fusiform gyrus (i.e. close to the FFA), rather than the parahippocampal gyrus proper (Nasr et al., 2011). Based on the findings from numerous fMRI studies, the PPA is known to respond preferentially to images of scenes, relative to objects, faces, and other non-spatial stimulus categories (Epstein and Kanwisher, 1998). Importantly, differences in the low level properties of these categories cannot entirely account for the PPA's preference for scene-stimuli, because images of Lego blocks arranged to form spatial configurations elicit significantly greater activity in the PPA than images of the same Lego blocks that were combined to form complete 'objects' (Epstein et al., 1999). Interestingly though, more recent investigations have suggested that one of the critical stimulus features to which the PPA responds is the rectilinearity of visual stimuli (Nasr et al., 2014), which may in turn partly account for why the PPA has been found to respond more to indoor scenes, relative to naturalistic outdoor scenes (Henderson et al., 2007). The PPA is thought to support viewpoint-specific representations of spatial scenes. Evidence in favour of this proposition comes from a study by Epstein et al., (2003), who presented images of scenes, each containing a main foreground object. After a scene was presented, participants were then exposed to either: a) the same scene + object image, b) an image of the same scene with a different foreground object, c) an image of the same scene from a different viewing angle, d) an image of a different scene containing the same object, or e) an image of the same scene containing additional objects. The authors found that the PPA BOLD response to the second stimulus was attenuated/diminished when participants viewed the same scene + object image or the same scene image with a different foreground object in it (i.e. repetition suppression occurred for the scene regardless of the foreground object), whereas presentation of the same scene from a different viewpoint was associated with an increase in the BOLD response. This suggests that the different-view scene images are not linked to the original scene representation by the PPA, but are instead treated as entirely new stimuli and do not, therefore, trigger repetition-suppression. Analogous to the role of the LOC in constructing viewpoint-specific object representations, the PPA therefore

appears to support viewpoint-specific scene representations, and cannot by itself integrate different-viewpoints of the same scene into a single view-invariant scene representation, which must be achieved elsewhere.

Another scene-selective EVC region was originally reported to be localised on the Transverse Occipital Sulcus (Tootell et al., 1997), and is therefore frequently referred to as the TOS. More recent investigations have, however, localised this category-sensitive region on the transverse occipital gyrus, rather than within the sulcus itself (Nasr et al., 2011), so it is also sometimes referred to as the occipital place area; to maintain consistency with the majority of the literature, however, I will continue to refer to this region as the TOS. Whereas the PPA has been extensively studied in terms of its role in the representation of space and its differential functional response to different spatial stimulus manipulations, the function of the TOS is less clear. Some authors suggest that the TOS may stand in the same relation to the PPA, as does the OFA to the FFA. That is to say, that the TOS may be the first scene-selective cortical region within a more distributed scene perception network, which also incorporates other more anterior regions, including the PPA and retrosplenial cortex (Dilks et al., 2013; see also Fig 1.9). In support of this, TOS responds preferentially to both indoor and outdoor scenes, relative to more object-like stimuli (Bettencourt and Xu, 2013). Analogous to the putative role of the OFA in face-part processing, the TOS may be involved in processing relatively basic properties of visual scenes, which may then be integrated with other spatial features at more anterior regions of the scene perception network (e.g. the PPA and posterior HC).

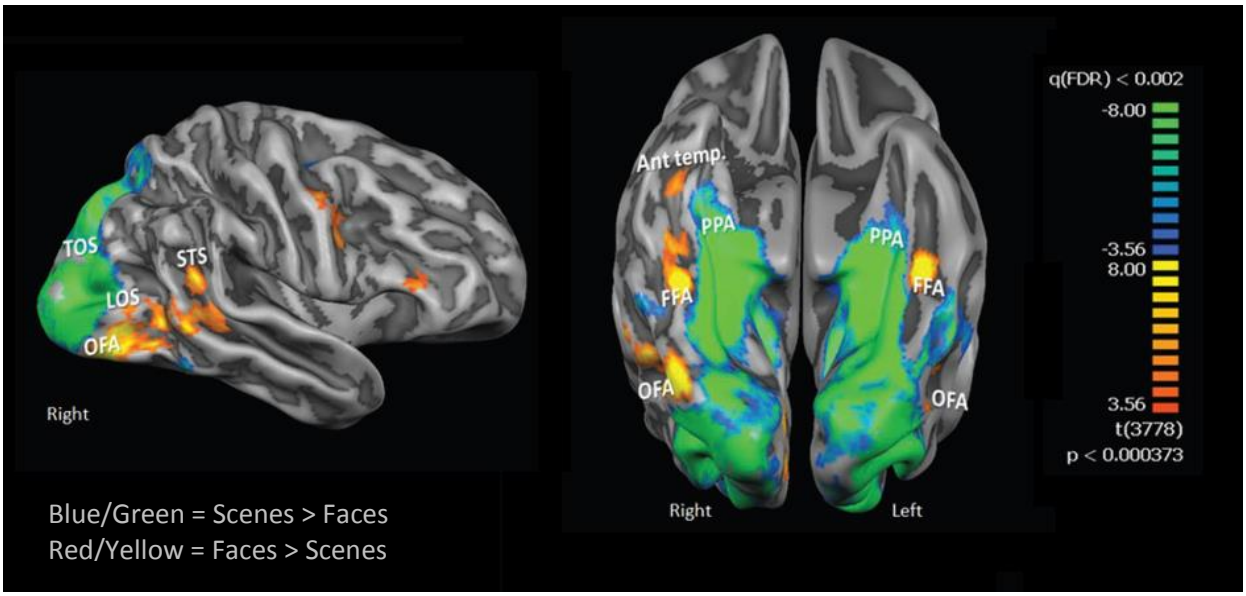

Fig 1.9. Illustration of differential face and scene-selective activity patterns across the EVC, on the lateral (left) and ventral (right) surfaces of the brain. Blue/Green = preferential activation in response to scenes; Red/Yellow = preferential activation in response to faces. OFA = Occipital Face Area; FFA = Fusiform Face Area; STS = Superior Temporal Sulcus; LOS = Lateral Occipital Sulcus; Ant temp. = Anterior Temporal Cortex; TOS = Transverse Occipital Sulcus; PPA = Parahippocampal Place Area. Figure adapted from Avidan et al., (2014).

There remains a contentious debate about the extent to which these category-sensitive regions represent focal 'modules' that are specialised for processing specific stimulus categories (Kanwisher, 2010), as opposed to constituting parts of broader cortical 'maps' with graded sensitivities to different categories of stimuli (Op de Beeck et al., 2008; Behrmann and Plaut, 2013). Nevertheless, it is the orthodox view that the EVC contains hierarchically organised brain regions that are critical for normal visual perception, and that damage to these hierarchies has a disproportionate impact on the ability to process specific categories of stimuli.

1.3: The MTL and declarative memory

In contrast to the EVC, structures within the MTL are widely believed to collectively form a highly specialised memory system, with little or no role in visual perception. Before presenting evidence contrary to this view, I will discuss literature that led to this conceptualisation of the MTL as a memory system.

In 1954, Scoville reported patient H.M., who had been suffering with debilitating and intractable epileptic seizures. H.M. underwent an experimental surgical procedure to remove a substantial portion of his MTL bilaterally. The rationale was that the HC had previously been determined to possess epileptogenic properties, so a temporal lobe resection might relieve H.M. of his seizures. The procedure, however, destroyed tissue up to 8cm posterior to the tips of the temporal lobe bilaterally, thereby damaging not only the HC, but also the amygdala, ERC, PHC, and PRC.

Post-surgery, H.M. immediately presented with severe impairments in his ability to acquire new memories (anterograde amnesia), and to a more limited extent, deficits in his ability to retrieve old memories (retrograde amnesia). Systematic investigations revealed that H.M. was severely impaired relative to healthy controls in remembering lists of word-pairs (Scoville and Milner, 1957), and his face recognition scores were poor relative to a patient with frontal lobe damage (Milner et al., 1968). In contrast to these face recognition and word recall deficits, other cognitive abilities were thought to be intact; assessments of H.M.'s general intelligence showed a slight improvement, and his parents declared no adverse personality change. H.M. could also perform the perceptual Mooney 'Closure' task at a level that was superior to several age-matched healthy controls (Milner et al., 1968). This task requires detection of a face 'stimulus' that is composed of multiple black and white patches that form no complete contours. That H.M. performed better than controls on this task was taken to indicate that his amnesia was not accompanied by impairments in perception.

H.M. was able to acquire new skills and information under certain conditions. He was able to learn (after just 10 trials) to trace the outline of a star which, along with his hand, was visible to him only via it's reflection in a mirror; he showed good retention of this ability after 3 days, despite having no recollection of ever having performed the task (Milner, 1962). These observations prompted researchers to distinguish between two types of memory. The ability to consciously recognise or recall facts and events was termed 'declarative memory', and was presumed to be supported by the MTL,

whilst other forms of memory, such as skill learning, perceptual learning, habit learning, and simple conditioning, were referred to collectively as 'non-declarative memory', and considered not dependent upon the MTL (Squire, 2004).

H.M., therefore, suggested two distinct memory systems, with the MTL – as a whole – responsible for declarative memory. As the precise spatial distribution of the damage to H.M.'s temporal lobe could not be defined at the time, the unique contribution of each MTL sub-region to declarative memory was unknown. Animal studies, however, where lesions could be made to specific MTL substructures, provided a way to understand the memory impairments seen in individuals like H.M.

For this endeavour to succeed, researchers needed to develop a paradigm that is sensitive to the animal equivalent of the behavioural memory impairments seen after damage to the human MTL. One such paradigm is the delayed non-match to sample task (DNMS). During a given trial, a subject is exposed to a stimulus, and after a pre-determined delay, is presented with two stimuli; one is entirely novel, the other is the stimulus to which the subject was pre-exposed. To solve the task and obtain a reward, the subject must select the novel stimulus. Unique stimuli are presented on each trial so this paradigm does not require extensive periods of training, so successful task performance is unlikely to be dependent upon skill-learning or other forms of non-declarative memory.

The DNMS task was initially administered to nonhuman primates and rodents with large bilateral MTL lesions designed to approximate the damage sustained by H.M., with a view to reproducing his striking recognition memory deficits. These lesions incorporated the HC, amygdala, PRC and PHC (Squire et al., 1991), and, as anticipated, were found to impair DNMS performance (Zola-Morgan et al., 1982). These findings suggested that the integrity of the MTL is critical for recognition memory in the animal model, as well as patient H.M.

Subsequent studies sought to refine the animal model in order to identify the specific MTL subregions that contribute to DNMS performance. Monkeys with lesions limited to the amygdala were unimpaired in the DNMS task, suggesting that the amygdala is not a critical component of the MTL recognition memory system (Zola-Morgan et al., 1989a; Fig 1.10). This was supported by findings that monkeys with combined HC and amygdala lesions were impaired in the task, but no more than monkeys with circumscribed HC lesions. Another study showed that lesions of the PRC and PHC impaired DNMS performance to the same extent as lesions incorporating the HC, amygdala, and adjacent cortical regions (Zola-Morgan et al., 1989b; Fig 1.10). Such

findings were taken to indicate that the HC, PRC, ERC, and PHC, but not the amygdala, form a highly specialised declarative 'memory system' (Squire and Zola-Morgan, 1991), and that damage to these components was responsible for H.M.'s apparently selective declarative memory deficit.

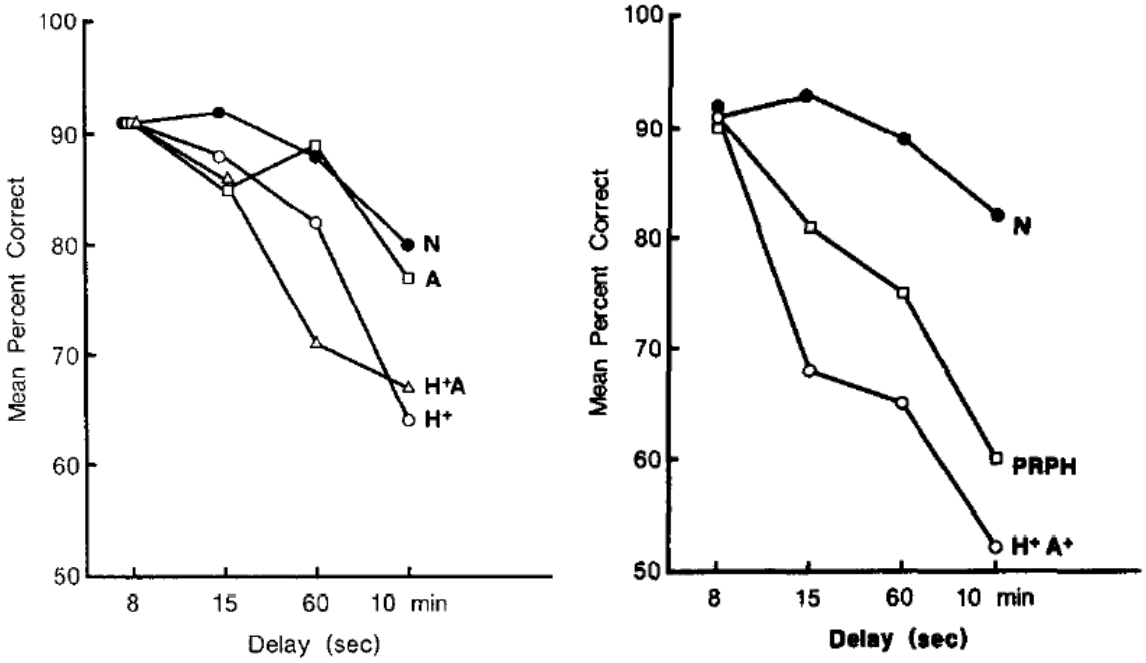

Fig 1.10. DNMS performance in 'normal' monkeys (N), monkeys with HC lesions (H+), monkeys with amygdala lesions (A), monkeys with combined HC and amygdala lesions (H+A), monkeys with combined lesions of the HC and amygdala that also damaged adjacent cortices (H+A+), and monkeys with conjoint lesions of the PRC and PHC (PRPH), with a variable delay between stimulus exposure and test. Figure- left and figure-right were adapted from Zola-Morgan et al., (1989a) and Zola-Morgan et al., (1989b), respectively.

1.3.1. Unitary Process Account of MTL function

These findings prompted researchers to develop theoretical accounts of MTL function. In the following sections, I provide a brief description of several accounts from this literature, along with some empirical work that has been interpreted to support each account. The primary focus of the current Thesis is on EVC/MTL contributions to perception rather than memory, so this summary is not intended to explicate all of the subtle nuances of these models, or to provide an exhaustive review of the studies that

they have generated. Rather, it is intended to highlight that the MTL has until recently been studied almost exclusively in terms of its role in declarative memory.

One such account of MTL function is the unitary process account, according to which the HC, ERC, PRC and PHC support declarative memory by rapidly binding together stimulus features processed in other distributed cortical sites (Squire et al., 1991). After a lengthy period of consolidation, the memory is then stored in these other cortical regions, so that MTL damage will impair the ability to form new memories, but remote memory will be preserved (as seen in patient H.M.). This account does not explicitly propose that the MTL acts as a single coherent functional unit, with all substructures playing the same role in forming new declarative memories, but it does state that the degree of declarative memory impairment will be correlated with the size of lesions in the MTL. Indeed, both amnesic patients and monkeys with lesions limited to the HC have been reported to present with less substantial declarative memory impairments relative to those with more diffuse MTL lesions including the subjacent temporal cortex (Squire et al., 2004).

1.3.2. Dual-process Accounts

A set of competing accounts propose that declarative memory is actually supported by two largely independent processes; recollection and familiarity (Aggleton and Brown, 1999; Yonelinas, 1994). Stimulus recollection is characterised as 'remembering' the details and context associated with a previously encountered item, and is often described as a threshold-based process (i.e. it either fails or succeeds) that also allows the free recall of episodic information. By contrast, familiarity is characterised as 'knowing' that an item was previously encountered without necessarily being able to recall the details or context of this encounter, and is often described as a continuous strength-based signal-detection process providing a measure of stimulus-recency. Furthermore, prominent 'dual-process' accounts, such as that developed by Aggleton and Brown (1999), propose that recollection and familiarity have distinct neural substrates *within* the MTL; with recollection supported by an extended HC-fornix-MB-ATN network, and familiarity dependent on PRC. Unitary and dual-process accounts therefore differ in that the former predicts that MTL damage will impair declarative memory generally, whereas the latter makes the additional prediction that the location of the damage within the MTL (HC versus PRC) will determine what type of declarative memory 'process' is impaired.

Several procedures have been developed in an attempt to systematically dissociate recollection and familiarity-based recognition memory judgements in humans, and test the differential contributions of the HC/PRC to these processes. These include confidence-based receiver-operating characteristic (ROC) recognition paradigms. These require participants to assign a degree of confidence to their old/new recognition judgements to test stimuli (some of which are pre-studied, whereas others are entirely novel), often using a 6-point confidence scale; performance at each level of confidence (hits versus false alarms) is then plotted as an ROC, and a dual-process signal detection model of recognition is applied to the data in order to extract quantitative estimates of familiarity and recollection (Yonelinas, 1994). Aggleton et al., (2005), for example, administered a verbal ROC paradigm to a patient with HC pathology due to meningitis (patient KN), and reported abnormally low estimates of recollection in the context of preserved familiarity.

This neuropsychological evidence suggests a role for the HC in tasks that tax recollection, but not those that can be supported by familiarity alone. Patients with selective PRC damage are extremely rare, making it difficult to attribute familiarity impairments to PRC involvement. One study, however, reported a patient with temporal lobe epilepsy (Patient N.B.), who underwent surgery to remove a portion of the left anterior temporal lobe which included the amygdala, PRC, ERC, but not the HC, after which her post-surgical cognitive impairment profile was assessed (Bowles et al., 2007). N.B. was asked to perform a number of recognition memory tasks, which included an ROC recognition paradigm. N.B. demonstrated marked impairments in familiarity relative to healthy controls, but estimates of recollection were within the normal range; consistent with dual-process accounts. Taken together then, neuropsychological studies suggested a double-dissociation between the role of the HC and PRC in recollection and familiarity, respectively.

Functional MR imaging (fMRI) studies of memory also provided evidence for a differential contribution of the HC and PRC to recollection and familiarity, respectively. In fMRI studies of memory, participants are scanned while they study stimuli in an appropriate memory encoding task. The participant then typically completes a subsequent memory task *outside* the scanner, which includes both pre-studied stimuli and a series of novel distractor stimuli. This allows researchers to test whether the activity of a given region-of-interest (ROI) at encoding is predictive of subsequent memory success in particular task conditions, or at particular response criteria. A number of researchers have used fMRI in conjunction with ‘source memory’ (SM) paradigms to investigate the differential contributions of the PRC/HC to item and item-

source memory, respectively. Davachi et al., (2003) administered a SM encoding task to participants whilst they received an event-related fMRI scan. During the task, participants were presented with a series of adjective words (e.g. 'dirty'), and prompted to either read the word, or to imagine a place that may be described using that word (e.g. a rubbish dump). In a subsequent memory task participants were presented with the pre-studied words along with a series of novel distractor words and asked to: a) identify whether each word was pre-studied or novel (i.e. old or new), and b) the context under which the word was studied (i.e. its source-context: 'read' versus 'place'). Consistent with dual-process accounts, encoding-related activity in the PRC was predictive of subsequent item recognition, but not source recognition, whereas encoding-related activity in the HC was predictive of source recognition, but was not correlated with individual item recognition (see also Rugg et al., 2012).

1.3.3. Alternative accounts

Not all accounts of MTL function describe the functional specialisation that exists across MTL sub-regions in terms of the different memory *processes* that these regions support. One such account is the 'Binding of Item and Context' model (BIC; Diana et al., 2007), which instead describes this functional specialisation in terms of the different kinds of *information* that the different MTL sub-regions are involved in encoding/retrieving. BIC proposes that the PRC is involved in encoding/retrieving information about individual *items* (not explicitly constrained to any particular stimulus category), whereas the posterior PHC stores information about the *context* in which the item was encountered (both spatial and non-spatial). These two separate streams of information remain segregated as they pass through the ERC, but are bound together into item-context associations by the HC. BIC is distinguishable from dual-process accounts by its proposal that recollection of individual items or contexts can actually be supported by the PRC and PHC, respectively, and that it therefore does not necessarily rely on the integrity of the HC. The HC is only critical for recollection of item-context associations. Like dual-process accounts, BIC does, however, propose that only the PRC will be associated with familiarity-based recognition judgements for individual items, because contextual information is not required to make a judgement about the item's prior occurrence. BIC can therefore accommodate much of the data that has previously been interpreted to support dual-process accounts of MTL function, but can, in addition, account for evidence for increased activity in the PHC as well as the HC during accurate SM judgements (Diana et al., 2007).

The unitary process, dual process, and BIC accounts of MTL function differ in terms of how they characterise the nature and the extent of the functional specialisation that exists within the MTL. Nevertheless, they share a number of important assumptions about MTL function that will be challenged in the next section. The first is that the MTL is a highly specialised declarative memory system that is not required for other functions such as high-level visual perception or non-declarative forms of memory (e.g. perceptual learning). Another is that neither the HC nor the PRC are preferentially engaged by different visual categories. Given these shared assumptions about MTL function, such models will be referred to collectively as 'memory system' accounts, as a convenient means to distinguish them from more recent representational accounts of MTL function, which will be introduced shortly.

1.4: Going beyond declarative memory in the MTL

In this section I review evidence that: a) the PRC and HC make a differential contribution to non-spatial and spatial processing, respectively, and b) that they contribute to a number of cognitive domains beyond declarative memory. I begin by reviewing evidence highlighting a preferential role for the PRC in object processing.

1.4.1. The PRC and object processing

As outlined in section 1.2., the orthodox view of object processing is that this is carried out sequentially and hierarchically along the VVS, and that this 'object-analyser' stream ends, prior to the PRC, at area TE (Fig 2) (Murray and Wise, 2012). As Murray et al., (2007, pp102) point out, however, as well as receiving direct inputs from area TE, the PRC also possesses reciprocal connections with "the higher-order cortical fields for each sensory system, together with multimodal cortical regions", and that it is, therefore, "in a position to construct higher-order visual and multimodal representations of objects". As well as these anatomical grounds for suspecting a role for the PRC in high-level object perception, a number of lesion studies in animals are also suggestive.

Eacott et al., (1994) administered a matching-to-sample task to macaque monkeys with combined bilateral lesions of the PRC and ERC, and reported good performance following a short delay between exposure and test, but impaired performance relative

to controls when the delay was increased. The authors also reported a modified version of the task, called simultaneous match-to-sample, in which, at test, both the old and the novel stimulus were presented to the animal simultaneously on a screen. After increasing the perceptual demands of the task by removing the colour and reducing the size of the stimuli, the authors found that the PRC + ERC lesion monkeys were impaired in the task even when there was no delay between exposure and test. This finding is consistent with earlier DNMS findings in monkeys with PRC damage (Zola-Morgan et al., 1989b), and is suggestive of a role for the PRC in object perception based on the assumption that long term memory would make a negligible contribution, if any, to such a discrimination task. Subsequently, Buckley and Gaffan (1997) reported that monkeys with PRC lesions were able to learn to make a small number of concurrent visual discriminations (N = 10), but were impaired at learning larger sets. They proposed that this pattern arose due to the increased perceptual demands placed on discrimination between large sets of items.

To account for these novel findings, it was proposed that PRC is best understood as a 'visual' rather than a 'memory' area. More specifically, PRC may operate as the most anterior component of the VVS, storing representations of object feature-conjunctions that are even more complex than those supported by area TE, and other more posterior regions of the VVS (Fig 1.11; Bussey & Saksida, 2002; Murray & Bussey, 1999). This new perspective was termed the Perceptual-Mnemonic Feature Conjunction model (PMFC) of PRC function, and was an important precursor to the representational accounts outlined below. According to PMFC, the PRC is important for high-level object perception because it affords the representation of complex conjunctions of stimulus features, and important for object memory because it also maintains these complex representations. If this framework is correct, then the complex conjunctive representations that are normally instantiated in PRC should enable a subject to resolve 'feature ambiguity', which arises when stimuli are presented which share similar individual stimulus features, and which can only be identified by processing of their unique conjunctions of these features. For example, although an individual feature (e.g. wheels) may not be diagnostic of a target stimulus (e.g. a plane) because it also occurs in other distractor stimuli (e.g. a car), the conjunction of this feature with another feature (e.g. wings) may be unique to the target item. The ability to form and maintain conjunctive representations in the PRC may therefore be key to performance in memory and perception tasks in which the stimulus set contains multiple exemplars with overlapping features, combinations of which have to be processed in order to successfully distinguish distinct exemplars.

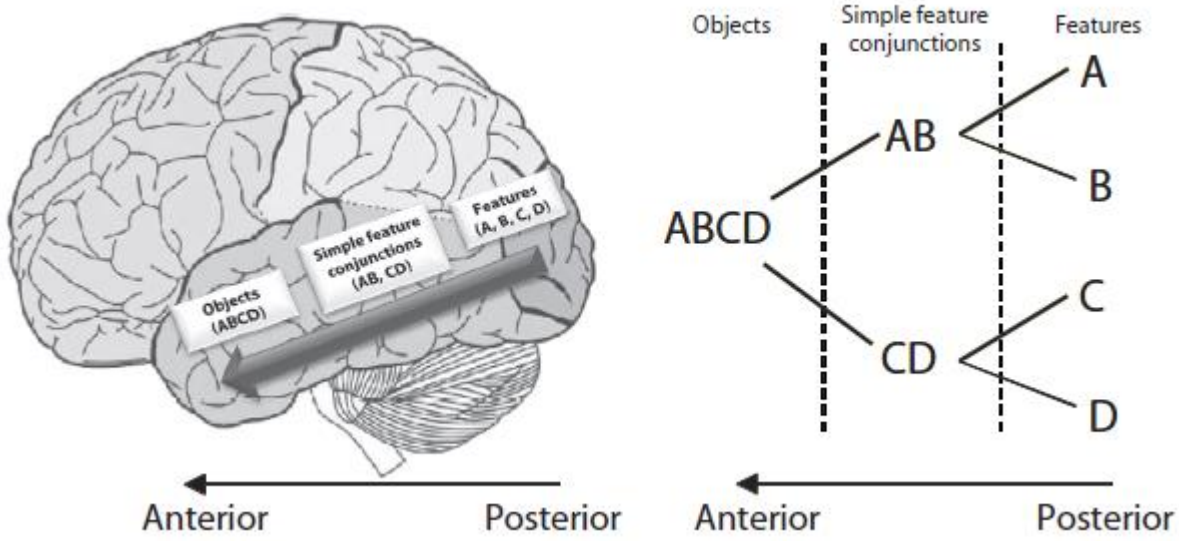

Fig 1.11. Illustration highlighting that the anterior regions of the VVS process more complex feature-conjunctions relative to more posterior regions (left), and a schematic diagram highlighting how representations of feature-conjunctions may be combined at each level of this hierarchy (right). A, B, C, and D refer to the simple stimulus features represented in more posterior VVS regions. As the PRC is proposed to sit at the apex of the VVS, it would house the most complex conjunctive representations of visual objects. Figure adapted from Barense et al., (2012).

1.4.2. The PRC and concurrent visual discrimination

A number of approaches have been developed to create stimuli that can be used to investigate the role of the PRC in resolving feature ambiguity. Each approach involves systematically varying the extent to which target and distractor stimuli share overlapping features. These include: a) morphing together prototype stimuli so that there is a variable degree of feature overlap across the resulting target and distractor stimuli (Bussey et al., 2003), and b) systematically controlling the presence/absence of specific features across target and distractor stimuli (Bussey et al., 2002).

PRC lesions have been found to impair performance in single-pair discrimination learning tasks involving pairs of visually similar, morphed stimuli. Bussey et al., (2003), morphed together pairs of prototype clipart images (e.g. flowers) to create pairs of test stimuli to be discriminated by monkeys with PRC lesions in exchange for a food reward. By varying the amount of morphing applied to the original prototype stimuli,

they were able to create a low ambiguity condition in which the target and distractor stimuli were visually distinct, and a high ambiguity condition in which the target and distractor stimuli had a high degree of feature overlap, and were thus less visually distinct. The lesioned animals were only impaired in acquiring discriminations between concurrently presented visual stimuli in the high ambiguity condition.

In another study, Bussey et al., (2002) specifically tested the proposal that the putative conjunctive representations of the PRC enable subjects to resolve feature ambiguity, by training monkeys with PRC lesions to discriminate pairs of visual stimuli over a number of repetitions. The stimuli were created by combining eight greyscale images of individual objects (ABCDEFGH) into stimulus pairs, and using these to create three conditions; minimum ambiguity, in which no individual features were shared across the rewarded/unrewarded stimuli (i.e. AB+, CD+, EF-, GH-); intermediate ambiguity, in which half of the stimulus features was shared across the rewarded/unrewarded stimuli (i.e. AB+, CD+, CE-, AF-); and maximum ambiguity, where all features occurred in both rewarded/unrewarded stimuli (i.e. AB+, CD+, AC-, BD-) (Fig 1.12). With greater ambiguity, this task places increasing demand on the ability to process *conjunctions* of features in order to correctly identify the rewarded items. Consistent with their predictions, monkeys with PRC lesions demonstrated preserved performance in the minimum ambiguity condition of the task. They were, however, impaired in both the intermediate and maximum ambiguity conditions, making significantly more errors-to-criterion relative to healthy controls. Monkeys with HC lesions are, by comparison, unimpaired on these tasks (Saksida et al., 2006). These findings are consistent with the proposal that the PRC plays a role in representing the feature-conjunctions that comprise target versus distractor stimuli, and that the integrity of this structure is therefore critical for ‘high ambiguity’ discrimination tasks.

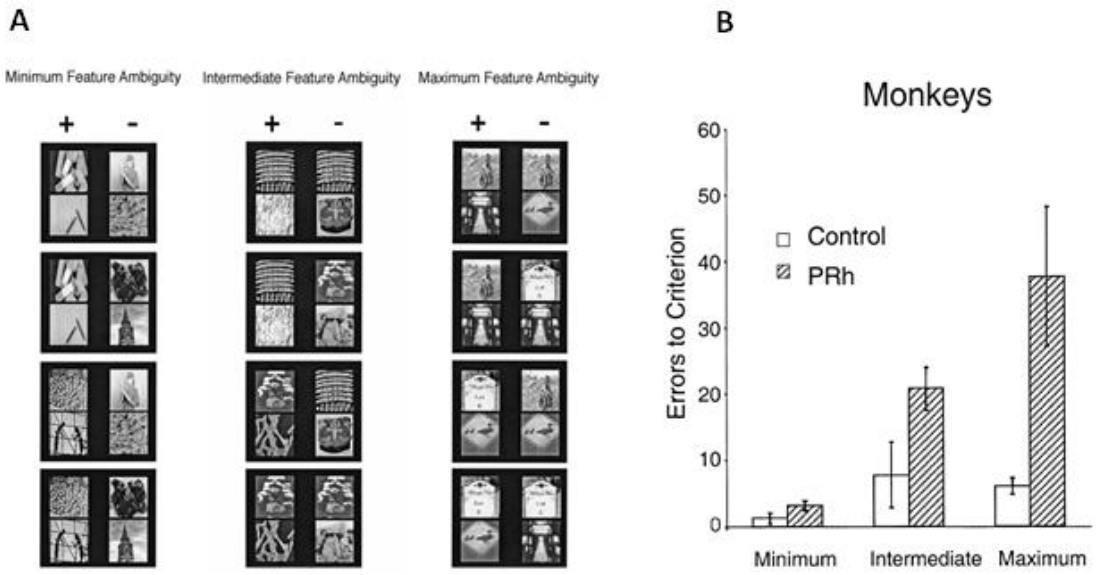

Fig 1.12. (A) Example stimuli from the minimum, intermediate, and maximum ambiguity conditions in the Bussey et al., (2002) study, and (B) the performance of monkeys with PRC lesions (PRh) relative to that of controls. Monkeys were required to learn to distinguish the rewarded stimulus (+) from the distractor stimuli (-). The feature ambiguity of these problems was manipulated by systematically varying the extent to which individual stimulus features were present in both rewarded and unrewarded stimuli. Figure adapted from Bussey et al., (2002).

PRC contributions to visual perception have also been assessed in patients with MTL lesions. Patients with focal PRC lesions are extremely rare, so researchers have frequently used a subtraction approach to investigate PRC versus HC function. In studies that use this approach, the performance of patients with focal HC lesions (Fig 1.13*A*) and those with more extensive MTL lesions that incorporate both HC and PRC (Fig 1.13*B*) are compared. Any behavioural deficits, relative to healthy controls, that are present in both the HC and MTL patient groups, are attributed to the HC damage that is shared across both groups. Any additional impairment in the MTL group is then attributed to the extra PRC damage that is present in this group alone.

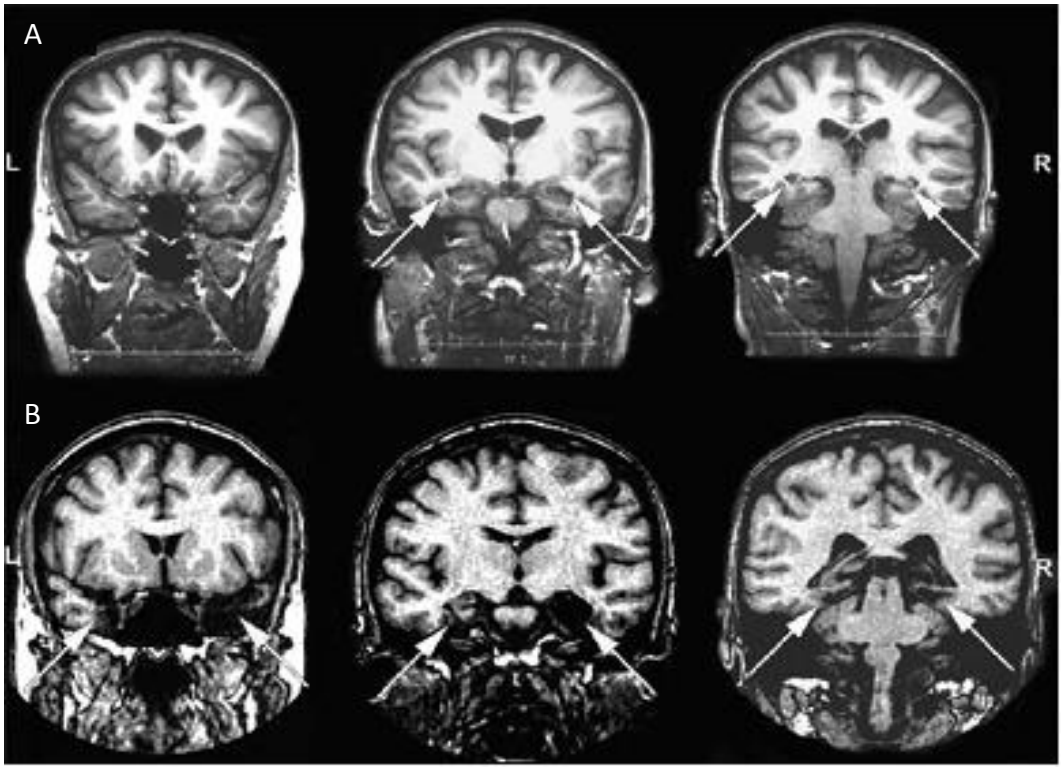

Fig 1.13. Three coronal MRI scans for (A) a patient with circumscribed HC damage, and (B) a patient with more diffuse MTL damage that incorporates PRC as well as the HC. Arrows indicate regions of significant damage. Figure adapted from Barense et al., (2005).

For instance, a modified version of the 'ambiguous' concurrent visual discrimination paradigm introduced above, was also administered to patients with focal HC lesions, and a group of patients with more diffuse MTL lesions encompassing both the PRC and HC (Barense et al., 2005). Four new categories of stimuli were created for this experiment, including barcodes, blobs, bugs, and beasts. For each stimulus category, feature ambiguity was systematically manipulated by varying the extent to which individual stimulus features were shared across the target and distractor stimuli, to create a minimum, intermediate, and a maximum ambiguity condition (e.g., 'Bug' stimuli; Fig 1.14*A*). As with the macaque monkeys in Bussey et al., (2002), patients with focal HC lesions were unimpaired in this task at all levels of feature ambiguity, for all 4 categories of stimuli, whereas those with more diffuse MTL lesions were impaired in both the intermediate and maximum ambiguity conditions (Fig 1.14B). Importantly, the number of discriminations to-be-acquired was the same in all conditions, highlighting that impaired performance was related to the increase in feature ambiguity, and not to potential differences in memory load across these conditions. This translational approach, across both nonhuman primates and humans, offers strong

support for a contribution of the PRC to representing complex feature-conjunctions in primates.

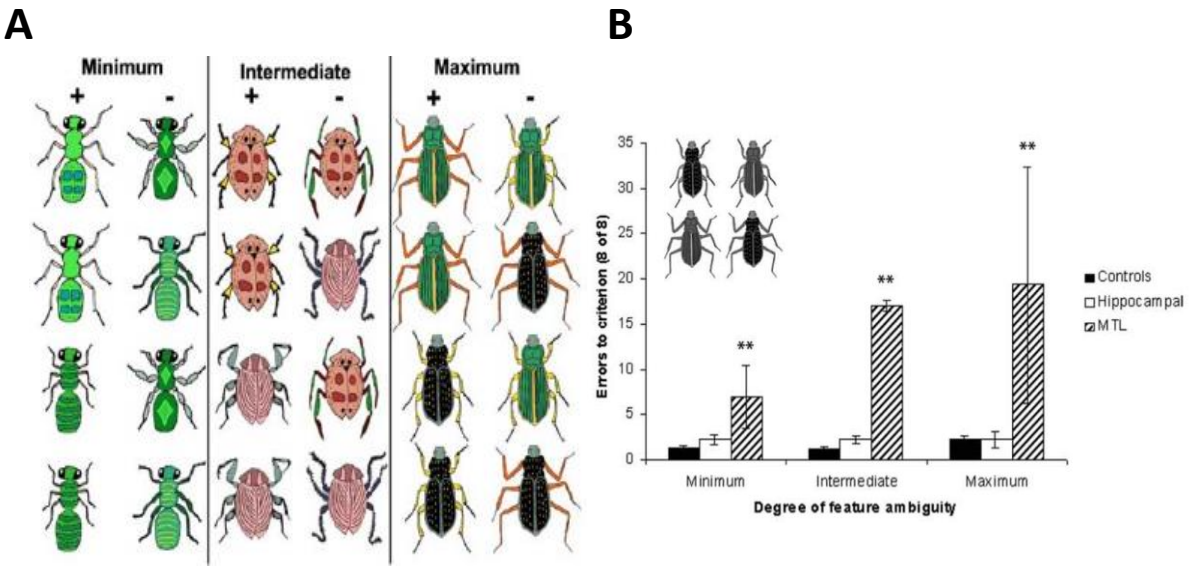

Fig 1.14. (A) Example 'Bug' stimuli from the minimum, intermediate, and maximum ambiguity conditions administered by Barense et al., (2005), along with (B) the mean errors to criterion (8 consecutive correct responses) for patients with HC pathology (white bars), patients with more diffuse MTL pathology (striped bars), and healthy controls (black bars). Error bars indicate SEM. ** $p < 0.01$ (MTL group versus control). Figure adapted from Barense et al., (2005).

That these paradigms were originally developed in animals does, however, pose a problem of interpretation. Animals need extensive training in order to acquire concurrent visual discriminations. This paradigm, therefore, may not represent a means of assessing process-pure perceptual discrimination, because prior learning about a given set of stimuli may make a contribution to subsequent discrimination judgements (Kim et al., 2011). Hampton (2005) has also argued that increasing the ambiguity of a discrimination problem increases the number of feature-conjunctions that the subject has to commit to working memory in order to make a correct judgement on a subsequent test trial. More ambiguous discrimination problems may, therefore, simply exceed the working memory capacity of patient groups. Indeed, Knutson et al., (2012) recently administered a discrimination paradigm to patients with focal HC damage, and a single individual with additional PRC pathology. The participants had to identify the

unique object from an array of twin-pairs of perceptually similar objects. These stimuli were presented to participants at 8 levels of increasing difficulty, which was manipulated by increasing the number of stimuli within a trial, and the number of individual features to be processed within each of these stimuli. These stimulus manipulations were designed to vary memory load, rather than a perceptual property of the stimuli. The authors reported that both patient groups were impaired in the most difficult task conditions, and consequently argued that: a) impairments in these perceptual tasks are due to deficits in working memory capacity, and b) that the HC is involved in processing object as well as spatial features/stimuli. Notably, however, the stimuli in the most difficult conditions of this task were not only made more confusable by increasing the gross number of stimulus features, but also by manipulating the size, shape, and orientation of these features. Given that the HC network has previously been implicated in processing spatial stimulus features (e.g. Buckley et al., 2004; see section 1.5.), the behavioural impairments of both patient groups in the high-difficulty conditions of this task could also be attributed to perceptual impairments in processing these spatial feature-discrepancies.

Evidence for the involvement of PRC, but not HC, in higher-level object perception was augmented by the findings of Lee et al., (2005a), who administered a visual discrimination paradigm involving trial-unique pairs of faces, objects, scenes, and colour stimuli to patients with focal HC and broader MTL lesions. In each of these conditions, participants were required to judge which of two trial-unique stimuli was most similar to a target stimulus. Trial-unique stimulus pairs were created by morphing two prototype images together (one of which was the target stimulus) so that the resulting pairs of test-images contained a different blend of features from each original item (e.g., face 1 and 2: 0-9%, 10-19%, 20-29%, 30-39%, and 40-49%). On some trials, the pairs were, therefore, easy to discriminate on the basis of individual stimulus features (i.e. low feature overlap trials), whereas in others, the pairs were more challenging based on a high degree of feature overlap. Both patient groups performed at levels comparable to controls in a control colour discrimination condition, but were impaired for high feature-overlap scene stimuli, even in a version of the task where the original target stimulus was presented above the test stimuli. Only in the patients with diffuse MTL lesions was there evidence of difficulties with face/object discrimination impairments, which, again, were related to the degree of feature overlap. Notably, the MTL lesion group was more consistently impaired in the face than the object condition. This pattern of findings is consistent with differential roles for the HC in high-level spatial discrimination, and the PRC in high-level discrimination of non-spatial stimulus

categories like faces and objects, particularly when feature ambiguity or overlap is stressed. It also suggests that face stimuli are more sensitive to PRC lesions than are objects, perhaps because faces inherently possess a high degree of feature overlap/ambiguity (i.e. all faces contain similar features), and so the discrimination of face stimuli is naturally more dependent on the complex representations in PRC.

This study was criticised based on the fact that all of the test stimuli for a given condition were generated from the same prototype target stimuli, so that stimulus-related learning could still have made some contribution to overall performance measures; whilst controls may have benefited from such learning, the patients might not, leading to the discrepancies evident in performance across these groups. Indeed, Shrager et al., (2006) administered a similar object and face discrimination paradigm, but with trial-unique prototype stimuli, to HC patients, MTL patients, and healthy controls, and found that performance was not significantly different across these groups. The stimuli used by Shrager et al., (2006) were, however, easily discriminable on the basis of individual stimulus features and were therefore unlikely to challenge conjunctive processing (Graham et al., 2010). Further, the performance of both the patient and control groups in the original Lee et al., (2005a) study did not improve over the course of the task, suggesting that the category-sensitive patterns of perceptual impairment cannot in fact be easily attributed to the inability of the patient groups to benefit from learning mechanisms available to controls.

1.4.3. The PRC and visual oddity judgements

To tackle these criticisms, researchers also investigated higher-level perception using stimulus oddity paradigms. In oddity tasks, an individual must identify the incongruent stimulus from an array of concurrently presented visually similar stimuli (i.e. the 'odd-one-out'). Buckley et al., (2001) administered an oddity paradigm to monkeys with PRC lesions, in which the animals were required to make odd-one-out judgements based on simple stimulus features (e.g. size, shape, and colour) or more complex stimuli that encourage the processing of more complex feature-conjunctions (faces, objects, and scenes). There were several levels of discrimination difficulty for each of the 'simple features' conditions. Within each trial of the object and face oddity conditions, the distractor stimuli could be presented from either the same viewpoint, or from different viewpoints (the latter placing greater demands on the ability to process the target and the distractor images at the object-level). Within each trial involving scene stimuli, a single view of a target scene that was populated by several foreground objects was

presented among multiple identical images of another scene containing foreground objects. PRC lesions did not impair the discrimination of simple stimulus features, even at the highest difficulty levels, but did impair discrimination of objects and faces when the test stimuli were presented from different viewpoints. These findings imply that PRC supports flexible view-invariant representations of complex object-like stimuli, which, unlike the viewpoint-specific representations instantiated throughout the EVC, enable control subjects to recognise multiple different-view images of an object as corresponding to the same stimulus. PRC lesions in the monkeys also impaired scene-oddity, but this is most likely explained by a difficulty in distinguishing the discrepant objects across the target/distractor stimuli, rather than being driven by spatial processing impairments *per se*.

As discussed for the concurrent visual discrimination paradigms, in order to perform these oddity judgement tasks, monkeys were pre-trained which means that, although there was evidence of preservation and impairment for simple and complex stimuli, respectively, the deficits could be due to difficulties with learning rather than perception. The translation of this paradigm into patients with MTL pathology, however, has enabled some traction on this issue, in particular via the use of trial-unique stimuli. In Experiment 2 of Lee et al., (2005b), patients with MTL pathology were given an oddity paradigm involving trial-unique face and scene stimuli (Fig 1.15*A*-*D*). Again, the distractor stimuli could be presented from either the same, or from different viewpoints. In this task, scene stimuli were computer-generated rooms without objects, which had the added benefit of removing the possibility that the target/distractor items could be distinguished on the basis of the presence/absence of any foreground objects; a strategy that could be adopted by healthy subjects to solve the scene oddity task originally reported by Buckley et al., (2001). Patients with selective HC pathology demonstrated preserved performance in both the same and different-view face-oddity conditions and the same-view scene-oddity condition of this task (Fig 1.15*E*). They were, however, significantly impaired in the different-view scene-oddity condition. Patients with both HC *and* additional PRC pathology presented with preserved same-view oddity performance for both faces and scenes, but were impaired in both different-view face and scene conditions. This study provided some of the most compelling evidence to date that the PRC contributes to high-level process-pure perception of complex, visually similar object-like stimuli, particularly for view-invariant representations of such stimuli. The different-view scene-oddity impairments of the HC patients highlighted an additional key role for the HC in trial-unique scene perception,

particularly in tasks that place demands on the ability to form view-invariant representations of complex visual scenes.

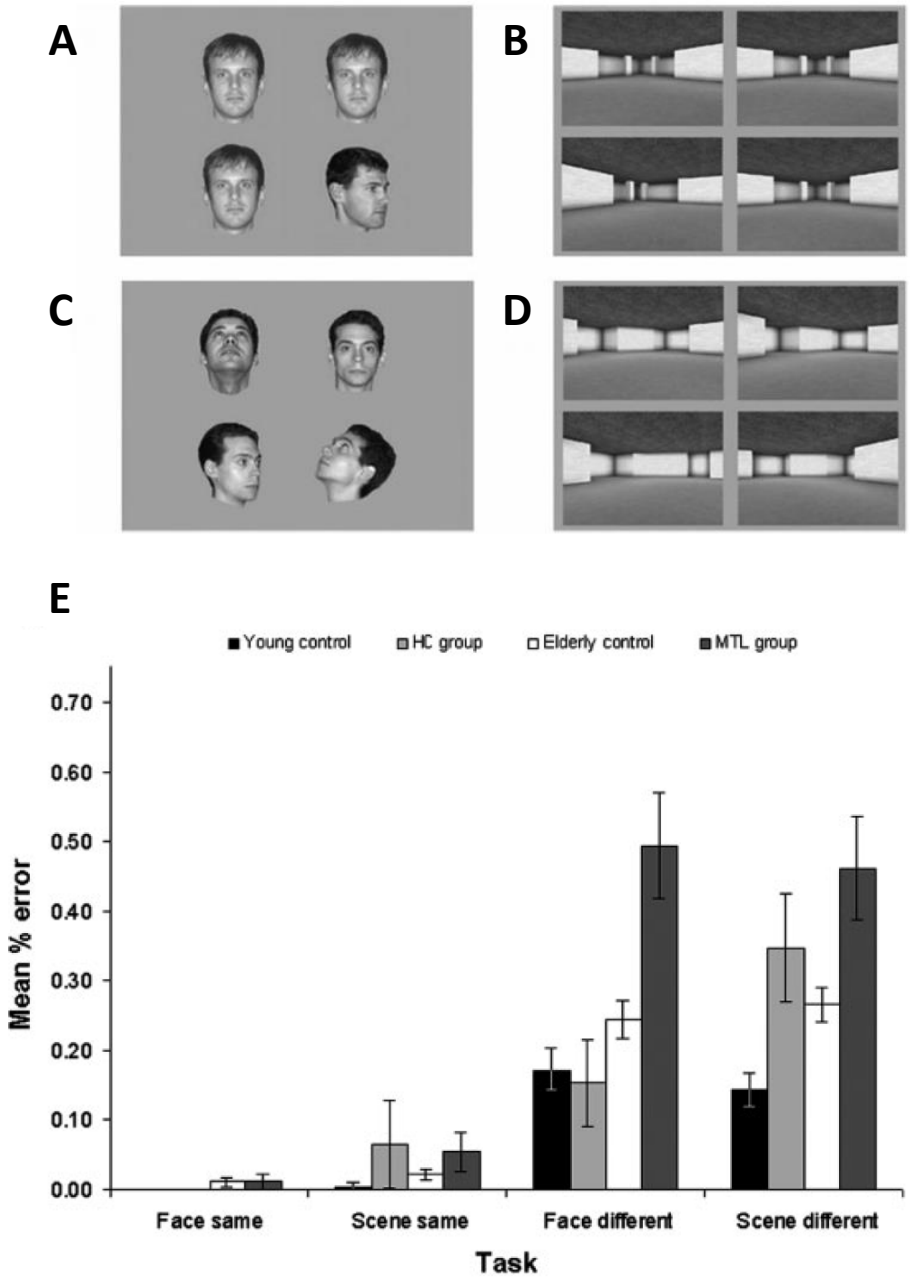

Fig 1.15. Trial-unique face and scene oddity trials from Lee et al., (2005b). Conditions included: (A) same-view face, (B) same-view scene, (C) different-view face, and (D) different-view scene oddity. (E) Performance of each participant group in each oddity condition as measured by mean % error. Figure adapted from Lee et al., (2005b).

The concern that deficits in perceptual discrimination tasks after MTL damage may actually be due to poor stimulus-related learning or working memory was further countered by evidence that patients with lesions including the PRC are also impaired on judgements of the structural coherency of individual object drawings. Lee & Rudebeck (2010) administered a same/different concurrent object discrimination task to a patient with bilateral HC lesions, and a patient with broader MTL damage that included PRC. The patients also undertook an additional task in which they were required to indicate whether trial-unique object images were either 'possible', or, like the well-known Penrose stairs, geometrically 'impossible'. Both patients were unimpaired in the concurrent discrimination task, which could be solved relatively easily based on the presence/absence of individual features across the two stimuli presented in each trial. The patient with PRC damage (but not the individual with HC injury), did, however, demonstrate significant behavioural impairments in the possible/impossible judgement task. The pattern of eye movements during this latter task was also analysed, revealing that the MTL patient with PRC damage spent significantly less time fixating on the geometrically impossible region of the 'impossible' objects in this task compared to controls. The patient with focal HC damage also spent significantly less time fixating on the impossible regions of the impossible objects, but unlike the PRC patient, did not demonstrate concomitant behavioural impairments. A further innovation in this study was administration of a face/object/scene functional localiser task whilst the patients underwent an fMRI scan. This was a working-memory paradigm in which the patients were required to press a response key whenever they detected two consecutive presentations of the same face/object/scene, during blocks of sequentially presented images from these visual categories. By contrasting the BOLD response across the whole brain to the face, object, and scene images during this task, the researchers were able to confirm that there were category-selective responses in the FFA, LOC, and PPA of both patients. This finding indicates that any behavioural impairment in the main experimental tasks is unlikely to be due to additional damage to the non-MTL 'perception areas'. Together, these studies provide strong evidence in favour of a role for the PRC in trial-unique perception for individual objects, a finding that is hard to reconcile with a memory system account of MTL function.

1.4.4. Complementary fMRI evidence for PRC contributions to object perception in healthy participants

Numerous complementary fMRI studies have been reported, in which the differential contribution of the HC and PRC to perception for scenes and faces, respectively, has been investigated. Devlin and Price (2007) investigated the contribution of the PRC to oddity judgements for single features (e.g. colour and shape) and to both easy and difficult object-oddity judgements (operationalised by presenting the object stimuli from either the same or different viewpoints, respectively). They found bilateral activation in the PRC (relative to baseline) during this task, but only during the complex, different-view object oddity condition. This was interpreted to indicate that individual stimulus features are integrated at the level of the PRC to form flexible view-invariant object representations that can support higher-level perception.

In a related study, Lee et al., (2008) administered the trial-unique different-view face, and scene oddity tasks from Experiment 2 of Lee et al., (2005b), along with an additional size-oddity condition to healthy participants whilst they underwent fMRI scanning. The BOLD response in the HC and PHC was found to be enhanced during scene relative to size and face oddity trials, whereas the PRC BOLD response was greater during face, compared to size and scene oddity trials. As stimuli were repeated across trials, the researchers also examined the potential effect of subsequent trial-repetitions on activation within PRC, HC, and PHC. The BOLD response in the posterior HC and PHC was found to be attenuated by stimulus repetition (indicating that these regions treated the stimuli as 'familiar'), this was not the case for the anterior HC and the PRC. This lack of a repetition-suppression effect in PRC is consistent with an additional role for this structure in face perception, outside the mnemonic domain. In contrast, the attenuated BOLD response of the posterior HC to repeated presentation of scene oddity trials is compatible with a role for this ROI in spatial perception, but also highlights its contribution to scene memory encoding.

The fMRI studies cited above were the first to provide compelling evidence that MTL regions including the PRC and the HC are engaged during higher-level perceptual tasks. The reader will note that it is difficult to conclusively rule out the possibility that MTL activations detected during these tasks may in fact be due to the incidental engagement of memory encoding processes. A study by O'Neil et al., (2009), however, provided evidence that this is not necessarily the case. Participants were administered a face oddity task, as well as the retrieval phase of an orthogonal face recognition task, whilst they underwent an fMRI scan; the study phase for the recognition task was

conducted prior to scanning. When behavioural performance was matched between these two tasks, the authors found comparable levels of activation in the PRC across both tasks. Further, activity in the right PRC was found to be predictive of accurate performance in both perception and memory. Considered together, these findings demonstrate that the PRC can make a performance-related contribution to perceptual, as well declarative memory tasks, and that increased mnemonic demand does not necessarily result in greater PRC engagement.

Going beyond oddity paradigms, Mundy et al., (2012) presented participants with blocks of visually similar or visually distinct face, animate object, inanimate object and scene exemplars. Participants performed a temporal duration-detection task whilst these items were presented, pressing a response button whenever an exemplar was presented for slightly longer (500ms) than the majority of the other items in the block (300ms). This task was adopted to separate the task requirements (temporal detection) from the experimental manipulation (different levels of perceptual similarity). Any activity elicited in the PRC/HC whilst participants performed this task would therefore be independent of any explicit mnemonic *or* perceptual demands. The results were striking; activity in the bilateral PRC was greater for animate/inanimate objects and faces compared to scenes, whereas the HC responded preferentially to scenes compared to faces and objects. As with the other studies reviewed above, this finding suggests a preferential role for the PRC and HC in perception for faces/objects and scenes, respectively. Interestingly, the authors also found that within the 'preferred' stimulus category of each of these MTL regions, greater activity was elicited by the visually *similar*, compared to the visually *distinct* blocks of stimuli. The effect of both stimulus category and feature overlap upon the BOLD response in the FFA, LOC, and PPA was also examined bilaterally. Consistent with their a priori predictions, these EVC ROIs also responded maximally to stimuli of their 'preferred' type (FFA = faces, LOC = animate/inanimate objects, PPA = scenes), but in contrast to their counterpart regions in the MTL, these EVC ROIs responded preferentially to blocks of visually *distinct*, relative to blocks of visually *similar* exemplars. The differential patterns of activation across the EVC and MTL during this task is consistent with a role for the former in the construction and maintenance of perceptual representations of individual stimulus features that are sufficient to support the discrimination of visually distinct stimuli, but lack the prerequisite conjunctive complexity to distinguish between visually similar exemplars. By contrast, that the MTL regions responded preferentially to blocks of visually similar stimuli is consistent with a role for these more anterior brain regions in

supporting the kind of complex feature-conjunction representations that can be recruited to distinguish complex stimuli with overlapping features.

1.4.4. The HC and spatial processing

The neuropsychological and neuroimaging findings reviewed in the previous section challenge memory system accounts of MTL function in favour of the PMFC model of the representations supported by the PRC. They also produced evidence, however, for HC contributions to scene perception which is not accounted for by the PMFC model. Before introducing recent representational accounts of MTL function that *can* accommodate findings of both PRC and HC contributions to higher-level perception, I will now review previous lines of research that are consistent with a role for the HC in spatial processing generally.

HC contributions to spatial cognition have been evident since O'Keefe and Dostrovsky (1971) demonstrated neurons in the rat HC that fire selectively when the rat is in a particular spatial location. Nearby cells responded preferentially to other locations, so that across the HC, the entire spatial environment was encoded. Given the location-specific response profile of these neurons, they were termed 'Place Cells', and taken to indicate a critical role for the HC in spatial processing. Indeed, subsequent research has extended our understanding of these place cells, so that we now know that whilst they are sensitive to changes in the shape of the local environment, they are not sensitive to changes in the specific features in the environment (i.e. they are sensitive to 'spatial' but not 'object' features) (O'Keefe & Burgess, 1996; Cressant et al., 1997). The enhanced response of HC place-cells to a specific location can also endure for several weeks. One proposed function of the HC consistent with these findings is that the HC may continuously construct and maintain allocentric 'cognitive maps' of the subject's spatial environment able to support a variety of functions including spatial navigation and memory (O'Keefe and Nadel, 1978).

Consistent with this view, a number of early studies in animals demonstrated that spatial memory paradigms are especially sensitive to HC damage (e.g., the water maze task; Morris, 1981). In this task, animals (usually rats or mice) are placed in a circular pool of water, made opaque by adding milk or other suitable substances. The rat then has to swim around the pool to locate and climb onto a submerged platform, thus escaping from the water. The initial search pattern is necessarily random, but over repeated testing the rat typically demonstrates a reduced escape-latency, which is

taken to indicate that it has learnt the spatial location of the platform. Rats with HC lesions do not show improvements over repeated trials, however, suggestive of impairments in spatial memory (Morris et al., 1982).

One reason that HC pathology may be associated with episodic memory impairments in human amnesia, therefore, is that the patient is no longer able to encode or retrieve the spatial context of a given event, which is an important component of episodic memories (Burgess et al., 2002). Indeed, some authors have argued that the key role of the HC in cognition is related to spatial processing, and that the HC is therefore implicated in episodic memory "only to the extent that spatial information is needed for some kinds of memory" (Gaffan, 2001, pp9; also Maguire and Mullaly, 2013). Whilst some authors have argued that such interpretations of HC function are too simplistic (Squire and Cave, 1991), it is consistent with neuropsychological studies in which HC damage was reported to be associated with a disproportionate impact upon *spatial* memory tasks; Taylor et al., (2007) studied memory for faces and scenes in patients with focal HC damage and individuals with more diffuse MTL pathology that included the PRC. The patients provided pleasant/unpleasant judgements to these stimuli, prior to undertaking a subsequent memory test in which they were asked to distinguish the previously studied target stimulus from a novel, visually similar, distractor stimulus. Critically, the stimuli could either be presented from the same viewpoint as that encountered during the previous study phase, or they could be presented from a different viewpoint. Patients with broad MTL damage were impaired in both the face and scene memory tasks, whereas the performance of the HC patients in the face memory condition was comparable to that of controls. Performance in the different-view scene memory condition was significantly lower in the HC patients compared to controls, however, indicating impairments in allocentric scene memory over a delay.

Adding to this literature, Maguire and colleagues found that inter-individual variation in spatial navigation expertise was predictive of HC macrostructural properties. Maguire et al., (2000) compared structural MRI images of the HC in London taxi drivers (a group of individuals with extensive spatial navigation experience) with those of control subjects, and found that not only was the posterior HC of the taxi drivers larger relative to controls, but it's overall volume was also related to the length of time served as a taxi driver. Although it's difficult to determine the direction of causality in such correlational research designs (i.e. does taxi experience drive posterior HC volume, or does a larger posterior HC predispose individuals to enter occupations in which superior navigation ability is an advantage), it is interesting to note that the structural properties of the HC are associated with spatial navigation experience.

The ability to imagine new, spatially coherent scenes, is, however, not thought to be so dependent on spatial *memory*. It is therefore interesting that imagining fictitious scenes is associated with a comparable HC BOLD response in healthy participants, to that elicited by the recall of real scenes (Hassabis et al., 2007a); this suggests that the role of the HC in spatial processing extends beyond the declarative memory domain. Further studies have confirmed that patients with HC pathology have profound impairments in imagining new spatially coherent scenes (Hassabis et al., 2007b). FMRI research has also shown that HC activity during scene imagination is correlated with the number of boundaries constraining the scene (Bird et al., 2010). Similarly, Mullaly et al., (2012) presented HC patients with a picture of a scene and asked them to mentally extend this scene and report what it might look like. Whilst the patients could provide appropriate details for such a scene, they could not imagine it 'in their mind's eye', and their responses typically contained fewer spatial details compared to healthy controls (e.g. "on the left" or "above").

HC damage in humans has also been reported to impair numerous non-declarative forms of memory when the task or stimuli place demands on spatial processing. For example, HC damage impairs learning to categorize sets of visually similar scenes on the basis of perceived similarities and differences between individual exemplars, whereas categorization of other complex visual categories (e.g. faces) is preserved (Graham et al., 2006). Together, these findings suggest that spatial processing is a core HC function, and that this structure will contribute to any cognitive task that places a demand on spatial processing, regardless of whether or not the task explicitly challenges declarative memory (Maguire and Mullaly, 2013). Such a view is consistent with the findings reviewed in the previous section, in which HC damage is also associated with impairments in scene discrimination and 'odd-one-out' judgements in the context of preserved perception for faces and objects, whereas PRC damage impairs the face/object perception in these same tasks but spares spatial perception.

The oddity paradigms that were administered to healthy participants whilst they underwent fMRI scans also highlight that the HC is activated during scene perception (Lee et al., 2008). Again, proponents of 'memory system' accounts of MTL function might argue that these activations could reflect incidental memory encoding rather than perceptual processing. Recently, however, Lee et al., (2013) used fMRI to scan neurologically healthy participants whilst they performed a scene oddity task that did not include any explicit memory demands. A subsequent surprise memory test was undertaken outside the scanner. The conjunction of these two tasks meant that each scanned oddity trial could be categorised according to both oddity accuracy, and

success in the subsequent recognition task. This afforded an investigation of whether HC activity during scene oddity is related to perceptual processing, or whether it simply reflects incidental memory encoding for the scene stimuli. If the former were the case, then we would expect HC activity to be predictive of oddity performance, but if the latter were the case, then we would expect that HC activity could *only* be predictive of subsequent memory success. The analyses revealed several clusters of voxels in the HC (one in the left anterior HC, and one in each of the right anterior and right posterior HC), in which activity was significantly greater during correct relative to incorrect oddity trials. Importantly, this difference was not related to whether or not the trials were subsequently remembered successfully (i.e. HC activity was predictive of perceptual performance even if the stimuli were subsequently forgotten). This shows that perceptual processing demands are sufficient to elicit HC activity, and that this activity is not necessarily related to subsequent memory success.

1.5: Representational accounts of memory and perception

The novel proposal of the PMFC model of PRC function was that the gradient of representational complexity that exists along the VVS does not end at area TE, but continues into the PRC where the feature-conjunctions that comprise individual objects are represented at an exquisite level of complexity (Bussey et al., 2002). The literature reviewed above, however, indicates an additional role for the HC in scene perception. Researchers were therefore prompted to extend the PMFC model to account for the contributions of the PRC and HC to object and scene perception, respectively.

1.5.1. The representational hierarchical account

The outcome of this model-extension was the representational-hierarchical account of MTL function (Saksida and Bussey, 2010; see also Bussey and Saksida, 2005). This account retains the core features of the PMFC model in regards to the role of the PRC in processing visual objects. Thus, the PRC is proposed to represent an anterior component of the VVS, constructing and maintaining complex conjunctive representations of object stimuli, in contrast to the more posterior regions of the VVS representing individual stimulus features. PRC damage is therefore anticipated to impair the discrimination of object stimuli that share multiple visual features, because this depends on processing of feature-conjunctions, but spares the ability to distinguish

stimuli that are visually distinct, because this could be achieved on the basis of the simple representations in posterior VVS regions. Like the PMFC model, the representational-hierarchical account can accommodate previous findings implicating the PRC in visual discrimination and oddity judgements for face/object stimuli with overlapping features.

The representational-hierarchical account proposes that the putative role of the PRC in resolving feature ambiguity in a perceptual context, can also account for the delayed object *recognition* impairments associated with MTL amnesia. The argument is that by supporting conjunctive representations that are each unique to a specific target object, the PRC effectively buffers recognition memory judgements against interference from distractor stimuli that share individual features with the target item, but not the full set of feature-conjunctions diagnostic of that particular target. In a forced-choice recognition paradigm incorporating a minimal exposure-test delay for example, the PRC of healthy subjects can construct and maintain a complex conjunctive stimulus representation of a target item comprised of features A, B, C, and D. In a subsequent test phase, the target item (ABCD) may share a number of individual features with a visually similar distractor stimulus (ABEF). Whilst several features of both the target and distractor stimulus will be familiar to the subject, the conjunction of features unique to the distractor stimulus will not be as familiar as that of the target stimulus. The representational complexity supported by the PRC therefore enables the subject to correctly distinguish the old/novel stimuli on the basis of the differential familiarity of the conjunction of features that is unique to the target stimulus, even if these items are difficult to distinguish on the basis of their individual features.

The suggestion that the PRC buffers against interference is also consistent with the findings of Bartko et al., (2007) who administered a spontaneous object-recognition task to rats with and without lesions of the PRC. In a given trial of this task, animals were exposed to two compound stimuli, BC and AD, in two separate sample phases, so that all four of features A, B, C, and D, would be familiar to the animal in a subsequent choice phase. In the choice phase, the animal was presented with one of the original sample stimuli (BC), and a new compound stimulus that comprised a novel conjunction of individually familiar stimulus features (e.g. stimulus AB). To perform this task properly, the animal was required to choose the novel compound stimulus in the choice phase. Given that all of the features presented in the choice phase, across both the pre-exposed and novel stimuli, are equally familiar, the novel stimulus could not be determined on the basis of representations of individual stimulus features; this could only be achieved via the novel conjunction of features A and B. Rats with PRC lesions

were impaired in this task relative to controls, whereas they were unimpaired in another condition in which the novel item could be identified successfully on the basis of individual feature representations.

The above study demonstrates that the integrity of the PRC is important for visual recognition memory across a minimal delay but also the severe delay-dependent recognition memory impairments characterising MTL amnesia. Here, the argument is that during a stimulus exposure-test interval, a subject may experience multiple visual stimuli, both real and imagined, which will each possess features that are common to many items (e.g. line orientations or colour). Such features will therefore become highly familiar prior to a subsequent test phase likely to contain stimuli that possess these simple stimulus features. Even if the item is a distractor or foil stimulus, it could therefore be judged to be familiar on the basis of an individual stimulus feature. In this sense, the item possesses feature ambiguity, and cannot be distinguished from the pre-exposed item on the basis of low-level representations of individual stimulus features in posterior VVS; the ambiguity can only be resolved on the basis of the complex conjunctive representations in the PRC. As Saksida and Bussey (2010, pp2379) note: “This feature-ambiguity based mechanism for producing a delay-dependent deficit is effectively an interference account of amnesia: perirhinal cortex damage compromises object-level conjunctive representations, leaving the subject susceptible to interference from incidental lower-level visual information”. Indeed, recent studies have confirmed that rats with PRC lesions are impaired at object recognition when interfering stimuli are presented after or even before the original sample stimulus (Bartko et al., 2010).

That the PRC may buffer recognition memory against the effects of perceptual interference has also recently been tested in fMRI with healthy human participants. Watson and Lee (2012) administered a novel interference match-to-sample task to participants while they underwent an fMRI scan. Each trial of this task involved a study phase, an interference phase, and a test phase; in all conditions, the stimuli were individual objects superimposed over a virtual reality scene image. In the study phase, participants were exposed to one such object-scene compound image. In the interference phase that followed, the participant performed a 1-back working memory task whilst viewing several more object-scene images which were either: 1) images of the studied object and a background scene that differed slightly from the studied scene, or 2) images of the studied scene and a novel object that differed slightly to that of the studied stimulus. Participants were thus exposed to a period of object or spatial interference prior to the test phase, in which the participant had to distinguish the pre-

studied stimulus and reject a novel and visually similar distractor stimulus. Importantly, the distractor stimulus comprised either: 1) the studied object and a visually similar scene, or 2) the studied scene and a visually similar object. In the former case, the trial would challenge spatial memory, whereas in the latter, object memory would be stressed. This design enabled the authors to distinguish the effects of object and spatial interference upon PRC activity during object versus scene retrieval. They reported that PRC activity was greater during object recognition judgements that were preceded by a period of object interference, compared to that elicited by object recognition judgements preceded by a period of scene interference. PRC activity did not differ across scene recognition trials that were preceded by either object or spatial interference. These findings are consistent with a role for the PRC in buffering object recognition against the effects of object-level interference by resolving the feature ambiguity of target and distractor stimuli.

A role for the PRC in buffering against interference between object-like stimuli has also been demonstrated in patients with PRC pathology. Barense et al., (2012) recently developed a visual matching task in which participants were required to make a same/different judgement to two concurrently presented, trial-unique 'blob' stimuli. Each 'blob' was defined by three features: an inner shape, an outer shape, and a texture. Although each 'blob' was trial-unique, its constituent features were repeated across the stimulus set. Two levels of feature ambiguity were developed. In the low ambiguity condition, the two blobs in a given trial differed in terms of all 3 features (so a feature-based discrimination strategy would be sufficient to solve the problem), but in a high ambiguity condition, the blobs could only be distinguished on the basis of 1 discrepant feature (so a conjunction-based discrimination strategy was optimal). Consistent with previous findings, patients with PRC damage were impaired in the high but not the low ambiguity condition, relative to healthy controls and patients with circumscribed HC pathology. Importantly, the impairment was only observed in the PRC patient group in the second half of the paradigm. This latter finding suggests that patients with PRC pathology were unable to buffer their later object-level discrimination judgements against a build-up in feature-ambiguity that had occurred over the course of previous trials as a result of the individual blob features recurring across the stimulus set. Indeed, when the 'high ambiguity' trials were interspersed with trials that involved discriminating visually dissimilar real-world objects that shared no features with the blob stimuli (thereby reducing the cross-trial build-up in blob feature-ambiguity), the PRC patients were no longer impaired. As stated by the authors, this novel approach offered the seemingly paradoxical but compelling conclusion "that intact memory for

irrelevant, lower-level features processed on previous trials can impair *perception* in cases with *memory* disorders" (Barense et al., 2012, pp161). This further undermines the notion of a MTL declarative memory system, in favour of representational accounts according to which PRC is critical for both object perception and memory.

The role of the PRC in resolving feature-ambiguity, as proposed by the representational-hierarchical account, therefore provides a common mechanism with which we can understand why PRC damage has an adverse impact upon memory and perception for visual objects. Importantly though, the representational hierarchical view also proposes a representational role for the HC in cognition.

1.5.2. The representational hierarchical account and the HC

The representational-hierarchical account proposes that the PRC offers a level of representational complexity that can resolve feature-level ambiguity, which exists whenever multiple object stimuli share rewarded features. One task that produces such feature ambiguity, in which rats with PRC lesions are known to be impaired, is object recognition involving trial-unique stimuli (Eacott et al., 1994). Saksida and Bussey (2010) argue, however, that object recognition tasks that involve repeated presentation of a specific set of items lead to a higher level of ambiguity, which they term "object ambiguity". This arises in such tasks because not only do the individual features comprising the target and distractor objects become increasingly familiar with successive presentations, but so too do the unique sets of feature-conjunctions comprising both the target and distractor objects. In this situation, the familiarity of the target object's feature-conjunctions is no longer diagnostic of being the rewarded item, because the feature-conjunctions comprising the distractor object have also become familiar. The object-level representations in the PRC lack the representational complexity to resolve *object* ambiguity, however, which must therefore be resolved at a level of the representational hierarchy that is higher than the PRC. Based on previous evidence that the HC is involved in the representation of complex information, including the "where" or "when" aspects of episodic memory (Maguire and Mullaly., 2013), Saksida and Bussey (2010) argue that spatial representations in the HC may offer the level of representational complexity required to resolve object-level visual ambiguity.

This notion is similar to an idea that Gaffan (1994) outlined within his proposal that the HC and other related structures support representations (or "snapshot memories") of visual scenes and the spatial arrangement of the objects within them. Gaffan argued

that memory for individual objects could be insufficient to support performance in object-learning tasks that take place within a given background scene, if the subject also encounters other visually similar objects in the context of different visual scenes. This is because the memories of the task-irrelevant non-target objects that occurred in other scenes could potentially interfere with the memory of the current target object. The memory of the scene in which the target was uniquely encountered could therefore be beneficial to such object-learning tasks because it would enable the subject to recognise that a given object is only ever rewarded when it is encountered within a specific place within a specific scene. In a sense, memory for the background scene helps resolve the object-ambiguity that is present in such tasks. Gaffan tested the idea that the extended HC network (section 1.1.3.) was involved in such scene-specific memory for objects by administering an object-in-place task to monkeys with, and without a fornix transection. In this task, the monkey was required to learn a series of background 'scene' and foreground 'objects, where the correct response to a given discrimination problem was to a particular object that always occupied a particular place within a unique background scene. Monkeys with fornix-transections were severely impaired in this task, relative to control animals.

These object-in-scene memory tasks are considered an effective model of the episodic memory impairments seen in patients with MTL amnesia than DNMS tasks, on the basis that the former challenge the ability to recognise a foreground object that is embedded in a specific scene, which is how humans experience most events. To the extent that we recollect an object, we tend to recall the scene in which it was encountered. Whilst successful performance in DNMS tasks may depend on the animal equivalent of human recognition memory, the retrieval of contextual details associated with a stimulus that is associated with human recollection, may be better challenged by object-in-place tasks. This also highlights that the differential impact of HC and PRC damage upon recollection and familiarity, respectively, may be explained by considering the type of representations instantiated in these structures (spatial and non-spatial, respectively), without the need to invoke different memory 'processes'.

There is also a substantial and growing body of evidence that the HC is involved in processing spatial stimulus features outside a declarative memory context in both humans and animals, as suggested by the representational-hierarchical view. Studies in humans that highlight impairments in making discrimination or oddity judgements to visually similar trial-unique scenes following HC damage have been reviewed above (Lee et al., 2005b), and these suggest that the high-level spatial representations of the

HC can also support spatial perception, but not perception of individual object-like stimuli which is dependent on PRC representations (see Lee et al., 2012).

Beyond this previously reviewed literature, Buckley et al., (2004) administered a concurrent visual discrimination learning paradigm to macaque monkeys. In this task, the monkeys were required to learn to discriminate between highly similar "tadpole" stimuli that were individually defined by a number of spatial variables (e.g. position on a screen, tail length, and tail orientation angle; Fig 1.16). The authors reported impaired performance in this task following fornix transection, suggesting that this lesion impacts on the higher-level spatial representations stored in the HC and needed to resolve the object-level ambiguity of the many tadpole stimuli in this task.

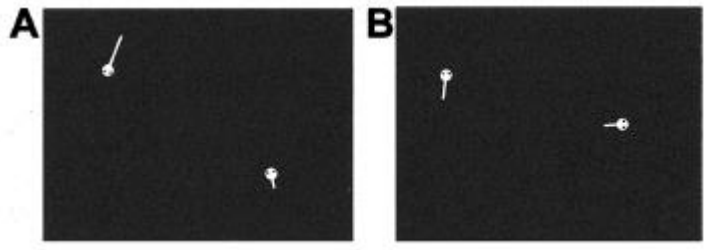

Fig 1.16. Two representative tadpole-discrimination problems administered to monkeys by Buckley et al., (2004). Figure adapted from Buckley et al., (2004).

Whilst this study focused on the role of the HC in *concurrent* spatial visual discrimination learning, recent evidence demonstrates an additional role in the discrimination of *consecutively* presented spatial stimuli in humans (computer generated rooms), along with a dissociable role for the PRC in discriminating consecutively presented non-spatial stimuli (faces). In a study by Mundy et al., (2013), patients with focal HC or broader MTL lesions incorporating the PRC were required to make same/different discrimination judgements to a number of rapidly and sequentially presented pairs of visually similar faces, scenes, and dot patterns. This type of discrimination-learning paradigm involves perceptual learning, a form of non-declarative memory that supports gradual improvements in discrimination speed/accuracy following exposure to stimuli, compared to when stimuli are completely novel. According to unitary accounts of MTL function, perceptual learning, like process-pure perception, is not critically dependent on the MTL 'declarative memory system' (Squire et al., 2004). Evidence in favour of this position was taken from studies in which

the performance of amnesic patients on a dot prototype learning paradigm was found to be comparable to controls (Knowlton and Squire, 1993). In Mundy et al., each trial involved presentation of a stimulus for 500ms, followed by a high-contrast visual noise mask for 300ms, and then a second (identical or different) stimulus for 500ms, after which the participant was able to make a same/different response. Like the previously reported data, neither of the two patients with MTL lesions showed deficits on the dot pattern condition, presumably because these stimuli possess simple stimulus attributes that can be represented in posterior VVS regions. Notably, however, the HC patient was unable to learn to discriminate between complex scenes, despite demonstrating unimpaired learning for faces. The patient with diffuse MTL pathology, including PRC, presented with both face and scene discrimination learning impairments. This study was important in bringing together findings from previous perceptual learning studies in amnesic individuals, whilst highlighting a critical role for the HC in high-level perceptual discrimination learning for scenes but not faces, and for the PRC in supporting high-level perceptual representations of faces. Further, these findings suggest that earlier studies on perceptual learning in amnesia may have failed to detect impaired perceptual learning in their MTL patients simply because they did not administer the complex stimulus categories of that are actually represented by MTL substructures.

Evidence that the HC supports spatial representations outside a mnemonic context also comes from Clelland et al., (2009), who trained rats to discriminate between locations on a computer screen that were spatially displaced from one another by a variable amount. Animals with damage to the dorsal HC, or impaired neurogenesis in the HC dentate gyrus, were impaired in this task when the locations were separated by a small distance, but were unimpaired when the locations were separated by an intermediate or large distance. The learning and memory demands were equivalent across the minimal, intermediate, and maximum separation conditions of this task, so the behavioural impairments could not be attributed to differences in mnemonic factors; the only difference was the perceptual similarity of the stimuli.

1.5.3. The Emergent Memory Account

That damage to the HC and PRC is associated with selective impairments in the processing of spatial and non-spatial stimuli, respectively, across a number of cognitive domains, in multiple species, and that these structure-behaviour dissociations are corroborated by the findings of numerous functional imaging studies, provides strong support to representational accounts of MTL function. From the representational

hierarchical perspectives, the critical factor which determines whether a given MTL region might contribute to task performance is not the kind of memory process challenged by the task, but the level of representational complexity required to solve the task. In this section, I consider the overlapping predictions of another representational account.

Like the representational-hierarchical view, the Emergent Memory Account (EMA, Graham et al., 2010) proposes that there is a gradient of increasingly complex, hierarchically-organised representations of visual stimulus features that are distributed along a posterior-anterior axis between early visual areas and the MTL. Importantly, the account proposes that representations along the full extent of this hierarchy can be recruited to support both memory and perception provided that they offer sufficient representational complexity to meet the current task demands (e.g. to resolve feature ambiguity). Accordingly, EMA makes several key predictions: 1) representations throughout the hierarchy can be recruited to support performance in both memory and perception tasks, 2) the factor driving MTL involvement is not the cognitive 'function' challenged by the task, but the extent to which the task challenges the ability to process conjunctions of features across visually similar stimuli, 3) the PRC and HC support complex conjunctive representations of objects/faces and scenes, respectively, and 4) diffuse damage to the MTL impairs both memory and high-level perception for faces/objects and scenes because these patients are no longer able to construct or retain distinct representations of visually similar exemplars from these categories. As with the representational-hierarchical account of MTL function, EMA therefore argues that the boundary that is commonly drawn between memory and perception, is largely based on a phenomenological distinction; we may experience memory and perception as distinct processes, but actually, they both depend upon the activation of the same set of distributed visual representations.

1.6: Questions addressed by the current Thesis

The predictions of the EMA have been broadly corroborated by the neuropsychological and neuroimaging research reviewed above. The reader will note, however, that, to date, studies aimed at testing these emerging representational models have typically focused on: a) how damage to individual MTL regions disproportionately affects higher-level visual perception for particular categories of stimuli, or b) the preferential

activation of these individual MTL sub-regions during perception for different stimulus categories. And yet both the EMA and the representational-hierarchical account explicitly propose that representations of complex stimuli are hierarchically distributed across both the EVC and the MTL; this prompts us to go beyond a focus on individual brain regions, and consider instead the role of broader *networks* in perception for distinct visual categories.

1.6.1. Distributed brain networks and visual processing

The important role of distributed networks in visual processing was recently discussed by Behrmann and Plaut (2013). These authors highlight that whilst previous research has identified several brain regions (e.g. FFA) that respond maximally to a particular stimulus category (faces), this does not indicate that these regions support the visual processing of their 'preferred' stimulus category independently of the rest of the brain (i.e. as highly specialised 'cognitive modules'). Indeed, as we have seen, multiple spatially distinct brain regions can be preferentially engaged by the same stimulus category (e.g. OFA, FFA, and PRC). This suggests that individual brain regions do not suffice for the successful visual processing of a given stimulus; rather, an extended multi-regional network is likely to underpin its successful processing. Furthermore, category-sensitive brain regions typically respond to 'non-preferred' as well as 'preferred' stimulus categories (section 1.2; Downing et al., 2006), so that the extended visual networks that subserve perception for two highly distinct visual categories, can in fact be partially integrated and overlapping. According to Behrmann and Plaut (2013), visual processing for a given category of stimuli does not, therefore, depend merely upon the activation profile of individual category-sensitive brain regions, but also upon successful interactions between multiple widely distributed brain regions that demonstrate graded sensitivities to different stimulus categories. From this perspective, "functional specialization is not simply an intrinsic property of individual regions that compute specific representations and/or computations in isolation, but, rather, is an emergent property of the interactions between a set of spatially distributed nodes and their functional and structural connections" (Behrmann and Plaut, 2013, pp211). The critical point here is that the task-related activity of individual category-sensitive ROI's in either the EVC or MTL are not the only important factors driving successful visual perception; their ability to interact is also relevant.

This point can be elucidated in the context of congenital prosopagnosia (CP): the face processing impairments associated with this condition need not necessarily be the result of damage to a specific face-processing region, such as the FFA, because CP can also occur in conjunction with normal face-selective activation patterns in this region (Avidan et al., 2005). The impairment could, alternatively, arise due to a failure to successfully propagate information about a face stimulus from the FFA to higher-level face processing regions in the temporal lobe, such as PRC (i.e. a 'disconnection' account of prosopagnosia; Berhmann and Plaut, 2013). Consistent with this view, studies have demonstrated that the functional connectivity (i.e. the statistical dependence of activity across distinct brain regions) of several core face processing regions is reduced in CP relative to controls (Avidan et al., 2014).

Further evidence for this relative 'disconnection' account of congenital prosopagnosia comes from studies using Diffusion Tensor Imaging (DTI) in conjunction with white-matter tractography techniques in order to reconstruct and quantify the white matter pathways that may facilitate communication between spatially distinct face processing regions, including the OFA, FFA, and PRC (e.g. the ILF; section 1.1.4.2). As DTI is employed in several Chapters here, I will briefly outline some of the basic principles before returning to show how it has been used to study the role of an extended network of regions in higher-level face processing.

DTI is a magnetic resonance imaging technique which exploits the diffusion properties of water molecules in the tissue of the living brain, in order to quantify and reconstruct in vivo the trajectories and microstructure of the white matter tracts that connect spatially distinct brain regions. In a DTI study, the researcher modifies MRI pulse-sequence parameters in order to sensitize the MR signal to the mean displacement of water molecules in the brain of a participant (Mori & Zhang, 2006). By applying a diffusion tensor model to the data, an estimate can then be derived at each voxel of the resulting image, of the direction "in which the diffusivity of the fitted tensor is greatest (i.e. the principle eigenvector)" (Jones, 2010). This eigenvector is assumed to reflect the orientation of an underlying white matter tract (Stieltjes et al., 2001), and is exploited by single tensor DTI-based tractography techniques to "produce voxel-wise maps of fiber orientation or integrated to form continuous trajectories" (Jones, 2010). This means that the three-dimensional trajectories of white matter connections can be reconstructed by tractography algorithms using the eigenvector maps that are calculated as part of the tensor framework. Tractography based on a single tensor

model of diffusion is known to be less successful in faithfully reproducing white matter pathways that pass through voxels containing multiple rather than a single fiber orientation/population (Jones et al., 2008). Recently, however, several approaches have been devised to improve the resolution of crossing fibers, including modelling diffusion within each voxel with multiple rather than a single diffusion tensor (Behrens et al., 2007), and extracting multiple fiber orientation peaks from an orientation density function at each voxel (Tournier et al., 2008). Tractography is limited by the available MRI voxel resolution, which is inherently coarse with respect to the spatial scales that are spanned by individual axons. Nevertheless, comparisons of white matter tracts that have been reconstructed using tractography with those found during post-mortem neuroanatomical dissections in humans, and tract-tracer studies in nonhuman primates, have demonstrated that tractography can provide accurate reconstructions of white matter tracts *in vivo* (Lawes et al., 2008; Stieltjes et al., 2001).

The diffusion tensor framework also produces several useful voxel-wise metrics. One such measure is the fractional anisotropy (FA) estimate – an index of the extent to which the diffusion of the water molecules within the voxel occurs predominantly along a single axis (Mori & Zhang, 2006). FA is measured on a scale of 0 to 1, with '0' indicating that diffusion is occurring freely in all directions (e.g. in cerebral spinal fluid; CSF), whereas a value of '1' indicates diffusion occurring predominantly along a single axis (e.g. along an axonal bundle). If a tractography algorithm has been used to reconstruct a tract, then FA can be averaged across all voxels contained in that tract-solution, to provide a tract-specific mean-FA measure. Importantly, FA is known to be modulated by a number of white matter microstructural properties that may influence the efficiency with which information can be propagated between spatially distinct brain regions, including axon myelination, diameter, density, and configuration (Jones et al., 2010). Another commonly reported diffusion MRI measure that is sensitive to these white matter properties is the mean diffusivity (MD); this metric indicates the average magnitude of water diffusion, and because it too is sensitive to variation in white matter properties like axon myelination and diameter, it is often reported alongside FA in the literature (Gschwind et al., 2012; Metzler-Baddeley et al., 2011).

Thomas et al., (2009) used a DTI-tractography protocol to extract FA from the ILF in cases of CP and control subjects. They found that ILF FA was reduced, bilaterally, in CP patients relative to controls, and that it was predictive of errors in a face recognition task. These findings suggest a role for the ILF in facilitating communication between spatially distinct regions involved in processing face stimuli, and are consistent with the notion that effective functional interactions within an extended network underpin

successful face processing. More generally, these findings illustrate how diffusion MRI techniques can be used to investigate the role of white matter pathways in supporting the relay of information along spatially dispersed visual networks. The results of such analyses can complement those obtained using functional MRI and provide us with a broader understanding of how visual perception for particular visual categories is supported by the healthy brain.

1.6.2. EMA and the two streams perspective

In the context of extending the EMA and other representational accounts, it is, therefore, not only important to understand why individual regions across both the EVC and the MTL are differentially engaged by face, object, and scene stimuli, but also to understand how these spatially distinct category-sensitive brain regions interact with one another, and to what extent their ability to interact with one another underpins successful perception in humans. With these outstanding questions in mind, I offer a proposal, below, about how perception for scenes and object-like visual categories may be supported by distinct streams in the human brain, and briefly outline how this is tested by the experiments reported in subsequent Chapters of this Thesis.

In the representational hierarchical account of Saksida and Bussey (2010), the HC is discussed in terms of its positioning at the apex of the ventral visual processing stream, and its role in using spatial representations to resolve object-level ambiguity in more posterior VVS regions. From this perspective, the HC represents another level of representational complexity along the VVS. It was noted in section 1.2, however, that there are also brain regions in the early EVC that respond preferentially to scene stimuli (e.g. TOS and PPA), whereas others respond preferentially to object-like stimulus categories (e.g. LOC and OFA). It has also been noted that whereas the PHC (and consequentially, posterior HC) primarily receives inputs from dorsal-medial visual areas involved in visuospatial processing, such as the posterior parietal cortex, posterior cingulate cortex, and retrosplenial cortex, the PRC primarily receives inputs from ventral-lateral visual association areas in the temporal lobe, such as areas TE and TEO of the VVS (see section 1.1.2; also Kravitz et al., 2011; Kravitz et al., 2013).

It is, therefore, plausible that there are actually two relatively segregated but parallel visual processing networks or ‘streams’; an extended ventral-lateral stream (culminating in the PRC) that contains hierarchically-organised representations of non-spatial feature conjunctions that are most useful in the context of memory and

perception for individual object-like stimulus categories (e.g. artificial objects and faces), and another more medial stream (culminating in posterior HC), which contains hierarchically-distributed representations of spatial feature-conjunctions that are more useful in the context of scene memory and perception. The ventral-lateral stream may culminate in PRC but should also comprise functionally-defined regions along the posterior-anterior extent of the classic VVS, including the LOC, OFA and FFA. The medial stream may culminate in posterior HC but should also comprise the various posteromedial cortices that have previously been implicated in scene processing; these include the TOS and PPA (section 1.2), but also, potentially, the lingual gyrus, posterior parietal cortex and retrosplenial cortex (Nasr et al., 2011; Aly et al., 2013; Epstein and Kanwisher, 1998; Epstein, 2014; Zeidman et al., 2014). If this network-level perspective of visual processing is valid, then successful perception for object-like stimulus categories (artificial objects and faces) should depend largely upon the activity of individual regions within the putative ventral-lateral stream, but also their ability to communicate with one another effectively via their functional/structural connections. Similarly, successful scene perception should depend largely upon the activity of regions within the more medial stream and successful inter-regional functional interactions between these regions.

Note that this framework retains the core predictions of the representational accounts of MTL function outlined above and should not, therefore, be seen as a distinct and competing account. Rather, it is intended as a complementary proposition which clarifies that the processing of scenes and object/face stimuli are differentially dependent upon distinct visual streams converging on the posterior HC and PRC, respectively. In a sense, this notion simply extends the classic 'What' versus 'Where' conception of how visual processing is organised in the EVC (section 1.1.1), and should not, therefore, be entirely controversial. For instance, the authors of the BIC model of MTL function (section 1.3.3) also noted that the PRC and PHC are preferentially connected to regions involved in processing object and spatial information, respectively (Diana et al., 2007). Indeed, it was partly on this basis that the PRC and PHC were proposed to support the mnemonic encoding/retrieval of individual items and contexts, respectively. Unlike BIC, however, the current proposal is that the spatial 'stream' continues from PHC into posterior HC. Also in contrast to BIC, the current framework proposes that both PRC and posterior HC can contribute to higher-level perception as well as memory for their 'preferred' stimulus categories (e.g. objects/faces and scenes, respectively). This framework also extends a recent proposal by Dilks et al., (2013); that a number of scene-processing regions including

the TOS and PPA may be organised hierarchically along a posterior-anterior axis in the same manner as are core face-processing regions including the OFA and FFA according to prominent models of face processing (Haxby et al., 2000; see Fig 1.9).

Whilst the two streams conception resembles similar proposals in the literature, it is nevertheless useful in the context of extending existing representational accounts like the EMA. This is because it affords the generation of clearer predictions with respect to the distinct patterns of functional and structural (white matter) connections that support PRC/posterior HC contributions to successful higher-level perception for their 'preferred' categories. For instance, if successful visual perception for scenes and object-like stimuli are particularly dependent on distinct hierarchical visual streams culminating in the posterior HC and PRC, respectively, then:

1) Within a single experiment, it should be possible to demonstrate that both the PRC and ventral-lateral EVC regions (e.g. LOC and FFA) respond preferentially to blocks of object-like stimuli (artificial objects and faces) during visual perception, whereas both the posterior HC and posteromedial EVC regions (e.g. PPA) respond preferentially to blocks of scenes. In addition, EVC regions should respond preferentially to blocks of visually dissimilar stimuli, whereas MTL regions should respond preferentially to visually similar stimuli because only the latter would place great demands on the ability to create complex and highly distinctive stimulus representations.
2) The PRC should demonstrate preferential functional connectivity (i.e. a statistical dependence of activity) with ventral-lateral EVC regions, particularly during presentation of its 'preferred' stimulus categories (faces and objects). By contrast, the posterior HC should demonstrate preferential functional connectivity with posteromedial EVC regions, particularly during the presentation of visual scenes.
3) The PRC and posterior HC should possess different patterns of structural connectivity with earlier visual processing regions. More specifically, PRC should demonstrate preferential structural connectivity (i.e. possess more reproducible structural connections) with ventral-lateral object/face-selective EVC regions, whereas the posterior HC should demonstrate preferential structural connectivity with posteromedial scene processing regions of EVC.
4) Inter-individual variation in structural measures of the white matter pathways providing inputs/outputs for the PRC or the posterior HC, should be related to the magnitude of face/object and scene-selective BOLD responses within these regions, respectively.

5) Inter-individual variation in structural measures of the white matter pathways providing inputs/outputs for the PRC or the posterior HC should also be predictive of behavioural markers of perception for faces and scenes, respectively.

These predictions will be tested sequentially in this Thesis using a combination of behavioural paradigms and MR imaging techniques as outlined below:

In Chapter 2, I introduce a modified version of the fMRI experiment described in Mundy et al., (2012), which has previously been used to demonstrate that category-sensitive sub-regions of the MTL (e.g. HC and PRC) and EVC (e.g. PPA and FFA) are preferentially activated by blocks of visual stimuli with a high and low degree of feature overlap, respectively (section 1.4.4). This experiment includes modifications designed to address some potential confounds in the original study, and test Prediction 1 outlined above. In a novel departure from the previous study, I also submit the fMRI data to a functional connectivity analysis pipeline (O'Reilly et al., 2012). This latter analysis enables investigation of the distinct patterns of functional interactions that allow the PRC and HC to contribute to higher-level perception for faces/objects and scenes, respectively (i.e. testing Prediction 2 above). The results of both analyses are discussed in the context of the representational accounts outlined in this Chapter, and, for comparison, both the memory system accounts of MTL function outlined in section 1.3, and another recent network-based account of how visual processing is organised in the brain (Behrmann and Plaut, 2013).

In Chapter 3, I report the results of a study in which I use the functional data from Chapter 2 to localise face, object, and scene-sensitive EVC regions (OFA, LOC, and TOS), and then apply an established probabilistic tractography pipeline to reconstruct and quantify the white matter connections between these category-selective EVC ROIs and the PRC/HC. The data is then used to investigate whether the PRC does indeed possess more reproducible structural connections with ventral-lateral EVC regions involved in visual processing for object-like stimulus categories (OFA/LOC), whereas the posterior HC possesses more reproducible connections with scene-processing EVC regions (TOS) (i.e. testing Prediction 3 above). In this same Chapter, I also report the results of a combined fMRI and deterministic tractography analysis. This is carried out to investigate how inter-individual variation in diffusion MRI measures of the macro- and microstructural properties of the fornix and the ILF - which provide inputs/outputs to the HC and PRC, respectively (section 1.1.4) – relates to the magnitude of category-selective BOLD responses in the PRC and the HC (i.e. testing Prediction 4 above).

In Chapter 4, I present data from an experiment in which deterministic tractography was once again employed, but this time to investigate whether inter-individual variation in diffusion-MRI measures of the macrostructure and microstructure of the fornix and the ILF are also differentially predictive of participants' discrimination accuracy for scenes or faces, in a previously reported visual discrimination paradigm (Mundy et al., 2013) (i.e. testing Prediction 5 above).

During the discrimination paradigm reported in Chapter 4, participants were required to make discriminations between pairs of visually similar stimuli over a number of repetitions. Over time, therefore, stimulus-related learning may, arguably, have contributed to the overall performance measures (Kim et al., 2011). In Chapter 5, therefore, I present data from a follow up study that employed the same deterministic tractography approach as that reported in Chapters 3 and 4, to investigate whether structural properties of the fornix/ILF are also differentially predictive of markers of perception for trial-unique pairs of scenes versus faces using a modified version of a previously reported change-detection paradigm (Aly et al., 2013) (i.e. providing a more rigorous test of Prediction 5).

The results of these experiments are summarised and interpreted in the context of representational accounts during the General Discussion in Chapter 6. More broadly, this final chapter will highlight the novel contributions of the current Thesis to our understanding of the role of distributed visual processing streams converging on the PRC and the posterior HC, along with their white matter pathways, in successful perception for different visual categories. I will also highlight new questions that emerge from the current work and suggest how these may be addressed in future studies.

Chapter 2: Brain regions involved in perceptual processing for scenes, objects and faces

2.1. Introduction

In Chapter 1, I described several representational accounts of visual perception (Graham et al., 2010; Saksida and Bussey, 2010). According to these accounts, brain regions along the EVC support representations of individual visual stimulus features and low-level feature-conjunctions, whereas the HC and PRC support highly complex representations of spatial and non-spatial visual feature-conjunctions, respectively. The representational complexity that is afforded by the PRC and the HC enables the construction of perceptual representations of the unique set of non-spatial and spatial feature-conjunctions, respectively, that comprises an individual stimulus and help distinguish it from other visually similar exemplars (i.e. it enables the resolution of 'feature ambiguity'; section 1.4.1). These accounts therefore extend the putative posterior-anterior visual processing hierarchy (i.e. the Ventral Visual Stream; VVS) beyond the EVC and into the MTL. An important proposal of these accounts is that higher-level face/object perception is supported by the non-spatial feature-conjunction representations that are constructed in the PRC, whereas scene perception is more dependent upon the spatial representations instantiated in the HC. Indeed, fMRI studies confirm that the PRC and HC are differentially engaged during perception for objects/faces and scenes, respectively (Lee et al., 2008). At the end of Chapter 1, I also outlined a 'two streams' conception of how higher-level visual perception is organised along the EVC and MTL (section 1.6.2). This retained the core predictions of representational accounts but explicitly states that the processing of spatial and non-spatial stimuli are differentially dependent upon distinct visual processing streams converging on the posterior HC and the PRC, respectively.

These representational accounts predict that the PRC and HC will respond preferentially to object/face and scene stimuli, respectively. In addition, these regions should be preferentially engaged by blocks of visually similar (high feature overlap; HFO) compared to visually dissimilar (low feature overlap; LFO) stimuli from within their 'preferred' category, because only the former will place great demands on the ability to construct highly distinct representations of successive exemplars. Recent investigations have sought to test these predictions, which are novel with respect to

many contemporary accounts of MTL function (e.g. ‘memory system’ accounts; section 1.3). Mundy et al., (2012), for example, recently used fMRI to test the proposition that visual similarity, as well as stimulus category, is a critical factor determining whether the posterior HC or PRC is engaged by a set of stimuli. In their study, healthy participants viewed blocks of visually similar (high feature overlap; HFO) and visually dissimilar (low feature overlap; LFO) faces, animate objects, inanimate objects, and scenes whilst they performed a stimulus duration-detection task in an MRI scanner. An independent functional localiser scan was also administered to localise category-sensitive brain voxels corresponding to the FFA, LOC, PPA (section 1.2), as well as the PRC and posterior HC. The main experimental data was then used to investigate how stimulus category and within-block visual similarity modulated activity within each of these category-sensitive ROIs during the duration-detection task. Firstly, both the EVC and the MTL ROIs were found to respond maximally to those categories of stimuli with which they have previously been most strongly associated (FFA = faces, PPA = scenes, LOC = objects, PRC = faces/objects, and posterior HC = scenes). Secondly, each EVC ROI responded preferentially to LFO compared to HFO blocks of exemplars from its preferred stimulus category, whereas the MTL ROIs responded more to HFO compared to LFO blocks from their preferred category (Fig 2.1).

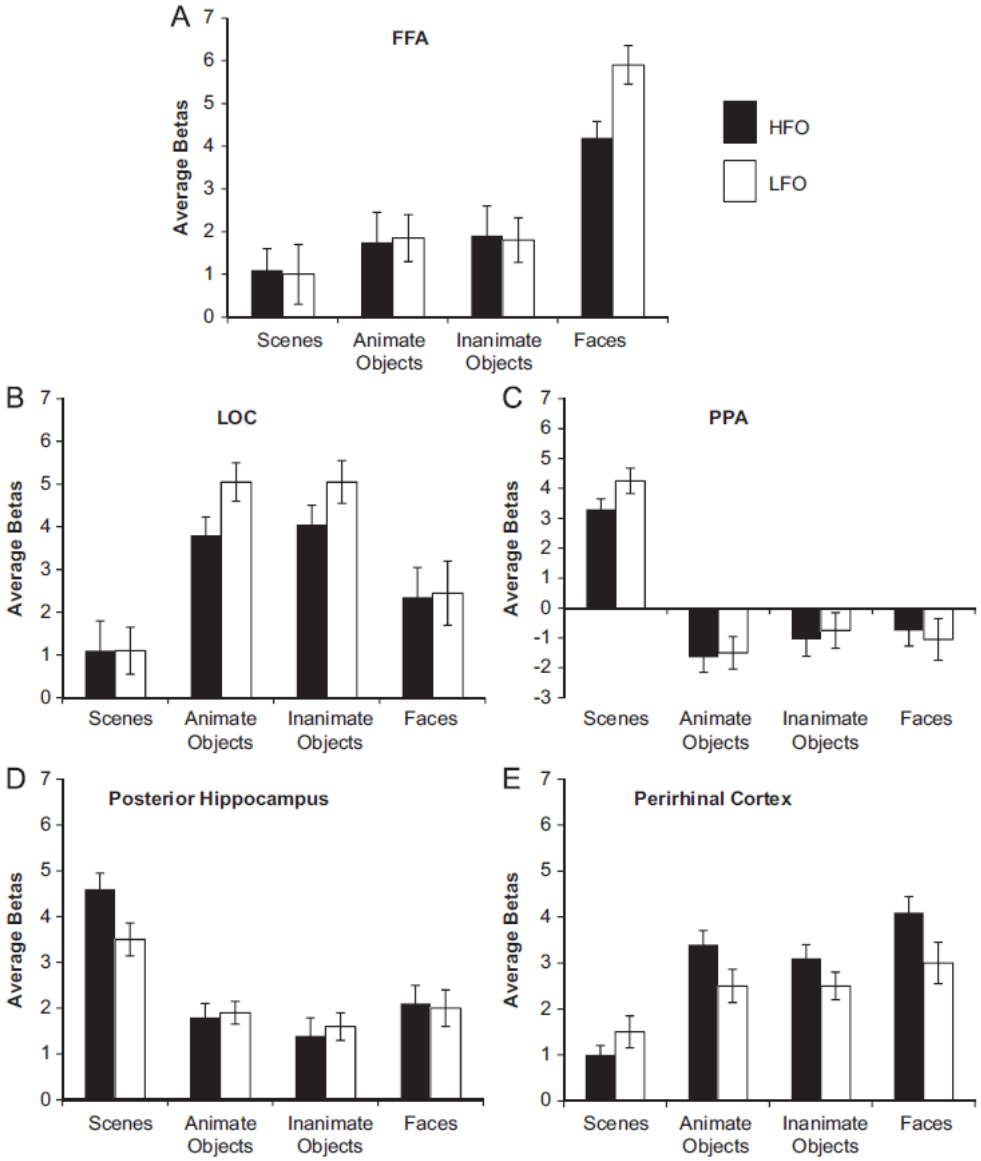

Fig 2.1. Average Beta values for each stimulus category reported in Mundy et al., (2012), presented separately by feature overlap (HFO = high feature overlap; LFO = low feature overlap) and functional ROI [(A) FFA; (B) LOC; (C) PPA; (D) posterior HC; (E) PRC]. The data was collapsed across hemisphere for clarity. Figure adapted from Mundy et al., (2012).

Consistent with representational accounts, Mundy et al., (2012) argued that EVC regions responded maximally to LFO blocks within their preferred stimulus category because exemplars within these blocks were easier to distinguish from one another on the basis of representations of their distinctive individual features, relative to the stimuli that comprised the HFO blocks. Furthermore, HFO blocks may have triggered a repetition suppression-like effect in these ROIs (a phenomenon associated with an attenuated neural response to repeated relative to novel stimuli; Grill-Spector and

Malach, 2001b), because the repeated presentation of visually similar exemplars was more likely to produce a significant overlap in the neural populations responding to these images, compared to the LFO blocks. In contrast, MTL regions may have responded maximally to HFO rather than LFO blocks, because these regions are involved in the construction of distinct representations of the unique sets of feature-conjunctions that comprise individual exemplars from sets of visually similar stimuli. The gradual build-up of feature ambiguity during HFO blocks would have therefore placed a greater demand on the ability to create these distinct MTL representations.

Mundy et al., (2012) highlighted some limitations of their experimental design, however, which mean that in the context of testing the predictions of representational accounts of visual perception (including the novel predictions outlined in section 1.6.2 of the present Thesis), their findings should be treated with caution pending replication. One such limitation related to the within-category differences between the material that comprised the HFO and LFO stimulus blocks (Fig 2.2). The HFO and LFO face stimuli, for example, were artificial and real-world faces, respectively; the HFO and LFO scenes were artificial rooms and real-world photographs of outdoor scenes, respectively. The within-ROI and within-category differences in activation during the HFO versus LFO blocks could therefore potentially be attributable to differences in material-type for these categories, rather than visual similarity *per se*. Further, the stimuli that comprised the HFO and LFO blocks of the object stimuli were drawn from real-world semantic categories with different levels of semantic as well as perceptual similarity; the HFO and LFO animate objects were images of fish from the same taxonomic family and mammals from different taxonomic families, respectively; and the HFO and LFO inanimate objects were photographs of chairs and tools, respectively. That differences in the perceptual similarity of the HFO and LFO object stimuli were confounded with differences in semantic similarity, may affect the interpretation of the findings reported by Mundy et al., (2012) in the PRC, because PRC atrophy has been linked to impairments in the “disambiguation” of semantically confusable objects (Kivisaari et al., 2012), and the BOLD response of the PRC to semantically confusable objects has been shown to be greater than that to semantically distinct objects, even after controlling for differences in the low level visual similarity of the individual items (Clarke and Tyler, 2014).

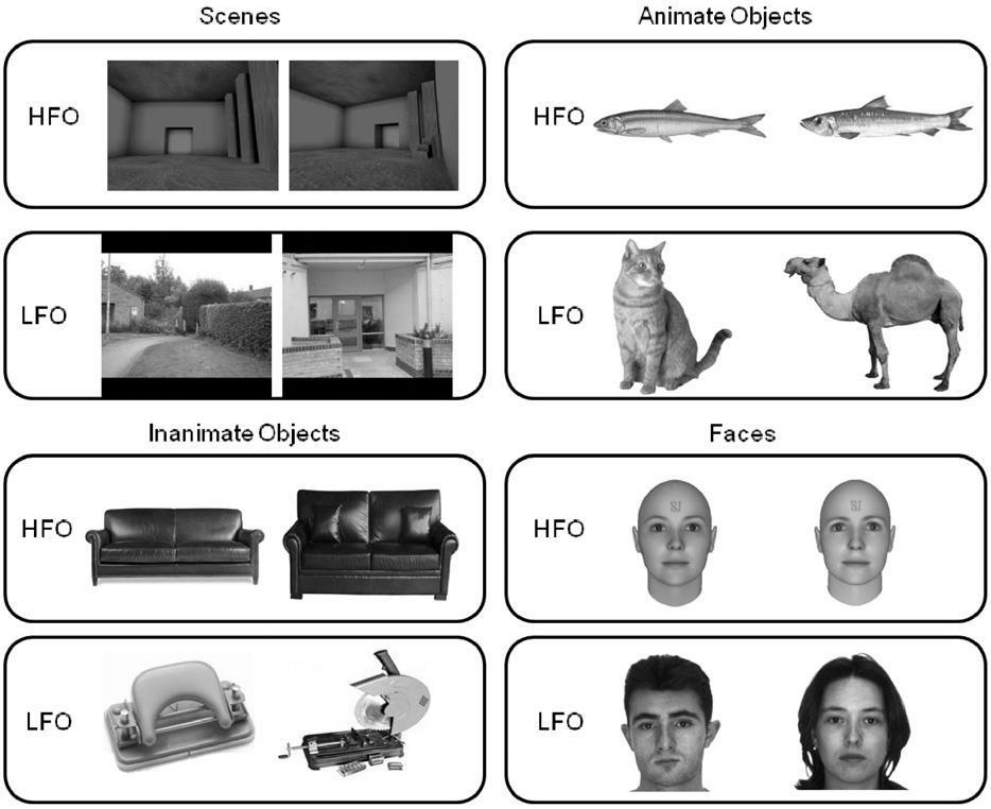

Fig 2.2. Example HFO and LFO stimuli from each of the visual categories that were presented to participants by Mundy et al., (2012). Figure from Mundy et al., (2012).

In the current Chapter, I report, therefore, a study that was carried out in order to test whether the findings of Mundy et al., (2012) with respect to the effect of stimulus category and visual similarity upon activity across EVC/MTL regions, could be replicated when the visual similarity of the stimulus set is more systematically manipulated across LFO and HFO blocks, thereby removing several potential confounds present in the original experiment. Category-sensitive voxels corresponding to the FFA, LOC, PPA, PRC and posterior HC were initially identified as functional regions-of-interest (ROIs) in a sample of healthy participants using an independent functional localiser scan. The same participants also viewed blocks of visually similar (HFO) and visually dissimilar (LFO) faces, objects, and scenes whilst they performed a duration-detection task in an MRI scanner. Data from the latter task was then used to investigate how within-block stimulus category and visual similarity modulated the activity within each of the above category-sensitive ROIs. Importantly, the face, object, and scene stimuli that were constructed for both the HFO and LFO blocks were all of the same 'type', so that the effect of feature overlap on within-ROI activity would not be confounded with differences in stimulus type. Further, the object stimuli were a class of

artificial objects that would be completely novel to the participants at test, thereby reducing the potential for the engagement of semantic processing during these blocks. By addressing several confounds present in the original study, the pattern of results produced by this replication study should reflect a more rigorous test of the predictions of representational accounts of visual perception. Consistent with the findings of Mundy et al., (2012) and representational accounts, it was anticipated that the posterior HC and PRC would respond preferentially to scenes and faces/objects, respectively, and that these MTL regions would be preferentially engaged by HFO relative to LFO stimuli, whereas their counterpart category-sensitive regions in the EVC would be preferentially engaged by LFO stimuli.

As explained in Chapter 1, category-sensitive brain regions do not act as independent visual processing 'modules', but must interact with other functionally related brain areas within their broader neural networks in order to contribute to perception for their 'preferred' stimuli (section 1.6.1). Therefore, I also report an exploratory functional connectivity analysis that was conducted using the data from the main experimental task and a method called psychophysiological interactions (PPI); this second analysis goes beyond a focus on activity within individual category-sensitive ROIs, and instead investigates the different patterns of functional *interactions* that support PRC and posterior HC contributions to higher-level perception. According to O'Reilly et al., (2012, pp 604): "PPI is a measure of what is generally referred to as functional connectivity – a statistical dependence between activity in between brain areas". PPI is not the only method that can be used to investigate functional connectivity; others include, resting state connectivity analyses (Biswal et al., 1995), Dynamic Causal Modelling (DCM; Friston et al., 2003), and Independent Components Analysis (ICA; Hyvarinen, 1999). Unlike these alternative approaches, however, PPI specifically aims to identify brain voxels in which activity is more strongly correlated with the activity of a seed region of interest *in one context compared to another*. Such a context-dependent increase in the statistical relationship between two brain regions suggests that these regions exchange information with one another, but only in particular contexts. This is the pattern of functional interactions that would be expected across visual networks that are relatively specialised for processing particular visual categories. A key face processing region, for example, is more likely to interact with other face processing regions when the individual is viewing a face rather than a scene, whereas a scene processing region is more likely to interact with other scene processing regions when the individual is viewing a scene. The PPI approach was therefore employed here because it was expected to be sensitive to the kind of category-dependent functional

interactions that may underpin PRC and posterior HC contributions to higher level perception.

Given that representational accounts propose that the PRC is part of an extended 'object analyser pathway' that is specialised for the perceptual processing of non-spatial stimulus categories (Murray et al., 2007; Saksida and Bussey, 2010), it was anticipated that the PPI analysis would reveal that PRC activity is more strongly correlated with that of regions along the ventral-lateral VVS during the presentation of faces and/or objects compared to scenes. In contrast to the PRC, representational accounts propose that the posterior HC is relatively specialised for scene perception; posterior HC activity should therefore be more strongly related to that in other more posteromedial scene-sensitive cortices when participants view images of scenes, rather than objects and faces. This pattern would indicate that the PRC and posterior HC contribute to perception for faces/objects and scenes, respectively, through *distinct* patterns of functional interactions with other category-sensitive visual areas along the VVS, consistent with representational accounts of visual processing (see also section 1.6.2).

2.2. Method

2.2.1. Participants

Forty healthy participants with normal or corrected-to-normal vision were recruited for this study. The data for 10 of these participants could not be obtained or submitted to subsequent analyses, however, due to participant illness on the day of scanning (N = 2), technical difficulties during scanning (e.g. E-prime software faulting intermittently; N = 7), or excessive movement during scanning (N = 1). The data described below corresponds to the remaining 30 participants (2 male; age range = 18 – 27; mean = 20.37; SD = 2.14). All participants gave written informed consent to participate in this study, which was approved by the Cardiff University Ethics Committee.

2.2.2. Stimuli

To investigate the effects of stimulus category and feature overlap upon EVC/MTL ROIs, 40 'families' of faces, objects, scrambled-objects, and scenes, were created as described below. Each 'family' contained 16 exemplars from a particular stimulus category. The stimuli were designed so that within-family exemplars shared a large number of features (high feature overlap; HFO), whereas exemplars from different families shared few features and were more visually distinct from one another (low feature overlap; LFO). 32 families per stimulus category were randomly selected from the larger stimulus pool for the purposes of the duration detection task. Note that whereas Mundy et al., (2012), used different 'types' of stimuli for their HFO and LFO conditions (e.g. artificial versus real-world), all of the present face, object, and scene stimuli were artificially generated, ensuring that differences in feature overlap are not confounded with differences in stimulus type.

In more detail, each face family was created in Facegen Modeller 3.5 (Singular Inversions, Toronto, Canada) by generating a random face. The genetic similarity function was then used to generate 16 unique but visually similar 'family members' based on this initial 'prototype' (Fig 2.3*A*). The genetic similarity factor was fixed at 0.3, while the gender, age, and distinctiveness parameters were fixed so that they could not vary across exemplars. Each face was rendered as a 400 x 400 pixel colour image.

Each object family comprised exemplars from a class of artificial objects known as 'Fribbles' (Hayward & Williams, 2000), which have been employed in previous studies to demonstrate that patients with PRC damage present with impairments in higher-level perception for visual objects (Barense et al., 2007). Unlike the object stimuli reported in Mundy et al., (2012), which were drawn from real-world semantic categories, all fribbles would be entirely novel to the participants at test. Individual fribbles were constructed from a main body part and 4 appendages. Each appendage had 2 possible variants that were unique to each fribble family. The series of possible combinations of these appendage-variants afforded the construction of 16 unique exemplars per family (Fig 2.3*B*). 12 fribble families were created by recycling the body parts and appendages from a subset of the exemplars from 4 pre-existing fribble families that were freely available online. The shape of the main body part was shared across some of these 12 families but its colour and texture were family-unique. The colour/texture of the main body part was manually altered in 9 of these 12 families using Strata Design 3D CX 7 (Strata, Santa Clara, Utah, USA). The same software package was used to generate a set of 28 additional fribble families, each of which contained completely family-unique

body parts and appendages. Each fribble was rendered as a 400 x 400 pixel colour image.

Each scene family contained 16 photorealistic outdoor scene stimuli that were created in Terragen 2 (Planetside Software, Cheshire, UK). Within each scene, 4 salient spatial variables were defined (e.g. water level, steepness, surface spacing and area length), each of which had two possible levels. The series of possible combinations of the different levels of these 4 variables afforded the construction of 16 visually similar exemplars for each family (Fig 2.3*C*). Importantly, different outdoor scene 'types' (e.g. beaches, mountain ranges, fields) possess different visual characteristics and so the precise spatial variables that were altered were necessarily different across each scene family (e.g. water level is a useful variable for Alpine lake scenes, but inappropriate in the context of desert scenes). All scene stimuli were rendered as 400 x 400 pixel images.

A custom image filter was used to produce scrambled versions of every fribble exemplar in Adobe Photoshop 6. The filter divided each input image into a grid of 10 x 10 pixel sections, and then randomly rearranged these sections. Each resulting scrambled-fribble image therefore contained the same low level visual properties as the original fribble image from which it was created (e.g. mean intensity and colour), but lacked the structural coherence of the original stimulus. This procedure afforded the creation of a scrambled fribble for every intact fribble exemplar.

The stimuli used in the independent functional localiser task included 32 greyscale exemplars from each of the following visual categories: 1) real-world objects, 2) artificial faces, and 3) artificial indoor scenes. The stimulus-set also included 16 grayscale exemplars from a 'scrambled objects' category. All stimuli were orthogonal to those used in the main experimental task. The object stimuli were photographs of chairs from the Hemera object database Vol. 1-3. The artificial faces and scenes were created in FaceGen Modeller 3.3 (Singular Inversions, Toronto, Canada) and Deus Ex (Ion Storm Inc., Austin, TX, USA), respectively. Scrambled object stimuli were 20 x 20 grids of randomly rearranged square sections of photographs of flowers and chairs (Watson, Wilding, & Graham, 2012). The stimulus dimensions were as follows: faces = 400 x 400 pixels; objects = 300 x 300 pixels; scenes = 640 x 512 pixels; scrambled objects = 400 x 400 pixels.

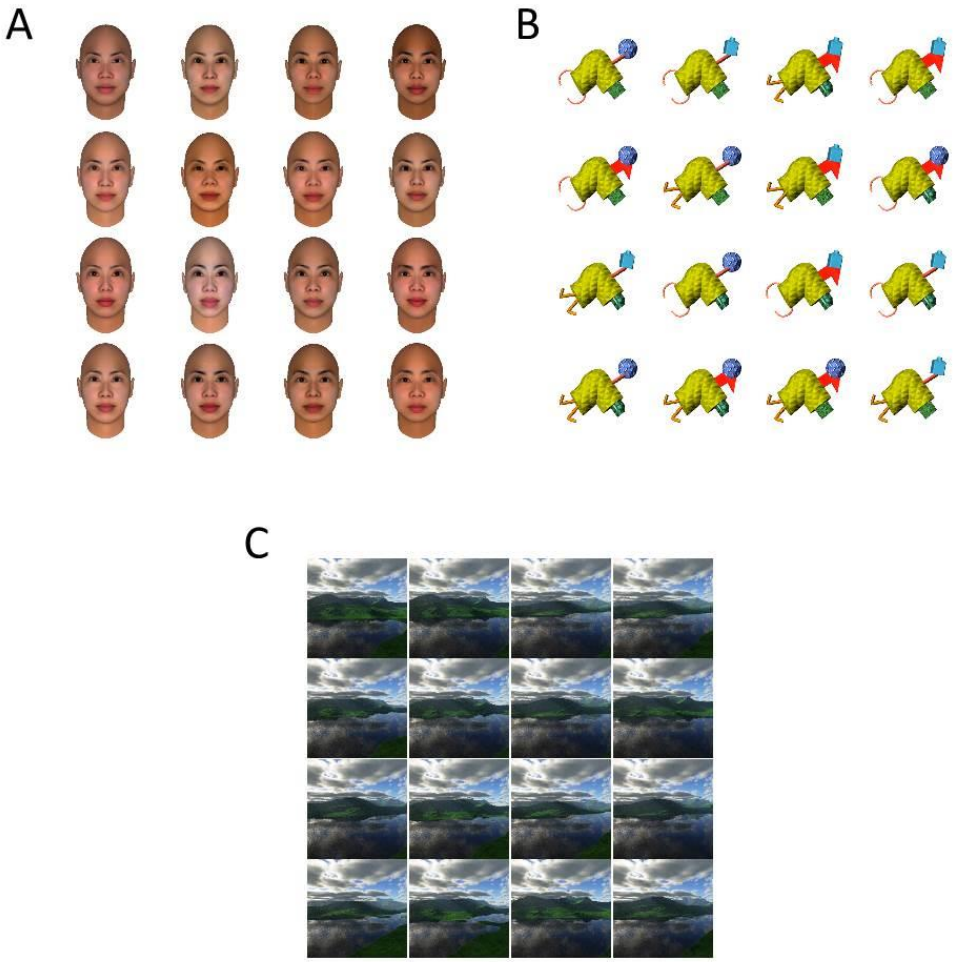

Fig 2.3. Examples of a family of (A) face, (B) object, and (C) scene stimuli from the duration detection task.

2.2.3. Experimental Procedure – Duration Detection Task

A blocked experimental design was used to manipulate stimulus category and feature overlap during the duration detection task, which was split into 2 runs and administered with E-Prime (Psychology SoftwareTools Inc., Sharpsburg, Pennsylvania, USA). Each run contained 8 unique blocks for each of 8 conditions: 1) high feature overlap faces (HFO faces), 2) high feature overlap objects (HFO objects), 3) high feature overlap scenes (HFO scenes), 4) low feature overlap faces (LFO faces), 5) low feature overlap objects (LFO objects), 6) low feature overlap scenes (LFO scenes), 7) scrambled objects (SCRAM), and 8) crosses (CROSS). This resulted in 64 blocks per run. For both runs, the presentation order of the 8 conditions was varied over the 64 block sequence according to a latin-square counter-balanced design which ensured that no

block could be preceded or followed by another from the same condition. The starting condition for this sequence was counterbalanced across participants.

Each HFO block contained all 16 exemplars from 1 particular family. This consumed 16 of the 32 families created for each stimulus category. LFO blocks contained 1 exemplar from each of the remaining 16 families, thereby consuming the remaining 16 families per stimulus category. The allocation of stimulus families to HFO and LFO conditions was counterbalanced across participants. SCRAM blocks contained scrambled versions of the LFO object blocks, and CROSS blocks contained 16 black crosses positioned centrally on a white background. The SCRAM and CROSS data is not relevant to the present hypotheses and was neither analysed nor reported below (the SCRAM data is reported in Chapter 3 where it is relevant for that experiment).

During both runs of the duration-detection task, participants were required to press a response button with their right index finger whenever they detected a stimulus that was presented for slightly longer than the others in the sequence. All stimuli were presented on a white background, on a projector screen with a resolution of 1024 x 768 pixels. In each block, the majority of the stimuli were presented serially for 300ms, with a 450ms inter-stimulus-interval (ISI). One or two stimuli within each block were assigned to be temporal 'deviants', however, and were instead presented for 600ms (mean number of deviants per block = 1.5). In each block, the 'long' and 'short' trials were distributed in a pseudorandom order, which was constrained to ensure that 'long' trials could not occur until at least 3 'short' trials had occurred, and that two 'long' trials could not occur consecutively. Each run lasted ~16 minutes.

2.2.4. Experimental Procedure - Independent Localiser Task

The localiser task was described by Mundy et al., (2012), and began immediately after both duration-detection task runs were completed. The task, which was administered via Presentation software (Neurobehavioral Systems, Albany, California, USA), was a working memory paradigm in which participants were required to press a response key with their right index finger whenever they detected that a stimulus had occurred twice in immediate succession. Stimuli were presented serially within blocks of objects, faces, scenes, and scrambled objects. Each block contained 16 stimuli, each of which was presented for 200ms with an ISI of 800ms. Within each block, the number of repeats was randomised and stimuli were drawn from the stimulus set with replacement.

There were 12 blocks for each of the 4 categories employed in this task, all of which were presented on a white background in the same alternating sequence across participants. In addition, there were four blocks of fixation crosses which occurred at blocks 1, 18, 35, and 52 within the overall 52-block sequence. The task lasted ~15 minutes.

2.2.5. MRI acquisition

FMRI data was acquired from participants with a General Electric 3T HDx MR scanner using an 8 channel receive-only head coil. The same gradient-echo, echo-planar imaging (EPI) sequence was used during both the localiser and duration-detection tasks (TR = 3000ms, TE = 35ms, flip angle = 90°, FOV = 220mm, slice thickness = 2.4mm with a 1mm inter-slice gap, in-plane resolution = 3.4 x 3.4mm). 46 slices covering the whole-brain, were acquired per participant along an oblique-axial plane tilted 30 degrees from the AC-PC plane (posterior down) with a view to minimising signal dropout in the MTL (Weiskopf et al., 2006). High-order shimming was also used to reduce signal dropout. The first three volumes from each EPI run were automatically discarded.

A T1-weighted 3D FSPGR sequence with the following parameters was used to acquire structural images from our participants: TR = 7.8ms, TE = 3ms, TI = 450ms, flip angle = 20°, FOV = 256mm × 192mm × 172mm, 1mm isotropic resolution. Two additional 3D FSPGR images were acquired (TR = 20ms, TE = 7ms and 9ms, aligned to the slice orientation of the fMRI images) in order to produce participant-specific field-maps, which were later used to correct for regional distortions in the EPI data during data pre-processing (Jezzard & Balaban, 1995).

2.2.6. fMRI pre-processing

Data pre-processing and analysis was conducted with FEAT (fMRI Expert Analyses Tool) in FSL (www.fmrib.ox.ac.uk/fsl). The pre-processing pipeline included motion correction with MCFLIRT (Jenkinson et al., 2002), non-brain removal using BET (Smith, 2002), and fieldmap-based EPI unwarping using PRELUDE & FUGUE (Jenkinson, 2003). High-pass temporal filtering (Gaussian-weighted least-squares straight line fitting, with sigma=20.0s), mean intensity normalisation, and spatial

smoothing with a Gaussian kernel of FWHM 4.0mm were also applied. The EPI data was registered to the participant-specific FSPGR structural scans and a Montreal Neurological Institute (MNI) standard template image using FLIRT (Jenkinson et al., 2002).

2.2.7.1. Analysis 1

As the first analysis reported here was an attempt to replicate the findings of Mundy et al., (2012), the imaging analysis pipeline was near identical to that of the original study. The EPI data for each duration detection task run was first submitted to a mixed effects general linear model. The block onset times were used to define a single regressor for each of 7 conditions (HFOfaces, HFOobjects, HFOscenes, LFOfaces, LFOobjects, LFOscenes, SCRAM); these were then convolved with a standard model of the haemodynamic response function. CROSS blocks were not modelled, thereby providing an implicit baseline. Although the scrambled object (SCRAM) blocks were modelled, they were not analysed further here because, as indicated above, they do not relate to the current hypotheses. Analysis of this data is, however, reported in Chapter 3. The data from the two runs of the task were then combined using a higher-level fixed-effects analysis in FLAME (FMRIB's Local Analysis of Mixed Effects; Beckmann, 2003; Woolrich, 2008).

For the localiser task, the face, scene, object, and scrambled object blocks were modelled as predictors of interest. As per Mundy et al., (2012), whole brain statistical contrasts between these conditions were then established to define category-sensitive EVC ROIs in each participant individually, with a cluster creation threshold of $Z \geq 2.3$, $p \leq 0.05$, corrected for multiple comparisons. The FFA was localised by contrasting faces with scenes (F > S), the LOC by contrasting objects with scrambled objects (O > SO), and the PPA by contrasting scenes with objects (S > O). As per Mundy et al., (2012), for each of these contrasts, the peak voxel in an area that corresponded well with previously reported anatomical locations and mean Talaraich coordinates was identified [i.e. FFA (-39, -52, -12; 40, -50, -11; Kanwisher et al., 1997; Peelen and Downing, 2005); PPA (-27, -44, -6; 22, -40, -5; Epstein and Kanwisher, 1998; Peelen and Downing, 2005); LOC (-45, -75, 4; 43, -73, 5; Grill-Spector et al., 1998)]. A $9mm^3$ sphere was then defined around this peak voxel and binarised. The resulting sphere was intersected with all significant voxels in the appropriate contrast image and re-binarised for subsequent use. This process resulted in a participant-specific ROI for the FFA, LOC, and PPA in each hemisphere.

To identify category-sensitive voxels in the PRC of each hemisphere, analyses of the localiser data were restricted to the region described by Devlin and Price (2007). This bilateral PRC mask was initially binarised and warped into participants' native space using FLIRT (Jenkinson, et al., 2002). Category-sensitive voxels within the boundaries of this mask were identified by contrasting activation for faces and scenes, with a cluster creation threshold of $Z > 2.3$, $p \leq 0.05$, corrected.

To identify category-sensitive HC voxels, analyses were restricted to a bilateral mask of the posterior HC, because previous fMRI studies have consistently localised scene-sensitive voxels in the posterior, but not the anterior HC in humans (Aly et al., 2013; Mundy et al., 2012; Lee and Rudebeck, 2010), and lesions to the dorsal but not the ventral HC consistently result in significant maze-learning impairments in rodents (Moser and Moser, 1998). This focus on the posterior HC is also consistent with Mundy et al., (2012). The posterior HC mask was created by binarising a probabilistic mask that had been thresholded to include only those voxels that had at least a 50% probability of overlapping with the HC of either hemisphere according to the Harvard-Oxford subcortical structural atlas (Desikan et al., 2006), and then applying an anterior cut-off to the mask at $y = -24$ in Talaraich space. The resulting binary and bilateral mask of the posterior HC was then warped into participants' native functional space. A lower statistical threshold was applied for the purpose of localising scene-selective voxels in the posterior HC, because these were found to be less reproducible relative to category-sensitive voxels in the other ROIs described above. As Rossion et al., (2012, pp140) point out, however, variability in the signal-to-noise ratio across the brain, coupled with the variability of the shape and height of the haemodynamic response function across not only the individual brain but also across individual participants, does make it "practically impossible to use the same statistical criterion to define all functional brain areas in all participants of a study". To ensure that scene-sensitive voxels were identified in the posterior HC of each hemisphere for a satisfactory number of participants, activation for scenes within the bilateral HC mask was therefore contrasted with that for faces with a statistical threshold of $Z \geq 2.3$, $p \leq 0.05$, uncorrected. This process resulted in a participant-specific mask for each MTL ROI in each hemisphere.

Featquery was then used to extract parameter estimates for each of the main experimental conditions from within the boundaries of each of the above functionally defined EVC/MTL ROIs. These parameter estimates were converted into percent signal change estimates ready for analysis. These data were then submitted to a series of 3 (Category: Faces, Objects, or Scenes) x 2 (Feature Overlap: HFO versus LFO)

repeated measures ANOVA's, as per Mundy et al., (2012), in order to investigate the effect of stimulus category and feature overlap on activity within each ROI.

2.2.7.2. Analysis 2

To investigate PRC/posterior HC functional connectivity, the generalised form of PPI was conducted. This has been found to provide better model fits for experimental designs that involve more than 2 conditions (McLaren et al., 2012), compared to the standard PPI approach described by O'Reilly et al., (2012). In more detail, the EPI data for each duration detection task run was again submitted to a mixed effects general linear model. The seed regions were the participant-specific PRC and posterior HC clusters extracted from each hemisphere during Analysis 1. The physiological component of the PPI term (i.e. the timecourse) was extracted from each ROI separately for each run in FSL. Psychological factors were obtained by convolving a regressor for each of the duration detection block types with a standard model of the haemodynamic response function. For each MTL seed ROI, interaction (PPI) terms were then generated for each condition of the duration detection task by multiplying the physiological and psychological factor regressors. Statistical contrasts between the resulting PPI terms for each of the 6 main experimental conditions (HFOfaces, HFOobjects, HFOscenes, LFOfaces, LFOobjects, LFOscenes,) were then set up in order to identify brain regions in which activity was more strongly correlated with that of the PRC/posterior HC of each hemisphere during blocks of:

a) Faces compared to scenes (F > S)
b) Objects compared to scenes (O > S)
c) Faces and objects compared to scenes (F + O > S)
d) Faces compared to objects and scenes (F > O + S)
e) Objects compared to faces and scenes (O > F + S)
f) Scenes compared to faces (S > F)
g) Scenes compared to objects (S > O)
h) Scenes compared to faces and objects (S > F + O)

These contrasts were employed because they afforded a test of the proposition that the PRC and posterior HC contribute to higher-level perception for faces/objects and scenes, respectively, via distinct patterns of inter-regional functional interactions. These contrasts were conducted separately for each participant-specific seed ROI and run. The resulting participant-specific contrast images from the two task runs were

combined using a higher-level fixed-effects analysis in FLAME. Participant-specific mean contrast images were then fed into a higher-level cross-subjects mixed-effects analysis in order to test the group-level effect of these contrasts. Given that PPI analyses are associated with relatively low statistical power (O'Reilly et al., 2012) the group-level contrasts were restricted to a mask of occipito-temporal cortex in order to limit the number of necessary statistical comparisons. This mask was created by thresholding (50%), binarising, and combining masks of the occipital and temporal lobes, which were obtained from the MNI structural atlas in FSL. The resulting statistical images were thresholded at $Z \geq 2.3$, $p \leq 0.01$ (voxel-wise, uncorrected). To reduce the risk of reporting false positive results, Monte-Carlo simulation (AFNI's 3dClustSim, http://afni.nimh.nih.gov/pub/dist/doc/program_help/3dClustSim.html) was used to determine a cluster-extent threshold at an alpha level of $p \leq 0.01$ (34 voxels).

2.3. Results

2.3.1. Behavioural performance – duration detection task

Table 2.1. Mean proportion of Hits and False Alarms (FA) during each duration detection task condition, presented separately by Feature Overlap. Standard deviations are provided in brackets.

Condition	Hits	FA
HFO Faces	0.506 (0.186)	0.004 (0.006)
LFO Faces	0.522 (0.194)	0.002 (0.004)
HFO Objects	0.496 (0.183)	0.005 (0.008)
LFO Objects	0.476 (0.169)	0.003 (0.004)
HFO Scenes	0.519 (0.171)	0.005 (0.005)
LFO Scenes	0.481 (0.202)	0.003 (0.004)

The mean proportion of Hits and False Alarms during each condition of the duration detection task was collapsed over both runs and is reported in Table 2.1. For each participant, overall behavioural performance was measured as the proportion of Hits – False Alarms (FA) for each of the main experimental conditions of interest. Responses made between 0 – 300ms post stimulus onset were treated as delayed responses to the previous stimulus because this time window would not enable the participant to distinguish the 'short' from the 'long' trials (presented for 300 and 600ms, respectively). Hits were therefore defined as responses to 'temporal deviants' between 300 – 1350ms post stimulus onset. Other than repeated responses (e.g. the second of a 'double-click') to a 'temporal deviant', which were discarded prior to analysis, all other responses made during the task were treated as False Alarms. A 3 (Category: faces, objects, or scenes) x 2 (Feature Overlap: High versus Low) repeated measures ANOVA revealed no significant main effect of Category (F (2, 58) = 1.137, p = 0.328) or Feature Overlap (F (1, 29) = 0.736, p = 0.398) upon performance, and there was no significant interaction between these factors (F (2, 58) = 1.818, p = 0.171). Behavioural performance was, therefore, well matched across the main experimental conditions.

2.3.2. Behavioural performance – Localiser task

Table 2.2. Mean proportion of Hits and False Alarms (FA) during each condition of the functional localiser task. Standard deviations are provided in brackets.

Condition	Hits	FA
Faces	0.476 (0.212)	0.031 (0.018)
Objects	0.702 (0.140)	0.035 (0.021)
Scenes	0.618 (0.192)	0.036 (0.018)
Scrambled Objects	0.479 (0.231)	0.021 (0.016)

Table 2.2 reports the mean proportion of Hits and False Alarms during each condition of the functional localiser task. Overall behavioural performance was measured as the

proportion of Hits – False Alarms for each condition. Responses made between 200-1000ms post stimulus onset to a stimulus which had occurred in both the current and the preceding trial, were coded as Hits. All other responses were coded as False Alarms. A repeated measures ANOVA revealed a significant effect of category upon behavioural performance in this task (F (3, 87) = 16.722, p < 0.001). Bonferonni-corrected post-hoc pairwise comparisons revealed that performance was higher for Object relative to Face, Scene, and Scrambled Object blocks (all p's < 0.035). Performance was also lower during Scene (p = 0.005), but not Scrambled Object (p = 1) blocks. Performance was significantly higher during Scene compared to Scrambled Object blocks (p = 0.027).

2.3.3. Imaging Data - Analysis 1

For each ROI (FFA, LOC, PPA, PRC, and HC), the percent signal change to each condition of the main experimental task was submitted to a 3 (Category: Faces, Objects, and Scenes) x 2 (Feature Overlap: HFO and LFO) repeated measures ANOVA as per Mundy et al., (2012). Some of these ROIs were localised successfully in different numbers of participants across the left and the right hemispheres. These analyses are, therefore, reported separately by hemisphere as well as ROI and information is provided about how many individuals showed significant activation in the localiser task. This is consistent with Mundy et al., (2012), who also analysed their data separately by hemisphere.

2.2.3.1. FFA

In the left and right FFA, which were successfully localised in 28/30 and 29/30 participants, respectively, there was a significant main effect of Category (left: F (2, 54) = 67.224, p < 0.001; right: F (2, 56) = 97.116, p <0.001). Planned pairwise comparisons revealed that in both hemispheres, this was driven by a greater BOLD response to Faces compared to both Objects and Scenes, and a greater response to Objects than Scenes (left: all t's (27) ≥ 6.514, p's ≤ 0.001; Fig 2.4*A*; right: all t's (28) ≥ 7.562, p's ≤ 0.001; Fig 2.4*B*). The main effect of Feature Overlap was also significant, with this ROI responding preferentially to LFO relative to HFO blocks of stimuli generally (left: F (1, 27) = 48.923, p < 0.001; right: F (1, 28) = 30.330, p <0.001). There was also a

significant Category x Feature overlap interaction (left: F (2, 54) = 6.753, p = 0.002; F (2, 56) = 97.116, p < 0.001). In more detail, the magnitude of the preferential response to LFO relative to HFO blocks, was greater for Faces relative to both Objects and Scenes (left: both *t's* (27) ≥ 2.809, p ≤ 0.009; right: both *t's* (28) ≥ 4.562, p < 0.001), but statistically equivalent for Objects and Scenes (left: t (27) = -0.311, p = 0.758; right t (28) = -0.272, p = 0.787). This data indicates that across hemispheres, the FFA responded preferentially to the present face stimuli, but also that it 'prefers' blocks of visually dissimilar stimuli regardless of their category (see Fig 2.4).

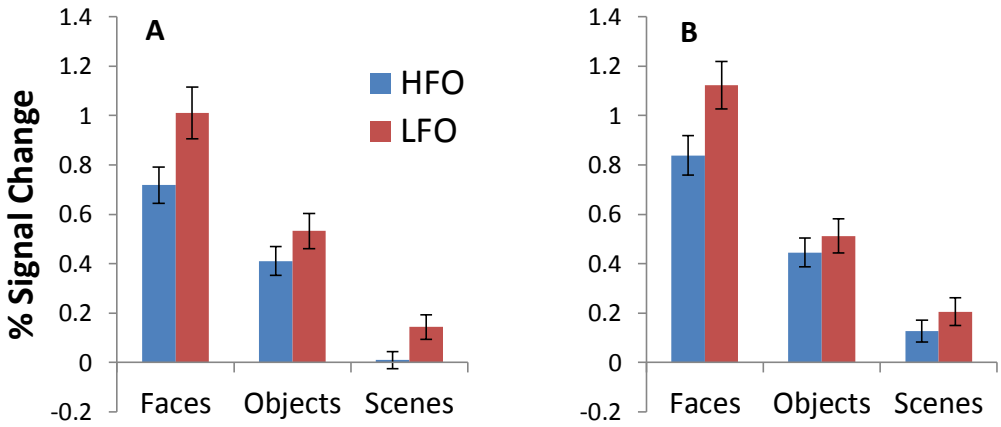

Fig 2.4. Percent signal change during each experimental condition in (A) the left and (B) the right FFA. Error bars represent the standard error of the mean for each condition.

2.2.3.2. LOC

Both the left and right LOC were successfully localised in 29/30 participants, and across both hemispheres, there was a significant main effect of Category (left: F (2, 56) = 111.656, p <0.001; right: F (2, 56) =90.007, p <0.001), with activity for Objects > Faces > Scenes (left: all t's (28) ≥ 6.345, p's ≤ 0.001, Fig 2.5*A*; right: all t's (28) ≥ 4.126, p's ≤ 0.001; Fig 2.5*B*). Across both hemispheres there was also a significant main effect of Feature Overlap, which reflected the overall response-preference of this ROI for LFO relative to HFO blocks (left: F (1, 28) = 50.758, p <0.001; right: F (1, 28) = 46.033, p <0.001). In the left hemisphere, there was also a significant Category x Feature Overlap interaction (F (2, 56) = 3.394, p =0.041), driven by the fact that the magnitude of the preferential response to LFO relative to HFO blocks, was statistically greater for Objects relative to Scenes but not Faces (t (28) = 2.495, p = 0.019; t (28) = -

1.856, p = 0.074, respectively), but equivalent for Faces and Scenes (t (28) = 0.556, p = 0.583). In the right hemisphere, the Category x Feature Overlap interaction was not statistically significant (F (2, 56) = 0.525, p = 0.594).

These findings indicate that the LOC of both hemispheres responded preferentially to the object stimuli compared to other visual categories, and that it 'prefers' visually distinct blocks of stimuli regardless of stimulus category (see Fig 2.5).

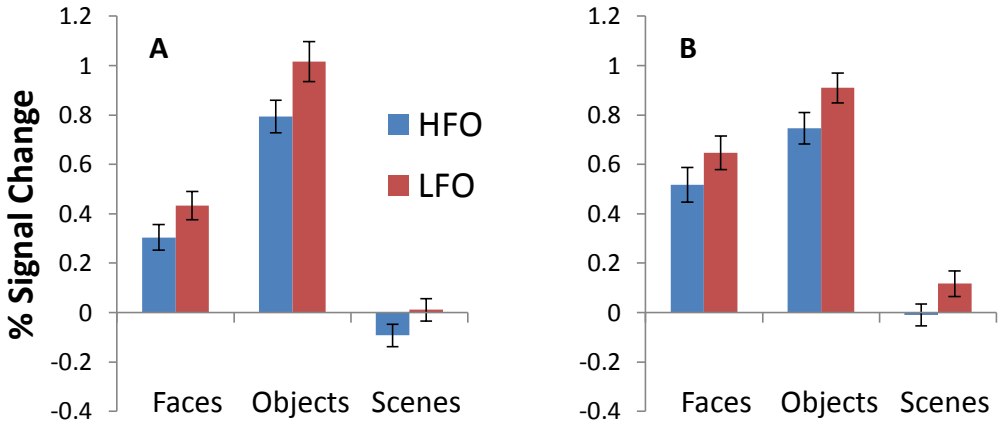

Fig 2.5. Percent signal change during each experimental condition in: (A) the left and (B) the right LOC. Error bars represent the standard error of the mean for each condition.

2.2.3.3. PPA

The PPA was identified in 30/30 participants bilaterally, and within this ROI there was a significant main effect of Category (left: F (2, 58) = 151.078, p <0.001; right: F (2, 58) = 183.075, p <0.001), with activity for Scenes > Objects > Faces (left: all t's (29) ≥ 8.555, p's ≤ 0.001; Fig 2.6*A*; right: all t's (29) ≥ 9.124, p's ≤ 0.001; Fig 2.6*B*). The main effect of Feature Overlap was also significant, with the ROI demonstrating an overall response-preference for LFO relative to HFO stimuli (left: F (1, 29) = 91.884, p <0.001; right: F (1, 29) = 105.288, p <0.001). Across both hemispheres, the Category x Feature Overlap interaction was also significant (left: F (2, 58) = 7.961, p = 0.001; right: F (2, 58) = 3.885, p = 0.026). In the left hemisphere, the interaction was driven by the fact that the magnitude of the preferential response to LFO relative to HFO blocks, was statistically greater for Objects relative to both Faces and Scenes (t (29) = 3.700, p = 0.001; t (29) = -3.109, p = 0.004, respectively), but equivalent for Faces and Scenes (t (29) = -0.532, p = 0.599). In the right hemisphere, the magnitude of the preferential

response to LFO relative to HFO blocks, was statistically greater for Objects relative to Faces but not Scenes (t (29) = 2.955, p = 0.006; t (29) = 1.145, p = 0.262, respectively), but equivalent for Faces and Scenes (t (29) = 1.533, p = 0.136).

In contrast to the LOC and the FFA, the PPA of both hemispheres responded preferentially to scene stimuli, but it too 'preferred' visually distinct blocks of stimuli regardless of stimulus category (see Fig 2.6).

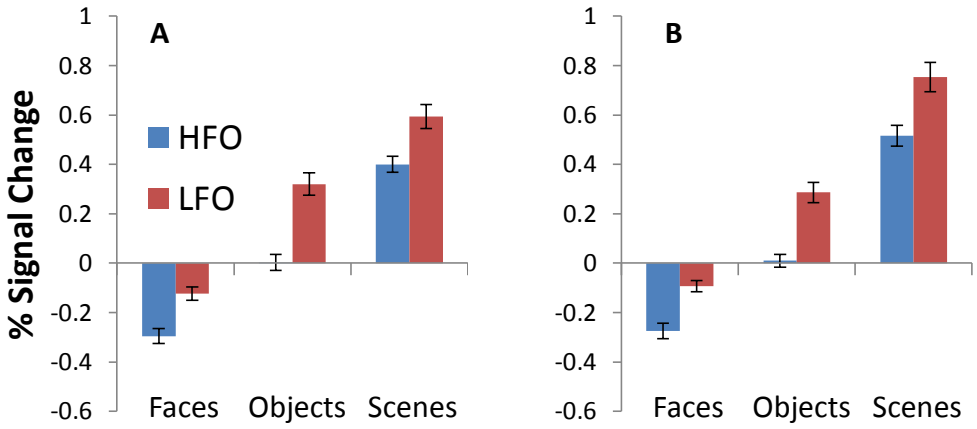

Fig 2.6. Percent signal change during each experimental condition in: (A) the left and (B) the right PPA. Error bars represent the standard error of the mean for each condition.

2.2.3.4. PRC

In the left and right PRC, category-sensitive voxels were successfully localised in 17/30 and 14/30 participants, respectively. Analyses of the effects of Category and Feature Overlap on both left and right PRC activity were therefore conducted in a smaller group of participants relative to the EVC regions reported above. Across both hemispheres, the main effect of Category upon the activity of this ROI was statistically significant (left: F (2, 32) = 18.774, p <0.001; right: F (2, 26) = 8.131, p = 0.002). In the left hemisphere, this was driven by greater activity in response to Faces relative to both Objects and Scenes (t (16) = 4.115, p = 0.001; t (16) = 5.785, p < 0.001, respectively); the responses to Objects and Scenes were equivalent (t (16) = 1.676, p = 0.113; Fig 2.7*A*). In the right hemisphere, there was an overall response-preference for blocks of Faces relative to Scenes (t (13) = 4.431, p = 0.001), but no preference for Faces relative to Objects, or for Objects relative to Scenes (t (13) = 2.017, p = 0.065; t (13) = 1.917, p = 0.077, respectively; Fig 2.7*B*). Across both hemispheres, neither the main effect of

Feature Overlap nor the Category x Feature Overlap interaction were statistically significant (left: F (1, 16) = 0.467, p = 0.504; F (2, 32) = 0.984, p = 0.385, respectively; right: F (1, 13) = 1.853, p = 0.197; F (2, 26) = 0.574, p =0.570, respectively). The PRC was therefore found to respond preferentially to images of faces, but its activity was not modulated by feature overlap (see Fig 2.7).

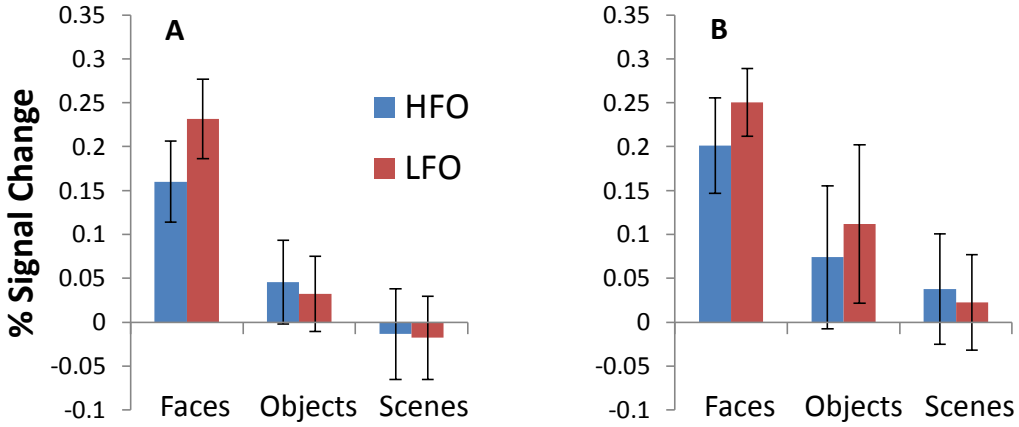

Fig 2.7. Percent signal change during each experimental condition in the left (left) and right (right) PRC. Error bars represent the standard error of the mean for each condition.

2.2.3.5. Posterior HC

Category-sensitive voxels were successfully localised in the left and right posterior HC of 27/30 and 25/30 participants, respectively. Across both hemispheres, there was a significant main effect of Category (left: F (2, 52) = 10.491, p < 0.001; right: F (2, 48) = 9.255, p < 0.001), with activity during blocks of Scenes greater than that for both Objects and Faces (left: both *t's* (26) ≥ 2.984, p ≤ 0.006, Fig 2.8*A*; right: both *t's* (24) ≥ 3.223, p ≤ 0.004, Fig 2.8*B*), but equivalent during blocks of Faces and Objects (left: t (26) = 1.739, p = 0.094; right: t (24) = 0.443, p = 0.662). There was also a main effect of Feature Overlap bilaterally, with this ROI demonstrating a response preference for LFO relative to HFO stimuli (left: F (1, 26) = 5.511, p =0.027; right: F (1, 24) = 8.543, p = 0.007). The Category x Feature overlap interaction was not significant (left: F (2, 52) = 2.024, p = 0.142; right: F (2, 48) = 0.160, p = 0.853). The left and right posterior HC, therefore, responded preferentially to scene rather than object or face stimuli, and 'preferred' LFO relative to HFO blocks of all stimulus categories (see Fig 2.8).

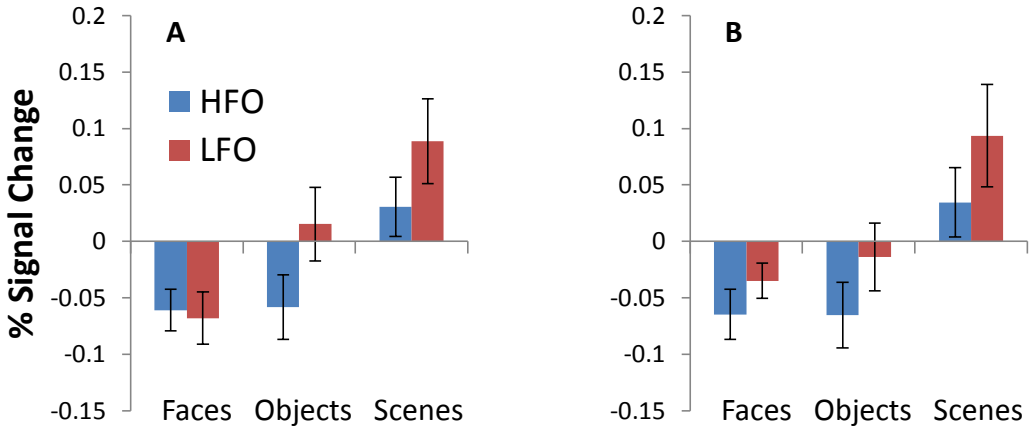

Fig 2.8. Percent signal change during each experimental condition in: (A) the left and (B) the right posterior HC. Error bars represent the standard error of the mean for each condition.

2.3.4. Imaging Data - Analysis 2

The PPI analyses detected no supra-threshold clusters of voxels within occipito-temporal cortex in which activity was more strongly correlated with that of the left PRC during some conditions of the main experimental task compared to others. The planned contrasts for this analysis did, however, reveal a cluster of voxels in the right temporal occipital fusiform cortex in which activity was more strongly correlated with that of the right PRC during Face compared to both Object and Scene blocks (i.e. the F > O + S contrast); the peak voxel of this cluster was localised slightly posterior to previously reported coordinates for the FFA (Zmax = 2.93, x = 46 y = -60 z = -20, voxels = 37; Fig 2.9). There were no other clusters in which activity was more strongly correlated with that of the PRC of either hemisphere during the presentation of particular visual categories compared to others.

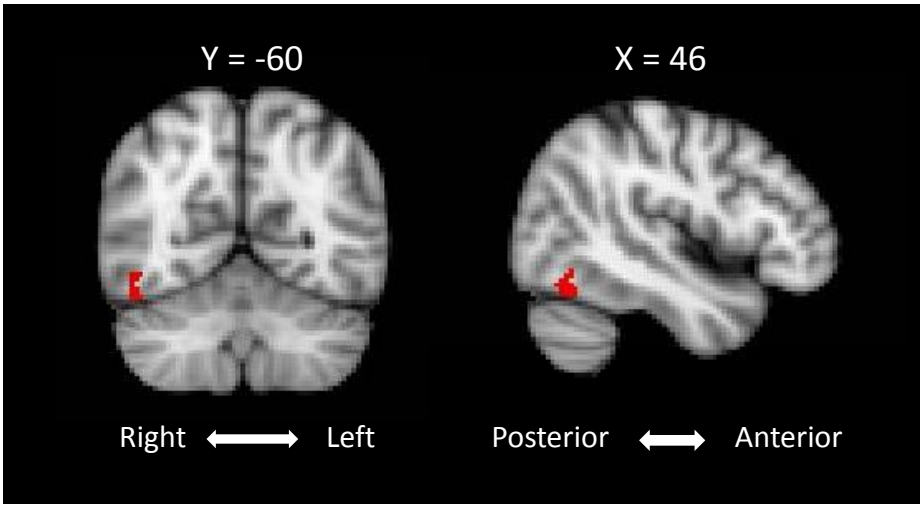

Fig 2.9. A cluster in the right temporal occipital fusiform cortex (i.e., FFA) in which activity was more strongly correlated with that of the right PRC during presentation of Faces compared to Objects and Scene stimuli (F > O + S). The cluster (red voxels) is shown on a standard Montreal Neurological Institute (MNI) 152 2mm brain template.

The analysis also revealed a cluster in the right lingual gyrus, in which activity was more strongly correlated with that of the left posterior HC during the presentation of Scenes compared to both Faces and Objects (i.e. the S > F + O contrast; Zmax = 3.05; x = 10 y = -88 z = -4; voxels = 38; Fig 2.10*A*). The same cluster was revealed when posterior HC connectivity patterns during Scene blocks were contrasted with that during Face blocks alone (i.e. the S > F contrast), along with an additional slightly more inferior cluster in the right lingual gyrus (Zmax = 3.22, x = 8 y = -90 z = -2, voxels = 43; Zmax = 3.22, x = 8 y = -90 z = -2, voxels = 43, respectively; Fig 2.10*B*).

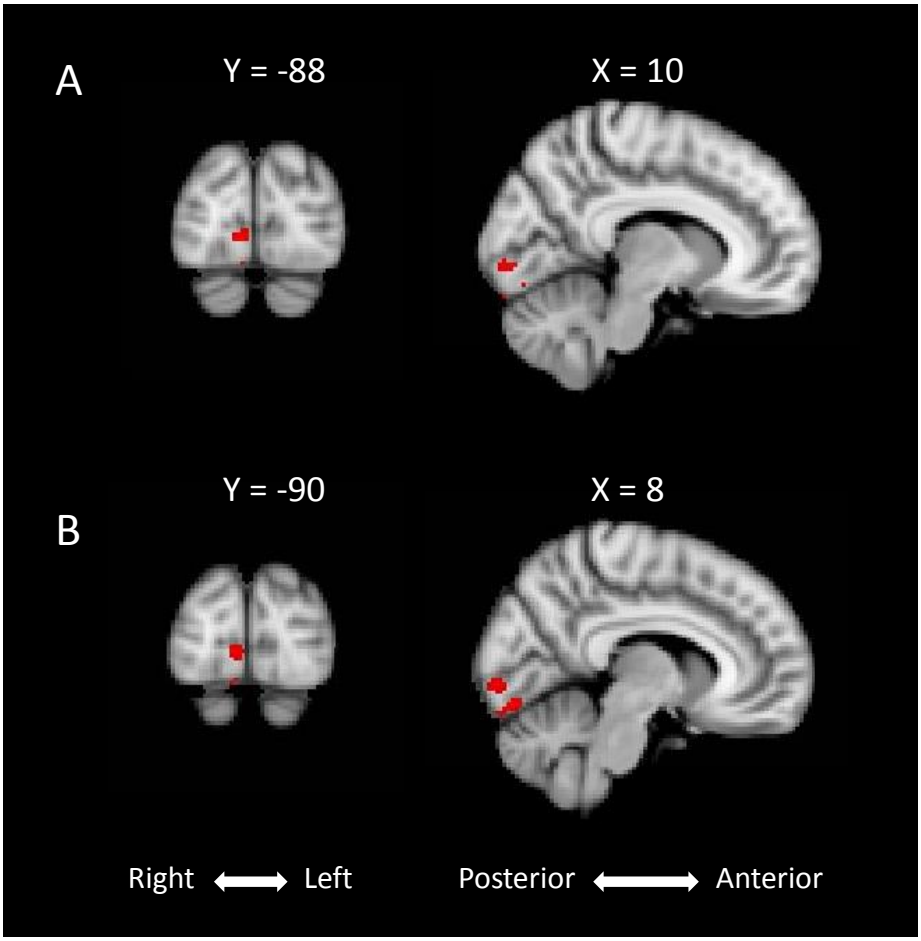

Fig 2.10. Clusters in the right lingual gyrus/occipital pole in which activity was more strongly correlated with that of the left HC during presentation of Scenes compared to (A) both Faces and Objects, or (B) Faces alone.

The analysis also revealed a cluster in the left superior temporal pole, in which activity was more strongly correlated with that of the right posterior HC during the presentation of Scenes compared to Objects (i.e. the S > O contrast; Zmax = 3.04; x = -52 y = 6 z = -6; voxels = 35; Fig 2.11*A*), and another in the left inferior temporal pole in which activity was more strongly correlated with that of the right posterior HC during the presentation of Scenes compared to Faces (i.e. the S > F contrast; Zmax = 2.97; x = -40 y = 8 z = -38; voxels = 36; Fig 2.11*B*). There were no other clusters in which activity was more strongly correlated with that of the posterior HC of either hemisphere during the presentation of particular visual categories compared to others.

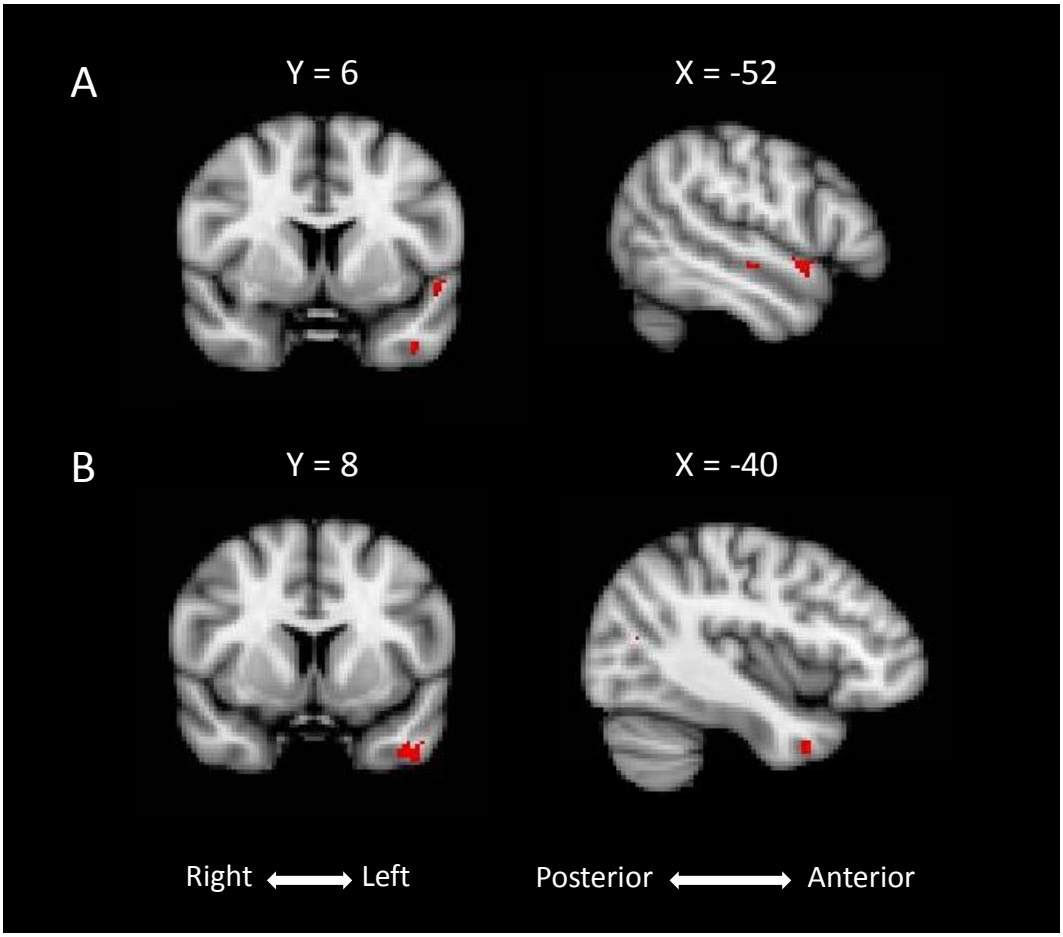

Fig 2.11. (A) A cluster in the left superior temporal pole in which activity was more strongly correlated with that of the right HC during presentation of Scenes compared to Objects. (B) A cluster in the left inferior temporal pole in which activity was more strongly correlated with that of the right HC during presentation of Scenes compared to Faces.

2.4. Discussion

The first analysis reported in this Chapter was designed to test whether Mundy et al.'s (2012) finding of interactions between stimulus category and visual similarity in EVC/MTL brain activity could be replicated with a design that addressed several potential confounds present in the original experiment. The principal importance of this analysis, however, in the context of the broader aims of this thesis, was that the results were expected to be informative in terms of testing the predictions of representational accounts of how perception for different visual categories is supported in the brain. An independent functional localiser task and a modified version of the duration-detection paradigm reported in Mundy et al., (2012) were administered to healthy participants during an fMRI scan. The localiser analysis identified several category-sensitive EVC regions (FFA, LOC and PPA), as well as face and scene-sensitive voxels within the PRC and the posterior HC, respectively. The activity within these category-sensitive ROIs was interrogated further using the data acquired during the duration detection task. These analyses confirmed that all 3 EVC regions responded preferentially (but not exclusively) to those visual categories with which they have previously been associated (i.e. FFA = faces, LOC = objects, PPA = scenes), and that the PRC and posterior HC responded preferentially to faces and scenes, respectively. All 3 EVC ROIs and the posterior HC were found to respond preferentially to LFO relative to HFO blocks for all stimulus categories; activity in the left/right PRC was not modulated by visual similarity. The findings in the EVC and the MTL are discussed separately with respect to previous studies and competing theoretical models. I will then discuss the findings of the additional functional connectivity analysis.

The pattern of category-sensitivity observed here in each EVC ROI is consistent with the findings of Mundy et al., (2012), and with the literature reviewed in Chapter 1 that led to the view that the FFA, LOC, and PPA represent spatially distinct brain regions that are relatively but not absolutely specialised for the processing of face, object and scene stimuli, respectively (section 1.2). A substantial body of previous work has shown that whilst the FFA responds to numerous stimulus categories (e.g. food, cars, and scenes), it responds maximally to images of faces (Downing et al., 2006). Similarly, the LOC has consistently been shown to respond preferentially to images of intact compared to scrambled visual objects (Grill-Spector et al., 2001a), whereas the PPA responds maximally to images of visual scenes compared to other visual categories (Downing et al., 2006).

Both the present study and that reported by Mundy et al., (2012) detected significant interactions between stimulus category and feature overlap in the FFA, LOC and PPA. In Mundy et al., (2012), these interactions reflected the fact that each EVC ROI responded more to LFO compared to HFO blocks containing it's 'preferred' stimulus category, whereas it responded equivalently to LFO and HFO blocks from 'non-preferred' categories. Here, the BOLD response of all three EVC ROIs was found to be attenuated for HFO relative to LFO blocks for both 'preferred' and 'non-preferred' categories, but in each ROI, the magnitude of the LFO > HFO effect was statistically greater for one particular stimulus category compared to the others. Mundy et al., (2012) attributed the enhanced response of EVC regions to LFO relative to HFO blocks from 'preferred' stimulus categories to the fact that the former contain stimuli with more diverse visual features than do the latter. The visual distinctiveness of the LFO exemplars means that they are unlikely to repeatedly engage highly overlapping neural populations within EVC ROIs and trigger repetition suppression (Grill-Spector and Malach, 2001b). By contrast, the visually similar exemplars comprising HFO blocks are likely to repeatedly engage overlapping neural populations within the EVC ROI that 'prefers' that category of stimuli, and will consequentially trigger repetition suppression. This argument can be adapted to account for the additional main effect of feature overlap that was detected in each EVC ROI here; HFO blocks from non-preferred as well as preferred stimulus categories may have triggered repetition suppression in each EVC ROI because a subset of their neural populations may have been consistently engaged during these blocks by 'critical' features or feature-conjunctions that can occur across stimulus categories. The PPA, for example, responds more strongly to rectilinear compared to non-rectilinear polygons (Nasr et al., 2014), and Nasr et al., argue that the sensitivity of the PPA to basic rectilinear features may itself account for the strong response of this ROI to multiple categories of complex 'carpentered' stimuli, including images of isolated buildings (Levy et al., 2004), and inanimate objects (Ewbank et al., 2005), as well as images of scenes and places (Epstein and Kanwisher, 1998). If a subset of the neural populations within the category-sensitive EVC regions studied here are sensitive to visual features/conjunctions that can occur across multiple categories, then repeated presentation of identical or highly visually similar exemplars from non-preferred as well as preferred categories could potentially trigger repetition suppression, leading to a generally attenuated response to HFO relative to LFO stimuli, as reported in the current study. Indeed, repetition suppression has been observed following repeated images of inanimate objects in the PPA and FFA as well as the LOC, and to images of places in the LOC as well as the PPA (Ewbank et al., 2005; Pourtois et al., 2009).

Although a repetition-suppression mechanism can therefore account for the present pattern of EVC ROI sensitivity to the feature overlap of stimuli from both 'preferred' and 'non-preferred' visual categories, there remains the discrepancy with the findings of Mundy et al., (2012), who reported that EVC ROIs were only sensitive to the feature overlap of stimuli from their 'preferred' categories. In addressing the discrepancy across the two sets of findings, it is worth noting differences in visual similarity between the stimuli that comprised the HFO blocks in the two studies. In Mundy et al., (2012) the HFO stimuli for each visual category were 'visually similar' by virtue of being drawn from a sub-category 'type' in which the exemplars are typically quite visually similar (faces = artificial faces; animate objects = fish; inanimate objects = chairs; scenes = artificial rooms; Fig 2.1). In the current study, not only were the HFO stimuli drawn from a particular sub-category 'type', but further, all exemplars within a given block were members of the same 'family', and could therefore be described as subtle variations of the same 'prototype' (Fig 2.3). The added level of visual similarity of the HFO stimuli reported here may have rendered the present design more sensitive to a category-general repetition suppression effect across all 3 EVC ROIs, compared to the design reported by Mundy et al., (2012). This interpretation could be tested in future studies in which the visual similarity of the exemplars comprising the stimulus *families* themselves is varied parametrically across multiple levels. In the case of face stimuli, for example, this would involve generating several 'families' of artificial faces. LFO face blocks would be populated by face exemplars from multiple face-families. HFO face blocks could be filled with exemplars from a single family so that all of the stimuli in these blocks would be somewhat confusable. Some face-families would, however, be systematically constructed to possess a greater intra-family visual feature overlap than others. This would allow researchers to test whether repetition suppression is most likely to occur within a non-face-selective EVC ROI (e.g. LOC) during presentation of the most visually similar face-families (HFO+ Faces), less likely to occur following presentation of families characterised by an intermediate level of intra-family visual similarity (HFO Faces), and potentially non-evident following those families characterised by the lowest level of intra-family visual similarity (HFO- Faces).

The above interpretation of the main effects of stimulus category and feature overlap upon EVC activity is, notably, also consistent with another recent 'distributed coding' account of visual processing by Behrmann and Plaut (2013). Briefly, this account proposes that category-sensitive ROIs do not correspond to distinct cortical modules that are exclusively specialised for the processing of specific visual categories, but rather, they correspond to patches (i.e. local 'peaks') within more distributed and

overlapping representational networks that possess graded sensitivities to a variety of visual categories (Behrmann and Plaut, 2013; also Haxby et al., 2001). It is not clear, however, that the EVC findings reported here support this distributed coding account at the expense of the representational accounts outlined above (Graham et al., 2010; Saksida and Bussey, 2010; section 1.6.2). This is because the latter are actually fairly agnostic with respect to category-selectivity across the EVC. In other words, representational accounts propose that EVC regions support perceptual representations of lower-level stimulus features/feature-conjunctions, but they do not specify whether these representations are organised in a category-specific or a category-general manner across individual EVC ROIs; each EVC region may therefore simply support representations of particular kinds of visual features/conjunctions at a level of complexity that is *relatively* more useful in the context of processing some visual categories (e.g. faces) compared to others (scenes). By extension, the BOLD response of each EVC ROI may be sensitive to the visual similarity of blocks of stimuli from multiple stimulus categories, but the greatest MR signal attenuation would still be expected during HFO relative to LFO blocks from the preferred stimulus category. Indeed this pattern was observed in the current ROI analyses for the FFA bilaterally and the left LOC. The current EVC findings are therefore informative because they highlight that the nature of category-sensitivity across the EVC should be addressed in future theoretical revisions to representational accounts, but they alone cannot currently distinguish between representational and alternative distributed coding accounts of visual perception.

Turning to the findings in the MTL, the response-preferences of the PRC and the posterior HC for face and scene stimuli, respectively, across both the current functional localiser and the duration-detection task, is consistent with the findings of Mundy et al., (2012). It is also consistent with previous studies highlighting impaired performance in scene processing tasks following HC damage, and additional face processing impairments following MTL damage that extends to PRC. This pattern is seen across a range of perceptual/mnemonic tasks, including visual oddity (Lee et al., 2005b), perceptual learning (Mundy et al., 2013; Graham et al., 2006), and recognition paradigms (Taylor et al., 2007). FMRI studies have also demonstrated that PRC activation is greater during perceptual discrimination and perceptual learning for face compared to scene stimuli, and vice versa for the HC (Lee et al., 2008; Mundy et al., 2013). The response-preference of the PRC and posterior HC for faces and scenes, respectively, is consistent with the predictions of representational accounts, according to which the PRC supports complex representations of non-spatial visual feature

conjunctions that enable fine-grained discriminations between distinct but visually similar exemplars from non-spatial stimulus categories, whereas scene discrimination is more dependent upon spatial representations instantiated in the HC (Graham et al., 2010; Saksida and Bussey, 2010). Other contemporary distributed coding accounts of visual processing make no clear predictions, however, with regard to how distinct visual categories will differentially engage the PRC/posterior HC (e.g. Behrmann and PLAUT, 2013; Plaut and Behrmann, 2011). The category-preferences identified here in the PRC/posterior HC therefore favour representational accounts over distributed coding accounts.

The category-selectivity of the PRC and posterior HC is also difficult to reconcile with 'memory system' accounts of MTL function which typically focus on the differential contribution of the PRC and HC to particular memory processes (e.g. familiarity and recollection, respectively; Aggleton and Brown, 1999), and make limited predictions about the extent to which different visual categories will differentially engage the PRC/HC. Aly et al., (2010) have, however, previously argued that the mnemonic processing of faces may be disproportionately dependent upon familiarity compared to recollection. From this perspective, the response-preference of the PRC to faces reflects incidental familiarity-based mnemonic encoding for faces, rather than the task-independent construction of perceptual representations of their non-spatial feature-conjunctions. As participants' subsequent memory for the studied items was not assessed here, it was not possible to test whether PRC activity at study was correlated with subsequent memory performance, which would offer *some* support to the proposition that PRC activity reflects incidental mnemonic encoding. O'Neil et al., (2009), however, report findings that are relevant here; in their study, participants were scanned during a face oddity task, and the retrieval phase of an orthogonal face recognition task (the recognition task study phase was conducted prior to scanning). When behavioural performance was matched, the authors found comparable levels of PRC activation across both tasks (i.e. mnemonic demands do not necessarily increase MTL engagement). Furthermore, PRC activity was predictive of accurate perception as well as memory. These findings suggest that the present face-selective PRC activations, could, indeed, reflect the task-independent construction of complex face representations that can be recruited to support both perception and memory judgements, as anticipated by representational accounts. Similarly, advocates of 'memory system' accounts of MTL function could argue that posterior HC activations during scene blocks must reflect incidental scene memory encoding. Lee et al., (2013), however, recently administered a scene oddity task with no explicit memory demands

to healthy participants during an fMRI scan; they found that HC activity was predictive of participants' performance in this perceptual paradigm, but not in a subsequent surprise test of their memory for the scene stimuli. These findings support the proposition that the HC can make a performance-related contribution to scene perception tasks, and that the activity that is elicited by such tasks does not necessarily reflect incidental memory encoding.

Mundy et al., (2012) reported that the PRC response to objects is comparable to that for faces, and greater than that for scenes. Those findings, which imply a role for the PRC in the task-independent higher-level perceptual processing of non-spatial stimuli generally, were not replicated here, as the PRC response to objects was significantly lower than that to faces, and statistically equivalent to that for scenes, bilaterally. In addressing the inconsistency across these two sets of findings, it is worth noting that PRC damage has been less consistently associated with visual discrimination impairments for objects compared to faces (Lee et al., 2005a). This might indicate that face stimuli inherently possess a higher degree of feature overlap/ambiguity than most classes of objects, and so the processing of face stimuli is more dependent upon the complex representations instantiated within the PRC than are objects. Nevertheless, previous studies have demonstrated a role for PRC in higher-level object perception under certain conditions. Barense et al., (2007) reported that patients with PRC pathology were impaired at discriminating visually similar, but not visually dissimilar exemplars of the kind of artificial object stimuli employed here, but only when the exemplars were presented from different viewpoints. Further, PRC activity during discrimination of visually similar objects is greater when the exemplars are presented from different as opposed to the same view-point (Barense et al., 2010). Similarly, patients with PRC pathology have been reported to be impaired at discriminating pairs of differently-rotated 'blob' stimuli that share multiple features in common (i.e. HFO blobs), but not at discriminating differently-rotated 'blobs' with little feature overlap (i.e. LFO blobs); in the same study, activity in the PRC of healthy controls was also greater during the HFO relative to LFO rotated-blobs condition (Barense et al., 2012). Whilst activity can therefore be elicited in the PRC during perception for artificial objects, as well as faces, in the case of the former, the effect may be more contingent upon task conditions that further tax the ability to process the distinct feature-conjunctions comprising individual exemplars (e.g. presenting successive visually similar exemplars from different viewpoints).

Differences in the type of object stimuli employed across the two studies may also partly account for the inconsistency across the findings reported here, and those of

Mundy et al., (2012). All object stimuli employed here were artificial fribbles that were novel to the participant at test, whereas Mundy et al., (2012) employed animate and inanimate object stimuli from real-world semantic categories. The HFO and LFO animate objects, for example, were pictures of fish from the same taxonomic family and mammals from different taxonomic families, respectively. PRC activity during those object blocks could arguably reflect an additional contribution of this region to semantic processing. Indeed, recent research has shown that atrophy of the medial PRC, but not the ERC or HC in patients with Alzheimer's disease, is predictive of overall naming performance for living (typically share several semantic features) relative to non-living (typically share few semantic features) things, which suggests that the PRC contributes to the binding of the semantic properties of visual objects, which in turn, enables their "disambiguation from other similar objects and thus comprehension" (Kivisaari et al., 2012, pp3357). After controlling for both categorical and low-level visual similarities between individual stimuli, PRC activity is also greater for semantically confusable relative to semantically distinct objects (Clarke and Tyler, 2014). Together, these studies suggest that the significant PRC response to the objects employed by Mundy et al., (2012), particularly in the HFO conditions, could reflect the combined contributions of this region to semantic as well as perceptual disambiguation. It is, however, also possible that the visual complexity of the real-world object stimuli employed by Mundy et al., (2012) was such that they were more dependent on the construction of complex stimulus representations in the PRC, than were the artificial objects used here. It will, therefore, be important for future studies to employ object stimuli that are sufficiently complex, without drawing exemplars from real-world semantic categories which would confound the contributions of the PRC to perceptual and semantic feature-binding (e.g. fribble stimuli that are comprised of more features/conjunctions). As noted above, however, whilst previous studies using visually similar sets of artificial objects/'blobs' have detected behavioural impairments in perception following PRC damage, and elicited PRC activity in healthy controls, it may be necessary to present such stimuli from different viewpoints.

Another finding reported here was that neither the PRC nor the posterior HC responded preferentially to HFO relative to LFO stimuli from their 'preferred' categories. PRC activity was not significantly modulated by feature overlap; activation was, on average, actually greater for LFO compared to HFO faces across both hemispheres, though this difference did not reach significance. In the posterior HC, there was, across categories, an LFO > HFO response preference; this reflected reduced *activation* to HFO relative to LFO stimuli in the context of scenes, but increased *deactivation* to HFO

relative to LFO faces and objects. The posterior HC was, therefore, only positively 'engaged' by the HFO/LFO *scene* stimuli, consistent with representational accounts. However, representational accounts propose a role for the PRC and the HC in resolving feature ambiguity across visually similar exemplars from their 'preferred' categories, so within these ROIs they predict an enhanced rather than attenuated response to HFO objects/faces and scenes, respectively. This prediction distinguishes representational accounts from alternative accounts of visual processing that do not specify a role for the PRC/HC in resolving feature ambiguity (e.g. Plaut and Behrmann, 2011), and was corroborated by the findings of Mundy et al., (2012), but not those reported here. Mundy et al., (2012) interpreted their findings to indicate that the PRC/posterior HC construct conjunctive stimulus representations of sufficient complexity to enable fine-grained discriminations between visually similar stimuli, and that this process is increasingly engaged over the course of HFO blocks so that each successive exemplar is assigned a distinct representation. They state that this interpretation "depends on the proposition that participants noted, at least at some level, the subtle differences among stimuli in HFO blocks, even though doing so was not a requirement of the task. In the absence of direct evidence for this, however, it is possible that in these conditions the sequence of items simply appeared to participants as a string of highly repeated identical stimuli. If this were the case, however, we would have expected repetition suppression to be evident (e.g. the opposite pattern to that seen in our data, LFO > HFO)" (Mundy et al., 2012, pp3059). This provides a potential explanation for the lack of response-enhancement in the PRC to HFO > LFO face/object stimuli in the current study, and, further, the significant preference for LFO > HFO scene stimuli in the posterior HC. As with Mundy et al., (2012), there was no direct evidence that the current participants noted the subtle differences between successive HFO exemplars because these differences were task-irrelevant. The stimuli comprising the HFO blocks may, therefore, have appeared as a string of repeated identical stimuli. In this situation, a unique stimulus representation may not have been constructed in the PRC/posterior HC on each HFO trial, leading to repetition-suppression as per the EVC ROIs discussed above. Indeed, previous studies indicate that repeated presentation of scenes and object-like stimuli can trigger repetition suppression in the HC and PRC, respectively, as well as EVC regions (Goh et al., 2004; Rubin et al., 2013).

Again, this interpretation of the current findings could be tested in a future design in which the visual similarity of individual stimulus families is varied parametrically across each visual category (producing LFO, HFO-, HFO, and HFO+ blocks as described

above). The prediction would be that the PRC/posterior HC would be engaged by their 'preferred' categories at all levels of feature overlap. The PRC/posterior HC BOLD signal would, however, be attenuated during HFO+ (relative to LFO) blocks, which are expected to trigger repetition suppression because participants should struggle to perceive any differences across successive exemplars. PRC/HC activity should be enhanced during HFO- blocks because whilst the stimuli that comprise these blocks are visually similar by virtue of being drawn from a single 'family', the cross-exemplar differences should be salient enough for participants to assign each of them a distinct MTL representation. HFO blocks should elicit an even greater BOLD response, provided that the participants can still detect the differences across the exemplars. The differential discriminability of the HFO-, HFO, and HFO+ blocks could be verified in advance in an independent sample.

A PPI analysis was also conducted here in order to investigate the patterns of inter-regional functional interactions that enable the PRC and posterior HC to contribute to face/object and scene perception, respectively. This revealed a cluster roughly corresponding to the right FFA, in which the BOLD response was more strongly correlated with that of the right PRC during the presentation of faces compared to other visual categories. In contrast, activity in the left and right posterior HC was more strongly correlated with that in clusters within the right lingual gyrus and left temporal pole, respectively, during the presentation of scenes compared to other visual categories. Given the exploratory nature of this analysis, these findings should be considered with caution pending replication. Nevertheless, that the PRC and FFA may interact with one another in the service of face perception in particular is consistent with O'Neil et al., (2014); who recently demonstrated reliable resting state functional connectivity between the PRC and FFA, and that inter-individual differences in the strength of this PRC-FFA connectivity was predictive of participants' increased accuracy for upright relative to inverted faces in a face recognition task (i.e. PRC/FFA connectivity has behavioural relevance for face processing). This pattern of PRC/FFA connectivity is also consistent with representational accounts proposing that the PRC is part of an extended ventral object analyser pathway' involved in the hierarchical processing of faces and objects (e.g. Graham et al., 2010). Similarly, that the posterior HC may contribute to scene perception via interactions with posteromedial visual processing regions including the lingual gyri, is consistent with the findings of Aly et al., (2013), who reported increased functional connectivity between the posterior HC and lingual gyri with levels of response confidence in a scene discrimination task. Similarly, Zeidman et al., (2014) recently demonstrated HC interactions with an even more

distributed set of postero-medial brain regions during scene processing (e.g. PHC, posterior inferior parietal lobule, posterior cingulate cortex, and occipital gyrus). That HC contributions to scene perception may depend on interactions with numerous posteromedial scene processing regions, whereas PRC contributions to face/object perception may depend on interactions with more lateral brain regions along the lateral occipito-temporal cortex/VVS, is consistent with the 'two streams' framework of visual processing outlined in Chapter 1 (section 1.6.2). In this context, it is also worth noting that neither the PRC nor the posterior HC demonstrated more synchronised activity with other brain regions during perception for their 'non-preferred' relative to 'preferred' stimulus categories. This finding is easily accommodated within the two streams framework (section 1.6.2), according to which the visual streams that culminate in the PRC/posterior HC are indeed relatively specialised for the processing of non-spatial and spatial stimulus categories, respectively. The same finding is, however, more difficult to reconcile with alternative accounts of visual processing which suggest that regions along the VVS support visual processing for all complex stimulus categories (e.g. Behrmann and Plaut, 2013); if this were the case, then the PRC, for example, should have demonstrated functional interactions with other occipitotemporal brain regions during perception for scenes as well as faces. Taken together with the results of the ROI-based analyses discussed above, the results of the current functional connectivity analysis therefore support the notion that a lateral visual processing stream culminating in the PRC supports the processing of non-spatial stimuli like faces, whereas a more medial stream culminating in the posterior HC supports the processing of spatial stimuli like visual scenes.

It should be noted, however, that the PRC did not demonstrate preferential functional connectivity with ventral-lateral EVC areas during the presentation of objects compared to scenes. Furthermore, the preferential connectivity of the right PRC with the right FFA during face perception was detected by contrasting the BOLD response to faces with that to both the scenes *and* objects. This might be taken to indicate that object processing is not dependent upon ventral-lateral EVC interactions with PRC. As noted above, however, PRC contributions to higher-level object perception may be better investigated using stimuli and task demands that further tax feature-conjunction processing across object exemplars. Under such circumstances, the PRC may be shown to interact with other distinct ventral-lateral EVC regions during higher-level object perception. This possibility and its potential implications are discussed further in section 6.4.1.

This latter shift in emphasis towards the role of extended representational networks in visual perception sets the tone for the remaining chapters of this thesis. In Chapter 3, I introduce a novel combination of functional and structural MRI approaches to investigate the *structural* connections that may differentially support the propagation of information about stimuli from distinct visual categories across these networks. In Chapters 4 and 5, I use a combination of behavioural paradigms and structural MRI to investigate how inter-individual variation in the structural properties of these pathways relates to markers of participants' perception for distinct categories of visual stimuli.

In summary, this Chapter has confirmed that multiple regions across both the EVC (FFA, LOC, PPA) and the MTL (PRC and posterior HC) respond preferentially to stimuli from particular visual categories during a task that includes no explicit discrimination or recognition demands. BOLD response to visually similar blocks of stimuli, was, across categories, generally attenuated compared to that for visually distinct stimuli in many of these regions (FFA LOC, PPA and posterior HC). The PRC and posterior HC were also found to interact with distinct sets of brain regions during the presentation of their 'preferred' stimulus categories. These findings are consistent with lesion studies demonstrating that damage to the PRC as well as category sensitive regions of the EVC, can disproportionately impair visual memory and perception for non-spatial categories of visual stimuli, whereas HC damage impairs memory and perception for spatial stimulus categories (Lee et al.., 2005b; Graham et al., 2006; Mundy et al., 2013). The findings are also partially consistent with representational accounts of higher-level visual perception (Graham et al., 2010; Saksida and Bussey, 2010; section 1.6.2). In the next Chapter, we will consider how the white matter of the healthy brain maps onto category-sensitive regional activation in the brain, and how inter-individual variation in the structural properties of pathways converging on the PRC and the posterior HC relates to the magnitude of category-selective BOLD responses in these ROIs.

Chapter 3: White matter connections supporting perception for scenes, objects and faces

3.1. Introduction

Chapter 2 confirmed that regions within the EVC and MTL were preferentially engaged by particular categories of visual stimuli. Further, these regional activations were found under task conditions that placed no explicit demand on declarative memory, with these activations elicited during a temporal duration-detection task. These findings support hypotheses from representational accounts of perception (Graham et al., 2010; Saksida and Bussey, 2010), which propose that the PRC and HC are anterior components of an extended visual processing hierarchy that contributes to visual perception for object-like (e.g. artificial objects/faces) and scene stimuli, respectively.

Moving beyond these simple regional analyses, the functional connectivity analysis (PPI) suggested the contributions of the PRC and the posterior HC to perception for object-like and scene stimuli, respectively, are potentially driven via functional interactions with category-sensitive EVC brain regions (e.g. FFA [faces] and lingual gyrus [scenes], respectively). This result is consistent with the 'two-streams' conception of visual processing outlined in Chapter 1, according to which there are two relatively segregated but parallel visual processing networks; an extended ventral-lateral processing stream (culminating in the PRC) that contains hierarchically-organised representations of feature conjunctions that support memory and perception for object-like stimuli, and another more medial stream (culminating in the posterior HC), which contains hierarchically-distributed representations of spatial feature-conjunctions that can be used to support memory and perception for scene stimuli. Chapter 2 highlighted, therefore, that higher-level perception for a given category of stimuli is not simply dependent upon the activity of individual category-sensitive MTL sub-regions like the PRC and posterior HC, but rather upon the activity of multiple regions along at least two relatively segregated and distributed visual processing streams, and the ability of the components of these two streams to propagate information to one another effectively (see also Behrmann and Plaut, 2013; Kravitz et al., 2011; Kravitz et al., 2013).

Whilst the functional connectivity analysis reported in Chapter 2 identified some of the gray matter regions with which the PRC and posterior HC may interact in the service of perception for their 'preferred' stimulus categories, one can only indirectly infer how functionally-related gray matter regions are *anatomically* interconnected with one another on the basis of *functional connectivity* analyses (Gschwind et al., 2012). In other words, structural connectivity analyses are required in order to understand how the distributed white matter of the healthy brain supports inter-regional functional interactions. A key aim of the study described in this Chapter, therefore, was to investigate the white matter connections that enable the PRC and posterior HC to interact with regions in EVC, and identify how PRC and posterior HC white matter pathways may support the processing of object-like and scene stimuli, respectively.

In the current study, the direct white matter connectivity profiles between the PRC/posterior HC and the more posterior functionally-defined regions of the EVC were investigated using a combination of non-invasive fMRI, diffusion tensor imaging (DTI), and white matter tractography in healthy participants (for details of the principles underpinning DTI and tractography techniques, the reader is referred to section 1.6.1). There are, broadly speaking, two approaches to white matter tractography: deterministic and probabilistic. In deterministic tractography, a single fiber trajectory is reconstructed at each step of the propagation of a white matter streamline. Typically, some additional external constraints are imposed in order to prevent the reconstruction of anatomically implausible tracts and those that enter gray matter regions of the brain (Jones et al., 2008). This means that whilst deterministic tractography can produce accurate reconstructions of *prominent* white matter pathways, it is not ideally suited to tracking white matter connections near or within cortical brain regions. Furthermore, because only a single fiber trajectory is estimated at each step of the reconstruction of a given white matter streamline, deterministic tractography provides no indication of the confidence with which a given tract was reconstructed. This is an issue for analysis 1 of the current study where I aim to demonstrate differences in the reproducibility of direct white matter connections between the PRC/posterior HC and multiple spatially distinct category-selective regions of EVC. For this type of analysis, some indication of the *likelihood* of a direct ROI-to-ROI connection is required.

Rather than reconstructing a single trajectory in a deterministic fashion at each step of the streamline propagation, in probabilistic tractography, "the direction in which to step next is drawn from a distribution of possible orientations. The end result is a set of multiple pathways passing through the seedpoint, which is then conventionally summarized by assigning to each voxel the percentage of pathways, launched from the

seedpoint, that pass through the voxel" (Jones et al., 2008). The resulting images essentially represent the likelihood that a connection can be reproduced between a given voxel and a given tractography seedpoint. Importantly, because probabilistic tractography protocols implicitly model the noise in the estimated fiber orientation at each voxel or sub-voxel step, it is not so important to impose additional external constraints designed to prevent the reconstruction of tracts within gray matter regions (Gschwind et al., 2012). Fiber tracking in or near cortical sites is therefore expected to be more sensitive in probabilistic as opposed to deterministic tractography, and can produce some measure of the 'reproducibility' of a connection between spatially distinct gray matter regions. Gschwind et al., (2012), for example, used probabilistic tractography to demonstrate that face-selective regions of occipito-temporal cortex (e.g. OFA and FFA) are characterised by greater structural connectivity to one another compared to other local cortices.

In analysis 1 of the current study, therefore, an established *probabilistic* tractography pipeline (Behrens et al., 2003, 2007) was used to quantify the reproducibility of direct white matter connections (i.e. the 'connectivity probability') between the PRC/posterior HC, and several category-sensitive EVC regions, namely, OFA (faces), LOC (objects) and TOS (scenes). These regions are an interesting set of target EVC ROI's for the current connectivity analysis because all 3 have been described as early components of extended category-sensitive visual processing networks (Dilks et al., 2013; Taylor and Downing, 2011). Briefly, direct transcranial magnetic stimulation (TMS) of the OFA is known to temporarily impair the discrimination of face parts (Pitcher et al., 2007), and this region has been described as the earliest region within a 'core' network of face processing regions (Haxby et al., 2000). By contrast, TMS of the LOC is known to impair object categorization (Mullin and Steeves, 2011), and this region has been described as an early object processing region (Taylor and Downing, 2011). Finally, TMS of the TOS impairs scene discrimination, and so this region may represent the earliest component of a scene processing network (Dilks et al., 2013). If visual processing for faces/objects and scenes depends upon two distinct visual streams converging on the PRC and posterior HC, respectively, then we would anticipate different patterns of PRC/posterior HC connectivity across the OFA, LOC and TOS.

As well as being an interesting selection of target ROI's on a conceptual level, the OFA, LOC, and TOS are also suitable functional ROI's for probabilistic tractography on practical grounds. More specifically, the OFA, LOC, and TOS are all spatially displaced from the PRC and the posterior HC by a similar extent along the anterior-posterior axis of the brain. This is important because connections between adjacent cortical areas are

more likely to be reproduced than are connections between highly spatially distinct cortical regions due to an accumulated error problem that is inherent in probabilistic tractography. This arises due to the uncertainty in fiber orientation at each step of the propagation of a tract, which accumulates as the length of the streamline increases (Jones, 2008). If cortical regions that are not spatially displaced from the PRC/HC by a comparable distance were used as target ROI's for tractography (e.g. FFA and PPA), then it would be ambiguous whether any significant differences in the resulting connectivity probabilities are attributable to differences in connection-reproducibility per se, or simply to this distance bias.

Given that much of the literature reviewed in Chapter 1 suggests that visual processing typically proceeds in a feed-forward and sequential fashion from posterior to anterior regions of the VVS (e.g. Tanaka et al., 1991), it might seem counter-intuitive to attempt to reproduce *direct* connections between regions that are spatially displaced by as great a distance as are, for example, the OFA and the PRC. Tract tracer studies in animals have, however, revealed that information is not necessarily relayed along visual networks in an *exclusively* sequential fashion. Indeed, a growing body of evidence shows that the putative occipito-temporal object processing pathway is actually a complex recurrent network that contains direct feedback as well as feed-forward connections, some of which bypass intermediate cortical regions, thereby allowing early and late regions of the hierarchy to interact with one another directly (see Kravitz et al., 2013). The PRC in monkeys, for instance, possesses direct connections with visual areas as early as area V1, bypassing intermediate occipito-temporal regions like areas TE and TEO (Clavagnier et al., 2004). Similarly, in Chapter 1, I outlined how the posterior HC predominantly receives inputs from local MTL structures like the PHC (Aggleton, 2012). Tract tracer studies in monkeys, however, have shown that it is also directly connected to early regions of parietal visual cortex whose function is important for spatial navigation, including the inferior parietal lobule (pIPL; Kravitz et al., 2011; Clower et al., 2001), thereby bypassing the PHC and several other medial brain regions that are known to be involved in aspects of spatial processing (e.g. PPA). Whilst it is important to bear in mind that the results of structural connectivity studies conducted in rodent and primate brains may not map directly onto human brain anatomy, the evidence for direct connections between the PRC/HC and early as well as intermediate EVC justifies the present long-range connectivity approach.

Consistent with the 'two streams' conception of visual processing outlined in Chapter 1 and recent representational accounts of MTL function (e.g. Graham et al., 2010), it was anticipated that the PRC would demonstrate a greater connectivity probability with

early visual cortices that are known to respond preferentially to object-like (OFA and LOC; Gauthier, 2000; Grill-Spector et al., 2001a) compared to scene (TOS; Dilks et al., 2013; Nasr et al., 2011) stimuli. In contrast, the posterior HC should demonstrate a greater connectivity probability with earlier visual cortices that respond preferentially to scene (TOS) compared to object-like (OFA and LOC) stimuli.

A second analysis was motivated by the functional connectivity results reported in Chapter 2, and by previous research demonstrating that the face recognition impairments that characterise congenital prosopagnosia (CP) can manifest even in the context of normal patterns of activation in core face processing regions (Avidan et al., 2005). Again, this suggests that the activity of individual gray matter regions is not sufficient to support successful higher-level face processing. Indeed, subsequent research has revealed that the functional connectivity between face-selective regions is reduced in CP (Avidan et al., 2014). This indicates that face processing impairments in CP can also arise from a failure to successfully propagate information about face stimuli between multiple widely distributed brain regions. Such findings are interesting in the context of the current Thesis because they suggest that PRC and posterior HC's engagement in processing of their 'preferred' visual stimuli (faces versus scenes, respectively), may be related to their ability to communicate with other brain regions that are also functionally-sensitive to these categories. As highlighted above, these functional interactions are likely to be supported by white matter connections.

Two specific and prominent white matter pathways are of particular interest here, because one acts primarily as a HC input/output pathway, whereas the other acts as an input pathway to regions of anterior temporal cortex, including PRC; these are the fornix and the inferior longitudinal fasciculus (ILF), respectively (anatomical descriptions in section 1.1). That the fornix may be critical for relaying information about visual scenes to/from the HC is consistent with evidence that fornix transection in nonhuman primates impairs performance in a number of spatial processing tasks, including the learning of object-in-scene associations (Gaffan, 1994), and concurrent visual discriminations of spatial feature-conjunctions (Buckley et al., 2004). Furthermore, inter-individual variation in measures of human fornix tissue microstructure has also been shown to predict memory performance, particularly for scene stimuli (Rudebeck et al., 2009). The fornix has even been proposed to constitute a key component of an extended HC network that is critical for the construction of scene representations (Gaffan, 1994).

In the case of the ILF, this white matter fascicle has been shown to contain connections between multiple distributed face processing regions (e.g. OFA, FFA, and anterior temporal lobe; Gschwind et al., 2012; Pyles et al., 2013), and significant reductions in measures of ILF microstructure have been observed in both clinical cases of prosopagnosia and children with object recognition deficits (Thomas et al., 2009; Ortibus et al., 2012). Each of these findings is consistent with a role for the ILF in relaying information about object-like stimuli between category-sensitive EVC areas and regions of anterior temporal lobe, including PRC.

Previous investigations of fornix and ILF contributions to scene and object/face processing, respectively, have, however, tended to employ stimulus recognition paradigms (Rudebeck et al., 2009; Ortibus et al., 2012) or discrimination paradigms involving repeated presentation of a small number of stimuli (Buckley et al., 2004) so that learning and memory mechanisms may have contributed to performance measures over time (Kim et al., 2011). It is currently unclear, therefore, whether the roles of the ILF and the fornix in visual processing for objects/faces and scenes, respectively, extend to perception as well as memory. If PRC and posterior HC contributions to object/face and scene perception are indeed dependent upon the ability of these MTL regions to interact with other areas via the ILF and the fornix, then inter-individual variation in the magnitude of category-sensitive BOLD responses in the PRC/posterior HC during trial-unique perception should be related to differences in structural properties of the ILF/fornix that affect the efficiency with which information can be transferred along these pathways.

As explained previously in section 1.6.1, the diffusion tensor framework produces several voxel-wise diffusion-MRI indices that may be useful in this context. Fractional Anisotropy (FA) and Mean Diffusivity (MD) measures extracted from white matter pathway reconstructions are, for instance, known to be modulated by a number of white-matter microstructural properties that may influence the efficiency with which information can be propagated between spatially distinct brain regions, including axon myelination, diameter, and density (Jones et al., 2010). Studies highlighting a link between these diffusion MRI measures of white-matter pathways and activity within the gray matter regions to/from which they project, include that reported by Toosy et al., (2004), in which it was found that FA measures in the optic radiations were positively correlated with the BOLD response of the early visual cortex during photic stimulation (for a review of combined DTI-fMRI studies, see Bennett and Rypma, 2013). It is also possible to estimate certain macrostructural properties of white-matter pathways that have been reconstructed with established tractography protocols. One such

macrostructural measure is the tissue volume fraction (*f*; Pasternak et al., 2009); *f* indicates the fraction of the diffusion-weighted MR signal attenuation that is due to diffusion occurring in tissue rather than in free water (Metzler-Baddeley et al., 2012), and can be used to describe the proportion of a tract reconstruction that is composed of tissue (i.e., its relative tissue volume).

In analysis 2, therefore, a deterministic tractography protocol was used to obtain tract-specific measures of white matter microstructure (FA and MD) and macrostructure (*f*) from *in vivo* reconstructions of the fornix and the ILF. We then investigated whether the magnitude of category-sensitive BOLD responses in the PRC and posterior HC during the duration-detection task reported in Chapter 2, was related to inter-individual variation in the structural properties of their primary input/output pathways. For the PRC it was anticipated that inter-individual variation in the magnitude of the face/object-selective BOLD response of this region would correlate with measures of ILF macro- and microstructure. In contrast, it was anticipated that the magnitude of scene-selective BOLD responses in the posterior HC would correlate with measures of fornix macro- and microstructure.

3.2. Method

3.2.1. Participants

The 30 participants that contributed fMRI data to the analyses reported in Chapter 2 also underwent a diffusion-weighted MRI scan (DWI) during the same scanning session for the purposes of the current study. The DWI data for one of these participants did not transfer from the scanner successfully and was not available for subsequent analysis. The fMRI/DWI data described below therefore corresponds to the remaining 29 participants (2 male; age range = 18 – 27; mean = 20.38; SD = 2.18). All participants gave written informed consent to participate in this study, which was approved by the Cardiff University Ethics Committee.

3.2.2. Duration Detection Task - Stimuli

The stimuli that were used to localise category-sensitive EVC ROIs in this study were the faces, scenes, objects, and scrambled objects constructed for the duration detection task reported in section 2.2.

3.2.3. Duration Detection Task - Experimental Procedure

The reader is referred to section 2.2 for details of the duration detection task design.

3.2.4. MRI acquisition

The gradient-echo echo-planar imaging (EPI) sequence reported in Chapter 2 was used to acquire fMRI data from participants whilst they performed both runs of the duration-detection task in the MRI scanner. The reader is referred to Chapter 2 for details of the T1-weighted 3D FSPGR sequences used to obtain: a) high-resolution participant-specific anatomical images, and b) participant-specific fieldmaps for correction of regional distortions in the EPI data during data pre-processing.

Whole-brain diffusion-weighted MRI data were acquired using a diffusion-weighted single-shot EPI sequence (with TE = 87ms, field of view = 23 x 23 cm^2, 96 x 96 acquisition matrix, 60 contiguous slices acquired along an oblique-axial plane with 2.4mm thickness and no gap), and the scans were cardiac-gated using a peripheral pulse oximeter. Gradients were applied along 60 isotropically-distributed orientations with b = 1200 s/mm^2 (Jones et al., 1999). Six non-diffusion-weighted images (DWI) with b = 0 s/mm^2 were also acquired.

3.2.5. fMRI pre-processing

fMRI data pre-processing was conducted in FEAT as described in section 2.2, and included motion correction, non-brain removal, fieldmap-based EPI unwarping, high-pass temporal filtering, intensity normalisation, spatial smoothing, and registration to participant-specific anatomical images and a standard MNI template.

3.2.6.1. DWI pre-processing 1

For the purpose of investigating the differential connectivity profiles of the posterior HC and the PRC, a probabilistic DWI pre-processing pipeline was carried out using command-line FSL tools and FMRIB's diffusion toolbox, FDT 2.0. This pre-processing pipeline included the application of corrections for motion artefacts and eddy current-induced geometric distortions, along with non-brain removal (BET) and fieldmap-based unwarping (FUGUE) for each individual DWI dataset. A probabilistic diffusion model that uses Bayes rules to account for noise and uncertainty in the measured data was then fitted to the corrected DWI's using bedpostx (Behrens et al., 2003). A 2-fiber probabilistic diffusion model was applied to improve the modelling of crossing fiber populations (Behrens et al., 2007). For each participant, the first b = 0 s/mm^2 image was registered to a Montreal Neurological Institute (MNI) standard template image using FLIRT (Jenkinson et al., 2002). The resulting transformation matrix was subsequently inverted to enable standard space coordinates/masks to be warped back into participants' native diffusion space. FA images were also normalized to the FMRIB58 FA template using FNIRT (Jenkinson et al., 2012); the resulting transformation matrices were subsequently used to normalise participant-specific connectivity probability maps so that they could be combined into group-level images.

3.2.6.2. DWI pre-processing 2

A *deterministic* tractography approach was adopted for the purpose of accurately and reliably reconstructing the fornix/ILF of the participants, and to extract diffusion MR measures of white matter micro-/macrostructure from these prominent fiber bundles (required for analysis 2). The DWI pre-processing pipeline that preceded individual-subject tractography was automated in the non-commercial graphical MR diffusion toolbox, ExploreDTI (Leemans et al., 2009), and included non-brain removal, along with the application of corrections for participant motion and eddy current-induced geometric distortions. Custom MATLAB scripts were also used to carry out a free-water-elimination (FWE) procedure that applies post-hoc voxel-wise correction for partial volume errors due to free-water contamination in diffusion indices prior to individual-subject tractography (Pasternak et al., 2009). Not only does this procedure improve the accuracy of the mean FA and MD measures that were subsequently estimated along the fornix/ILF, but it also produces voxel-wise maps of the tissue volume fraction *f*. These images were later intersected with the results of the individual-subject tractography protocol (below) to extract *f* from the reconstructions.

3.2.7.1.1. Analysis 1 – Selection of ROI's

To identify face, object, and scene-sensitive EVC cortices to act as target ROIs for the probabilistic tractography analysis, the EPI data for each run of the duration detection task was again submitted to a mixed effects general linear model. A single regressor was defined for each of the 7 conditions (HFOfaces, HFOobjects, HFOscenes, LFOfaces, LFOobjects, LFOscenes, SCRAM), each of which was convolved with a standard model of the haemodynamic response function. Whole brain statistical contrasts between these conditions were generated in order to define the OFA and the LOC in each participant individually. The OFA was localised by contrasting faces with scenes (F > S), whereas the LOC was localised by contrasting objects with scrambled objects (O > SO). Scene-selective voxels within the TOS were localised by contrasting scenes with scrambled objects (S > SO), within a search space that was restricted to those voxels circumscribed by a mask of the TOS from the ICBM Sulcal Atlas (Mazziotta et al., 1995). The data from the two task runs were then combined using a higher-level fixed-effects analysis in FLAME (FMRIB's Local Analysis of Mixed Effects; Beckmann, 2003; Woolrich, 2008). For each EVC target ROI, the peak voxel in an area that corresponded well with previously reported anatomical locations and peak Talairach coordinates was identified for each participant individually (LOC: -45 -75 4 and 43 -73 5, Grill-Spector et al., 1998; OFA: -42 -74 -8 and 42 -69 -5, Hasson et al., 2003; TOS: -34 -79 12 and 33 -77 12, Hasson et al., 2003). On those occasions where no clear-cut peak-activation voxel could be identified for a given ROI in an individual participant (even at a level of $p \leq 0.05$, uncorrected), the group-level coordinates for that ROI were used instead; this ensured a balanced number of all EVC ROIs which afforded the within-subjects inter-regional connectivity analysis described below (Gschwind et al., 2012). The peak coordinate of each EVC ROI was then warped into participants' native diffusion space using the FSL utility 'std2imgcoord'.

Each participant-specific EVC ROI was then projected onto the white matter of the brain by dilating a sphere around the peak voxel (in 1mm iterations) until the sphere contained a minimum of 30 voxels with FA ≥ 0.2, in order to improve trackability to these areas (Gschwind et al., 2012Hagmann et al., 2006). The resulting spheres (mean radius of dilatation kernel = 7.1mm, SD = 0.94mm, no hemispheric differences in paired t-tests; largest t (28) = 1.575, p = 0.090) were subsequently binarised and used as participant-specific target EVC ROIs.

Unlike the EVC ROIs, which can only be functionally localised, the posterior HC and the PRC were delineated using the thresholded (50%) and binarised anatomical masks described in section 2.2. These anatomical MTL ROI's were warped back into native diffusion space using FLIRT, and were subsequently used as seed ROIs for probabilistic tractography. This approach is similar to that adopted by Gschwind et al., (2012), who used anatomically defined masks of the amygdala (another prominent MTL gray matter structure) as seed-ROIs for probabilistic tractography.

This procedure resulted in a participant-specific ROI for the OFA, LOC, TOS, PRC, and posterior HC in each hemisphere.

3.2.7.1.2. Analysis 1 – Probabilistic tractography protocol

Probabilistic fiber tractography was initiated in FDT 2.0 (Behrens et al., 2007). 25,000 streamlines were propagated from every voxel within the PRC and posterior HC of each hemisphere, with a step size of 0.5mm and a curvature threshold of 0.2 (Gschwind et al., 2012). The number of PRC/posterior HC streamlines that subsequently reached each EVC ROI within the same hemisphere, was expressed as a proportion of all successful pairwise connections in each individual (Gschwind et al., 2012; Croxson et al., 2005; Eickhoff et al., 2010). This procedure resulted in normalized measures of the 'connectivity probability' between each MTL ROI (PRC and posterior HC) and each EVC ROI (LOC, OFA, and TOS) within each hemisphere, ready for analysis.

For each MTL seed ROI (posterior HC and PRC), the connectivity probabilities were then submitted to a 2 (Hemisphere: Left and Right) x 3 (Target ROI: OFA, LOC, and TOS) repeated measures ANOVA with a Greenhouse-Geisser adjustment for sphericity applied as per Gschwind et al., (2012), and a significance threshold of $p \leq 0.05$. Significant effects were interrogated further using planned pairwise t-tests with a significance threshold of $p \leq 0.05$.

3.2.7.2.1. Analysis 2 – Deterministic tractography protocol

Whole brain tractography was initially performed from all voxels in individual participants' (free-water corrected) native diffusion-space in ExploreDTI using a deterministic tractography algorithm based on constrained spherical deconvolution

(Tournier et al., 2008; Jeurissen et al., 2011). A step size of 1mm and an angle threshold of 30 degrees was applied to prevent the reconstruction of anatomically implausible fibers. A multiple region-of-interest (ROI) approach was then applied to isolate the fornix bilaterally (mean voxel count: 1449.2; SD = 335.6; range: 815 - 2134) from the results of this whole-brain tractography procedure (Fig 3.1*A*; Metzler-Baddeley et al., 2011). Mean FA, MD, and *f* indices were subsequently extracted from the reconstructions in ExploreDTI (Jones et al., 2005). Mean FA/MD/*f* indices were also obtained from the main occipito-temporal associative white-matter pathway, the inferior longitudinal fasciculus (ILF; Catani et al., 2003). The right and left ILF were reconstructed (mean voxel count: 2818.3; SD = 821.1; range: 1505 - 4306) using a two-ROI approach (Fig 3.1*B*; Wakana et al., 2007), and for comparability with the fornix, the average of the measures obtained from the two hemispheres was calculated to create a single value per participant. Note that for consistency, this same deterministic fornix/ILF tractography protocol was also adopted for the tractography analyses reported in Chapters 4-5.

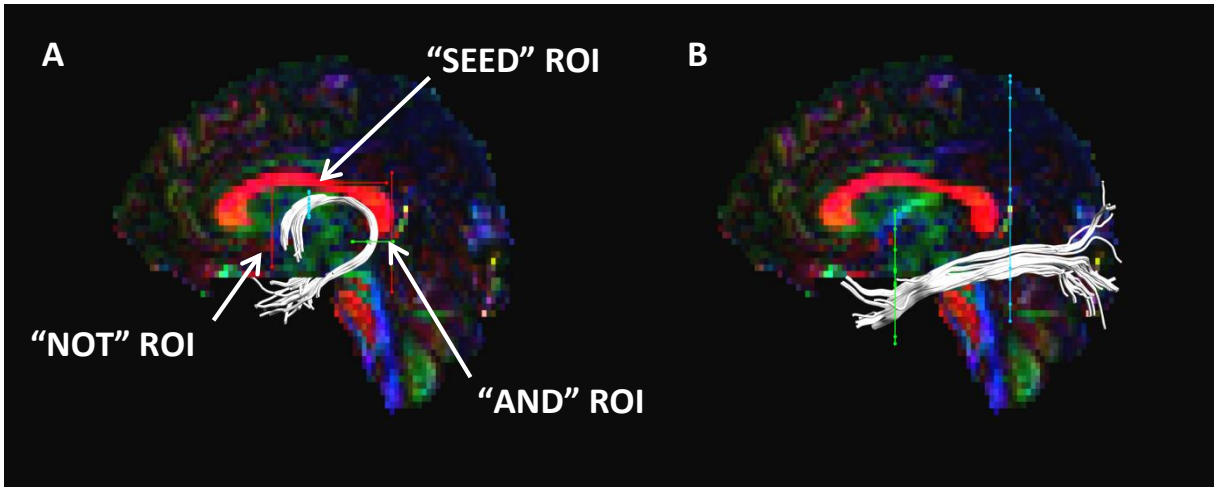

Figure 3.1. Mid-sagittal section of the orientation-coded FA map (red = left-right fibres; green = anterior-posterior; blue = superior-inferior) of a representative participant, which illustrates the manually drawn ROI's (the blue, red, and green lines) used to extract the fornix (**A**) and the ILF (**B**) bilaterally, in all participants.

3.2.7.2.2. Analysis 2 – fMRI analysis

The EPI data for each run of the duration detection task was again submitted to a mixed effects general linear model with a single regressor defined for each of the block types involved in this task. These were then convolved with a standard model of the

haemodynamic response function. Whole-brain statistical contrasts between the main experimental conditions of interest (i.e. HFOfaces, HFOobjects, HFOscenes, LFOfaces, LFOobjects, LFOscenes) were subsequently generated in order to identify voxels that responded preferentially to:

1) Faces compared to scenes (F > S)
2) Objects compared to scenes (O > S)
3) Faces and objects compared to scenes (F + O > S)
4) Faces compared to objects and scenes (F > O + S)
5) Objects compared to faces and scenes (O > F + S)
6) Scenes compared to faces (S > F)
7) Scenes compared to objects (S > O)
8) Scenes compared to faces and objects (S > F + O)

These specific contrasts were selected in order to identify voxels in both PRC and posterior HC that responded preferentially to object-like or scene stimuli. For each participant, the resulting contrast images from the two runs of the task were combined using a higher-level fixed-effects analysis in FLAME. The mean contrast images for each participant were then fed into a higher-level cross-subjects mixed-effects analysis. These analyses were initially conducted with bilateral probabilistic masks of the PRC and posterior HC in standard MNI space, which were thresholded and binarised at 50%. The DTI metrics that were extracted from the fornix and ILF (mean FA, MD and *f*) of all 29 participants were demeaned and included as covariates of interest for the group-level HC and PRC analyses, respectively. The resulting statistical images were thresholded at $p \leq 0.01$ (voxel-wise, uncorrected). Supra-threshold voxels demonstrated a significant *positive* association between the BOLD response for a given contrast and the FA/*f* metrics, or a n*egative* association with MD. To reduce the risk of reporting false positive results in the PRC/HC, Monte-Carlo simulation (AFNI's 3dClustSim, http://afni.nimh.nih.gov/pub/dist/doc/program_help/3dClustSim.html) was used to determine a cluster extent threshold at the experimental alpha level ($p \leq 0.01$: posterior HC = 10 voxels, PRC = 17 voxels). All reported clusters correspond to a cluster-extent corrected threshold of $p \leq 0.01$.

These BOLD/DTI covariate analyses were initially restricted to masks of the PRC and HC as outlined above, but the search space was subsequently widened to the broader but circumscribed mask of occipito-temporal cortex that was previously applied to the PPI analysis reported in Chapter 2 (section 2.2.7.2). This afforded identification of other visual regions in which the magnitude of a category-preferential BOLD response (e.g. F

> S) was related to inter-individual variation in the structural properties of a particular white matter pathway (as assessed by the mean FA, MD and *f* of the fornix/ILF). Given the large number of contrasts that this would entail, and the subsequent inflated risk of reporting false-positive effects in brain areas for which we had limited or no specific predictions, these follow-up analyses were only performed for those statistical contrasts that initially revealed significant clusters in either the PRC or posterior HC masks. At our experimental alpha level of $p \leq 0.01$, only clusters within the broader occipito-temporal cortex that exceeded an extent threshold of 34 voxels are reported (also determined via AFNI's 3dClustSim; section 2.2.7.2).

3.3. Results

3.3.1. Behavioural performance – duration detection task

Behavioural performance over the two runs of the duration detection task was averaged and assessed as the proportion of Hits – False Alarms for each of the conditions of interest (Table 3.1 above). Performance for the Face, Object, and Scene conditions was collapsed across Feature Overlap, as this was not a relevant factor here. Hits were defined as responses to 'temporal deviants' between 300 – 1350ms post stimulus-onset. Responses made between 0 – 300ms post stimulus onset were treated as delayed responses to the previous stimulus. Other than repeated responses to the same stimulus (e.g. the second of a 'double-click'), which were discarded prior to analysis, all other responses made during the task were treated as false alarms. A repeated measures ANOVA revealed no significant main effect of condition upon duration detection performance (F (3, 84) = 0.229, p = 0.876).

Table 3.1. Mean proportion of Hits and False Alarms (FA) during the Face, Object, Scene, and Scrambled Object conditions of the duration detection task, collapsed over Feature Overlap. Standard deviations are provided in brackets.

Condition	Hits	FA
Faces	0.506 (0.186)	0.003 (0.004)
Objects	0.496 (0.183)	0.005 (0.005)
Scenes	0.519 (0.171)	0.004 (0.003)
Scrambled Objects	0.485 (0.178)	0.003 (0.004)

3.3.2. Analysis 1 – Differential connectivity profiles of the PRC and posterior HC

Participant-specific PRC/posterior HC probabilistic connectivity maps were regularised in MNI space and thresholded to show all voxels – overlapping in at least 14 of 29 participants – that were intersected by at least 5 x 10^{-5}% of the streamline samples. The resulting images were then visually inspected in order to ensure that the orientation, trajectory and location of any reconstructed projection pathways were consistent with the known anatomy of the brain (with reference to Wakana et al., 2007; Catani et al., 2003).

For the posterior HC, the analysis reproduced a posteromedial pathway which connected the posterior HC to posterior parietal/superior occipital cortex (Fig 3.2*A*); the orientation, trajectory and location of this projection pathway corresponded well with the known anatomy of the parahippocampal cingulum. The posterior HC was also connected to parietal/superior occipital cortex via a more posterolateral projection pathway, the orientation, trajectory and location of which overlapped with the known anatomy of the posterior portion of the inferior fronto-occipital fasciculus (IFOF), but also the optic radiations and the ILF. At its most lateral extent, this latter pathway was also contaminated with some fibers from the posterior portion of the superior longitudinal fasciculus (Fig 3.2*B*); these false-positive fibers were presumably reconstructed as a result of a suboptimal resolution of multiple crossing-fiber populations in some voxels within this region (Jones, 2008).

For the PRC, the analysis reproduced a posterolateral pathway which connected the PRC to medial occipital cortex; the orientation, trajectory and location of this

posteromedial projection pathway overlapped with the known anatomy of the posterior portion of the ILF, the IFOF and the optic radiations (Fig 3.2*C*). It is also noteworthy that PRC projections to frontal brain regions were reproducible in this analysis; these corresponded well with the known anatomy of the prominent fronto-temporal pathway – the uncinate fasciculus – and the anterior portion of the IFOF (Fig 3.2*D*).

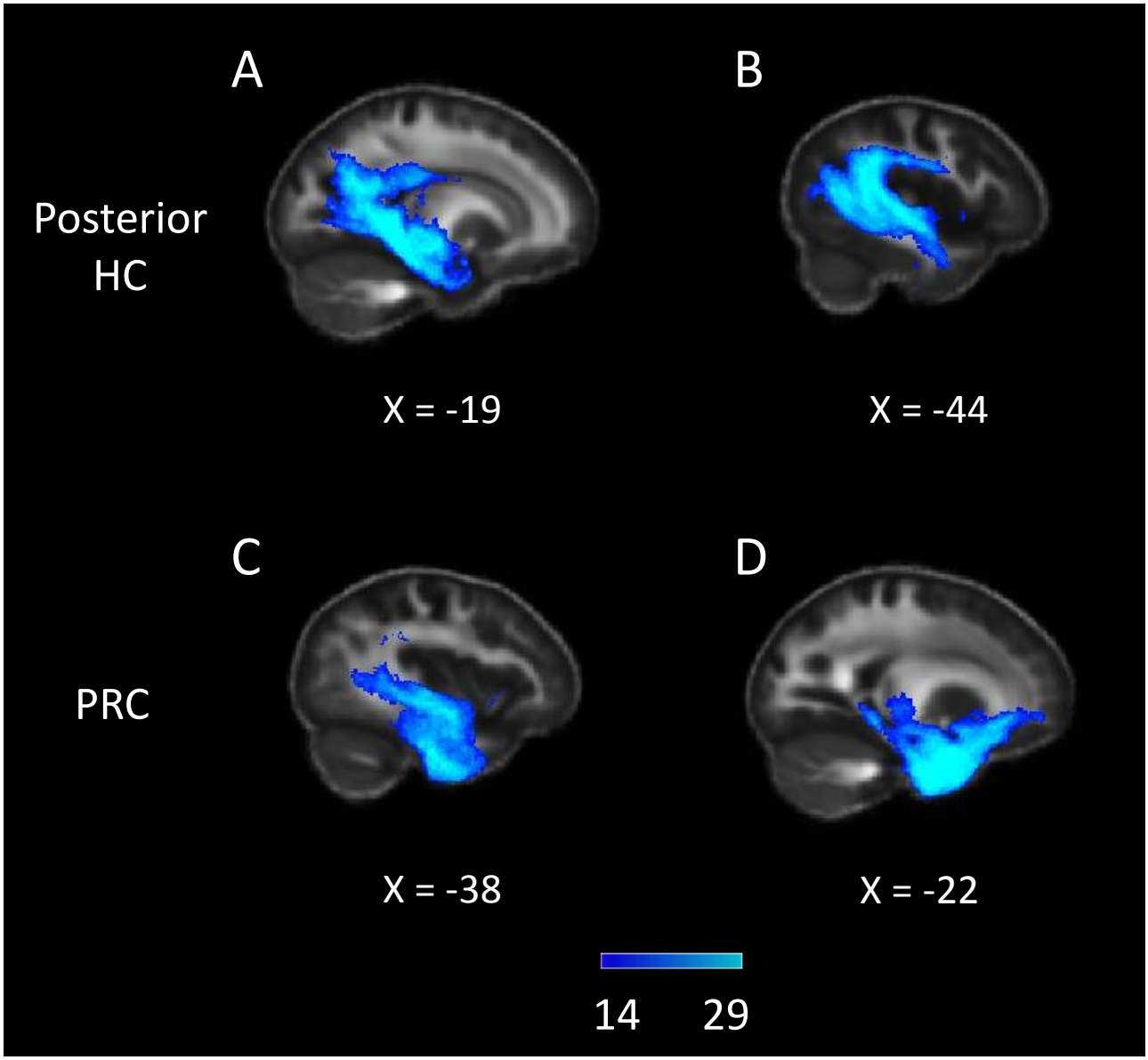

Figure 3.2. White matter connectivity probability maps highlighting (**A**) posterior HC projections via the parahippocampal cingulum, (**B**) posterior HC pathways via the ILF/IFOF/optic radiations, (**C**) PRC projections via the ILF/IFOF/optic radiations, and (**D**) PRC projections via the IFOF/uncinate fasciculus. The maps show all voxels – overlapping in at least 14 of 29 participants – that were intersected by at least 5 x 10^{-5}% of the streamline samples. All

connectivity maps are overlaid on sagittal sections of the group-mean FA image in standard MNI space.

The ROI-to-ROI connectivity probabilities between the posterior HC/PRC and the OFA, LOC, and TOS within each hemisphere were then quantified for each participant individually (Fig 3.3). The probability of connectivity between two ROIs is quantified as the number of successful connections, expressed as a proportion of all successful pairwise connections. For each MTL seed ROI (posterior HC and PRC), these connectivity probabilities were submitted to a 2 (Hemisphere: Left and Right) x 3 (Target ROI: OFA, LOC, and TOS) repeated measures ANOVA with a Greenhouse-Geisser adjustment for sphericity applied as per Gschwind et al., (2012), and a significance threshold of $p \leq 0.05$.

These analyses revealed that for the posterior HC (Fig 3.3*A*), there was no significant main effect of Hemisphere upon the connectivity probability metrics (F (1, 28) = 0.339, p = 0.565). There was, however a significant main effect of Target ROI (F (1.358, 38.023) = 63.891, p < 0.001), which subsequent planned pairwise comparisons revealed to be driven by a greater probability of connectivity with the TOS compared to both the OFA and the LOC (t (28) = -7.274, p < 0.001; t (28) = -6.374, p < 0.001, respectively); the probability of connectivity with the OFA was comparable to that with the LOC (t (28) = -1.914, p = 0.066). The Hemisphere x Target ROI interaction did not quite reach statistical significance (F (1.216, 34.047) = 3.834, p = 0.051). This pattern of results indicates that, consistent with the study predictions, the probability of direct connectivity between the posterior HC and an EVC region that responds preferentially to scene stimuli (TOS) is greater than that between the posterior HC and EVC regions that respond preferentially to object-like stimulus categories (OFA and LOC).

Turning to the PRC (Fig 3.3*B*), there were no significant main effects of Hemisphere or Target ROI upon the probability of connectivity with the OFA, LOC, and TOS (F (1, 28) = 0.077, p = 0.784; F (1.136, 31.803) = 3.595, p = 0.062, respectively), and the interaction between these factors was non-significant (F (1.308, 36.635) = 0.015, p = 0.946). This pattern of results indicates that, contrary to the present predictions, the probability of connectivity between the PRC and EVC regions that respond preferentially to object-like stimulus categories (OFA and LOC), was no greater than those between the PRC and the TOS, the latter of which responds preferentially to scene stimuli.

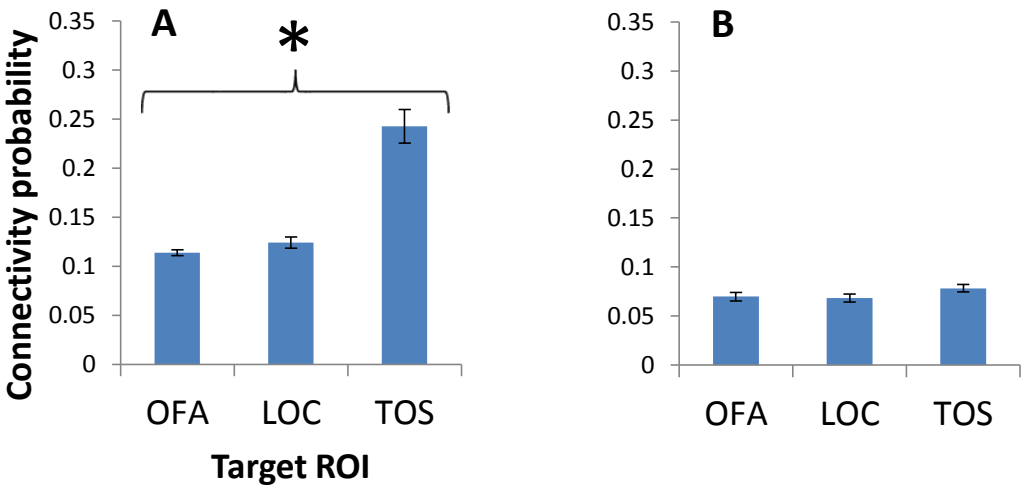

Figure 3.3. (**A**) Connectivity probabilities between the posterior HC and the OFA, LOC, and TOS. (**B**) Connectivity probabilities between the PRC and the OFA, LOC, and TOS. The connectivity probability between two ROI's is quantified as the number of successful connections, expressed as a proportion of all successful pairwise connections. The data is collapsed across Hemisphere for clarity. Asterisk indicates a significant difference between connectivity probabilities at $p < 0.001$ across both hemispheres. Error bars indicate the standard error of each pairwise connectivity probability.

It is possible that direct connections between the posterior HC and the TOS were more reproducible relative to connections between posterior HC and OFA/LOC, not because the former are in fact preferentially connected with one another, but simply because of the inherent proximity bias that is associated with probabilistic tractography.

Although the EVC target ROIs adopted for this study were selected precisely because they are spatially displaced from the HC/PRC by a comparable extent along the posterior-anterior axis of the brain, streamlines were, therefore, once again propagated between the posterior HC and each target EVC ROI, but with the 'distance correction' function enabled in FDT. This multiplies the number of connections successfully propagated between a given seed and target ROI by the average length of the streamlines reaching the target. As the resulting connectivity maps were essentially weighted by the average distance between the seed and target ROIs, it was possible to investigate whether the differential connectivity probabilities between the HC and the TOS/OFA/LOC reported above can actually be explained in terms of ROI-to-ROI

spatial-displacement rather than preferential connectivity *per se*. For each participant, the total number of the distance-weighted streamlines successfully propagated between the posterior HC and each ROI, was again expressed as a proportion of the total number of successful pairwise distance-weighted connections between the posterior HC and *all* target EVC ROI's, and submitted to a 2 (Hemisphere: Left and Right) x 3 (Target ROI: OFA, LOC, and TOS) repeated measures ANOVA.

After weighting the streamlines by distance-travelled, there was a significant main effect of Hemisphere on the connectivity probability metrics, which was driven by a generally higher probability of connectivity between MTL and EVC ROI's in the right compared to the left hemisphere (F (1, 28) = 15.712, $p < 0.001$). There was also a main effect of Target ROI (F (1.290, 36.120) = 72.988, $p < 0.001$), driven by a greater probability of connectivity with the TOS compared to both the OFA and LOC (t (28) = -9.824, $p < 0.001$; t (28) = -8.109, $p < 0.001$, respectively), and a greater probability of connectivity with the LOC compared to OFA (t (28) = -2.089, $p = 0.046$). The Hemisphere x Target ROI interaction effect was also significant (F (1.177, 32.947) = 16.140, $p < 0.001$), and was driven by a greater probability of connectivity with the TOS in the right compared to the left Hemisphere (t (28) = -4.342, $p < 0.001$), whereas the probability of connectivity with both the OFA and the LOC was comparable across Hemispheres (t (28) = -0.355, $p = 0.725$; t (28) = -0.749, $p = 0.460$). These follow-up results should be considered with caution because the linear approach to applying corrections for the distance bias in probabilistic tractography, which is made available by FDT, is unlikely to be optimal. Indeed, recent investigations have found that with increasing distance between the seed and target ROIs, both the true-positive and false-positive connection rate increase when this distance correction procedure is applied (Azadbakht et al., 2015). This underscores the importance of having initially taken account of the distance bias problem on a largely *a priori* basis, by focusing on target ROI's that are spatially displaced from the target ROI by a comparable distance along at least the posterior-anterior axis of the brain, and then interpreting the resulting data without these distance 'corrections'. Indeed, many similar studies do not adjust the connectivity probability metrics (e.g. Gschwind et al., 2012). Nevertheless, these additional findings are reported here as complementary to the main analysis reported above, as they do at least highlight that there was no evidence that the greater reproducibility of connections between the posterior HC and the TOS, relative to both the OFA and LOC, can be directly attributed to differential spatial displacement of these EVC regions from the posterior HC alone.

In summary, the findings reported above imply that the posterior HC is preferentially connected to scene-sensitive (e.g. TOS) compared to face (e.g. OFA) and object (e.g. LOC) sensitive visual cortices. There was no evidence for more reproducible direct white matter connections between the PRC and early visual cortices that we know from previous studies, and Chapter 1, respond preferentially to object-like visual categories (e.g. OFA and LOC) compared to those that respond preferentially to images of visual scenes (e.g. TOS).

3.3.3. Analysis 2 – Influence of ILF and fornix structure on PRC and posterior HC BOLD activity

3.3.3.1. Tractography measures

The reader is reminded that the second analysis conducted here was carried out to investigate whether the magnitude of category-selective BOLD responses in the PRC and posterior HC during the duration-detection task reported in Chapter 2 would be related to inter-individual variation in the structural properties of their primary input/output pathways. For the PRC it was anticipated that inter-individual variation in the magnitude of the face/object-sensitive BOLD responses of this region would correlate with measures of ILF macro- and microstructure. In contrast, it was anticipated that the magnitude of scene-sensitive BOLD responses in the posterior HC would correlate with measures of fornix macro- and microstructure.

Table 3.2 shows the mean and standard deviation of values obtained for FA, MD and *f* in the fornix and the ILF. Prior to reporting the analyses testing the key hypotheses (see above), the relationship between FA, MD and *f* was assessed by calculating correlation coefficients between each measure for each tract for all 29 participants. Fornix FA was correlated with both fornix *f* and MD (r = 0.765, p < 0.001, 95% CI [0.564, 0.890]; r = -0.584, p = 0.001, 95% CI [-0.790, -0.248], respectively). Fornix MD and *f* were also highly correlated (r = -0.608, p < 0.001, 95% CI [-0.812, -0.305]). Turning to the ILF, MD and *f* were highly correlated (r = -0.941, p < 0.001, 95% CI [-0.971, -0.888]). ILF FA was non-significantly correlated with both ILF MD and *f* (r = -0.071, p = 0.714, 95% CI [-0.502, 0.356]; r = 0.141, p = 0.464, 95% CI [-0.290, 0.576]). This pattern of inter-correlations (which is replicated in Chapters 4-5) indicates that the diffusion MRI measures reported here share a significant amount of variance, particularly in the fornix. The measures are not, however, proposed to be strictly independent. Indeed, there is no one-to-one correspondence between each of these

metrics and a specific component of white matter microstructure (Jones et al., 2013). These measures may, however, be differentially sensitive to variation in different white-matter properties which may in turn vary in their functional significance for a given task. Indeed, previous studies have reported significant structure-function correlations with one of either FA or MD, in the absence of a significant correlation using the other metric (e.g. Metzeler-Baddeley et al., 2011). The full range of structure-function correlations are therefore reported here for completeness.

Table 3.2. Mean FA, MD ($x10^{-3}mm^2\ s^{-1}$), and *f*, in both the fornix and the ILF of all 29 participants. Standard deviations are provided in brackets.

Tract	FA	MD	*f*
Fornix	0.373 (0.026)	1.044 (0.042)	0.721 (0.039)
ILF	0.422 (0.019)	0.749 (0.014)	0.898 (0.009)

3.3.3.2. Contrasts – PRC

Analyses within the bilateral PRC mask revealed a cluster of voxels in the left hemisphere in which there was a significant negative association between the inter-subject BOLD response to Faces + Objects > Scenes (F + O > S), and inter-individual variation in ILF MD (*x* = -27, *y* = -6, *z* = -41, zmax = 3.07, 30 voxels, Fig 3.4*A*). A larger cluster was detected for the association between the BOLD response to Faces > Scenes (F > S; i.e. once the object condition was removed from the statistical contrast) and ILF MD (*x* = -27, *y* = -4, *z* = -42, zmax = 3.71, 70 voxels, Fig 3.4*B*). The same substantial cluster was also evident for the association between the BOLD response to Faces > Objects + Scenes (F > O + S) and ILF MD (*x* = -27, *y* = -4, *z* = -42, zmax = 3.68, 68 voxels, Fig 3.4*C*).

Similarly, the BOLD response to Faces > Scenes was positively and significantly associated with ILF *f* (*x* = -27, *y* = -5, *z* = -42, zmax = 3.11, 49 voxels, Fig 3.*D*). The same cluster was evident for the association between the BOLD response to Faces > Objects + Scenes (F > O + S) and ILF MD (*x* = -27, *y* = -4, *z* = -42, zmax = 3.31, 54 voxels, Fig 3.4*E*). There were no PRC clusters reflecting a statistically significant

association between any other inter-subject BOLD response contrast (e.g. O > S or S > O) and diffusion properties of the ILF (FA, MD, or *f*).

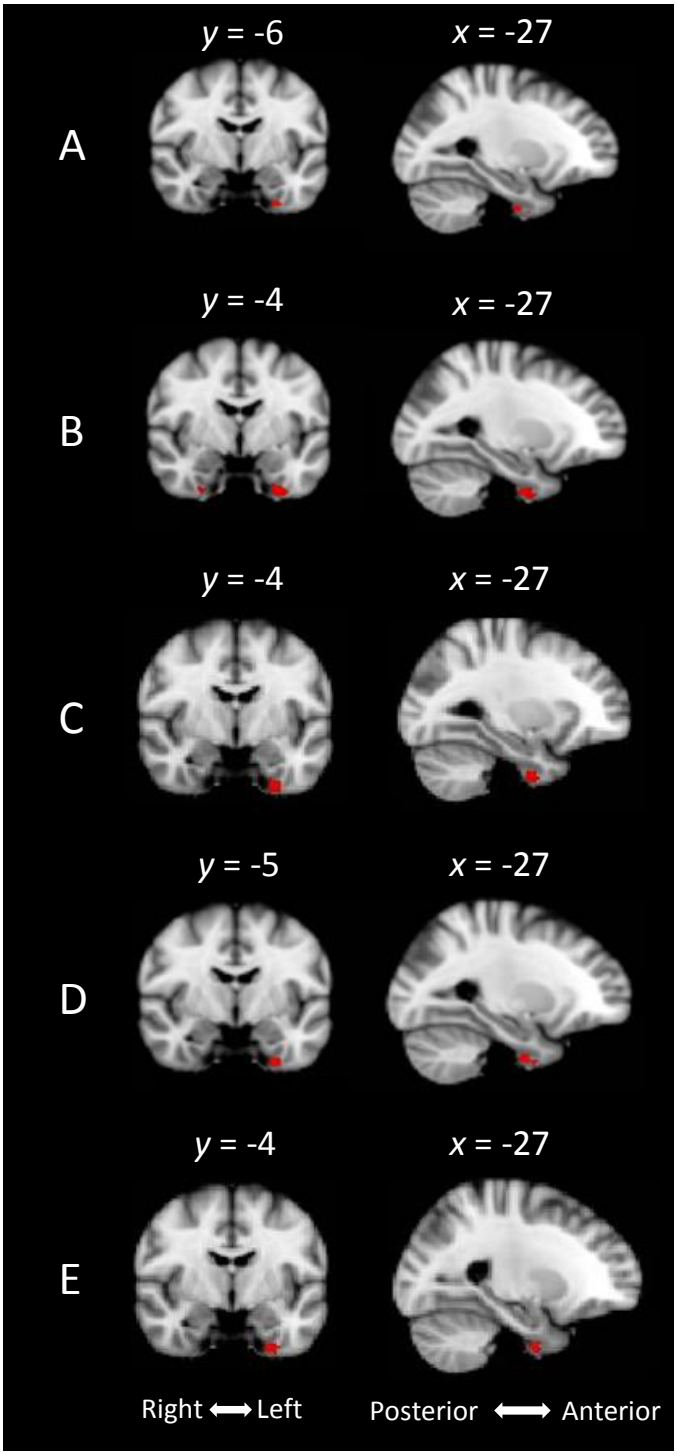

Figure 3.4. (**A**) Cluster in the left PRC reflecting a significant negative association between the inter-subject F + O > S BOLD contrast and ILF MD. (**B**) Left PRC clusters reflecting a significant negative correlation between the F > S BOLD contrast and ILF MD. (**C**) Left PRC clusters

reflecting a significant negative relationship between the inter-subject F > O + S BOLD contrast and ILF MD. (**D**) Left PRC cluster reflecting a significant positive association between the inter-subject F > S BOLD contrast and ILF *f*. (**E**) Left PRC cluster reflecting a significant positive association between the inter-subject F > O + S BOLD contrast and ILF *f*. All significant clusters (red voxels) are shown on a standard MNI 152 2mm brain template.

These findings are consistent with a role for the PRC in the processing of face stimuli in particular. They are also consistent with the proposition that the formation of complex face representations in the PRC is dependent upon the successful propagation of information between this region and other lower-level EVC regions, via the ILF. With a view to identifying some of these earlier regions, the 5 statistical contrasts that revealed significant clusters within the PRC (see above) were subsequently repeated within the broader search-space that is circumscribed by the mask of occipito-temporal cortex that was previously applied to the PPI analysis in section *2.2.7.2*. When applied to this broader search-space, these 5 contrasts revealed – in addition to the aforementioned clusters in PRC – several relatively posterior brain regions that have previously been implicated in face processing, including, notably, the OFA and superior temporal sulcus (STS; Table 3.3 below).

Table 3.3. Regions beyond the PRC in which inter-individual variation in the magnitude of the object and/or face-selective BOLD response was found to be related to inter-individual variation in ILF MD or *f*

N voxels	z-max	*x*	*y*	*z*	Brain Region
(Faces + Objects > Scenes) & ILF MD					
143	3.72	-32	-86	-15	Left occipito-fusiform gyrus (incorporates OFA)
(Faces > Scenes) & ILF MD					
166	3.94	-32	-87	-16	Left occipito-fusiform gyrus (incorporates OFA)
47	3.49	-54	-54	7	Left STS
(Faces > Objects + Scenes) & ILF MD					
146	3.79	-51	-53	7	Left STS
116	3.64	-34	-87	-16	Left occipito-fusiform gyrus (incorporates OFA)
(Faces > Scenes) & ILF f					
144	3.83	-32	-87	-16	Left occipito-fusiform gyrus (incorporates OFA)
38	2.67	-15	-97	4	Left occipital Pole
(Faces > Objects + Scenes) & ILF f					
122	3.66	-34	-87	-15	Left occipito-fusiform gyrus (incorporates OFA)
85	3.28	-50	-53	7	Left STS
70	3.86	1	-82	47	Left precuneus
62	2.93	-15	-96	0	Left occipital pole

3.3.3.2. Contrasts - HC

Analyses within the bilateral mask of the posterior HC revealed no clusters in which there was a significant association between any of the planned inter-subject BOLD contrasts (e.g. S > F, S > O, S > F + O, F > S etc) and fornix FA, MD, or *f*. Given the lack of an effect within this ROI, the analyses were not subsequently expanded to include broader regions of occipito-temporal cortex in order to avoid reporting false-

positive effects in regions for which we had limited or no specific hypotheses (see section *3.2.7.2.2*).

3.4. Discussion

Understanding how white matter pathways map onto category-sensitive functional activations across the healthy brain is necessary to enable researchers to describe the interactive functional networks that subserve visual perception for distinct stimulus categories. Further, identifying the relationship between inter-individual differences in properties of the structural pathways that support inter-regional communication within these networks, and the activity within their constituent regions will help us understand the neural factors underpinning inter-individual variation in behavioural measures of perception. This study has contributed findings relevant to both of these goals. The first analysis employed a combination of task-related fMRI, diffusion MRI and *probabilistic tractography* to demonstrate a greater probability of direct connectivity between the posterior HC and a functionally-defined EVC region that responds preferentially to scene stimuli (TOS), compared to other EVC regions that respond maximally to object-like stimulus categories (OFA and LOC); this difference could not be attributed to differences in the spatial displacement of the OFA, LOC, and TOS from the posterior HC. By contrast, the PRC was not found to possess more reproducible connections with the OFA and LOC compared to the TOS. In a second analysis, which employed task-related fMRI, diffusion MRI and *deterministic tractography*, the magnitude of face-sensitive BOLD responses in the left PRC was found to be related to inter-individual differences in measures of white matter micro- (MD) and macro-structure (*f*) in the ILF. The magnitude of scene-sensitive BOLD responses in the posterior HC, however, was not found to correlate with inter-individual differences in measures of fornix micro- (MD) and macro-structure (*f*).

That direct connections between the posterior HC and a scene-selective EVC region (TOS) are more reproducible than those between the posterior HC and EVC regions that are selective for other categories of stimuli (OFA and LOC), is consistent with the notion that higher-level scene perception depends upon HC interactions with other regions within an extended network or stream of scene processing regions (Zeidman et al., 2014). The TOS was of particular interest because it is known to respond preferentially to scenes compared to images of object-like stimuli (Bettencourt and Xu,

2013), and because transcranial magnetic stimulation (TMS) of the TOS impairs the discrimination of scenes but not faces (Dilks et al., 2013).

Compared to other scene-sensitive brain regions (e.g. HC and PPA), however, the precise role of the TOS in scene perception has received sparse attention in the literature, as has its connectivity to other anterior scene processing regions, including the posterior HC. Tract tracer work in animals has shown that the HC possesses both direct and indirect anatomical connections to early visual areas in posterior parietal cortex, including the posterior inferior parietal lobule (pIPL) (Kravitz et al., 2011; Rushworth et al., 2006). The pIPL, which actually overlaps the functionally defined TOS in some individuals (Baldassano et al., 2013), is, in turn, reciprocally connected to numerous subdivisions of the occipital cortex via an occipital-parietal pathway, thereby providing a potential, albeit indirect, route for HC-TOS interactions.

This is, however, the first study that has investigated *direct* white matter connections between the posterior HC and the TOS. Such connections might afford the rapid feed-forward transmission of lower-level spatial information to the posterior HC, thus bypassing sequential processing across intermediate occipito-temporal cortex. This proposal is similar to the notion that information about the affective relevance of face stimuli is rapidly propagated from occipital cortex to the amygdala via direct connections, thereby bypassing slower sequential processing in intermediate occipito-temporal regions (Vuilleumier et al., 2005), but should be treated cautiously given that little is presently known about the precise contribution of the TOS to early scene processing. Alternatively, direct HC-TOS connections might support feedback influences upon cortical processing within the TOS, in the same way that HC activity has been shown to exert a top-down influence on activity in a spatially distinct region of early visual cortex during a scene boundary-extension paradigm (Chadwick et al., 2013). It is important to note, however, that tractography produces bi-directional streamlines, so it is not possible here to determine whether a reconstructed connection is afferent or efferent in nature.

Whilst the current finding implies the presence of a direct connection between posterior HC and TOS, the limitations of DTI-based probabilistic tractography must be noted. For instance, when the reproducibility of a connection between two voxels is represented as being very high on a probabilistic tract map, this does not necessarily indicate that a direct connection between these points in space is present in the brain itself. In other words, false-positive connections can be returned by tractography (Jones, 2008). One cause of both false-positive and false-negative connections in tractography is the

crossing-fiber problem. This arises due to the lower spatial resolution of DTI with respect to the fine spatial scales that are spanned by individual axons, which means that a single diffusion tensor is inadequate to completely characterise all of the fiber orientations within a voxel (Jones, 2008). This can lead to the conflation of distinct fiber populations and orientations, reducing the accuracy of reconstructed streamline trajectories. This may be relevant here because the HC is situated just medial to several prominent white matter pathways that project towards/from posterior visual areas, including the optic radiations, ILF, and the fronto-occipital fasciculus. It is possible that direct connections between the HC and TOS may have been reconstructed as a result of the proximity of the HC to these prominent pathways. In addition, the HC borders the PHC, from which probabilistic tractography has been successfully employed to track connections with both posterior parietal (including pIPL) and superior occipital cortex (Rushworth et al., 2006). The broad PHC projection pathway that was reconstructed in this previous study incorporated a medial route in or adjacent to the parahippocampal cingulum, and lateral fibers of the optic radiations and the ILF. Although a 2-fiber probabilistic model was employed here to reduce the impact of crossing fibers on the accuracy of tract reconstructions, the same pathways could be visualised in the current study, suggesting that they could also have potentially arisen due to contamination with tracts emanating principally from PHC. Whilst the current study therefore highlights a stronger *probabilistic* connectivity of the posterior HC with the TOS, relative to the OFA/LOC, such a connection remains to be confirmed in the brain itself.

In contrast to the posterior HC, it was anticipated that connections between PRC and face/object-selective EVC regions (OFA and LOC) would be more reproducible than those between PRC and the scene-sensitive TOS. This would be consistent with a distinct role for the PRC as an anterior component of a visual network that is specialised for processing the non-spatial feature-conjunctions that define individual object-like stimuli (Graham et al., 2010; Saksida and Bussey, 2010). This pattern of preferential connectivity, however, was not borne out by the current study. This could, arguably, indicate that PRC contributions to face/object processing do not depend upon direct interactions with early face/object-sensitive EVC regions. Consistent with this interpretation, O'Neil et al., (2014) reported that the PRC demonstrates reliable resting-state functional connectivity with the FFA and amygdala, but not the more posterior face-sensitive OFA. On the basis of their findings, O'Neil and colleagues suggested that the FFA may act as a cortical hub through which the OFA may *indirectly* convey

lower-level information about face stimuli to the PRC. The notion that the FFA may act as an important hub for information – about face stimuli in particular – to be relayed to PRC is consistent with the findings of the functional connectivity analysis reported in section 2.3.4; activity in the right FFA was found to be more strongly correlated with that of the right PRC during the presentation of faces compared to other visual categories (objects and scenes). Against this view, however, long-range feedback connections have been successfully traced between PRC and visual areas as early as area V1 in monkeys (Clavagnier et al., 2004). Pyles et al., (2013) also recently demonstrated that some direct connections – travelling via the ILF – can be reconstructed between OFA and the anterior temporal lobe (which includes PRC) in humans. These previous findings suggest that human PRC contributions to perception may indeed require direct interactions with *some* early visual cortices, and that these interactions do not necessarily depend upon intermediate EVC hub regions. Furthermore, as discussed in further detail below, face-sensitive BOLD responses in both the left OFA and PRC were found to be correlated with diffusion MRI measures of ILF properties in the second analysis reported in section 3.3.3.2. This suggests that successful higher-level face perception may indeed be dependent upon direct functional interactions between early (OFA) and late (PRC) face processing regions, and that these interactions may be facilitated by direct white matter connections, for example via the ILF. Indeed, some successful connections could be reconstructed here between the PRC and both OFA/LOC, mostly via a posterolateral projection pathway that overlapped the known anatomy of the ILF; these connections were simply no more statistically reproducible than were those between the PRC and TOS.

In terms of why such direct PRC connections with OFA (but also potentially with LOC) were not found to be more reproducible here than those with TOS, this could potentially reflect technical difficulties associated with accurately reconstructing long-range white matter connections via probabilistic tractography. The limited spatial resolution of DTI-based tractography, for example, may render the technique insufficiently sensitive to small long-range PRC-EVC connections, although, as noted above, one small-scale tractography study (sample size N = 5) has recently reported that it is possible to reconstruct some anatomically plausible connections between the OFA and the anterior temporal lobe (Pyles et al., 2013). Difficulties in resolving crossing-fiber populations may also have been detrimental to the accurate and *selective* propagation of streamlines to the OFA/LOC. In this context it is worth noting that the prominent white matter bundle which is likely to carry PRC-EVC connections– the ILF – has been noted to pass through a region that contains multiple prominent fiber bundles, including

the fronto-occipital fasciculus, middle longitudinal fasciculus, superior longitudinal fasciculus and optic radiations (Martino et al., 2013). Even the 2-fiber probabilistic model used here may be sub-optimal for the accurate differentiation of all these fiber populations, thereby reducing the accuracy of the trajectories of the reconstructed streamlines. Indeed, whilst a set of posterolateral PRC projections to EVC via the ILF were reproducible here, these were contaminated with fibers from the superior longitudinal fasciculus (see section 3.3.2). The PRC has also been found to be connected to lateral orbitofrontal cortex (LOFC) via the fronto-temporal white matter pathway; the uncinate fasciculus (Ungerleider et al., 1989; Kondo et al., 2005). Though the LOFC and uncinate fasciculus are not directly relevant to the current thesis, at the thresholds reported here, streamlines reflecting the uncinate fasciculus were reconstructed from the PRC. Again, direct trackability of PRC-OFA/LOC connections via the ILF may have been hindered by contamination with these local uncinate fasciculus fibers. Technical improvements in diffusion MR imaging and fiber modelling may, however, facilitate informative investigations of probabilistic PRC connectivity.

The second analysis revealed that the magnitude of category-sensitive BOLD responses in the left PRC is related to inter-individual differences in the micro- and macrostructural properties of the ILF. More specifically, the preferential BOLD response of the left PRC to faces relative to scenes, in particular, was found to be related to individual differences in diffusion MR measures of ILF micro- (MD) and macrostructure (*f*). These findings are compatible with several fMRI studies in which PRC responses to face stimuli were found to be greater relative to those elicited by scene stimuli (Mundy et al., 2012; Barense et al., 2010; Lee et al., 2008), and with proposals that complex representations of the non-spatial feature-conjunctions that define individual object-like stimuli are constructed and maintained in the PRC (Graham et al., 2010; Saksida and Bussey, 2010). Those previous studies were important in highlighting previously undisclosed category-sensitive PRC contributions to higher-level visual perception, but the conclusions that we could derive from them regarding PRC function are limited because they tended to focus on the *unique* contributions of the PRC to perception. Brain regions do not contribute to cognitive functions in isolation, however, but through interactions with other spatially distinct and functionally-related regions (Behrmann and Plaut, 2013). A key aim of this second analysis, therefore, was to investigate how the ability of the PRC to *communicate with other brain areas* influences category-sensitive BOLD activity in this MTL structure.

The current findings contribute to this aspiration by highlighting for the first time that the ability to propagate visual information along the ILF – as assessed by differences in diffusion MR measures of ILF structural properties - is an important source of variability in the BOLD response of the left PRC to its 'preferred' stimulus categories. This relationship was evident even though the duration detection task did not involve making an explicit memory or discrimination judgement. These findings suggest that higher-level face perception may depend, not only upon activation of the PRC itself, but also upon its ability to interact with earlier category-sensitive extrastriate regions via the ILF. As noted above, these interactions may be feed-forward in nature, whereby earlier extrastriate regions process lower-level non-spatial stimulus features, before propagating this information downstream for it to be integrated into more complex conjunctive stimulus representations within the PRC (Graham et al., 2010; Saksida and Bussey, 2010). Alternatively, these PRC interactions could also reflect iterative feed-back modulations of activity within extrastriate regions (O'Neil, 2013; Nestor et al., 2011). That these dynamic intra-network interactions via the ILF are necessary for higher-level face perception is further implied by the finding that inter-individual variation in ILF micro- (MD) and macrostructure (*f*) was also related to the magnitude of face-selective BOLD responses in a cluster of voxels within posterior occipito-fusiform cortex that corresponded well with the OFA, and another in the STS; both of which have previously been labelled as components of a 'core' face processing network (Haxby et al., 2000). That the ILF may be involved in the relay of visual information about faces is also consistent with earlier investigations highlighting that the volume of the ILF is correlated with the size of the FFA but not the PPA (Scherf et al., 2014). These conclusions also converge with those of previous studies demonstrating that both the functional and structural connectivity of extrastriate and anterior temporal regions is compromised in congenital prosopagnosia (Thomas et al., 2009; Avidan et al., 2014).

In terms of why the magnitude of the PRC BOLD response to objects relative to that for scenes, was not related to individual variation in measures of ILF micro- or macrostructure, the reader is referred to section 2.4, where I point out that the PRC is less engaged by the current artificial objects compared to the face stimuli. Further, PRC damage has been less consistently associated with visual discrimination impairments for objects compared to faces (Lee et al., 2005a). This might indicate that face stimuli inherently possess a higher degree of feature overlap/ambiguity than most classes of objects, and so the processing of face stimuli is *de facto* more dependent upon the complex representations instantiated within the PRC than are objects. If this

interpretation is correct and faces are a special class of object-like stimuli that are particularly dependent on PRC representations owing to their relatively high visual complexity, then it may be possible for future studies to demonstrate a link between ILF properties and BOLD responses to non-face object-stimuli, but only for sub-categories of objects that are characterised by greater visual complexity than the artificial objects employed here (e.g. fribbles with more features/conjunctions or 'greebles'; see Barense et al., 2010).

Owing to the correlational nature of this second analysis, it is difficult to infer the direction of causality between ILF properties and PRC activity. Microstructural properties like axon myelination modulate the neural conduction velocity along white-matter pathways, and could therefore directly affect PRC function by influencing "the timing of sequential events" and the efficiency of information transfer across the extended object processing stream (Peters, 2002, pp585). This causal interpretation should be treated cautiously, however, as recent studies have reported experience-dependent changes in measures of white-matter microstructure in a number of pathways (Scholz et al., 2009); these findings suggest that variation in microstructural properties could also be a response to visual expertise. Neural activity-dependent mechanisms could stimulate myelination, for example, leading to increased efficiency of information transfer across a white matter pathway (McKenzie et al., 2014). This would be consistent with evidence that ILF microstructure undergoes protracted developmental changes that are tightly linked to age-related increases in the size of another functionally-defined face processing region that sits alongside the ILF; the FFA (Scherf et al., 2014). This interpretation (i.e. visual experience precedes changes in ILF macro-/microstructure) also offers a potential mechanism by which the visual processing stream that culminates in the PRC becomes organised and optimised for the successful processing of object-like stimuli over time (Scherf et al., 2014; Behrmann and Plaut, 2013).

MD but not FA was sensitive to the relationship between ILF microstructure and category-selective BOLD responses in the PRC. This may reflect the greater sensitivity of the former to age-dependent changes in microstructural attributes of the ILF (Scherf et al., 2014). It is not currently possible to attribute the discrepancy between our FA/MD findings to a single underlying white-matter attribute, however, because both of these metrics are sensitive to a wide range of axonal properties, including myelination, density, and diameter (Jones et al., 2013). MRI techniques that afford investigation of specific attributes of white-matter microstructure may offer a means for future studies to pursue more specific biological correlates of the effects reported here (e.g. axon

myelination; Alonso-Ortiz et al., 2014). *f* was also found to be related to the magnitude of the preferential PRC BOLD response to faces relative to scenes. This is interesting in the context of previous research highlighting that the overall volume of the ILF also increases with age (Scherf et al., 2014), which may indicate that experience-dependent macrostructural changes can also facilitate the gradual optimisation of the putative object processing stream over time.

There were no clusters in the posterior HC in which the magnitude of scene-sensitive BOLD responses was related to inter-individual variation in properties of the principal HC input/output pathway; the fornix. This might be taken to indicate that HC contributions to scene processing are not related to the ability of the posterior HC to communicate with other brain regions via the fornix. This seems unlikely given that fornix as well as HC damage produces behavioural impairments in spatial processing tasks. Fornix damage impairs, for example, the learning of concurrent visual discriminations based on multiple spatial stimulus features (Buckley et al., 2004), and performance in object-in-scene memory tasks (Gaffan, 1994).

It is, however, worth highlighting that whilst the current scene stimuli consistently activated both the PPA and posterior HC (sections 2.2.3.2 and 2.2.3.5, respectively), the participants were not required to make an explicit memory or perception judgement for each scene stimulus. This discrepancy between the current task demands and those employed in earlier fornix transection studies in nonhuman animals could potentially be informative here. It may be the case that: 1) the posterior HC is engaged by scene stimuli independently of any explicit demands on memory or perception, as demonstrated in Chapter 2, but 2) functional interactions across the 'extended HC network', of which the fornix is one component (Gaffan, 1994), are more important in the context of the explicit processing of the complex spatial properties comprising those visual scenes. For future studies of this kind, therefore, it will be important to investigate whether variation in fornix properties is indeed predictive of the magnitude of scene-sensitive BOLD responses in the posterior HC when the participant is required to provide explicit perception judgements to sets of visually similar scene stimuli. One paradigm that may be suitable here is the different-view scene oddity task, which requires participants to discriminate visually similar scenes presented from different viewpoints, and is known to elicit reliable BOLD responses in the HC (Lee et al., 2012; Lee et al., 2008). Another potentially suitable paradigm is the visual discrimination paradigm reported by Mundy et al., (2013), in which participants are required to make explicit same/different discrimination judgements to pairs of visually

similar faces and scenes. The scene discrimination condition of this latter task also engages the posterior HC (Mundy et al., 2013), and a version of this is described in more detail in Chapter 4, where it is employed to investigate the differential contribution of the fornix to visual discrimination accuracy for scenes versus faces.

An advantage of the targeted and deterministic tract reconstruction approach adopted for this second analysis was that it bypasses the technical difficulties associated with tracking directly from MTL gray matter regions via probabilistic tractography, and it affords the removal of false-positive streamlines that are not consistent with real brain anatomy or a specific tract-of-interest. Furthermore, by initially constraining the planned analyses to a small number of circumscribed tracts and regions-of-interest, this approach reduces the risk of reporting a) false-positive effects in regions for which we have no specific predictions and b) false-negative effects where true structure-function relationships are obscured due to corrections for large numbers of statistical comparisons. Another advantage of the targeted tract reconstruction approach adopted here is that it may be more sensitive to subtle long-range differences in white-matter microstructure compared to voxel-based DTI methods (Keedwell et al., 2012). Furthermore, the impact of partial volume artefacts upon the accuracy of diffusion MR indices of white matter microstructure is likely to be small when averaged across every voxel in the reconstruction, whereas they could have a substantial impact upon the accuracy of metrics extracted from individual voxels. To further improve the accuracy of FA/MD metrics here, however, rigorous correction for partial-volume artefacts due to free-water contamination was also applied to every voxel of the raw diffusion-weighted images, using the FWE method (Pasternak et al., 2009).

This is not to say that the deterministic tractography approach used in analysis 2 is superior to the probabilistic approach applied in analysis 1, or *vice versa*. As outlined in section 3.1, the two approaches are simply better suited to addressing different questions about ‘connectivity’. The probabilistic tractography protocol enabled the tracking of white matter connections from/toward/within specific gray matter ROIs and provides a measure of the reproducibility of direct connections between spatially dispersed brain regions. By contrast, deterministic tractography protocols typically include constraints designed to prevent white matter streamlines being propagated from/toward/within gray matter regions. Further, the deterministic approach does not produce any measure of the reproducibility of a given connection, and it would therefore have been unsuitable for the first analysis. The deterministic approach was, however, suitable in the context of the second analysis which sought to relate category-

sensitive BOLD responses in the PRC/posterior HC to variation in the structural properties of specific white matter pathways. This is because, as noted above, it enabled the removal of false-positive connections from the tract of interest, and ensured that the reconstructions were not contaminated with gray matter voxels, which would otherwise affect the accuracy of diffusion MRI estimates of white matter micro- and macrostructure extracted from the fornix/ILF. On a related point, it is important to note that there is no discrepancy in the findings of the two analyses reported here, because these analyses address different research questions. For example, fibers within the ILF could be reconstructed in both analyses. The results of the first and the second analysis with respect to the ILF could nevertheless be non-significant and significant, respectively, precisely because the two analyses addressed distinct questions about the role of this white matter tract in visual perception. More specifically, analysis 1 was designed to test whether direct connections between the PRC and face/object-selective EVC regions (OFA and LOC) were more reproducible than those between PRC and the scene-selective TOS, whereas analysis 2 asked whether individual variation in ILF properties would be predictive of the magnitude of face-selective PRC BOLD responses.

In summary, the current study provides evidence that direct connections between the posterior HC and a region of scene-sensitive extrastriate cortex (TOS) are more reproducible than those to local non scene-sensitive cortices (OFA and LOC), consistent with a role for the posterior HC as a component of an interactive network of scene processing regions. In addition, the magnitude of the preferential BOLD response of the left PRC to faces in particular, was related to individual differences in diffusion MR measures of ILF micro- (MD) and macrostructure (*f*), consistent with a role for the ILF in relaying visual information along the putative object processing stream. These novel findings extend recent representational accounts of MTL function (Graham et al., 2010; Saksida and Bussey, 2010) by highlighting category-sensitive contributions of white matter pathways, as well as gray matter functional nodes, to higher-level visual processing. It is important to understand the link between structure and category-sensitive functional activations in the healthy brain, but the present findings prompt us to ask whether inter-individual variation in the structural properties of MTL white matter pathways might also relate to behavioural outcome measures of perception. The current task did not require participants to make an active perception/memory decision, so this question is addressed in the remaining experimental Chapters using a combination of previously reported behavioural paradigms, diffusion MRI, and white matter tractography.

Chapter 4: Dissociable roles for the fornix and inferior longitudinal fasciculus in discrimination accuracy for scenes and faces

Note: Some of the work reported in this Chapter was also recently published in Postans et al., (2014).

4.1. Introduction

Previous MRI investigations of how the brain supports perception have frequently focused on the preferential BOLD response of functionally- or anatomically-defined ROIs to exemplars from specific visual categories, such as faces and scenes. In Chapter 2, for example, I reported a modified version of the fMRI experiment described by Mundy et al., (2012), which demonstrated that the FFA and PRC respond preferentially to images of faces compared to other visual categories, whereas the PPA and posterior HC respond preferentially to images of visual scenes (section 1.4.4). This work, as well as related studies outlined in Chapter 1, has provided valuable insights into how multiple regions within EVC and the MTL make distinct category-sensitive contributions to visual perception (Mundy et al., 2012; Downing, 2006), consistent with emerging representational accounts of these cognitive functions (Graham et al., 2010; Saksida and Bussey, 2010). Despite the striking degree of functional specialization that such studies imply, however, individual gray matter regions must interact with other functionally-related areas in order to support those 'emergent' cognitive processes with which they are associated (Behrmann et al., 2013). This point was elucidated in Chapter 2 with a functional connectivity analysis, the results of which suggested that the PRC and posterior HC contribute to face and scene processing, respectively, via distinct patterns of inter-regional functional interactions (e.g. PRC = FFA; posterior HC = lingual gyrus), consistent with the 'two streams' conception of visual processing (section 1.6.2). As explained in Chapter 3, PRC and HC interactions with other functionally-related brain regions are also supported by white matter connections. Two prominent white-matter pathways are of particular interest because one acts primarily as a HC input/output pathway and may therefore play an important role in higher-level

scene processing, whereas the other is a prominent input pathway for the PRC and may therefore play a relatively specialised role in higher-level face/object processing; these are the fornix and the ILF, respectively.

The reader is referred to section 1.1.4 for detailed anatomical descriptions, but briefly, the fornix is a prominent white-matter tract linking the HC to several subcortical (e.g. anterior thalamic nuclei [ATN], mammillary bodies [MBs]) and cortical (e.g. prefrontal cortex) brain regions (Saunders and Aggleton, 2007). Given that these gray matter areas are important for successful learning and memory (Aggleton, 2008), their ability to communicate with one another via the fornix, may, also be critical for performance in mnenomic tasks. Indeed, fornix transection in non-human primates is known to produce deficits in spatial memory paradigms that are also sensitive to HC lesions (e.g., object-in-scene memory tasks), consistent with the proposal that the fornix is one component of an extended HC-fornix-mammillary body-anterior thalamic network involved in the representation of complex visual scenes, and the arrangement of the objects within those scenes (Gaffan, 1994). More recently, Buckley et al., (2004) demonstrated that following fornix transection, macaque monkeys showed impaired concurrent visual discrimination learning between highly visually similar 'tadpole' stimuli that were individually defined by a number of spatial features (e.g. their orientation, position on a screen, and the length of their tails). In contrast to these spatial learning and memory impairments, however, fornix lesions in animals typically spare recognition of individual objects (Bussey et al., 2000).

Studies in humans with fornix damage and concomitant cognitive impairments also highlight a key role for this white matter pathway in memory. Vann et al., (2008) reported a clinical case study involving patient DN, who had bilateral damage to the anterior columns of the fornix and the left septum following surgery to remove a cavernous angioma from the left lateral ventricle; DN was found to be impaired in tests of memory which required the free recall of pre-studied verbal and visual stimuli, but his performance in forced-choice verbal/visual recognition memory tests was comparatively spared. These striking findings were taken as evidence in favour of dual-process models of recognition memory, according to which a mnemonic process called recollection – supported by the extended HC network – enables the free recall of the details and context associated with a previously encountered item, whereas a process called familiarity – supported by the PRC – provides a measure of stimulus-recency (section 1.3.2). Clinical case studies must be interpreted with caution, of course, because there may be a potential bias in this literature for the selective reporting of

idiosyncratic cases that happen to demonstrate the particular patterns of deficits and dissociations that are predicted by a given model of memory (Brown et al., 2010). Tsivilis et al., (2008) therefore augmented these earlier findings by administering a variety of memory tests to a larger group of patients at high risk for fornix damage due to having had surgery to remove a colloid cyst from the third ventricle (N = 38); this investigation confirmed, in a larger sample of patients, that fornix pathology is associated with impaired performance in tests of recall, whereas performance in forced-choice recognition tests is relatively preserved (also Vann et al., 2009).

In the context of addressing the research questions raised in the current Thesis, however, the conclusions that we can draw from clinical studies like those described above with respect to fornix function, are limited by at least two important considerations. Firstly, fornix damage in humans is never complete and independent of additional pathology in other gray matter regions that may have functional relevance, such as the MBs (Vann et al., 2009; Aggleton, 2008). This renders it extremely difficult if not impossible to directly attribute behavioural/cognitive impairments to fornix pathology in isolation through clinical case studies alone. Second, previous clinical investigations of human fornix function have clearly tended to focus on predicted dissociations between stimulus category-general memory processes (e.g. recollection versus familiarity; Vann et al., 2008). As a consequence, there has previously been little clinical investigation of the preferential contributions of the human fornix to spatial versus non-spatial learning, memory, and perception.

An alternative to this clinical research approach is to investigate whether inter-individual variation in the structural properties of the healthy fornix is related to memory and perception for particular categories of visual stimuli. One study is particularly relevant here; Rudebeck et al., (2009) administered an object and scene recognition memory paradigm to healthy participants. During separate object and scene stimulus-encoding phases, participants were asked to make a simple judgement to each exemplar within a series of target objects and scenes (objects: ‘Will it fit in a shoebox?’; scenes: ‘Is it indoor/outdoor?’). This was followed by a test phase in which participants were required to indicate whether each of a series of test stimuli was an old (i.e. pre-studied) or completely new item, and assign a degree of confidence to their response via a 6-point confidence scale (6 = Sure Old, 1 = Sure New). These confidence-based responses were used to perform a receiver operating characteristic (ROC) analysis and extract estimates of recollection and familiarity from individual participants (see section 1.3.2). A diffusion MRI measure of fornix microstructure (FA) was also computed for

each participant, and inter-individual variation in fornix FA was found to be predictive of recollection but not familiarity measures. Like the findings reported by Tsivilis et al., (2008), this was interpreted as evidence in favour of dual-process accounts of recognition memory. Importantly, however, the relationship between fornix microstructure and recollection was reported to be stronger in the case of the scene, as opposed to the object stimuli, which is suggestive of a preferential contribution by the fornix to *scene* processing.

Unlike the fornix, which acts primarily as a HC input/output pathway, the ILF carries association fibres from the early visual processing regions of the EVC to various regions of the anteromedial temporal lobe, including the PRC (Pyles et al., 2013; Gschwind et al., 2012; Catani et al., 2003). Given that this white matter pathway effectively traverses the posterior-anterior extent of the 'extended ventral visual stream' (Murray et al., 2007), the ILF may be involved in the relay of information critical for the successful representation and hierarchical processing of the features that comprise object-like visual stimuli, including faces. Indeed, the ILF possesses highly reproducible connections with a number of core face processing regions along the VVS, including the OFA, FFA, and anterior temporal lobe (Pyles et al., 2013; Gschwind et al., 2012). Further, as noted above, the study reported in Chapter 3 demonstrated that inter-individual variation in structural properties of the ILF is predictive of the magnitude of faces -sensitive BOLD responses in the PRC (section 3.3); consistent with a role for the ILF in relaying information about faces to/from the PRC. Furthermore, congenital prosopagnosia (CP) has been associated with lower FA in the ILF (Thomas et al., 2009); in the same study, Thomas et al., also reported that inter-individual variation in ILF FA is predictive of the number of errors made in a face recognition task. Reductions in FA have also been reported in the ILF in a group of children with object recognition deficits, relative to a group of typically developing children (Ortibus et al., 2011). In contrast to the fornix, these findings collectively suggest a key role for the ILF in higher-level face/object processing.

The aforementioned evidence that the fornix and the ILF may play key roles in the higher-level processing of scene and face/object stimuli, respectively, is interesting in the context of recent representational accounts of MTL function, which form the theoretical basis of the present Thesis (Graham et al., 2010; Saksida & Bussey, 2010). Briefly, these views propose that the HC is critical for scene memory but also higher-level perception, whereas the PRC supports memory and higher-level perception for individual objects and faces. Given that the fornix and the ILF act primarily as

input/output pathways to the HC and PRC, respectively, these representational accounts could also be said to anticipate the aforementioned evidence for category-sensitive contributions of these white-matter pathways to visual processing. The conclusions we can draw from the existing literature with regards to the differential contributions of the human fornix and ILF to performance in scene and face processing tasks are, however, actually limited by a number of important considerations. Firstly, much of the existing neuropsychological and MRI literature focuses on the contributions of these white matter pathways to visual processing in a recognition-memory context, whereas the primary focus of the current thesis is on how the healthy brain supports *visual perception*; it is therefore unclear whether the roles of these tracts in visual recognition paradigms extend to performance in visual discrimination tasks. Second, to the current author's knowledge, no previous study has directly compared the contributions of the fornix and ILF to scene and face processing *in the same sample of healthy individuals*, using tasks similar to those developed previously in animal studies (e.g., Buckley et al., 2004; Bussey et al., 2002). This means that it is currently unclear whether the contributions of these white matter pathways to face and scene processing are in fact dissociable, as suggested by representational accounts.

In this Chapter, therefore, I report the results of a novel study in which a deterministic white matter tractography protocol was applied in order to obtain diffusion-MRI indices of white matter microstructure (fractional anisotropy, FA, and mean diffusivity, MD) and macrostructure (tissue volume fraction, *f*) from the fornix and the ILF in a sample of healthy participants, in vivo. The participants also performed two tasks that both involved making rapid same/different judgements to pairs of highly visually similar scenes versus pairs of highly similar faces. As reported elsewhere in this Thesis (see section 1.4), analogous discrimination tasks have been shown to be sensitive to MTL lesions in non-human primates (Bussey et al., 2002) and humans (Barense et al., 2005; Mundy et al., 2013). Two tasks were administered in order to give some indication of the repeatability of the effects reported here. If, as part of an 'extended hippocampal network' (Gaffan, 1994), the fornix makes a preferential contribution to *spatial* discrimination, then it was anticipated that inter-individual variation in these fornix micro- and macro-structural measures would be associated with participants' overall scene, but not face, discrimination accuracy across both of the administered tasks. By contrast, the ILF carries association fibres from the early visual processing regions of the extrastriate cortex to various regions of the anteromedial temporal lobe, including the PRC. Given that this white matter pathway effectively traverses the posterior-anterior extent of the 'extended ventral visual stream' (Murray et al., 2007),

and may be involved in the relay of information critical for the successful representation of the non-spatial feature-conjunctions that comprise object-like visual stimuli, it was predicted that inter-individual variation in the ILF micro- and macro-structural measures would instead be associated with participants' overall face, but not scene, discrimination accuracy. The current study therefore adopts a novel correlational approach to testing the differential contributions of the fornix and the ILF to discrimination accuracy for scenes and faces.

4.2. Methods

4.2.1. Participants

Diffusion-weighted MRI and behavioural data were collected from 27 healthy participants. All participants provided written informed consent for participation in the study, which was approved by the Cardiff University School of Psychology Research Ethics Committee.

Analyses are reported on the two tasks separately, as not every participant completed both tasks (16 completed both). Task A included 21 participants (2 male; aged 18-22 years; mean = 19.0; SD = 1.1) and Task B, 22 participants (2 male; aged 19-23 years; mean = 19.9; SD = 1.0).

4.2.2. Stimuli

The two tasks reported here both involved making rapid sequential discriminations between pairs of highly similar scenes and faces (see Mundy et al., 2013, and example stimuli in Fig. 4.1*A*).

To create each pair of visually similar faces, grayscale photographs of two men or women with qualitatively similar facial features were obtained from an online yearbook and other online sources. These two images were then blended together in accordance with user-specified ratios with the software package Morpheus 1.85^{TM} (ACD Systems,

Saanichiton, British Columbia, Canada), which produced a series of intermediate faces that shared features from both faces 1 and 2. Two faces were then selected from this face 1 – face 2 continuum. The first of these (e.g. FP1) contained 56.6% of the features of 'original face 1' and 43.3% of the features from 'original face 2', while the second (FP1') contained 56.6% of the features from 'original face 2' and 43.3% of the features from 'original face 1'. 50% of the face-pairs administered in both of the reported tasks were male, and 50% were female.

For each scene-pair, a three-dimensional room 'scene' was initially generated using the commercially available computer game Deus Ex (Ion Storm L.P., Austin, TX, USA) and a freeware software editor (the Deus Ex Software Development Kit v1112f). Another visually similar version of this 'prototype-room' was then generated by manually changing the size, orientation, and/or location of three features of the original prototype room (e.g. a staircase, wall cavity and a window).

4.2.3. Tasks – Experimental Procedure

In Task A, which was administered on the same day that diffusion-weighted images (DWI's) were acquired, via a PC with Presentation software installed (Neurobehavioural Systems), participants made rapid same-different discrimination judgements to 8 unique pairs of highly similar faces and scenes. In a given discrimination trial (Fig. 4.1*B*), one stimulus from a given stimulus-pair (e.g. FP1) was presented for 500ms, and was followed by a 300ms masked inter-stimulus-interval (ISI), and then a second stimulus from the same pair (e.g. FP1') for 500ms. For each visual category, 96 discrimination trials were distributed over 2 task-runs. In each run, 4 pairs were repeated over ABCD blocks until participants had made 48 discriminations. Across both task-runs, 50% of the discrimination trials were 'Same' trials, and 50% were 'Different' trials. Consistent with Mundy et al., (2013), participants were pre-exposed to half of the pairs from each category. The pre-exposed pairs were the same for all participants.

In Task B, which was administered approximately 10 months later, participants made rapid discrimination judgements to 4 pairs of highly similar faces (50% males), scenes, and dot-patterns over ABCD blocks (total of 64 discriminations per category). Participants were pre-exposed to half of the pairs from each category, and the pre-

exposed pairs were counterbalanced across participants. Three of the 4 pairs of both the face and scene stimuli were taken from Task A. As the dot-pattern condition is not relevant to the current hypotheses, it is not discussed further. As noted above, the advantage of administering this second task was that it provided some indication of the repeatability of the white matter structure-behaviour effects established using Task A.

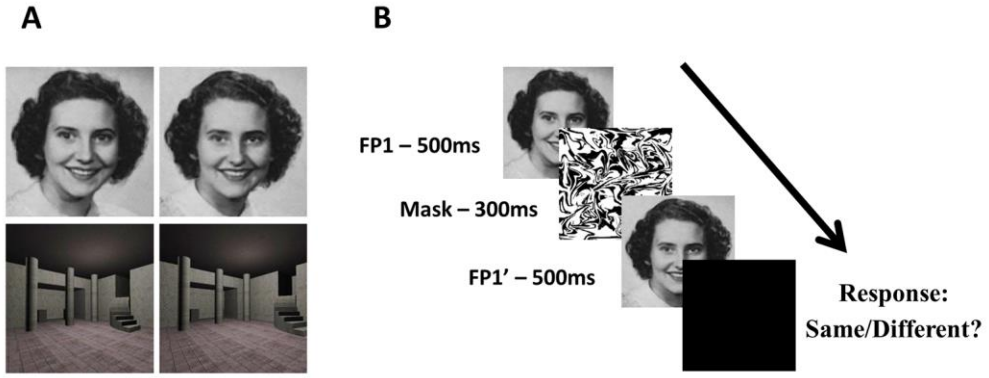

Fig 4.1. (A) Example face and scene discrimination pairs and (B) a schematic of a discrimination trial (see also Mundy et al., 2013).

4.2.4. MRI acquisition

Whole-brain diffusion-weighted MRI data were acquired using a 3T GE HDx Signa scanner with an eight-channel head coil at the Cardiff University Brain Research Imaging Centre (CUBRIC). Images were acquired using a diffusion-weighted single-shot spin-echo echo-planar imaging pulse sequence (with TE = 87ms, field of view = 23 x 23 cm^2, 96 x 96 acquisition matrix, 60 contiguous slices acquired along an oblique-axial plane with 2.4mm thickness and no gap), and the scans were cardiac-gated using a peripheral pulse oximeter. Gradients were applied along 30 isotropically-distributed orientations with b = 1200 s/mm^2 (Jones et al., 1999). Three non-diffusion-weighted images (DWI) with b = 0 s/mm^2 were also acquired. These images, which were acquired as part of a larger study within the research group, were subsequently co-opted and analysed by the current author in order to test the hypotheses of the current study.

4.2.5. DWI pre-processing

The same DWI pre-processing protocol described in section *3.2.6.2* was employed for the current analysis.

4.2.6. Tractography Protocol

Whole brain tractography was initially performed from all voxels in participants' (free-water corrected) native diffusion-space in ExploreDTI using a deterministic tractography algorithm based on constrained spherical deconvolution (Tournier et al., 2008; Jeurissen et al., 2011). A step size of 1mm, and an angle threshold of 30 degrees was adopted in order to prevent the reconstruction of anatomically implausible fibers.

A multiple region-of-interest (ROI) approach was then used to isolate the fornix bilaterally (mean voxel count: 1227.5; SD = 406.7; range: 460-1931) from the results of this whole-brain tractography procedure (Metzler-Baddeley et al., 2011; Fig 3.1*A*). Mean FA, MD, and *f* indices were subsequently extracted from the reconstructions in ExploreDTI (Jones et al., 2005).

Mean FA/MD/*f* indices were also extracted from the main occipito-temporal associative white-matter pathway; the inferior longitudinal fasciculus (ILF; Catani et al., 2003). The right and left ILF were reconstructed (mean voxel count: 2910.2; SD = 788.1; range: 1628-4655) using a two-ROI approach (Wakana et al., 2007; Fig 3.1*B*), and for comparability with the fornix, the average of the measures obtained from the two hemispheres was calculated to create a single value per participant.

4.2.7. Analyses

Two-tailed Pearson correlation statistics were calculated to establish whether fornix/ILF FA, MD, or *f,* were related to discrimination accuracy for scene or face pairs in either Task A or B. In order to control for false-positive effects, potentially arising through the calculation of multiple structure-behaviour correlation statistics across two distinct white matter tracts, a significance threshold of $p \leq 0.05$ was adjusted by a Bonferroni

correction factor of 2 (required $p \leq 0.025$). This is a more conservative approach to controlling for multiple comparisons compared to other similar and notable studies (e.g. Rudebeck et al., 2009), but should not unduly inflate the risk of reporting false negative effects. All correlations are, however, reported with 95% confidence intervals around the effect size estimates, based on 1000 bootstrapped samples of the data in order to provide additional information with respect to the reliability of the reported effect sizes. Directional t-tests for dependent correlations were used to determine significant differences between correlations, with a significance threshold of $p \leq 0.05$.

4.3. Results

Table 4.1. Mean FA, MD ($x10^{-3}mm^2\ s^{-1}$), and *f*, in both the fornix and the ILF of all 27 participants. Standard deviations are provided in brackets.

Tract	FA	MD	*f*
Fornix	0.373 (0.032)	1.056 (0.055)	0.727 (0.035)
ILF	0.428 (0.023)	0.757 (0.017)	0.896 (0.013)

Table 4.1 shows the mean and standard deviation of values obtained for FA, MD and *f* in the fornix and ILF. Prior to reporting the analyses testing our key hypotheses, we assessed the relationship between FA, MD and *f* by calculating correlation coefficients between each measure for each tract for all 27 participants. Fornix FA was strongly correlated with both fornix MD and *f* (r = -0.760, $p < 0.001$, 95% CI [-0.917, -0.487]; r = 0.685, $p < 0.001$, 95% CI [0.419, 0.851], respectively). Fornix MD and *f* were also highly correlated (r = -0.795, $p < 0.001$, 95% CI [-0.906, -0.603]). Turning to the ILF, MD and *f* were highly correlated (r = -0.969, $p < 0.001$, 95% CI [-0.986, -0.932]). ILF FA was correlated with ILF MD and *f* (r = -0.275, p = 0.166, 95% CI [-0.618, 0.169]; r =

0.338, p = 0.085, 95% CI [-0.100, 0.661]), but these correlations failed to reach statistical significance.

4.3.1. Behavioural Data

Table 4.2. Mean, standard deviation and performance range on Tasks A and B separated by condition (scenes and faces).

Task	Condition	Mean	SD	Range
A	Scenes	74.5	11.85	53.13 – 90.63
	Faces	72.12	5.55	63.54 - 80.21
B	Scenes	79.69	12.57	45.31 – 95.31
	Faces	70.03	11.04	43.75 – 87.5

Table 4.2 describes participants' performance in both tasks; analyses of this data are reported – separately by task - below.

4.3.2.1. Task A – Behavioural data

After dividing the discrimination test trials into 4 discrete time 'bins' (see Mundy et al., 2013), a 2 (Exposure: pre-exposed versus novel) x 2 (Category: scenes versus faces) x 4 (Bin number: 1, 2, 3 and 4) repeated measures ANOVA revealed no significant main effects of Bin number (F (2, 60) = 1.585, p = 0.202) or Category (F (1, 20) = 1.147, p = 0.297) on performance in Task A. There was a trend towards a main effect of Exposure as discrimination accuracy was numerically greater for novel relative to pre-exposed pairs (F (1, 20) = 3.965, p = 0.06). There was a significant Category x Bin number interaction (F (3, 60) = 7.45, p < 0.001), which post-hoc pairwise comparisons (Bonferroni-corrected) revealed to be driven by higher scene discrimination accuracy in Bins 2 and 3 relative to Bin 1 (p = 0.012, and 0.002 respectively). Scene discrimination accuracy in Bin 4 was non-significantly different from that obtained in Bins 1, 2 or 3 (p's = 0.135, 1.0, and 1.0 respectively). Face-pair discrimination accuracy did not differ across any of the 4 Bins (all p's > 0.773). These findings indicate that discrimination accuracy is similar across the two visual categories, and that there was no significant

and enduring improvement in discrimination accuracy from repetition or exposure to half of the stimuli prior to the discrimination test. This was true for both categories of stimuli.

4.3.2.2. Task A – Tractography

Fornix *f* correlated significantly with discrimination accuracy for scenes (r = 0.597, p = 0.004, 95% CI [0.174, 0.791]), but not faces (r = 0.278, p = 0.223, 95% CI [-0.222, 0.660]), and these correlations were significantly different (t (18) = 1.69, p = 0.054; see Fig. 4.3*A*). Likewise, fornix MD correlated significantly with discrimination accuracy for scenes (r = -0.729, p < 0.001, 95% CI [-0.908, -0.359]) but not faces (r = -0.138, p = 0.552, 95% CI [-0.515, 0.319]), and these correlations were also significantly different (t (18) = 3.986, p < 0.001; see Fig. 4.3*B*). There was also a significant correlation between fornix FA and discrimination accuracy for scenes (r = 0.545, p = 0.011, 95% CI [0.178, 0.816]) but not faces (r= 0.282, p = 0.215, 95% CI [-0.082, 0.592]). The difference between these correlations did not reach significance (t (18) = 1.34, p = 0.099; see Fig. 4.3*C*).

With regard to the ILF, *f* was non-significantly correlated with discrimination accuracy for both faces and scenes (r = 0.326, p = 0.149, 95% CI [-0.140, 0.652]; r = 0.389, p = 0.082, 95% CI [0.055, 0.653], respectively), and these correlations were non-significantly different (t (18) = -0.296, p = 0.385; see Fig 4.4*A*). The correlations between ILF MD and discrimination accuracy for both faces and scenes also failed to reach significance (r = -0.425, p = 0.055, 95% CI [-0.686, -0.046]; r = -0.436, p = 0.048, 95% CI [-0.711, -0.144], respectively), and were non-significantly different (t (18) = 0.054, p = 0.479; see Fig 4.4*B*). ILF FA was also non-significantly correlated with discrimination accuracy for both faces and scenes (r = 0.018, p = 0.939, 95% CI [-0.507, 0.514]; r = 0.084, p = 0.717, 95% CI [-0.383, 0.486], respectively), and these correlations were non-significantly different (t (18) = -0.285, p = 0.390; see Fig 4.4*C*). In summary, there were no Bonferroni-adjusted significant correlations between discrimination performance and micro- and macro-structural measures.

4.3.3.1. Task B – Behavioural data

Analyses on the behavioural data obtained from Task B were repeated for that obtained from Task B. This revealed that there was a significant main effect of Category upon discrimination accuracy in Task B, which reflected higher performance for scenes than faces (F (1, 21) = 17.153, p < 0.001). There was no main effect of Bin number, but the main effect of Exposure was significant, with discrimination accuracy being higher for pre-exposed pairs relative to those that were novel at test (F (1,21) = 6.621, p = 0.018). There was also a significant Category x Exposure interaction, which post-hoc tests revealed reflected better discrimination accuracy for pre-exposed compared to novel scenes (p = 0.005), but not faces (p = 0.483). All other interactions were non-significant. In brief, while there was no significant improvement in discrimination accuracy over the task, overall scene-pair discrimination accuracy did benefit from exposure to stimuli prior to the main task.

4.3.3.1. Task B – Tractography

As in Task A, fornix *f* correlated significantly with discrimination accuracy for scenes (r = 0.609, p = 0.003, 95% CI [0.397, 0.857]), but not faces *(*r = 0.235, p = 0.292, 95% CI [-0.158, 0.608]), correlations that were significantly different (t (19) = 2.26, p = 0.018, see Fig. 4.3*D).* Likewise, fornix MD correlated significantly with discrimination accuracy for scenes (r = -0.550, p = 0.008, 95% CI [-0.785, -0.205]) but not faces (r = -0.266, p = 0.231, 95% CI [-0.574, 0.157]), and the difference between these correlations showed a strong trend towards significance (t (19) = 1.61, p = 0.062, see Fig. 4.3*E*). There was also a marginally significant correlation between fornix FA and discrimination accuracy for scenes (r = 0.468, p = 0.028, 95% CI [0.180, 0.759]), but not faces (r = 0.263, p = 0.237, 95% CI [-0.111, 0.632]); the difference between these correlations was not significant (t (19) = 1.10, p = 0.144, see Fig. 4.3*F*).

Our ILF analyses revealed that ILF *f* was non-significantly correlated with discrimination accuracy for both faces and scenes (r = 0.143, p = 0.526, 95% CI [-0.285, -0.513]; r = 0.367, p = 0.093, 95% CI [-0.010, 0.733], respectively), and these correlations were non-significantly different (t (19) = -1.15, p = 0.133; see Fig 4.4*D*). Likewise, ILF MD was non-significantly correlated with discrimination accuracy for both faces and scenes (r = -0.179, p = 0.425, 95% CI [-0.569, 0.241]; r = -0.392, p = 0.071, 95% CI [-0.705, -0.063], respectively), and these correlations were non-significantly different (t (19) = 1.098, p = 0.143; see Fig 4.4*E*). The analyses did, however, reveal a significant correlation between ILF FA and overall face discrimination accuracy (r = 0.477, p =

0.025, 95% CI [0.008, 0.823]), but not scene discrimination performance (r = 0.170, p = 0.449, 95% CI [-0.350, 0.547]), and the difference between these two correlations showed a strong trend towards significance (t (19) = 1.67, p = 0.056; See Fig 4.4*F*). In summary, the only significant association in the ILF, was between FA and discrimination accuracy for faces, but not scenes, in Task B.

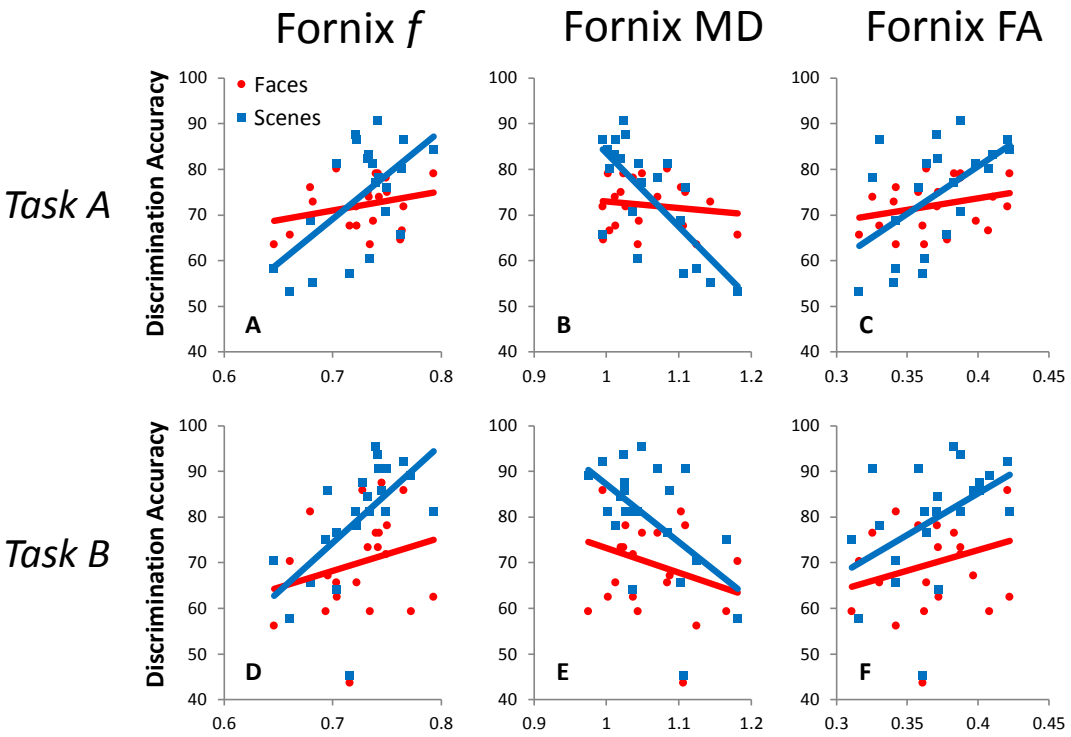

Fig 4.3. Relationship between face and scene discrimination accuracy (red and blue lines, respectively) and fornix *f,* MD (x10^{-3}mm^2 s^{-1}) and FA in Tasks A (top) and B (bottom).

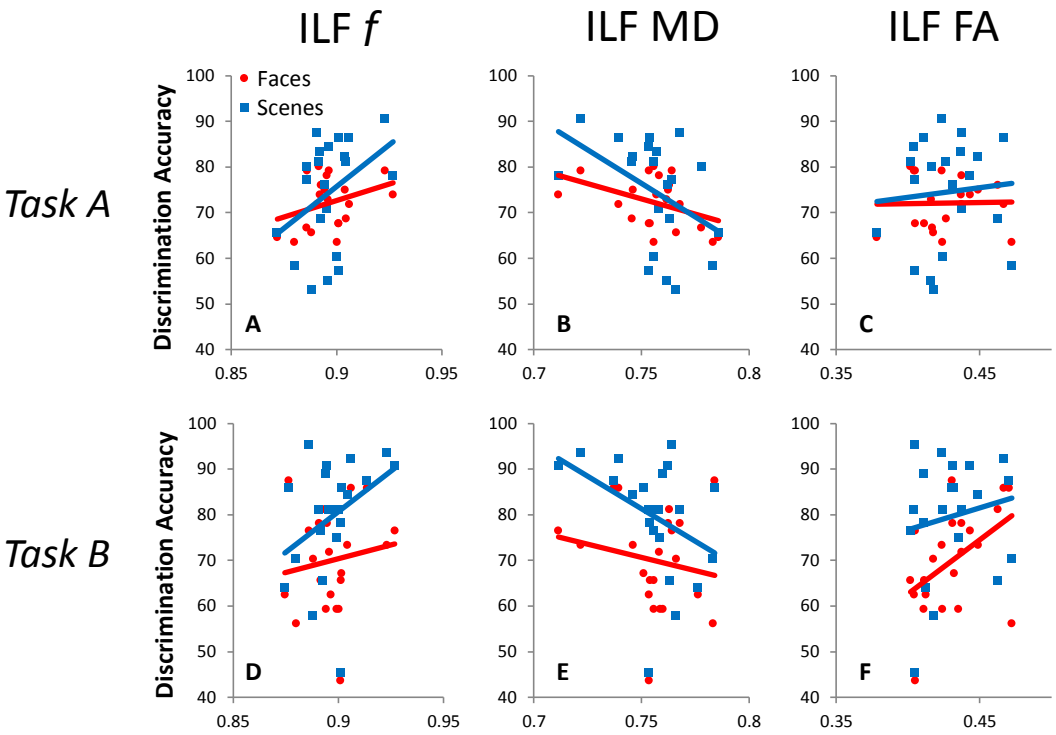

Fig 4.4. Relationship between face and scene discrimination accuracy (red and blue lines, respectively) and ILF *f,* MD (x10^{-3}mm^2 s^{-1}) and FA in Tasks A (top) and B (bottom).

4.4. Discussion

In the current Chapter I report the results of a study in which deterministic tractography and two visual discrimination tasks were employed to investigate the differential contributions of the fornix and the ILF to measures of discrimination accuracy for scenes and faces. The fornix and the ILF were of particular interest as tracts that may make differential contributions to scene and face perception, because whilst the former acts primarily as an input/output pathway for the HC, the latter is a prominent input pathway for the PRC. As discussed in previous Chapters, these two MTL gray matter structures are thought to be specialised for scene and face/object perception, respectively, according to representational accounts of memory and perception (e.g. Graham et al., 2010; Saksida and Bussey, 2010). Participant-specific diffusion-MRI

measures of white matter micro- and macrostructural properties were extracted from the fornix/ILF in vivo, and correlated with participant-specific measures of discrimination accuracy for scenes and faces. The analyses revealed that inter-individual variation in fornix micro- and macro-structure was related to visual discrimination accuracy for scenes, but not faces, across the two visual discrimination tasks. Importantly, this effect was not replicated in the ILF, implying specificity in the association between scene discrimination ability and fornix macro- and micro-structure. There was also evidence that ILF FA was associated with discrimination accuracy for faces, and not scenes, in Task B; an effect which was not replicated in the fornix, implying specificity in the association between face discrimination ability and ILF microstructure.

The scene-selective white matter structure-behaviour associations reported here in the healthy fornix highlight an important contribution of white matter pathways to performance in higher-level visual processing tasks. More importantly, they also indicate that individual white matter bundles can make a *preferential* contribution to the processing of particular visual categories. That inter-individual variation in structural properties of the fornix would be statistically related to measures of discrimination accuracy for scenes, and not faces, is consistent with the role of the fornix as a prominent input/output pathway for the HC; a region of the MTL that has previously been implicated in higher-level scene processing by studies reporting impaired performance in visual discrimination, oddity, discrimination-learning, and recognition paradigms involving scenes, but not faces, following HC damage in humans (Lee et al., 2005a, Lee et al., 2005b, Mundy et al., 2013, Taylor et al., 2007). HC contributions to scene processing are also reflected in an increase in HC BOLD response during presentation of visual scenes compared to other stimulus categories (Mundy et al., 2013, Mundy et al., 2012; Lee et al., 2008). The current findings augment the conclusions that can be drawn from these previous studies, however, because they highlight for the first time that as well as the activation profile of the HC itself, the ability of the HC to interact with other related brain areas via its white matter connections (i.e. HC connectivity; assessed here via variation in diffusion MRI measures of the fornix), may also be an important neural factor underpinning successful performance in scene discrimination tasks. In other words, successful scene discrimination is not simply a product of the activation of a highly specialised scene processing module in the HC, but is an emergent property of the HC and both its functional/structural connections with other functionally-related brain areas (see also Behrman and Plaut, 2013).

That HC contributions to scene processing tasks may partly depend upon inter-regional functional interactions via the fornix, is consistent with studies reporting impaired performance in spatial processing tasks following fornix transection in animals. Fornix transection in nonhuman primates, for example, has been shown to impair the ability to learn concurrent visual discriminations between spatial stimuli (Buckley et al., 2004), and produces deficits in other spatial memory tasks that are also sensitive to HC damage (e.g., object-in-scene memory tasks; Gaffan, 1994). The present findings extend those earlier findings by confirming that the specialised role of the fornix in spatial processing extends to healthy human participants with no known neurological pathology. In terms of which other brain regions the HC may need to engage with via the fornix, this prominent white matter tract does not project to the early posteromedial scene-sensitive cortices described in Chapters 1 (section 1.2), 2, or 3. Two more anterior regions in the medial diencephalon may, however, be relevant here: the mammillary bodies (MBs) and the anterior thalamic nuclei (ATN) (see section 1.5.2). Along with the HC and the fornix, these two regions have been proposed to form an extended HC-fornix-MBs-ATN network involved in the representation of complex visual scenes, and the arrangement of the objects within those scenes (Gaffan, 1994; see also Aggleton and Brown, 1999; sections 1.1.3. and 1.3.2.). Indeed, studies in rats confirm that damage to each of these gray/white matter structures results in impairments in the same tests of spatial learning (e.g. water maze tasks, see section 1.4.4), albeit with varying degrees of severity (Aggleton and Nelson, 2015). Further, fornix transection leads to reduced activity (as indexed by the expression of the immediate-early gene c-*fos*; a marker of neural activity) across both the HC and ATN (and also the medial septum; see Vann and Brown, 2000). The role that MTL-diencephalic interactions play in higher-level spatial processing remains a subject of open investigation (Vann, 2010; Jankowski et al., 2013), but, notably, the HC, MBs and the ATN are all known to contain head-direction cells (i.e. cells that discharge as a function of head-direction; Jankowski et al., 2013; Vann et al., 2010), and it has been proposed that these could potentially contribute to a variety of spatial processes that may be relevant to performance in scene processing tasks, including scene construction, mental imagery and mental navigation (Aggleton et al., 2010). The MBs and ATN are also known to include cells that fire rhythmically with theta (a sinusoidal oscillation of 6-12Hz; Jankowski et al., 2013). Theta rhythm is thought to play a key role in MTL function (Burgess et al., 2002), because, in rats, plasticity occurs between sequentially-activated HC place cells during theta epochs (Skaggs et al., 1996; Aggleton et al., 2010). Another key function that has therefore been proposed for the MBs/ATN, is in conveying theta to the HC (albeit via non-fornical back-projection

connections) in order to optimise synaptic plasticity (Aggleton et al., 2010; Vann, 2010). The fornix also contains reciprocal connections between the HC and the medial septum (Saunders and Aggleton, 2007); the medial septum also influences theta activity in the HC as evidenced by studies demonstrating that inactivation of the medial septum disrupts theta rhythmical discharges in both the HC and MBs (Bland et al., 1995). The present results are therefore consistent with a role for the fornix in facilitating inter-regional interactions with surrounding neo- and sub-cortical areas, which appear to be critical in supporting HC contributions to higher-level scene processing.

Turning to the ILF, the mean FA of this tract was associated with discrimination accuracy in Task B for faces, but not scenes. Although this finding needs to be considered with caution pending replication, that inter-individual variation in a measure of ILF microstructure would be specifically linked to measures of discrimination accuracy for faces, and not scenes, is consistent with the role of the ILF as an input pathway for the anterior temporal lobe, which includes the PRC (Pyles et al., 2013; Catani et al., 2003). In contrast to the HC, the PRC is a region of the MTL that has been implicated in higher-level face processing by studies reporting impaired performance in visual discrimination, oddity, discrimination-learning, and recognition paradigms involving faces following PRC damage in humans (Lee et al., 2005a; 2005b; Mundy et al., 2013; Taylor et al., 2007). The PRC BOLD response to faces is also greater than that to scenes (Mundy et al., 2013, Mundy et al., 2012; Lee et al., 2008; see also Chapter 2). The current findings augment the conclusions that can be drawn from these previous studies, however, because they suggest that as well as the activation profile of the PRC, the ability of the PRC to interact with other functionally-related brain areas via the ILF is also a neural factor that may underpin successful face *discrimination*. In other words, successful face discrimination is an emergent property of the PRC and its functional/structural connections with other functionally-related brain areas along the extended VVS (see also Behrman and Plaut, 2013). That higher-level face processing may depend upon interactions between the PRC and earlier VVS regions, via the ILF, is also, notably, consistent with previous evidence that ILF FA is reduced in individuals presenting with face and object recognition impairments (Thomas et al., 2009; Ortibus et al., 2011). Inter-individual variation in ILF FA has also been shown to be predictive of the number of errors made in a face recognition task (Thomas et al., 2009). The current findings augment this previous research, by showing that this 'supporting role' of the ILF in face recognition also extends to visual discrimination. More importantly, the current findings potentially highlight a *preferential* contribution of the ILF to visual discrimination for face compared to scene stimuli. This

category-sensitivity suggests that the ILF is actually relatively specialised for relaying information between gray matter regions involved in the processing of non-spatial stimulus categories like faces. This proposition itself is consistent with the findings reported in Chapter 3 of the present Thesis, where inter-individual variation in ILF structural properties was shown to be predictive of the magnitude of the preferential BOLD response to images of faces/objects compared to scenes in the OFA/PRC. In addition, the volume of the right ILF has, elsewhere, previously been shown to be linked to the size of the right FFA but not the PPA (Scherf et al., 2014). For the first time, the current findings therefore confirm that individual differences in structural properties of the ILF is an important source of inter-individual differences in visual discrimination as well as visual recognition performance, and that in contrast to the fornix, the ILF may be relatively specialised for the relay of visual information corresponding to non-spatial stimulus categories.

The category-sensitive white-matter structure-behaviour effects reported here in these HC and PRC white matter pathways are also consistent with recent representational accounts of MTL function (see section 1.5). The EMA (Graham et al., 2010), for instance, proposes that the HC and PRC support complex representations of spatial and non-spatial visual feature-conjunctions, respectively (for a similar conceptual framework, see Saksida & Bussey, 2010); the HC is therefore critical for scene memory and perception, whereas PRC supports memory and perception for individual objects and faces. Indeed, as noted above, patients with HC lesions have been found to be selectively impaired, relative to controls, in tests of both memory and perception for visual scenes, but not faces; whereas patients with more extensive MTL damage, that included the HC *and* PRC, present with additional face memory and perception impairments (Taylor et al., 2007; Lee et al., 2005b; Aly et al., 2013; Barense et al., 2007). That the category-sensitive impairments in visual processing tasks following HC/PRC damage are reflected here in the category-sensitive contributions of the fornix/ILF to discrimination accuracy, suggests that representational perspectives can offer new insights into the complex role of white-matter connections in human cognition; including previous evidence that fornix microstructure is more strongly related to recollection-based recognition memory for scenes than objects (Rudebeck et al., 2009). Representational accounts may also provide a useful framework for understanding how the ILF, as the major white matter tract traversing the visual ventral stream (Catani et al., 2003), contributes to typical and atypical face processing (Thomas et al., 2009).

Representational accounts could be extended to explicitly accommodate category-sensitive effects in both gray *and* white matter MTL structures. In Chapter 1 (section 1.6.2), I proposed one such extension, according to which there are two relatively segregated but parallel visual processing networks or 'streams'; an extended ventral-lateral processing stream (culminating in the PRC) that contains hierarchically-organised representations of feature-conjunctions that are most useful in the context of memory and perception for individual object-like stimuli, and another more dorsal-medial stream (culminating in the posterior HC), which contains hierarchically-distributed representations of spatial feature-conjunctions that are more useful in the context of scene memory and perception. This proposal retained the core predictions of existing representational accounts but explicitly states that the processing of spatial and non-spatial stimuli are differentially dependent upon distinct visual processing streams converging on the PRC and the posterior HC. This proposed extension of representational accounts like the EMA (Graham et al., 2010) thereby provides a framework to understand why the ILF – as a white matter pathway supporting the propagation of information about non-spatial feature conjunctions to the PRC – may be relatively specialised for the processing of faces and objects compared to scenes, whereas the fornix – as a prominent HC input/output pathway – may be relatively specialised for the processing of scenes compared to faces and objects. It is also worth noting that whilst the category-sensitive effects reported here in the fornix/ILF are consistent with representational accounts, they are less consistent with another notable network-based account of visual processing which makes no explicit distinction between how visual processing for spatial versus non-spatial stimulus categories is organised in the brain (see Behrmann and Plaut, 2013). Briefly, this latter account proposes that category-sensitive brain regions correspond to local 'peaks' within more distributed and overlapping hierarchical representational networks that possess graded sensitivities to all complex stimulus categories. In other words, multiple complex visual categories can engage common neural resources, even within ROI's that are optimised for the processing of particular categories. Similarly, the account suggests that the ILF plays an important role in propagating visual information about all kinds of complex visual stimuli to the anterior temporal lobe (e.g. scenes as well as faces). The category-sensitive effects reported here within the ILF therefore appear to distinguish between the representational accounts outlined here and the Behrmann and Plaut (2013) model in favour of the former.

With their emphasis on the distinct visual representations supported by the HC and PRC, 'representational' models differ from numerous other contemporary accounts that instead focus exclusively on the contributions of different MTL structures to declarative memory. The reader is referred to section 1.3.1 for a more detailed exposition of several such accounts, but briefly, unitary-process accounts of MTL function propose that, together, the HC, ERC, PRC and PHC support declarative memory by rapidly binding together stimulus features processed in other distributed cortical sites, where the memory is subsequently stored (e.g. Squire et al., 1991). By contrast, dual process accounts argue that declarative memory is actually supported by two largely independent processes; recollection and familiarity (e.g. Aggleton and Brown, 1999). Recollection and familiarity are proposed to have distinct neural substrates *within* the MTL; with recollection-based recognition supported by an 'extended HC network', and familiarity-based recognition supported by the PRC. Unitary and dual-process accounts therefore differ in that the former predicts that MTL damage will impair declarative memory, whereas the latter makes the additional prediction that the location of the damage within the MTL (e.g. HC versus PRC) will determine what 'type' of declarative memory process is impaired. Another contemporary account of MTL function describes the functional specialisation that exists across MTL sub-regions in terms of the different kinds of *information* that the different MTL sub-regions are involved in encoding/retrieving; this is the Binding of Item and Context model (BIC; Diana et al., 2007). BIC proposes that the PRC encodes/retrieves mnemonic information about individual *items*, whereas the posterior PHC stores information about the *context* in which the item was encountered (both spatial and non-spatial). These two streams of information remain segregated as they pass through ERC, but are bound together into item-context associations by the HC. In section 1.3.3, I also highlighted that whilst unitary process, dual process, and BIC accounts of MTL function differ in terms of how they characterise the functional specialisation that exists across MTL regions, they nevertheless share several assumptions about MTL function. One such assumption is that the MTL is a highly specialised declarative memory system that is not required for other functions such as higher-level perception, which led me to characterise them collectively, as 'memory system' accounts of MTL function. Another implicit assumption made by these 'memory system' accounts, is that neither the HC nor the PRC are optimised for the processing of particular visual categories. This is relevant here because whilst representational views of MTL function can readily accommodate the significant category-sensitive white matter structure-behaviour correlations reported here, the same findings are more difficult to reconcile with these category-general 'memory system' accounts. The current findings could, therefore, also be taken to

distinguish between representational and 'memory system' accounts of MTL function, in favour of the former.

Importantly, in contrast to 'memory system' accounts of MTL function, representational accounts suggest that MTL representations may have perceptual as well as mnemonic applications, and the current findings could be interpreted as supporting this view. There was no enduring improvement in discrimination accuracy over the course of either Tasks A or B, and there was no effect of prior exposure on discrimination accuracy in Task A. Particularly with Task A then, the behavioural data indicates that mnemonic processes *were not* necessarily recruited to support discrimination judgements. Notably, however, the stimuli used here were repeated across multiple discrimination trials (i.e. the stimulus pairs were not 'trial-unique'). Even though there was no statistically robust learning, it is therefore possible that memory processes could have contributed to participants' discrimination judgements over time. This argument can be elucidated with reference to a study by Kim et al., (2011). In their study, amnesic patients and healthy controls were administered a pair of visual discrimination tasks that involved discriminating pairs of visually similar faces and scenes. In one version of the task, all of the face and scene stimuli were completely trial-unique, whereas in another version, the same face and scene pairs were discriminated over a number of repetitions as per the design reported here. The performance of the patients was stable and well matched to the healthy controls over the course of testing in the trial-unique face and scene conditions. In the repeated face/scene conditions of that study, however, the patients were impaired relative to controls. This was because the performance of the controls gradually improved across testing for both the repeated face and scene conditions, whereas the performance of the patients remained stable. This was taken to indicate that the control participants – but not the patients – benefitted from the opportunity to learn about the stimuli over the course of the experiment; as a result overall performance measures for the controls in that study would reflect a contribution of learning and memory as well as perception. As outlined above, no statistically robust learning effects were evident in the present study, so it is unlikely that learning and memory made a contribution to participants' discrimination accuracy measures here. Nevertheless, further investigations focusing on the preferential contributions of particular white matter pathways to visual perception for different categories of stimuli should employ trial-unique stimuli to which the participant has not been pre-exposed prior to testing. This ensures that overall visual discrimination measures cannot benefit from any incidental within-trial learning about a given stimulus because it will not be encountered again in successive discrimination

trials. Any white-matter structure-behaviour correlations that are subsequently detected can then be taken as strong evidence in favour of a role for a given tract in process-pure perception, in addition to any established contributions to visual learning and memory. Such a trial-unique visual discrimination paradigm is reported in Chapter 5.

The strengths of the targeted tract reconstruction approach that was employed here to reconstruct and quantify structural properties of the fornix/ILF were outlined in section 3.4. It should, however, be noted that the fornix is a prominent white-matter bundle that provides the HC with both afferent and efferent connections to multiple functionally related areas (e.g. the ATN and MBs; Vann et al., 2011). It is not currently possible to distinguish these afferent and efferent connections using white matter tractography protocols, however, and so the precise functional node(s) with which the HC must interact in order to support performance in the current spatial discrimination tasks cannot be specified here. The same limitation extends to ILF tractography in that it is not currently possible to determine which gray matter regions contributing fibres to the ILF are most critical for face discrimination performance in these tasks. Future white-matter transection studies in non-human animals trained to perform a similar discrimination-learning paradigm could, however, provide some traction on this issue.

Whilst fornix MD correlated with scene-pair discrimination accuracy in the current study, fornix FA was less strongly associated with performance. This finding could reflect fornix MD's greater sensitivity to experience-dependent changes (Lebel et al., 2008; Hofstetter et al., 2013). As FA and MD are both affected by multiple axonal properties, including myelination, density, diameter and configuration, it is, however, not yet possible to attribute differences between the current FA/MD findings to a single white-matter subcomponent (Jones et al., 2013). For the same reason, it is not currently possible to attribute the significant correlation between ILF FA and face discrimination to inter-individual variation in a specific white-matter sub-component in the ILF. That fornix *f* was also associated with successful scene discrimination accuracy, as well as MD, additionally highlights a potential contribution of fornix macrostructure to variation in scene discrimination. Given the inter-correlations between all three imaging metrics in the fornix, the current findings may indicate that individual variation in some specific property of the fornix, to which multiple diffusion-MRI metrics are sensitive, is predictive of scene discrimination accuracy in the current tasks. It is also possible, however, that inter-individual variation in both the macro- *and* the microstructural properties of the fornix contributes to performance in the reported tasks (see also Saygin et al., 2013; Loui et al., 2011; Lebel and Beaulieu, 2011).

Owing to the correlation-based nature of the present white matter structure-behaviour analysis, it is difficult to infer the direction of causality between white matter properties in the fornix/ILF and measures of visual discrimination performance. Microstructural properties like axon myelination modulate the neural conduction velocity along white-matter pathways, and could therefore directly affect behavioural performance by influencing "the timing of sequential events" and the efficiency of information transfer across the extended HC network in the case of the fornix, and the extended VVS in the case of the ILF (Peters, 2002, pp585). This causal interpretation of the current findings should be treated cautiously, however, as recent studies have reported experience-dependent changes in measures of white-matter microstructure in a number of pathways (Scholz et al., 2009). Hofstetter et al., (2013), for example, recently reported significant changes in diffusion MRI measures of fornix microstructure following a short period of training in a spatial learning task, across both humans and rodents; further, in both species these microstructural changes were correlated with diffusion changes in the HC as well as behavioural measures of improvement in the spatial tasks. These striking findings suggest that variation in fornix microstructural properties could also be a response to differences in spatial processing expertise. Neural activity-dependent mechanisms could stimulate myelination along the fornix following a period of spatial processing, for example, leading to increased efficiency of information transfer across this white matter pathway over time (McKenzie et al., 2014). The same activity-dependent mechanisms could also account for recent evidence that ILF microstructure undergoes protracted developmental changes that are tightly linked to age-related increases in the size of a functionally-defined face processing region that sits alongside the ILF; the FFA (Scherf et al., 2014). Importantly, this alternative interpretation (i.e. visual experience precedes changes in white matter macro-/microstructure) offers a potential mechanism by which: 1) the extended HC circuit that includes the fornix may become organised and optimised for successful higher-level scene processing over time, and 2) the visual processing stream that culminates in the PRC becomes organised and optimised for the successful processing of object-like stimuli over time (Scherf et al., 2014; Behrmann and Plaut, 2013).

In summary, the current study demonstrates that inter-individual variation in fornix microstructure and macrostructure was related to discrimination accuracy for pairs of visually similar scenes, but not faces. This finding augments lesion studies in which hippocampal damage results in selective impairments in scene discrimination learning

(Graham et al., 2006; Mundy et al., 2013), and highlights a critical role for the human fornix in high-level scene, but not face, discrimination, consistent with representational accounts of MTL function (Graham et al., 2010). In addition, a measure of ILF microstructure was associated with discrimination accuracy for faces, and not scenes, which may indicate that this PRC-input pathway makes a preferential contribution to visual processing for faces and potentially other object-like stimuli, also consistent with representational accounts. These findings extend previous investigations and accounts of how the healthy brain supports memory and perception, by showing that inter-individual variation in the structural properties of the white matter pathways that project to category-sensitive MTL regions also make important category-sensitive contributions to these cognitive domains. It has already been noted, however, that in the two tasks reported in this Chapter, participants made discriminations to face and scene stimuli over a number of repetitions. Whilst there were no statistically robust learning effects in these tasks, it remains possible that over the course of performing the experiment, stimulus-learning mechanisms may have contributed to the overall discrimination performance measures (Kim et al., 2011). It therefore remains to be confirmed whether the category-sensitive contribution of these white matter pathways to visual processing may extend to process-pure perception. In the next Chapter, I therefore report the results of a similar structure-behaviour analysis that was conducted using behavioural data from a task in which participants were required to make discriminations to pairs of faces and scenes that were completely trial-unique. The results of that study will augment the work presented in this Chapter, by confirming that inter-individual variation in structural properties of the ILF and the fornix is also predictive of markers of trial-unique face and scene perception, respectively.

Chapter 5: Dissociable roles for the fornix and inferior longitudinal fasciculus in markers of perception for trial-unique scenes and faces

5.1 Introduction

The findings reported In Chapter 4 demonstrate for the first time that inter-individual variation in diffusion-MRI measures of fornix macro-structure and microstructure – a prominent HC input/output pathway – is predictive of discrimination accuracy for scenes, but not faces. This was shown in a discrimination task previously shown to (a) be sensitive to HC damage and (b) activate the HC when healthy participants perform this task in the MRI scanner (Mundy et al., 2013). There was also tentative evidence that inter-individual variation in a measure of the microstructure of the ILF – a prominent PRC-linked pathway – was predictive of discrimination accuracy for visually similar faces, but not scenes, in the same task. These findings provide new evidence in support of category-sensitive contributions of MTL white matter pathways to visual processing, consistent with representational accounts of MTL function (Graham et al., 2010; Saksida and Bussey, 2010).

Due to the nature of the discrimination task, however, stimuli in the paradigms reported in Chapter 4 were repeated several times during the task (i.e., they were not trial-unique). This poses an issue of interpretation, as previous studies have demonstrated that the performance of healthy participants, but importantly, not amnesic patients, can improve over the course of visual discrimination tasks that involve repeated sets of stimuli (Kim et al., 2011). That healthy participants can benefit from repeated exposure to stimuli over the course of such tasks suggests that the overall performance measures reported in Chapter 4 could potentially reflect a contribution of stimulus learning and memory as well as perception. Although no statistically robust learning effects were detected in the tasks reported in Chapter 4, nevertheless, it remains possible that over the course of the experiment, stimulus-related learning may have contributed to the participants' overall discrimination judgements. It remains to be confirmed, therefore, whether category-sensitive contributions of the fornix/ILF to visual processing will also be evident in a task that involves making discriminations to pairs of stimuli that are completely trial-unique.

In addition, the study reported in Chapter 4 treated visual discrimination as a unitary construct, but some authors have recently proposed that two functionally independent forms of perception may contribute to visual discrimination performance. I will review the literature underpinning this emerging view of perception; which I will henceforth refer to as the 'dual process' view. I will then highlight key differences between the dual process view and representational accounts of how perception is supported by the brain. This will stimulate some additional hypotheses about fornix/ILF contributions to higher-level perception, which can also be tested using a previously reported visual discrimination paradigm and trial-unique face and scene stimuli.

Aly and Yonelinas (2012) recently administered a trial-unique face and scene change-detection paradigm to healthy participants, who were required to use a 6-point confidence-based rating scale to indicate whether two consecutively presented images were identical or different. On 'different' trials, the second image was contracted or expanded slightly relative to the first (i.e., 'pinched' versus 'spherized'). The confidence-based responses were used to perform a receiver operating characteristic (ROC) analysis (Green and Swets, 1966). The left-most data-point in a perception ROC indicates the proportion of hits (y-axis) and false alarms (x-axis) for the most confident 'same' responses (i.e., 6 responses), and subsequent data-points indicate the cumulative proportion of hits and false alarms at decreasing levels of response-confidence. Examination of the ROCs plotted in Aly et al., (2012; Fig 5.1) suggested a contribution to discrimination performance from two types of perception. The first was referred to as 'Pd', and could be estimated from the point at which the ROC trend-line intersects the upper x-axis. The second was 'K', and was instead estimated from the curvilinearity of the trend-line. For complex stimuli like faces and scenes, both Pd and K were found to contribute to discrimination performance, so that the aggregate discrimination ROCs for such stimuli displayed curved trend-lines that were both asymmetrical with respect to the chance-diagonal, and shifted leftwards along the upper x-axis.

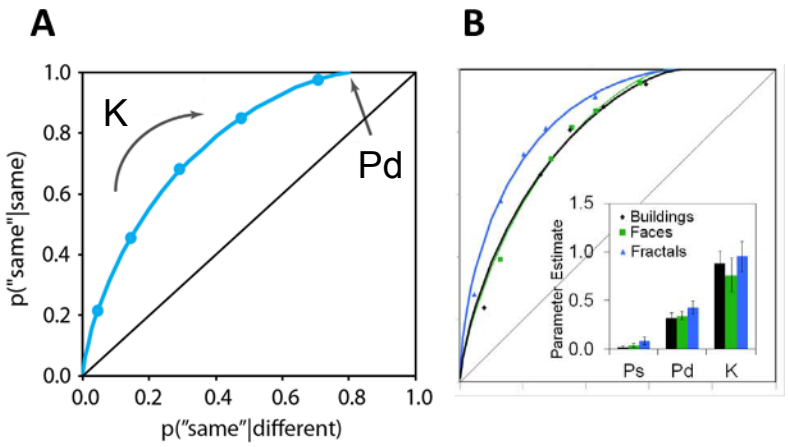

Fig 5.1. (A) An illustration of how Pd and K are estimated from the shape of the curve fitted to perception ROCs, and (B) the aggregate perception ROCs obtained from a building/face/fractal change-detection task. Note that unlike memory ROCs, in which the curve typically intersects the y-axis, perception ROCs tend to intersect the upper x-axis. Additional abbreviation: Ps = 'Perceive same'; another putative perception 'process' which, in practice, makes a negligible contribution to performance in the change-detection task (Aly and Yonelinas, 2012). Figures A and B adapted from Aly et al., (2014a; 2012, respectively).

Further experiments investigated the different functional characteristics of Pd and K. The change-detection paradigm was modified slightly so that participants were required to discriminate scene stimuli that differed in terms of either specific local details (e.g. in a given trial, a feature within stimulus 1 could be absent from stimulus 2), or more subtle and global configural information (e.g. stimulus 2 could be slightly pinched/spherized relative to stimulus 1). Analyses of the fitted ROCs and parameter estimates confirmed that both Pd and K contributed to performance under all task conditions. The contribution of Pd, however, was found to be greater under task conditions that required the detection of discrete local changes, whereas the contribution of K was greatest under conditions that required the detection of subtle configural changes.

Aly and Yonelinas (2012) also asked whether Pd and K map onto distinct subjective experiences and provide access to different sensory information. Another change-detection task was administered, in which participants were required to make confidence-based discriminations to scene images that contained specific distinguishing features. In addition to providing confidence-based same/different responses, the participants were also asked to introspect on their subjective experience during each trial and indicate whether they were able to 'Perceive' a

specific difference between the images or whether they simply 'Knew' the images were different. Finally, the participants were asked to justify each 'Perceive' and 'Know' response by reporting details of the specific distinguishing feature within each stimulus-pair. Pd and K estimates were derived from participant-specific ROCs, but also from the proportion of participants' subjective reports of 'Perceiving' versus 'Knowing' using a process dissociation procedure similar to that used to estimate recollection versus familiarity in the Remember/Know procedure (Tulving, 1985). ROC estimates of Pd were found to correlate with the subjective estimates of 'Perceiving', whereas ROC estimates of K correlated with subjective estimates of 'Knowing'. This was presented as evidence that Pd and K also map onto phenomenologically distinct experiences. ROC based Pd estimates also correlated with the proportion of trials in which participants successfully identified the distinguishing feature. After giving an accurate Know response, however, participants were just as likely to incorrectly as well as correctly identify the distinguishing feature, and twice as likely to provide no information about the distinguishing feature. The authors concluded that Pd is associated with participants being able to report specific local details that distinguish visually similar images ("Perceiving a difference"; Pd) whereas K enabled participants to provide an assessment of the overall match between two images, even if they could not identify specific distinguishing features ("Knowing" there is a difference; K).

Aly and Yonelinas (2012) argued that the fact that Pd and K were a) sensitive to distinct kinds of differences across visually similar stimuli (discrete and local versus global configural differences), b) linked to different subjective experiences ('Perceiving' versus 'Knowing'), and c) associated with access to different sensory information (local details versus overall match), suggests that they reflect two functionally independent 'processes' underlying discrimination performance. Pd was characterised as a discrete *state* in which participants become aware of specific local details distinguishing visually similar images (Perceiving), and K as a continuous *strength*-based form of perception that enables assessments of the overall match of two images (Knowing).

A parallel was then drawn between these putative state (Pd) and strength (K) based forms of perception, and the state- and strength-based 'processes' described in the recognition memory literature; recollection and familiarity, respectively. Dual-process models of recognition propose that recollection is supported by an extended HC-fornix-MB-ATN network, whereas familiarity is dependent upon PRC (Aggleton and Brown, 1999; see section 1.3.2 for details of studies purporting to support this conceptual and anatomical dissociation). Similarly, Aly and Yonelinas (2012; 2013) argue that Pd and K may be supported by distinct neural substrates. The HC was highlighted as a region

that may support K but not Pd (Aly et al., 2013), based on recent proposals that the HC supports the construction of relational 'bindings' of the disparate elements separated across space which make up an event; and that these relational representations can be recruited in the service of higher-level perception as well as memory (Olsen et al, 2012). The rationale here was that because K, but not Pd, was previously found to be sensitive to configural/relational differences across visually similar stimuli (Aly et al., 2012), then the relational binding functions of the HC should be important for strength (K) but not state (Pd) based perception.

Aly et al., (2012; 2013) noted that, if correct, this would have important implications for the circumstances in which perception impairments can be detected in patients with MTL damage. The argument is that legitimate impairments in one type of perception (e.g. K) could be obscured in studies that use single-point measures of perception when patients can recruit the intact form of perception (Pd) to support successful task performance. ROC markers of perception could, however, be more sensitive to perception impairments following MTL damage because they can separate the relative contributions of state and strength based perception to overall discrimination measures. For example, Aly et al., (2013) argued that if the HC constructs complex relational representations, then HC damage should be associated with impairments in strength-based perception due to difficulties with processing the global relational/configural match of visually similar scene stimuli in their change detection paradigm (K), whereas state-based perception for individual distinguishing features (Pd) should be preserved because other visual regions could potentially support such judgements independently of the MTL. With respect to the plotted ROCs, therefore, they predicted that patients with HC pathology (N=5; though the pathology incorporated additional MTL regions in at least 2 of these patients) would present with less curvilinear trend-lines relative to controls (N = 10), although the x-axis intercept should be equivalent across these two groups. Indeed, this pattern was observed in the aggregate ROCs (Fig 5.2), and analysis of the extracted parameter estimates confirmed impaired K, but preserved Pd in the HC patients.

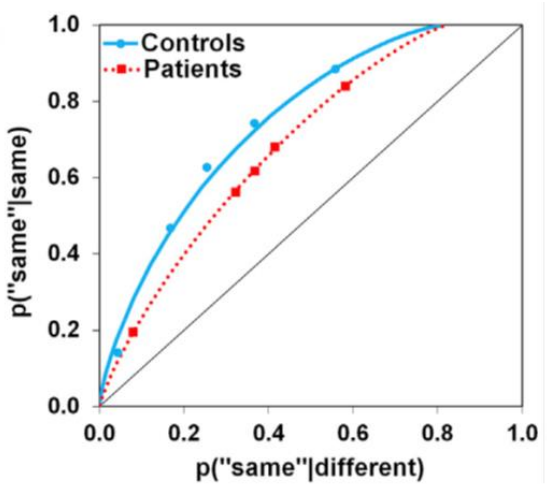

Fig 5.2. Aggregate ROCs for HC patients (red line) and healthy controls (blue line) in a scene change-detection task. The reduced curvilinearity of the patient relative to control ROC, and the matched upper x-axis intercepts has been proposed to indicate impaired strength- but preserved state-based perception. Figure adapted from Aly et al., (2013).

The authors noted that the groups were well matched at their most confident response criteria (left and right-most points on the ROC, respectively), but the patients performed less successfully at lower levels of response-confidence (i.e., the middle range of the ROC curve). This led them to argue that had they only collected binary discrimination responses and the participants had consistently adopted a strict response criterion (i.e., left and right-most points on the ROC) then the scene perception impairment could have potentially been obscured. Indeed, some studies that have assessed visual discrimination using binary responses and single-point performance metrics have failed to detect higher-level perception impairments in patients with MTL damage. Shrager et al., (2006), for example, administered discrimination tasks involving pairs of morphed faces, objects, and scenes, to patients with MTL pathology (either focal HC damage or damage incorporating both HC and PRC) and healthy controls. Performance was measured as discrimination accuracy per stimulus category, and, in contrast to the findings reported elsewhere (Lee et al., 2005a), the patients were found to be unimpaired in all three conditions. According to Aly et al., (2013), this inconsistency arises simply because binary discrimination responses and single-point performance metrics like discrimination accuracy conflate the independent contributions of different types of perception (Pd versus K), only some of which may be dependent upon the integrity of MTL substructures. As a result, the sensitivity of single-point performance metrics, with respect to MTL damage, may not be optimal. Furthermore, in the case of

the Shrager et al., (2006) study, the use of morphed stimuli has been criticised on the basis that exemplars can potentially be discriminated on the basis of local feature-discrepancy detection (Lee et al., 2012). Therefore, from the dual-process view, MTL damage may have impaired the ability of the patients to discriminate the stimuli on the basis of their overall match (i.e., K), but, arguably, Pd could have been recruited to make successful high-confidence discriminations to the stimuli based on local difference-detection alone, thus enabling patients to maintain a level of discrimination accuracy that was comparable to controls. The corollary, however, is that the independent measures of Pd and K that can be obtained using a response scale and ROCs may be more sensitive to MTL damage because they can separate the relative contributions of Pd and K based perception to discrimination performance.

I will briefly recapitulate some of the key proposals of the 'dual process' view to facilitate a clear contrast with the representational accounts that underpin the current Thesis. Firstly, single-point discrimination performance measures reflect the combined contributions of two functionally independent perception processes; state and strength based perception, or Pd and K, respectively. Second, the extent to which Pd versus K contributes to discrimination performance can be estimated by collecting response-confidence judgements and performing ROC analyses. Third, Pd and K may be supported by distinct neural substrates, with the HC, for example, contributing to successful strength- but not state-based perception. Fourth, when one of these processes is impaired due to damage to a core neural substrate, participants can rely on the intact process to support discrimination performance. Finally, ROC estimates of Pd and K may be more sensitive to impairments in higher-level perception relative to single-point performance metrics.

In contrast to the dual-process view, representational accounts argue that individual MTL (but also EVC) brain regions are not specialised to support particular memory or perception processes as such. Rather, these regions support different kinds of stimulus representations. The PRC is proposed to support representations of non-spatial feature conjunctions, which can be recruited to support the processing of objects/faces in both a memory and higher-level perception context (Graham et al., 2010; Saksida and Bussey, 2010). By contrast, the HC supports representations of spatial feature-conjunctions that can be recruited to support scene memory and perception (Graham et al., 2010; for a similar proposal, see Saksida and Bussey, 2010). In other words, the PRC and HC are *de facto* specialised, not for particular processes, but for the higher-level visual processing of objects/faces and scenes, respectively. Furthermore, even if within a given cognitive context, there are multiple 'processes' that can contribute to

task performance for a given stimulus category, these must nevertheless each interact with the same stimulus representations in the same brain regions. In the context of memory, for instance, many forms of memory are frequently distinguished according to whether they are thought to be 'declarative' or 'non-declarative' in nature (or explicit versus implicit; see section 1.3) and are often proposed to be supported by distinct neural substrates, with MTL regions thought to be critical for declarative but not non-declarative memory (Squire et al., 2004). This view is, however, undermined by evidence that HC damage impairs performance in both declarative (recognition) and non-declarative (categorization and perceptual learning) learning and memory tests involving scene stimuli, whilst PRC damage impairs declarative and non-declarative memory for faces (Taylor et al., 2007; Graham et al., 2006). Similarly, HC and PRC damage would be expected to impair perception for distinct categories of complex visual stimuli generally, but not distinct perceptual processes. So in stark contrast to the dual-process view of perception, representational accounts predict that HC damage will impair both Pd and K for scene but not object/face stimuli. Conversely, PRC damage should impair Pd and K for objects/faces but not scenes.

Dual-process and representational accounts therefore generate different predictions about how MTL damage will affect markers of perception in the various conditions of the change detection task. Given that the fornix and ILF act primarily as input/output pathways for the HC and PRC, respectively, these models also generate distinct predictions about how inter-individual variation in the properties of these two tracts will relate to the markers of perception that can be obtained from participants using the change-detection paradigm and ROC procedures described by Aly et al., (2012; 2013). Representational accounts, for instance, predict that variation in fornix properties will correlate with Pd and K for scenes but not faces, whereas variation in ILF properties will correlate with both Pd and K for faces but not scenes. The dual process view proposes that the HC supports K but not Pd for scenes, owing to its putative role in constructing high-resolution relational bindings (Aly et al., 2013; Yonelinas, 2013). Further, Yonelinas (2013) argues that the HC could also contribute to perception for visual objects when there is a demand to process the configural or relational information between their constituent features. Given the subtle but global impact that the image manipulations used in the standard change-detection task have upon the configuration of face as well as scene features, the dual-process view therefore predicts that fornix properties will be predictive of K but not Pd for faces as well as scenes here. The dual process view is currently under-specified with regard to the role of the PRC in Pd versus K for different stimulus categories. Yonelinas (2013, pp40)

does note, however, that “brain regions such as the perirhinal cortex can support perception of configural objects and faces”, so from this we might infer that the dual process view predicts that ILF properties would be predictive of K but not Pd for faces, and neither Pd nor K for scenes. The change-detection paradigm therefore affords a test of the representational accounts of perception that form the theoretical basis of the current Thesis, against the emerging dual-process view of perception. The task also affords a test of the proposition that the category-sensitive contributions of the fornix/ILF to higher-level visual processing, which were demonstrated in Chapter 4, extend to markers of perception for trial-unique stimuli.

In this Chapter, therefore, I report a study in which participants – for whom DWI’s were available – were administered a modified version of the confidence-based trial-unique face/scene change-detection paradigm described in Aly et al., (2012; 2013). Participants were required to use a 6-point confidence-based rating scale to indicate whether two consecutively presented images of a face or a scene were identical or different (‘different’ trials contained pinched/spherized stimuli). Participant-specific ROCs were then fitted to the data for each stimulus category, from which parameter estimates of Pd and K were subsequently extracted. As per Aly et al., (2012), the face stimuli comprised real-world face photographs; successful discrimination of such stimuli is associated with PRC activity (Mundy et al., 2013). The scene stimuli were photographs of houses in their natural context. These were employed to provide a bridge with the photographs of buildings employed as scene stimuli by Aly et al., (2012; 2013); the HC has been implicated in processing such stimuli, as evidenced by, for example, greater activity in the right HC during presentation of upright compared to inverted houses (Epstein et al., 2006). Another benefit of using this sub-category of real-world visual scenes is that, like the ‘face’ stimuli, this stimulus set is also characterised by a high degree of feature overlap (all houses contain windows, just as all faces contain lips).

If the HC supports representations of the spatial feature-conjunctions comprising scenes, as proposed by the EMA (Graham et al., 2010), then inter-individual variation in measures of the macro- and microstructure of the fornix should be predictive of both Pd and K for scene but not face stimuli. Considering the ILF, variation in ILF properties should correlate with markers of both Pd and K for faces but not scenes, because this pathway links to the PRC, which supports representations of the non-spatial feature conjunctions comprising faces/objects according to representational accounts (Graham et al., 2010; Saksida and Bussey, 2010). In contrast to representational accounts, Yonelinas (2013) argues that the HC could contribute to strength-based perception for

faces as well as scenes when there is a demand to process the configural/relational information between their constituent features. The current image manipulations affect the configuration of both face and scene features, so the dual-process view predicts that fornix properties will be predictive of K but not Pd for both faces and scenes. The dual process view does not currently specify a differential role for the PRC/ILF in Pd versus K within specific visual categories, but on the basis that its proponents accept that the PRC can support perception for *configural* objects, a somewhat speculative prediction would be that ILF properties will correlate with K but not Pd for faces but not scenes.

5.2. Method

5.2.1. Participants

Behavioural data was collected from 22 healthy participants for whom DWI's were already available as a result of their participation in a previous brain imaging study at CUBRIC (9 male; age range = 19-34, mean = 25.5, SD = 4.1). All participants provided written informed consent for participation in the current study, which was approved by the Cardiff University School of Psychology Research Ethics Committee.

5.2.2. Stimuli

Faces: 160 grayscale portrait photographs (80 females) were obtained from online face databases: male faces courtesy of Michael J. Tarr (Center for the Neural Basis of Cognition and Department of Psychology, Carnegie Mellon University, http://www.tarrlab.org), and female faces, courtesy of the University of Texas at Dallas Center for Vital Longevity (Minear and Park, 2004).

Scenes: The scene stimuli were 160 real-world grayscale photographs of houses in Pasadena, California, available online courtesy of the computational vision group at the California Institute of Technology (http://www.vision.caltech.edu/archive.html).

The photographs from each of these stimulus categories were distorted using the 'spherize' and 'pinch' tools in Photoshop, as per Aly et al., (2012; 2013). The 'pinch' function contracted the image inwards slightly, whereas the 'spherize' function expanded the image outwards slightly. No visual information was added or removed from the original stimulus, but the configuration of the face/scene features was altered as a result of these image manipulations. Each individual stimulus pair was therefore composed of a slightly 'pinched' and a slightly 'spherized' version of the original stimulus (Fig 5.3 shows example stimulus-pairs). The distortion effects resulting from both the 'pinching' and 'spherizing' techniques were greatest near the centre of the image, with a gradually diminishing impact towards the periphery of the image. Whilst the procedure used to generate the face- and scene-pairs was therefore identical, it is worth highlighting that the pinching/spherizing functions affect face and scene images slightly differently. For faces, the procedure affects the shape and configuration of the features (e.g. eyes, nose, and mouth) that comprise an individual face. By contrast, for scenes, the procedure additionally distorts spatial relationships between the perceptually distinct object 'features' that comprise a scene (e.g. distance between windows, a tree, and a drive-way).

Pilot testing was conducted to determine an appropriate amount of distortion to apply to the faces/scenes in order that overall behavioural performance in the main task would be similar across these categories. This confirmed that 12% and 16% pinching/spherizing – applied to the faces and scenes, respectively – was sufficient to match behaviour. Four additional pairs of practice stimuli were also created, using the same methods, for each of the stimulus categories.

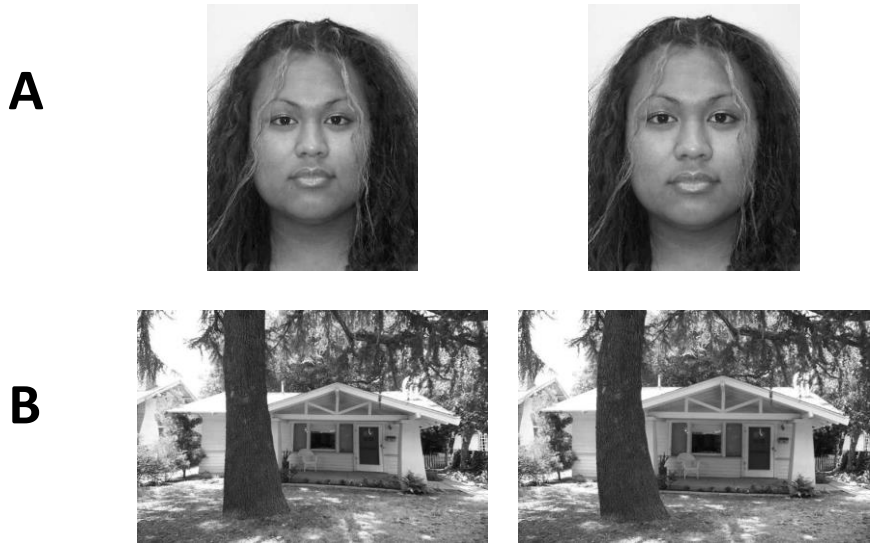

Fig 5.3. 'Pinched' (left) and 'Spherized' (right) versions of a representative Face (A), and Scene (B) stimulus-pair from the change-detection task.

5.2.3. Experimental Procedure

The change-detection task reported here involved making sequential discriminations between pairs of highly visually similar scenes and faces, and was administered to participants approximately 20 months after DWI's were acquired (mean = 20.4, SD = 3.3, range = 15-26). The task was undertaken using a laptop with Presentation software installed (Neurobehavioural Systems). The experiment began with an opportunity for the participant to inspect the 4 practice pairs for each stimulus category and complete a 4-trial practice block with a view to identifying the sort of stimulus manipulations to expect during each condition of the main task. During testing, the presentation order of the task conditions was counterbalanced across participants.

In both the practice and the main experimental task, each individual trial began with a blank screen for 1000ms. The participant was then exposed to one stimulus from a given pair for 1000ms, followed by a 50ms inter-stimulus interval (ISI; filled by a high contrast visual mask), and then a second stimulus from the same pair of images for a further 1000ms. A 6-point confidence scale followed presentation of this second stimulus, at which point the participant was required to indicate whether the stimulus changed during the masked ISI by pressing one of 6 number keys on the laptop keyboard (1 = "Sure-different"; 2 = "Maybe-different"; 3 = "Guess-different"; 4 = "Guess-

same"; 5 = "Maybe-same"; 6 = Sure-same"). The next trial was triggered by a response. Fig 5.4 illustrates an example trial.

Within each condition of the experimental task (faces/scenes) there was 1 trial for each of the 160 stimulus-pairs. The presentation order of the stimulus-pairs was randomised across participants. Similarly, the allocation of the 'pinched' and the 'spherized' stimulus to image 1 and 2 within each trial was also randomised, with the restriction that 'pinched' and 'spherized' stimuli occurred first and second in the trial sequence the same number of times, and that the overall proportion of 'Same' and 'Different' trials was matched (i.e., 50% same versus 50% different). All stimuli included in the experiment were trial-unique and so none of the derived performance measures should have benefitted from any incidental within-trial stimulus-related learning.

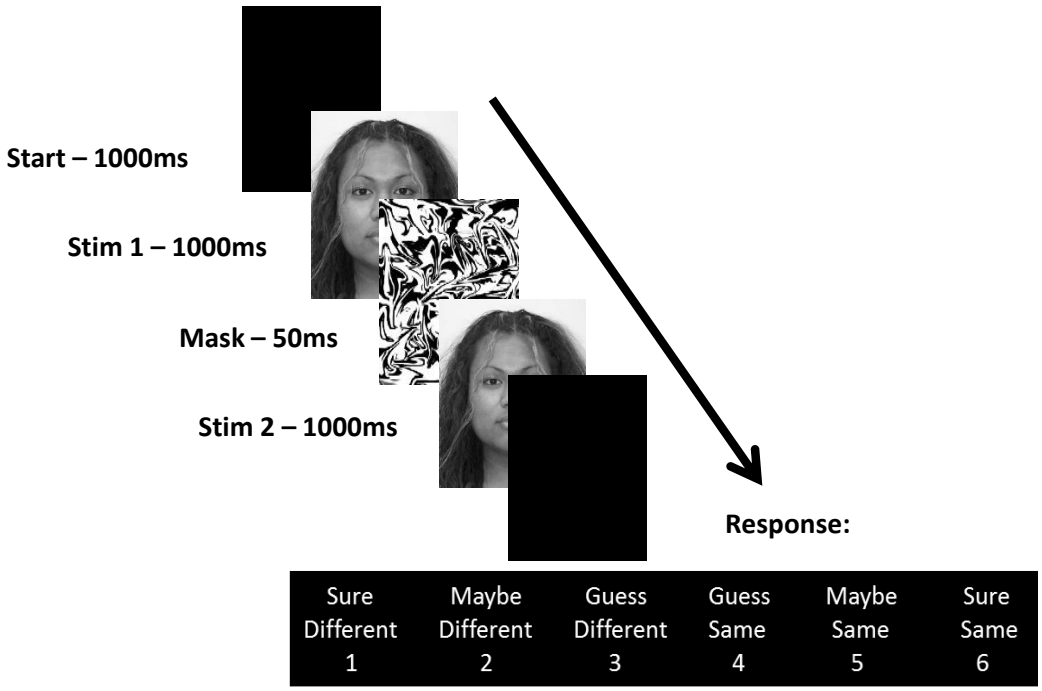

Fig 5.4. Trial schematic for the change-detection task.

For each participant, the cumulative proportion of 'hits' versus 'false alarms' was calculated for the most confident 'same' response (i.e., '6' responses) up to the most confident 'different' response (i.e., '1' responses). This data was used to plot participant-specific perception ROC's, which were subsequently fitted to state-strength theory using a maximum likelihood estimation procedure in an Excel solver, in order to derive separate quantitative estimates of Pd and K for each stimulus category (Aly et al., 2013, 2012).

5.2.4. MRI acquisition

Whole-brain diffusion-weighted MRI data were acquired using a 3T GE HDx Signa scanner with an eight-channel head coil, by researchers at the Cardiff University Brain Research Imaging Centre (CUBRIC). As per the acquisition protocol described in Chapter 4, images were acquired using a diffusion-weighted single-shot spin-echo echo-planar imaging pulse sequence (with TE = 87ms, field of view = 23 x 23 cm^2, 96 x 96 acquisition matrix, 60 contiguous slices acquired along an oblique-axial plane with 2.4mm thickness and no gap), and the scans were cardiac-gated using a peripheral pulse oximeter. Gradients were applied along 30 isotropically-distributed orientations with b = 1200 s/mm^2 (Jones et al., 1999). Three non-diffusion-weighted images (DWI) with b = 0 s/mm^2 were also acquired. The images were subsequently co-opted and analysed by the current author in order to test the hypotheses of this study.

5.2.5. DWI pre-processing

All DWI pre-processing was conducted as described in section 3.2.6.2.

5.2.6. Tractography Protocol

Consistent with the protocol described in Chapters 3-4, whole brain tractography was initially performed from all voxels in participants' (free-water corrected) native diffusion-space in ExploreDTI using a deterministic tractography algorithm based on constrained spherical deconvolution (Tournier et al., 2008; Jeurissen et al., 2011). A step size of 1mm, and an angle threshold of 30 degrees was adopted to prevent the reconstruction of anatomically implausible fibers.

A multiple region-of-interest (ROI) approach was then used to isolate the fornix bilaterally (mean voxel count: 1319; SD = 403; range: 549-2133) from the results of this whole-brain tractography procedure (Metzler-Baddeley et al., 2011). Mean FA, MD,

and *f* indices were subsequently extracted from the reconstructions in ExploreDTI (Jones et al., 2005).

As per Chapter 4, mean FA/MD/*f* indices were also extracted from the main occipito-temporal associative white-matter pathway; the inferior longitudinal fasciculus (ILF; Catani et al., 2003). The right and left ILF were reconstructed (mean voxel count: 3504; SD = 893; range: 2005-5457) using a two-ROI approach (Wakana et al., 2007), and for comparability with the fornix, the average of the measures obtained from the two hemispheres was calculated to create a single value per participant.

5.2.7. Analyses

Two-tailed Pearson correlation statistics were calculated to establish whether fornix/ILF FA, MD, or *f,* were related to Pd and/or K for each condition of the change-detection task. Consistent with the approach adopted in Chapter 4, a significance threshold of $p \leq 0.05$ was adjusted by a Bonferroni correction factor of 2 in order to control for false-positive effects, potentially arising through the calculation of more than one structure-behaviour correlation statistic across two distinct white matter tracts (required $p \leq 0.025$). Again, this is, notably, a more conservative approach to controlling for multiple comparisons compared to other similar studies (Rudebeck et al., 2009), but should not unduly inflate the risk of reporting false negative effects. To provide additional information with respect to the reliability of the reported effects, however, all correlations are again reported with 95% confidence intervals around the effect size estimates, based on 1000 bootstrapped samples of the data. Directional t-tests for dependent correlations were used to determine significant differences between correlations, with a significance threshold of $p \leq 0.05$.

5.3. Results

Table 5.1. Mean FA, MD ($x10^{-3}mm^2\ s^{-1}$), and *f*, in both the fornix and the ILF of all 22 participants. Standard deviations are provided in brackets.

Tract	FA	MD	*f*
Fornix	0.379 (0.025)	1.032 (0.036)	0.716 (0.050)
ILF	0.425 (0.024)	0.747 (0.012)	0.902 (0.008)

Table 5.1 shows the mean and standard deviation of values obtained for FA, MD and *f* in the fornix and the ILF. Prior to reporting the analyses testing our key hypotheses, we assessed the relationship between FA, MD and *f* by calculating correlation coefficients between each measure for each tract for all 22 participants. Fornix FA was correlated with both fornix *f* and MD (r = 0.583, p = 0.004, 95% CI [0.217, 0.844]; r = -0.452, p = 0.035, 95% CI [-0.770, -0.035], respectively). Fornix MD and *f* were also highly correlated (r = -0.598, p = 0.003, 95% CI [-0.886, -0.177]). Turning to the ILF, MD and *f* were highly correlated (r = -0.937, p < 0.001, 95% CI [-0.975, -0.855]). By contrast, the association between ILF FA and ILF MD was not significant; similarly, there was no significant correlation between ILF FA and *f* (r = -0.011, p = 0.960, 95% CI [-0.522, 0.438]; r = 0.144, p = 0.523, 95% CI [-0.328, 0.624]).

5.3.1. Behavioural data

Table 5.2. Mean, standard deviation, and the range of overall discrimination performance in the change-detection task, separated by condition.

Performance Metric	Mean	SD	Range
Faces Accuracy	80.00	9.62	60.00 – 98.13
Scenes Accuracy	79.88	9.86	62.50 – 94.38

Participants' same/different discrimination judgements were initially dichotomised (i.e., all 6-4 responses = 'same' responses, all 3-1 responses = 'different' responses) so that discrimination accuracy could be collapsed across levels of response-confidence, and compared across the two conditions of the task (see Table 5.2). A two-tailed paired samples t-test revealed no significant differences in discrimination accuracy across the Face and Scene conditions (t (21) = 0.058, p = 0.955). Before examining the ROC data, white matter structure-behaviour correlations were then calculated to investigate whether the micro- or macrostructure of the fornix/ILF was predictive of discrimination accuracy for either the Faces or the Scenes in the current task, as per the analyses reported in Chapter 4. In contrast to the findings reported in Chapter 4, measures of white matter micro- and macrostructure were not found to be predictive of discrimination accuracy in either the Face or Scene conditions of the change-detection task; this was true in both the fornix and the ILF (largest r = 0.333, p = 0.129, 95% CI [-0.040, 0.694])

5.3.2. ROC data

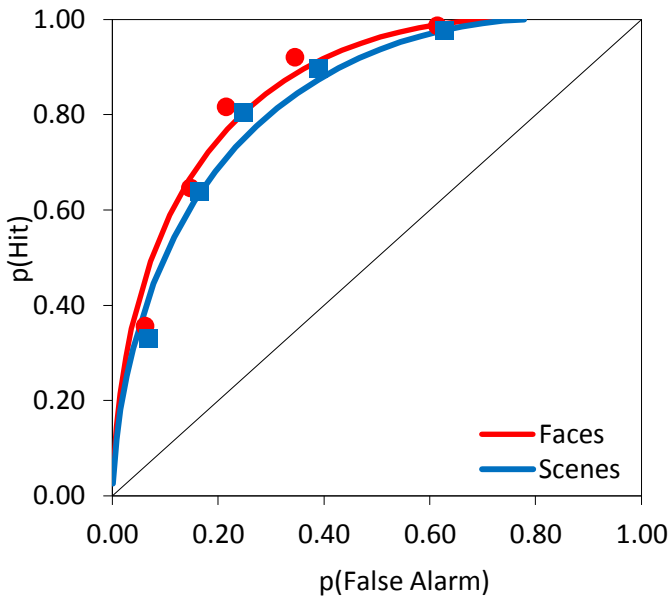

Fig 5.5. (A) Aggregate ROC's for the Face and Scene conditions (red and blue lines, respectively) of the change-detection task.

Table 5.3. Mean, standard deviation, and range of the parameter estimates of both 'state' and 'strength' based perception for Scenes and Faces.

Performance Metric	Mean	SD	Range
Faces Pd	0.34	0.23	0.00 – 0.89
Scenes Pd	0.36	0.23	0.00 – 0.93
Faces K	1.30	0.89	0.00 – 3.71
Scenes K	1.12	0.65	0.14 – 2.59

Fig 5.5 illustrates the participants' discrimination performance as separate aggregate ROC's for each core condition of the study. Visual inspection of the fitted aggregate ROC's confirms a similar pattern of performance across the Face and Scene conditions, resulting in comparably curvilinear trendlines (i.e., K) in which the intercept with the upper x-axis is shifted to the left of the ROC (i.e., Pd). It is also worth noting that the participants gave very few '1' responses during 'same' trials for all conditions of this task (3% for faces, and 6% for scenes). This indicates that participants seldom made a highly confident 'different' judgement to a pair of stimuli that were in fact identical, and were therefore using the confidence-based rating scale correctly (Aly et al., 2014b). Participant-specific parameter estimates of both Pd and K were subsequently extracted from the participant-specific ROC's for these conditions (see Table 5.3). Pair-wise repeated measures t-tests revealed that there were no significant cross-category differences in the parameter estimates for either Pd (t (21) = 0.259, p = 0.798) or K (t (21) = 0.956, p = 0.350); more specifically, the relative contribution of Pd and K to overall performance was well matched across these stimulus categories.

Two-tailed Pearson correlation statistics were calculated to determine whether there were any within-category correlations between Pd and K. These analyses revealed that estimates of Pd and K derived from the participant-specific Face ROC's were not significantly correlated with one another (r = -0.279, p = 0.209, 95% CI [-0.647, 0.326]). Similarly, neither did the estimates of Pd and K for the Scene stimuli show a significant association (r = 0.232, p = 0.299, 95% CI [-0.208, 0.592]). This is consistent with the notion that Pd and K make functionally independent contributions to overall

discrimination measures (Aly and Yonelinas, 2012), in the same way that ro and d' (i.e., recollection versus familiarity) can make functionally independent contributions to recognition memory performance according to some dual-process models of recognition memory (Yonelinas, 1994; Aggleton and Brown, 1999). It is, however, worth noting that for a small number of participants (3 for Faces; 1 for Scenes), a negligible or zero-estimate of Pd was derived from the participant-specific ROC's. Similarly, Aly et al., (2013) reported that one of their 10 healthy control participants, as well as one of their 5 HC patients, presented with zero-estimates of Pd for their scene stimuli. Zero-estimates of Pd may arise when individuals place a greater dependence on a K-based strategy for solving the rapid change-detection task in those participants. Indeed, for every single participant for whom a zero or negligible estimate of Pd was obtained in a given condition of the change-detection task, their corresponding K estimate (Faces: 1.38, 2.64, 3.72; Scenes: 2.06) was always greater than the mean for that condition (Faces: 1.30; Scenes: 1.12).

5.3.3. Task – Tractography

Macrostructure of the fornix, as assessed here using fornix *f,* did not show a significant association with Pd measures obtained for either Scenes or Faces (r = 0.244, p = 0.274, 95% CI [-0.240, 0.670]; r= 0.146, p = 0.517, 95% CI [-0.237, 0.461], respectively), and these correlations were not significantly different from each other (t (19) = 0.293, p = 0.387). Fornix *f* did not correlate significantly with K for either Scenes or Faces (r = -0.173, p = 0.442, 95% CI [-0.524, 0.224]; r= 0.159, p = 0.479, 95% CI [-0.221, 0.549], respectively), and these correlations were not significantly different from one another (t (19) = -1.32, p = 0.102). The correlations between fornix *f* and both Pd and K were also compared within each stimulus category in order to determine, statistically, whether variation in the macrostructure of this tract is more strongly related to a particular marker of perception for either Scenes or Faces. This revealed that the correlations between fornix *f* and both Pd and K were not significantly different from one another; this was true for both Scene and Face stimuli (t (19) = 1.559, p = 0.068; t (19) = -0.036, p = 0.486, respectively).

In contrast, fornix microstructure, as assessed by MD, showed a statistically significant association with Pd for Scenes (r = -0.479, p = 0.024, 95% CI [-0.744, -0.103]), but not Faces (r= 0.143, p = 0.525, 95% CI [-0.353, 0.590]), and these correlations were significantly different from each other (t (19) = -2.03, p = 0.029; Fig 5.6*A*). Fornix MD did not, however, show a significant correlation with K, a finding true for both Scenes

and Faces (r = 0.020, p = 0.929, 95% CI [-0.300, 0.288]; r= -0.242, p = 0.279, 95% CI [-0.568, 0.030]), and these K correlations for Scenes and Faces were not significantly different from each other (t (19) = 1.030, p = 0.158). Within-category comparisons also confirmed that fornix MD was more strongly related to Pd compared to K for Scenes (t (19) = -2.01, p = 0.03), whereas the correlations between fornix MD and Pd versus K for Faces were not significantly different from one another (t (19) = 1.084, p = 0.146).

Similar analyses applied for fornix FA – another microstructural measure – revealed no significant correlations. The correlation with Pd for both Scenes and Faces did not survive our robust statistical threshold (r = 0.274, p = 0.217, 95% CI [-0.108, 0.588]; r= -0.124, p = 0.583, 95% CI [-0.554, 0.256], respectively), and these correlations were not significantly different from each other (t (19) = 1.196, p = 0.123). Fornix FA was also not correlated with K for Scenes nor with Faces (r = -0.119, p = 0.597, 95% CI [-0.449, 0.254]; r= -0.028, p = 0.901, 95% CI [-0.418, 0.430], respectively) and these correlations were not different from each other (t (19) = -0.348, p = 0.366). The correlations between fornix FA and both Pd and K were not significantly different from one another, within either stimulus category (Scenes: (t (19) = 1.464, p = 0.08; Faces: t (19) = -0.263, p = 0.398).

In summary, the only significant association obtained in the fornix was between MD and Scene Pd. This association was significantly stronger than the corresponding Face Pd correlation, but also the corresponding Scene K correlation.

Turning to the ILF, *f* did not correlate significantly with Pd for either Faces or Scenes (r = 0.467, p = 0.028, 95% CI [0.046, 0.764]; r= 0.033, p = 0.884, 95% CI [-0.454, 0.618]); and the difference between these correlations did not reach statistical significance (t (19) = 1.387, p = 0.091). ILF *f* did not show a statistically significant correlation with K for either Faces or Scenes (r = -0.025, p = 0.912, 95% CI [-0.384, 0.528]; r= 0.267, p = 0.229, 95% CI [-0.038, 0.587]), and these correlations were not significantly different from each other (t (19) = -1.16, p = 0.131). Within both stimulus categories, the correlations between ILF *f* and both Pd and K were not significantly different from one another (Faces: t (19) = 1.481, p = 0.078; Scenes: (t (19) = -0.852, p = 0.203).

In contrast to the fornix, ILF MD showed a significant association with Pd for Faces (r = -0.509, p = 0.015, 95% CI [-0.768, -0.159]), but not Scenes (r= 0.021, p = 0.925, 95% CI [-0.539, 0.475]), and these correlations were significantly different (t (19) = -1.73, p = 0.05; Fig 5.6*B*). ILF MD did not, however, show a significant correlation with K, either

for Faces (r = 0.159, p = 0.480, 95% CI [-0.440, 0.479]) or Scenes (r= -0.091, p = 0.687, 95% CI [-0.398, 0.197]), and these correlations were not significantly different (t (19) = 0.973, p = 0.172). Within category comparisons confirmed that ILF MD was more strongly associated with Pd compared to K for Faces (t (19) = -2.07, p = 0.026); within the Scenes condition, however, the correlations between ILF MD and both Pd and K were not significantly different from each other (t (19) = 0.396, p = 0.349).

Finally, while ILF FA did not show a significant correlation with Pd for Faces (r = -0.165, p = 0.462, 95% CI [-0.591, 0.222]) nor for Scenes (r= 0.377, p = 0.084, 95% CI [-0.026, 0.666]); these correlations, however, were marginally different (t (19) = -1.69, p = 0.054). ILF FA did not show a significant association with K for either Faces or Scenes (r = 0.304, p = 0.169, 95% CI [0.039, 0.576]; r= 0.426, p = 0.048, 95% CI [0.074, 0.690]); and these correlations were not significantly different (t (19) = -0.514, p = 0.307). The additional within-category comparisons showed that the correlations between ILF FA and both Pd and K were not significantly different from one another, and that this was true within the data for both the Face and Scene conditions (t (19) = -1.34, p = 0.098; t (19) = -0.196, p = 0.424, respectively).

In summary, there was a significant association between ILF MD and Face Pd. This association was significantly stronger than the corresponding Scene Pd correlation, but also the corresponding Face K correlation.

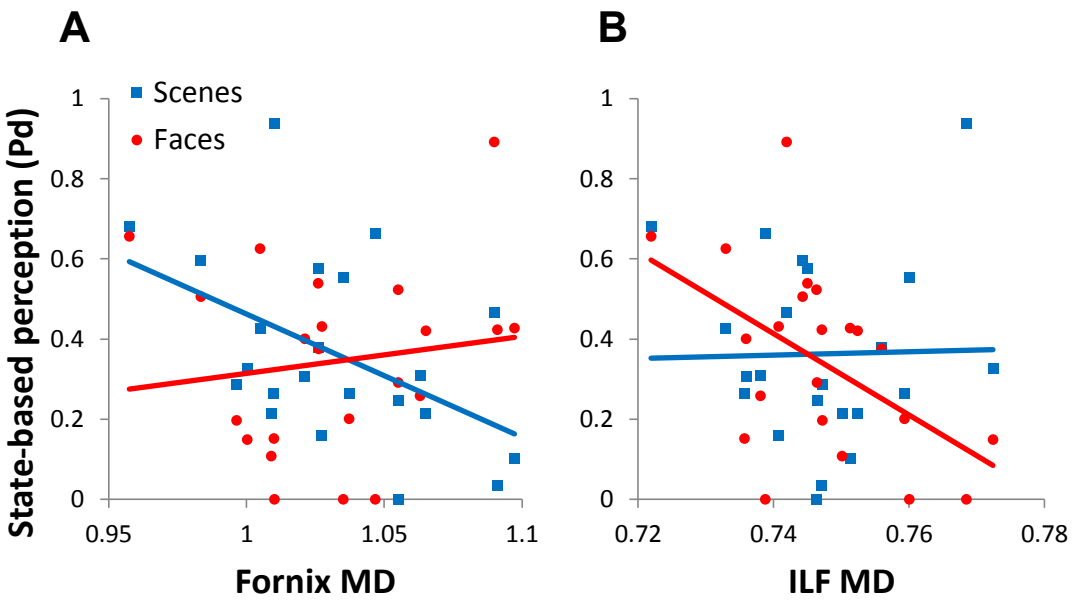

Fig 5.6. Relationship between the MD ($x10^{-3}mm^2\ s^{-1}$) of the fornix (A) and the ILF (B), and Pd for faces and scenes (red and blue lines, respectively).

5.4. Discussion

In Chapter 4, inter-individual variation in diffusion MRI measures of white matter microstructure (MD in particular) and macrostructure (*f*) in the fornix was shown to correlate with discrimination accuracy for scenes, but not faces, across two visual discrimination tasks. ILF microstructure, as assessed by FA, correlated with discrimination accuracy for faces but not scenes in one of two tasks. A limitation of that study, however, was the use of repeated stimuli, which meant that we do not yet know whether there are category-sensitive contributions of ILF/fornix microstructure to trial-unique perceptual discrimination. In addition, in Chapter 4, visual discrimination was considered a unitary construct; some authors have, however, suggested that two functionally independent forms of perceptual processing may contribute to visual discrimination performance. The relative contributions of these two components — termed *state* (Pd) and *strength* (K) based perception — can be separated using receiver operating characteristics (ROCs). Pd has been characterised as a discrete

state in which participants become aware of specific local details that distinguish visually similar images (i.e., Perceiving), and K as a continuous *strength*-based form of perception that enables assessments of the overall match between the images (i.e., Knowing). Here, we asked whether diffusion-MRI indices of ILF/fornix microstructure (FA and MD) and macrostructure (*f*), would correlate with markers of Pd and/or K for trial-unique faces and scenes. On the basis of representational accounts of perception (Graham et al., 2010l Saksida and Bussey, 2010), which propose that MTL sub-regions support distinct types of stimulus representations as opposed to memory or perception 'processes', it was predicted that fornix properties would correlate with both Pd and K for scenes but not faces, whereas ILF properties would correlate with Pd and K for faces but not scenes. These predictions were tested against those derived from the emerging 'dual-process' view of perception (Aly et al., 2012; 2013; Yonelinas, 2013), which predicted that fornix properties would correlate with K but not Pd for both faces and scenes, whereas ILF properties would correlate with K for faces but not scenes; and with Pd for neither faces or scenes. The analysis revealed that inter-individual variation in a diffusion MRI measure of fornix microstructure (MD) was predictive of Pd for trial-unique pairs of visually similar scenes, but not faces, in a confidence-based visual discrimination task. Bilateral ILF MD in the same participants was instead predictive of Pd for trial-unique faces, but not scenes.

That inter-individual variation in fornix and ILF properties would be differentially predictive of markers of perception for scenes and faces is consistent with the distinct roles that the fornix and ILF play as input/output pathways for the HC and the PRC, respectively. HC damage has been shown to selectively impair scene memory and perception, whereas MTL damage that incorporates PRC produces additional impairments in object/face memory and perception (Lee et al., 2005b; Bird et al., 2007; Aly et al., 2013). Like those reported in Chapter 4, however, the category-sensitive white matter structure-behaviour relationships reported here augment the conclusions we can derive about how the brain supports higher-level discrimination for distinct visual categories; successful performance in such tasks is not simply a product of highly specialised scene and face processing modules in the HC and PRC, respectively, but is likely an emergent property of the representations within these MTL regions *and* their functional/structural connections with other related brain areas (Behrman and Plaut, 2013). The notion that HC contributions to scene processing tasks may partly depend upon interactions with other brain regions via the fornix is consistent with studies reporting impaired performance in spatial discrimination-learning and object-in-scene memory tasks following fornix transection in animals

(Buckley et al., 2004; Gaffan, 1994). Conversely, that PRC contributions to higher-level face processing may depend upon the propagation of visual information along the ILF is consistent with evidence that individuals with face/object recognition impairments present with significant reductions in MRI indices of ILF microstructure (Thomas et al., 2009; Ortibus et al., 2011).

These category-sensitive structure-behaviour effects were demonstrated here using real-world face and scene stimuli. Photographs of faces were employed to match the stimuli reported in Aly et al., (2012), but the successful discrimination of such stimuli is also associated with PRC activity (Mundy et al., 2013). The current scene stimuli were photographs of houses. These provided a bridge with the photographs of buildings employed by Aly et al., (2012; 2013), but the HC has also been implicated in processing such stimuli, as evidenced by greater activity in the right HC during presentation of upright compared to inverted houses (Epstein et al., 2006). Photographs of houses also activate other scene-sensitive cortices; Epstein and Kanwisher (1998) demonstrated that houses elicit a greater PPA BOLD response than do both objects and faces. Interestingly, the houses employed by Epstein and Kanwisher were cut from their background; the PPA response to these images was itself attenuated relative to that for photographs of buildings presented intact within their broader spatial context. The houses in the current scene stimuli were not cut from their background, so as well as being comparable to the stimuli reported by Aly et al., (2013), they would be expected to prompt a substantial BOLD response in posteromedial scene-sensitive cortices.

Category-sensitive contributions of the fornix/ILF to visual discrimination judgements are also consistent with predictions from representational accounts of MTL function. The EMA (Graham et al., 2010), for instance, proposes that the HC and PRC support complex representations of spatial and non-spatial feature-conjunctions, respectively, and are required when paradigms stress processing of feature-conjunctions (see also Saksida and Bussey, 2010). Consequently, the HC is critical for higher-level scene memory (Bird et al., 2007), but also successful perceptual discrimination between items with overlapping spatial features (Lee et al., 2005b; Aly et al., 2013). The PRC, by contrast, supports higher-level object/face memory and perception, again in tasks that stress the processing of non-spatial feature-conjunctions (Lee et al., 2005b; Mundy et al., 2013).

The sensitivity of Pd to these category-sensitive structure-behaviour relationships is also compatible with representational accounts. To understand why representational accounts anticipate that fornix/ILF properties may correlate with Pd within their 'preferred' stimulus categories, it is important to note that in the current task, each condition comprises exemplars from stimulus categories that are characterised by a high degree of 'feature overlap'. This is relevant because Barense et al., (2012; see section 1.5.1) recently reported that over the course of a task that involved making discriminations to visually similar pairs of trial-unique 'blob' stimuli that shared lower-level features with blobs from other trials, the performance of patients with PRC damage declined relative to controls. Based on this finding, Barense et al., (2012) argue that the complex visual representations that are normally instantiated in PRC are required to buffer discrimination judgements for visually similar object-like stimuli against a gradual build-up in lower-level feature-ambiguity, which occurs over successive trials as visually similar features are repeatedly encountered across the stimulus set. If we accept the proposition that Pd reflects local-feature processing, and visually similar features recur during the change-detection task, then Pd may have been sensitive to a role for MTL representations in buffering visual discrimination against the build-up of feature ambiguity. This provides a parsimonious explanation for the significant correlation between ILF/fornix properties and Pd within their 'preferred' stimulus categories.

A number of tract-specific interpretations are also plausible. That ILF MD correlated with Pd but not K for faces may indicate a role for the ILF in relaying information about individual face features from posterior VVS regions, towards more anterior VVS regions proposed, by representational accounts, to integrate these features into more complex holistic face representations (PRC; Graham et al., 2010; Saksida and Bussey, 2010). The ILF is particularly suited to this role as it traverses the posterior-anterior extent of the extended VVS and possesses connections with numerous face-sensitive occipito-temporal regions (Pyles et al., 2013; Gschwind et al., 2012).

In contrast to the ILF, which receives dense inputs from early visual areas and projects to anteromedial temporal regions, the fibres comprising the fornix mainly originate/terminate in the HC. The correlation between fornix MD and Pd for scenes may therefore indicate that the representational complexity afforded by HC representations, enables the detection of local spatial differences within scenes. This proposition is relevant in relation to a recent review of anatomical and functional variation along the HC. Poppenk et al., (2013) point out that in rodents, the receptive

field of place cells (see section 1.4.4) is smaller in dorsal compared to ventral HC (Kjelstrup et al., 2013), and dorsal HC lesions impair fine but not coarse spatial location discriminations (McTighe et al., 2009). They also highlight that posterior HC activations often emerge in human fMRI memory studies when participants are required to process local spatial details, such as the precise locations of individual landmarks (Hirshhorn et al., 2012). Poppenk et al., (2013) argue that the posterior HC may be particularly important for 'finer-grained' spatial processing because it contains a higher proportion of dentate gyrus (DG) and lower proportion of CA1-3 subfields (section 1.1.2) relative to more anterior HC (Malykhin et al., 2010). The DG has been proposed to play a key role in constructing highly distinct, non-overlapping representations of similar events – an ability called pattern separation (Yassa and Stark, 2011). Consistent with this, very small changes in visual input can substantially alter correlated activity patterns in DG cells (Leutgeb et al., 2007). By contrast, other HC subfields (e.g. CA3) are associated with pattern completion; the putative process by which "incomplete or degraded representations are filled-in based on previously stored representations" (Yassa and Stark, 2011, pp515). Its high DG/CA ratio could therefore bias the posterior HC towards performing pattern separation on stimulus inputs, leading to especially 'sharp' representations in posterior HC. Whilst the HC may construct conjunctive spatial representations as per the EMA (Graham et al., 2010) those instantiated within posterior HC could be particularly 'fine-grained', potentially enabling local spatial-difference detection across visually similar scenes.

It is also worth noting that whilst the 'pinch' and 'spherize' effects that were applied to the present scene stimuli are global in that they expand/contract all stimulus features from/toward the centre of the image, they also affect multiple spatial properties (e.g. size, shape, location and orientation) of *individual objects* within the scenes. From Fig 3*B,* for example, it is clear that each pair of houses could potentially be discriminated based on the differential warping or relative position of their windows (or walls etc.). It is unlikely that the extended HC network – of which the fornix is a part – is required to detect differences in a single spatial property of an 'object' within a given scene-pair because HC damage does not impair size or shape oddity judgements (Lee et al., 2005b). The finding that fornix MD correlated with Pd might, however, be interpreted to indicate a role for the HC in processing conjunctions of spatial properties like the size, shape, orientation, *and* location of those objects. Some studies provide evidence consistent with this interpretation. Knutson et al., (2012), reported that patients with HC damage were impaired in a discrimination task that involved identifying the unique object from an array of twin-pairs of perceptually similar objects, even though most of

the patients had no pathology in PRC; a region in which damage is more frequently associated with object-processing impairments. Critically, the patients were impaired in only the most difficult task conditions, which involved discriminating objects whose appendages could differ along multiple subtle spatial dimensions, such as their size, shape, and orientation. Fornix-transected monkeys have also been shown to be impaired in learning to make discriminations between tadpole stimuli that are defined by conjunctions of spatial variables including their position, orientation, and tail-length. Further, the HC has been implicated in structural learning tasks, in which animals learn to discriminate visual stimuli that are comprised of the same individual features, but the particular spatial disposition of the features comprising the target stimulus is diagnostic of reward (Aggleton et al., 2007). Fornix properties were not, however, correlated with Pd for faces here, even though the image manipulations also influenced the spatial disposition of face-features. The current data therefore suggests that the fornix is relatively specialised for processing aspects of visual scenes. Nevertheless, future representational accounts could clarify whether the spatial properties of object-like stimuli and their constituent lower-level features can be partially supported by HC representations, or whether these are fully embedded within PRC representations.

From a representational perspective, variation in fornix/ILF properties was also expected to correlate with estimates of K for their 'preferred' categories. The lack of an association between white matter properties and K is particularly surprising with respect to the fornix, because whilst no previous study has examined PRC/ILF contributions to Pd versus K, Aly et al., (2013) recently reported that HC lesions disproportionately impair K for scenes. It is worth noting, however, that whilst *HC* lesions may impair K overall, it does not necessarily follow that inter-individual variability in *fornix* properties would be predictive of K for scenes. In this respect, it is interesting that recent neuro-computational modelling work has highlighted that HC subfield CA1 in particular produces the kind of graded strength-based signals associated with K when discriminating between similar stimuli (Elfman et al., 2014). This is relevant because investigations of the origin and topography of the fibres comprising the macaque fornix show that within the HC, it is subfield CA3 and the subicular cortices that contribute most fibres to the fornix, with CA1 contributing comparatively few (Saunders and Aggleton, 2007). If the fornix does not receive substantial inputs from the HC subfield that has been most clearly implicated in K, then the fornix micro-/macrostructure measures extracted here may simply lack sensitivity to the representations that underpin ROC estimates of K for scenes. The distinct contributions of the various HC subfields (and their white matter connections) to Pd

versus K in scene processing tasks is clearly an issue that could benefit from future studies using MRI scanners/sequences with the spatial resolution required to segment them accurately.

In considering why K was insensitive to fornix/ILF contributions to visual discrimination, it should also be noted that none of the previous change-detection experiments employed stimulus manipulations that systematically varied the feature-conjunctions comprising each stimulus-pair; rather, changes were introduced either to individual features or global stimulus configurations (Aly et al., 2012). A limitation of the current study, therefore, which may explain why K lacked sensitivity to fornix/ILF contributions to visual discrimination, is that it is not clear that the change-detection paradigm employs stimulus manipulations that stress the processing of 'feature-conjunctions' within a given trial (a key HC/PRC function according to representational accounts). Further, whilst Aly et al., (2013) sometimes use the terms 'configural/relational match' and 'conjunctive match' interchangeably when describing the stimulus properties to which K may be sensitive, there is currently no direct evidence that K is sensitive to the 'conjunctive match' of visual stimuli. This could be tested by administering a task, in which participants again make confidence-based discriminations to visually similar stimuli. In this modified task, each condition would comprise the same visual category, but the overall conjunctive-match of the stimulus-pairs would be varied parametrically across conditions. Multiple conditions could be generated using fribble stimuli, for example, because this stimulus category affords the construction of exemplars that differ in terms of a pre-determined number of features/conjunctions (see Chapter 2). The relative contributions of Pd versus K to task performance could then be compared across conditions characterised by different levels of 'conjunctive match', affording a test of whether K is indeed sensitive to the conjunctive-match of visual stimuli. Not only would this provide some justification for linking K to terms like 'conjunctive match' as well as 'configural/relational match', but a more conjunctive task version could potentially render ROC estimates of K more sensitive to a role for the ILF in discrimination for object-like stimuli compared to the same measures derived from the present – more configural –task. Similarly, fornix contributions to K for scenes may be better investigated using scene-pairs in which the exemplars differ in terms of specific spatial feature-conjunctions (e.g. roof angle and wall-length within artificial room stimuli). It is also important to note that the findings of Chapter 4 with respect to the category-sensitive correlations between fornix/ILF properties and discrimination accuracy were not replicated here. Again, this single-point performance measure may

have lacked sensitivity to variation in fornix/ILF properties here, because the configural stimulus manipulations did not sufficiently stress conjunctive processing.

Whilst further work is needed to test these interpretations, the present findings can therefore be reconciled with representational accounts. From this, it follows that it may be unnecessary to invoke distinct perceptual processes or neural substrates to account for Pd and K-based discrimination judgements; both may be partially supported by the same MTL representations. This conclusion contrasts with the emerging dual-process view of perception. This account proposes that not only do Pd and K reflect discriminations made based on different kinds of sensory information (local versus global configural/relational differences), but they also map onto distinct perception 'processes' (state versus strength). Consistent with this, ROC estimates of Pd and K were not significantly correlated here. The proponents of the dual process view argue further, however, that these 'processes' may also have distinct neural substrates. Aly et al., (2013), for example, argued that if the HC is involved in assessing the configural/relational match of complex stimuli (Olsen et al., 2012), rather than simply processing their individual features (Lee et al., 2012), then it should contribute to K but not Pd based discriminations. Consistent with this hypothesis, they found that patients with HC lesions presented with impaired K but preserved Pd for scenes. Given this previous finding, it is perhaps surprising that fornix MD in our healthy participants correlated significantly with Pd, but not K, for the current scene stimuli. The image manipulations employed here were identical to those of Aly et al., (2013), and as noted above, the scene stimuli employed here were similar to those used in the previous study. It would, therefore, be important to administer both the tasks reported here, and those reported in Aly et al., (2013), to a single sample of participants, in order to confirm that the correlation between fornix MD and scene Pd is stable across the two stimulus-sets. It would also be important to ask whether individuals with HC lesions would also show poor K, but not Pd, on the task used here as well as that reported by Aly et al., (2013). Nevertheless the association between fornix MD and Pd, but not K, for scenes, does not corroborate the proposition that the HC supports a strength (K) but not state (Pd) based perception 'process'. Further, since the Aly et al., (2013) study, Yonelinas (2013) has proposed that the HC could contribute to strength but not state-based perception for visual objects when there is a demand to process configural/relational information. The current finding that variation in fornix properties did not correlate with K for faces as well as scenes is, however, inconsistent with this prediction, and implies that the fornix is not specialised to support a category-general strength-based perception process, but the processing of scenes.

Nevertheless, as noted above, neuro-computational modelling work has subsequently been conducted to identify potential neural substrates for K *within* the HC (Elfman et al., 2014). HC subfield CA1 was of particular interest because it has been proposed to function as a 'comparator' of representations stored in CA3 with visual information arriving in the HC from entorhinal cortex (ERC; Duncan et al., 2012). In other words, CA1 may "derive a global match signal between what is currently being perceived and what was just presented" (Yonelinas, 2013, pp40). Indeed, Elfman et al., (2014) reported that CA1 generates the kind of continuous signals during perception that, behaviorally, have been associated with K (Aly et al., 2012). Interestingly though, during a recognition task, CA1 instead generated the kind of thresholded output signals that had previously been associated with recollection (section 1.3.2). Why might CA1 produce thresholded signals during memory but continuous strength-based signals during perception? The interpretation offered by Elfman et al., (2014) is that during memory tasks, pattern completion sometimes fails completely, leading to thresholded CA3 output signals. In perception, however, stimuli are presented with little if any delay, so pattern completion seldom fails and CA3 typically produces an output that is highly correlated with the input stimulus. The degree to which the input stimulus and CA3 output-signal correlate with one another can still vary, however, hence the continuous CA1 signals that may prove useful in the context of discriminating two stimuli. Elfman et al., (2014) therefore interpreted their data to indicate that CA1 provides a common neural substrate for both a strength-based perception process (K) and a state-based memory process (recollection). This work was important in showing that computational models can account for findings implicating the HC in both memory and perception, without altering assumptions about the neural architecture of the HC across these two cognitive contexts. Nevertheless, the current findings in the fornix suggest that further modelling work is needed to determine whether the HC can also produce thresholded signals consistent with Pd during scene perception. In this regard, it may prove useful to incorporate knowledge about the differential distribution of the various HC subfields along the HC, as its high DG/CA subfield ratio may render the posterior HC particularly sensitive to local scene differences (Poppenk et al., 2013).

Proponents of the dual-process view have also proposed that the PRC can support the processing of configural objects and faces (Yonelinas, 2013). No study has yet examined PRC contributions to Pd versus K, but from this it was inferred that the dual-process view would also predict that ILF properties would correlate with K but not Pd for faces. Contrary to this prediction, the current study detected an association between

ILF MD and Pd but not K for faces (ILF properties did not correlate with K for either faces or scenes). Overall, therefore, the current pattern of category-sensitive structure-behaviour correlations would appear to distinguish between representational accounts and the emerging dual process view of higher-level perception, in favour of the former.

The category-sensitive structure-behaviour relationships reported here in the fornix and ILF are also difficult to reconcile with the other accounts of MTL function outlined in section 1.3. These assume that: a) the MTL is a highly specialised declarative memory system (Squire et al., 2004), and b) any functional specialisation across the PRC and the HC network is best described in terms of the distinct memory 'processes' that these regions support (e.g. familiarity versus recollection; Aggleton and Brown, 1999), or, alternatively, the type of mnemonic information that they encode/retrieve (e.g. item versus context; Diana et al., 2007). The most serious difficulty for these 'memory system' accounts arises because unlike the tasks reported in Chapter 4, in which performance measures could have benefitted from learning/memory because the discriminations were not trial-unique, the current task involved making discriminations to completely trial-unique faces/scenes, separated by an extremely short inter-stimulus-interval. Trial-unique stimuli ensure that cross-trial learning and memory should make a negligible or zero contribution to discrimination measures, so that they in turn, should principally reflect participants' perception ability. Trial-unique designs have, therefore, previously been employed to demonstrate that, besides any established contributions to learning and memory, the HC/PRC also contribute to perception. Lee et al., (2005b) reported that patients with HC pathology presented with impaired performance in trial-unique different-view scene oddity tasks, but spared performance in different-view face oddity; patients with diffuse MTL pathology that included PRC, however, presented with additional face oddity impairments. Precisely because cross-trial learning and memory should not have benefitted performance in this trial-unique design, these category-sensitive impairments were taken to indicate critical roles for the HC and PRC in higher-level scene and face *perception*, respectively. Similarly, the use here of trial-unique face/scene stimuli ensured that any significant *white matter* structure-behaviour correlation would principally reflect a role for that tract in perception.

The advantages of the current deterministic tract reconstruction approach were outlined in section 3.4. It is, however, worth reiterating that tractography cannot distinguish the afferent and efferent MTL connections of the fornix, nor those comprising the ILF. Thus, it is not currently possible to specify which other gray matter nodes connected to the MTL via these white matter pathways may also contribute to

Pd for particular visual categories. These questions are unlikely to be addressed by white matter lesion studies in animals because animals require extensive training to perform behavioural tasks, so discrimination measures that should ideally reflect process-pure perception are inevitably confounded with learning and memory. Case studies of patients with white matter pathology may provide some insight because the current trial-unique perception task can be administered without prior training, but a concern remains that fornix/ILF damage may be highly variable, and accompanied by other functionally relevant pathology (Aggleton, 2008).

Consistent with the findings in the fornix highlighted in Chapter 4, MD was more sensitive to structure-behaviour relationships here than was FA. Unlike the findings reported in Chapter 4, which highlighted that fornix *f* as well as MD was consistently correlated with overall scene discrimination accuracy, *f* was less sensitive to the relationships between the structural properties of the fornix/ILF, and Pd for scenes and faces, respectively. ILF *f* was, however, marginally correlated with Pd for faces, which suggests that in future studies employing larger samples, inter-individual variation in tract-specific estimates of *f* as well as MD may be predictive of perception measures.

In summary, the current study demonstrates category-sensitive relationships between inter-individual variation in fornix and ILF microstructure, and a marker of perception for trial-unique scenes and faces, respectively. These findings confirm that the category-sensitive contributions of the fornix/ILF to visual processing extend to perception as well as discrimination-learning and memory. The current findings may also highlight a key role for the ILF in relaying information about lower-level face-features towards more anteromedial temporal areas involved in constructing more complex face representations (e.g. PRC). The association between fornix MD and Pd for scenes implies a broader role for the HC network in higher-level scene discrimination than was supposed by Aly et al., (2013); In particular, HC representations may facilitate the detection of local spatial differences across visually similar scenes. The current effects may also indicate a role for the fornix/ILF in buffering discrimination judgements for visually similar and trial-unique stimuli from ‘preferred’ categories against a build-up of feature-ambiguity. Representational perspectives can explain why some prominent white matter pathways may make category-sensitive contributions to higher-level perception. Such an integrated understanding of the collaborative roles of distributed white and gray matter regions in both memory and perception would be a major advance on the more modular accounts of how the brain supports these cognitive functions separately. In the next Chapter, I discuss how the findings of this Thesis add

to our understanding of how the brain supports higher-level visual perception. I also outline some limitations and directions for future research.

Chapter 6: General Discussion

In Chapter 1 (section 1.6), I noted that, to date, studies aimed at testing representational accounts (Graham et al., 2010; Saksida and Bussey, 2010), have typically focused on the unique contributions of individual MTL regions to higher-level perception for particular categories of complex stimuli. And yet these models explicitly propose that stimulus representations are hierarchically distributed across both the EVC and MTL, thereby prompting us to consider the role of broader *networks* in higher-level perception. This led me to outline a complementary 'two streams' conception of visual processing. This retained the core predictions of representational accounts, but proposed that successful perception for non-spatial stimuli (e.g. objects and faces) should depend largely upon the activity of regions within a putative ventral-lateral visual processing stream, and the ability of these regions to communicate with one another effectively via their functional/structural connections. Similarly, successful scene perception should depend largely upon the activity of individual regions within a more medial stream and successful functional interactions between these regions.

The experiments reported in the current Thesis used MRI techniques and behavioural paradigms in healthy participants to test key predictions that emerge from existing representational accounts and this latter proposal (for predictions, see section 1.6.2). In this General Discussion, I will summarise the key findings from these experiments in the context of representational accounts. I will also consider some limitations of the current work, and propose directions for future research.

6.1. Summary of findings

6.1.1. Regions across both the EVC and MTL respond preferentially to particular visual categories

Representational accounts predict that the PRC and HC will respond preferentially to object/face and scene stimuli, respectively. In addition, these regions should be preferentially engaged by blocks of visually similar (high feature overlap; HFO) compared to visually dissimilar (low feature overlap; LFO) stimuli from within their 'preferred' category, because only the former will place great demands on the ability to

construct highly distinct representations of successive exemplars. Mundy et al., (2012) recently conducted an fMRI experiment to test these predictions. Consistent with representational accounts, MTL regions responded preferentially to HFO relative to LFO stimuli from their preferred categories (posterior HC = scenes, PRC = faces/objects). By contrast, category-sensitive EVC regions 'preferred' LFO over HFO blocks of stimuli from their 'preferred' categories (PPA = scenes, FFA = faces, LOC = objects). A limitation of this previous study, however, was the fact that for each stimulus category, the stimulus material comprising the HFO and LFO conditions were different (e.g. HFO faces were artificial whereas LFO faces were real-world), so that any apparent effect of visual similarity on MTL activity, might have been driven by differences in material type. Further, the stimuli that comprised the HFO and LFO blocks of the object stimuli were drawn from real-world semantic categories with different levels of semantic as well as perceptual similarity. Differential PRC activations across these conditions could therefore, arguably, be attributed to an additional role for the PRC in disambiguation of semantically similar objects (Kivisaari et al., 2012).

In Chapter 2, therefore, I reported an fMRI experiment that was conducted to test whether the findings of Mundy et al., (2012) could be replicated when the visual similarity of the stimulus set was more systematically manipulated across LFO and HFO blocks, thereby removing several potential confounds of the original experiment. More specifically, the stimulus material comprising both the HFO and LFO blocks for each stimulus category were of the same type (faces = artificial faces; scenes = artificial Terragen scenes; objects = fribbles). In addition, the object stimuli were drawn from a class of artificial objects that were entirely novel to the participants at test, thereby reducing the potential for the engagement of semantic processing during these blocks.

I found that all 3 EVC regions showed a predicted category-preference (i.e. FFA = faces, LOC = objects, PPA = scenes), and that PRC and posterior HC also responded preferentially to faces and scenes, respectively. In addition, all EVC ROI's and the posterior HC responded preferentially to LFO relative to HFO blocks for all stimulus categories; activity in the left/right PRC was not modulated by visual overlap. In summary, regions across both the EVC and MTL responded preferentially to stimuli from particular visual categories in a manner that was consistent with contemporary representational, but not 'memory system' accounts of MTL function. There was, however, no evidence for a preferential engagement of MTL regions during HFO stimulus blocks (unlike the pattern reported in Mundy et al., 2012). The absence of the latter effect is a challenge for representational accounts, but as noted in section 2.4,

the visual similarity of the HFO stimuli used in this experiment may have been sufficiently high to trigger repetition suppression in MTL as well as EVC regions; future studies employing less homogenous stimuli within HFO blocks may, therefore, detect the HFO > LFO effect reported by Mundy et al., (2012).

6.1.2. PRC and HC contributions to perception are supported by distinct patterns of functional interactions

In Chapter 1 (section 1.6.1) I explained that extended multi-regional networks are likely to underpin the successful processing of complex visual stimuli. This point was elucidated in the context of congenital prosopagnosia (CP), a lifelong condition in which face processing impairments can manifest even in the context of normal activation patterns in individual face-sensitive EVC ROI's (Avidan et al., 2005). Some authors argue that these visual impairments could arise due to a failure to successfully propagate information about face stimuli between face-sensitive ROIs (Berhmann and Plaut, 2013). Consistent with this view, studies have shown that functional connectivity (i.e. the statistical dependence of activity across brain regions) of core face processing regions is reduced in CP relative to controls (Avidan et al., 2014).

In Chapter 2, therefore, I began to move beyond analysing regional activations during perception. A functional connectivity analysis was applied to the fMRI data acquired using the duration detection task to investigate the distinct category-dependent functional interactions that underpin PRC and posterior HC responses to their 'preferred' categories. As representational accounts propose that the PRC is part of an extended "object analyser pathway" that is specialised for the perceptual processing of non-spatial stimuli (Murray et al., 2007; Saksida and Bussey, 2010), I predicted that PRC activity would be more strongly correlated with that of regions along the ventral-lateral VVS during the presentation of faces and/or objects compared to scenes. In contrast to PRC, I hypothesised that posterior HC activity should be more strongly related to that in posteromedial scene-sensitive cortices when participants view images of scenes compared to objects and faces.

The analysis revealed a cluster of brain voxels, roughly corresponding to the right FFA, in which the BOLD response was more strongly correlated with that of the right PRC during the presentation of faces compared to other visual categories. In contrast, activity in the left and right posterior HC was more strongly correlated with that in clusters within the right lingual gyrus and left temporal pole, respectively, during the

presentation of scenes compared to other visual categories. Neither PRC nor the posterior HC demonstrated more synchronised activity with other brain regions during perception for their 'non-preferred' relative to 'preferred' stimulus categories. Whilst it would be important to replicate these findings, they are largely consistent with the view that two putative visual streams that culminate in the PRC/posterior HC are indeed relatively specialised for the processing of non-spatial and spatial stimulus categories, respectively.

6.1.3. Greater structural connectivity between the posterior HC and EVC regions involved in processing scenes compared to other visual categories

In Chapter 3, I used the functional data from Chapter 2 to localise face, object, and scene-sensitive EVC regions (OFA, LOC, and TOS), prior to applying an established probabilistic tractography protocol to reconstruct and quantify the white matter connections between these category-selective EVC ROI's and the PRC/posterior HC. The data was then used to investigate whether the PRC possesses more reproducible structural connections with ventral-lateral EVC regions involved in visual processing for object-like stimulus categories (OFA/LOC), whereas the posterior HC possesses more reproducible connections with scene-processing EVC regions (TOS).

The analysis confirmed a greater probability of connectivity between the posterior HC and a functionally-defined EVC region that responds preferentially to scene stimuli (TOS), compared to other EVC regions that respond maximally to object-like stimulus categories (OFA and LOC). The PRC, however, did not possess more reproducible connections with the OFA and LOC compared to the TOS, though this lack of an effect may have reflected technical difficulties in tracing pathways accurately and selectively between PRC and category-sensitive EVC regions. For instance, the prominent white matter bundle which is likely to carry PRC-EVC connections– the ILF –passes through a region that contains several other fiber bundles, including the fronto-occipital fasciculus, , middle longitudinal fasciculus, superior longitudinal fasciculus and optic radiations (Martino et al., 2013). Even the 2-fiber probabilistic model employed in this analysis may be sub-optimal for the accurate differentiation of all these fiber populations, thereby reducing the accuracy of the trajectories of the reconstructed streamlines.

6.1.4. The magnitude of category-sensitive BOLD responses in PRC is related to variation in structural properties of the ILF

In Chapter 3, I highlighted the ILF and the fornix as prominent white matter bundles that provide inputs/outputs to the PRC and the HC, respectively. I then argued that if higher-level face/object perception is dependent upon PRC activity but also the ability of this ROI to communicate with other related brain areas via its white matter connections, then variation in ILF structural properties may be predictive of the magnitude of face/object-sensitive BOLD responses in the PRC. Similarly, variation in fornix structural properties may be predictive of the magnitude of face/object-selective BOLD responses in the posterior HC.

To test this prediction, deterministic tractography was used to obtain tract-specific measures of white matter microstructure (FA and MD) and macrostructure (*f*) from in vivo reconstructions of the fornix and the ILF. A general linear model and statistical contrasts subsequently confirmed that the magnitude of face-sensitive BOLD responses in the left PRC was related to inter-individual differences in ILF MD and *f*. Variation in ILF properties was also predictive of face-sensitive BOLD responses in a number of other brain regions that have been implicated in face processing, including the OFA and STS. The magnitude of scene-sensitive BOLD responses in the posterior HC, however, did not correlate with inter-individual differences in measures of fornix micro- or macro-structure.

That ILF properties are predictive of face-sensitive BOLD responses in the PRC, but also the OFA, is consistent with a role for the ILF in relaying information about non-spatial stimulus features to the PRC, in order for these to be integrated into more complex representations. Notably, a similar effect was not observed for object-sensitive BOLD responses in PRC; this may simply reflect the fact that faces are typically more 'ambiguous' than most classes of objects (i.e. all faces contain very similar features) and that the former are therefore *de facto* more dependent upon the complex conjunctive PRC representations that are instantiated within the PRC than are the latter. Nevertheless, I propose that it may be possible for future studies to demonstrate a link between ILF properties and BOLD responses to non-face object-stimuli, but only for sub-categories of objects that are characterised by greater visual complexity than the artificial objects employed here (e.g. fribbles with more features/conjunctions or 'greebles'; see Barense et al., 2010). Fornix properties were not predictive of scene-sensitive BOLD responses in the posterior HC. Nevertheless, it seems unlikely that HC contributions to scene processing are not related to the ability of the posterior HC to

communicate with other brain regions via the fornix, because fornix as well as HC damage produces behavioural impairments in spatial processing tasks (Gaffan, 1994; Buckley et al., 2004). Fornix transection studies in animals that have implicated the fornix in spatial processing have, however, typically required monkeys to make explicit discrimination judgements to visual stimuli, whereas the current participants performed a duration detection task in which the visual properties of each successive scene were task-irrelevant and may not, therefore, have triggered HC functional interactions with other brain areas via the fornix. I propose, therefore, that it will be important to repeat these analyses using behavioural data from a task in which the participant is required to provide explicit scene perception judgements; such tasks could include the different-view scene/face oddity paradigm reported by Lee et al., (2008) or the visual discrimination paradigm reported by Mundy et al., (2013; see Chapter 4).

6.1.5. Dissociable roles for the fornix and the ILF in discrimination accuracy for scenes and faces

In Chapter 4, I moved from investigating the coupling between category-sensitive BOLD activations and specific white matter connections, towards investigating whether the ILF and the fornix make differential contributions to behavioural measures of successful perception for scenes and faces. Fornix transection is known to impair performance in spatial memory tasks (e.g. object-in-scene tasks; Gaffan, 1994). Similarly, the ILF has been linked to face processing by evidence that CP is associated with reductions in ILF FA (Thomas et al., 2009). It remained unclear, however, whether the roles of these tracts in visual recognition paradigms extend to performance in visual discrimination tasks. In addition, no previous study had directly compared the contributions of the fornix and ILF to scene and face processing *in the same sample of healthy individuals*, using tasks similar to those developed in animal studies (e.g., Buckley et al., 2004; Bussey et al., 2002). It was, therefore, unclear whether the contributions of these white matter pathways to face and scene processing are in fact dissociable, as representational accounts would predict.

Chapter 4 therefore reported a study that employed a deterministic white matter tractography protocol and a previously published visual discrimination paradigm (Mundy et al., 2013), to ask whether inter-individual variation in structural properties of the fornix and the ILF would be predictive of discrimination accuracy for scenes and faces, respectively.

The analyses revealed that inter-individual variation in several diffusion-MRI measures (MD and *f*) of the fornix was predictive of discrimination accuracy for scenes, but not faces. ILF MD was also found to correlate with face discrimination accuracy in one of the two discrimination tasks that were administered to participants, thereby providing tentative evidence in favour of a preferential contribution of the ILF to visual discrimination for faces compared to scenes. These findings were consistent with the notion that PRC and HC contributions to successful higher-level perception, for their preferred categories also depend upon interactions with other related brain areas via their key input/output white matter pathways.

6.1.6. Category-sensitive contributions of the fornix/ILF to visual discrimination extends to markers of perception for trial-unique stimuli

The stimuli that were administered to participants during the paradigms reported in Chapter 4, were repeated several times over the course of the task (i.e. they were not trial-unique). This means that stimulus learning and memory may have contributed to the overall performance measures over time (Kim et al., 2011). The significant white matter structure-behaviour correlations that were reported could therefore reflect roles for the fornix/ILF in memory rather than perception. For this reason, it was unclear whether the category-sensitive contributions of the fornix/ILF to visual processing would also be evident in a task that involves making discriminations to pairs of stimuli that are completely trial-unique.

In Chapter 5, therefore, I presented a follow up study that employed deterministic tractography to investigate whether structural properties of the fornix and the ILF are also differentially predictive of ROC markers of visual perception (Pd and K) for trial-unique pairs of scenes versus faces, using a modified version of a previously reported change-detection paradigm (Aly et al., 2013). A measure of white-matter microstructure (MD) in the fornix was found to be predictive of Pd for scenes but not faces, whereas in the ILF, MD was predictive of Pd for faces but not scenes. The findings confirmed that the role of the fornix/ILF in visual processing for particular stimulus categories extends to perception as well as discrimination-learning and memory.

6.2 General conclusions

The predictions of the network-level representational framework of visual perception that was outlined in section 1.6.2 were largely corroborated by the experimental work outlined in this Thesis. In particular, successful higher-level perception for a given complex stimulus is not merely dependent upon the activity of a particular category-sensitive EVC or MTL region. Rather, successful higher-level perception for individual exemplars from non-spatial stimulus categories is an emergent property of activity in individual regions within a ventral-lateral processing stream (e.g. the OFA and PRC), but also the ability of these regions to communicate with one another effectively via their functional/structural connections (e.g. the ILF). Similarly, successful scene perception is an emergent property of activity in the HC and its functional/structural connections with other posteromedial scene-sensitive cortices (e.g. TOS and PPA) but also with other functionally-related brain areas via the fornix. In section 6.4.2, I will provide further discussion of some of the other brain regions with which the HC may need to interact via the fornix in the service of higher-level scene perception.

The multi-modal research approach adopted in my Thesis afforded the testing of a diverse range of predictions. Numerous studies have previously employed fMRI and behavioural paradigms to investigate the category-sensitive contributions of individual EVC/MTL brain regions to higher-level perception (Mundy et al., 2013; Lee et al., 2008). These have been complemented by functional connectivity studies, which have, recently, provided insights into some of the inter-regional functional interactions that may underpin PRC and HC contributions to higher-level perception. O'Neil et al., (2014), for example, reported that the PRC interacts with the FFA even at rest. By contrast, Zeidman et al., (2014) have demonstrated that the HC interacts with a number of postero-medial scene-selective cortices during scene perception. The findings of those previous studies are complemented by the functional analyses reported here, and provide independent support for the network-level perspective outlined in section 1.6.2.

To date, comparatively few studies have combined functional and diffusion MRI techniques with behavioural paradigms, with a view to investigating the integrated white and gray matter networks that are relatively specialised for the processing of particular visual categories. Some notable exceptions include Scherf et al., (2014) who used a functional localiser task during an fMRI scan, diffusion MRI and white matter tractography to show that the volume of the ILF is related to the size of a key face processing region (the FFA) but not the PPA. This finding supports the current

interpretation that the ILF plays a greater role in relaying visual information between spatially distinct face but not scene processing regions (e.g. OFA and PRC). Osher et al., (in press) also recently demonstrated that it is possible to predict the magnitude of category-sensitive responses in individual brain voxels on the basis of their white-matter 'connectivity fingerprint' with the rest of the brain. These previous studies suggest that differences in category-sensitive regional brain activations are tightly linked to variation in local white matter properties. Indeed, diffusion and functional MRI were successfully combined here to show that the magnitude of category-sensitive BOLD responses in particular EVC/MTL ROIs, is related to the structural properties of their white matter pathways.

The work in Chapters 4 and 5 indicates that diffusion MRI techniques can also be integrated with behavioural paradigms to investigate how inter-individual variation in properties of specific white matter tracts may be a critical neural factor underpinning successful performance in higher-level perception as well as recognition memory tasks (Rudebeck et al., 2009).

The present multi-modal approach therefore enabled a number of complementary research questions to be addressed, and similar efforts in this direction may facilitate further progress in our understanding of how inter-individual variation in successful perception arises from the interplay between regional activations across the EVC/MTL, and the white matter connectivity within these extended functional networks.

These conclusions do of course need to be balanced by a frank acknowledgement that not all of the predicted effects were detected here (e.g. MTL regions did not respond preferentially to HFO relative to LFO stimuli in Chapter 2). In addition, some of the novel findings of the present work can, as I have outlined in the respective Chapters, potentially be reconciled with competing theoretical accounts (e.g. the fornix structure-behaviour correlations in Chapter 4 may potentially reflect a role for this tract in incidental spatial learning and memory). I have, however, also highlighted some of the study-specific limitations of the experimental designs and provided proposals for suitable modifications which may, in future, afford more rigorous tests of representational as against other competing accounts. Nevertheless, in the following sections I will address some of the more general limitations of the current work, and raise some new directions for future research.

6.3. Limitations of the current work

6.3.1. Incidental learning and memory

In Chapter 2, the PRC and posterior HC were found to respond preferentially to images of trial-unique faces and scenes, respectively. This was taken as evidence that the PRC and posterior HC construct perceptual representations of non-spatial and spatial feature-conjunctions, respectively, independently of any explicit perception or memory demands. This interpretation could be criticised on the basis that MTL activations could simply reflect incidental memory encoding. Furthermore, some authors have argued that the mnemonic processing of some visual categories (e.g. faces) may be more dependent on particular memory processes (familiarity) compared to others (recollection) (Aly et al., 2010). If face memory is more dependent on familiarity whereas scene memory is more dependent on recollection, then this argument could potentially explain the pattern of category-sensitive activations observed within the MTL in Chapter 2. The notion that MTL activations must reflect incidental if not explicit memory processing is a considerable challenge for representational accounts, but several authors have attempted to address it in their designs. Lee et al., (2013), recently administered a scene oddity task with no explicit memory demands to healthy participants during an fMRI scan; HC activity was found to be predictive of participants' performance in this perceptual paradigm, but not in a subsequent surprise test of their memory for the stimuli. These findings support the proposition that MTL regions can make performance-related contributions to higher-level perception tasks, and that the activity that is elicited by such tasks does not necessarily reflect incidental memory encoding (see also Barense et al., 2011). The duration detection task that was reported in Chapter 2 was not accompanied by a subsequent memory test, so it was not possible to test whether the MTL activations may have reflected mnemonic encoding. This is a legitimate limitation of the study but note that explicit stimulus perception judgements were not required from the participants during the duration detection task either, so that even if a subsequent memory test were included as part of the experimental design, it would not be possible to determine whether activity in the MTL regions could be predictive of *successful perception* as well as subsequent memory for the current stimuli. Nevertheless, subsequent memory tests should ideally be included in future studies of this kind.

A related limitation concerns the nature of the stimuli that were administered to participants in the visual discrimination paradigm reported in Chapter 4. As I explained in detail in section 4.4, the fact that the stimuli were repeated over the course of the task means that learning and memory processes could, arguably, have contributed to participants' discrimination judgements over time (Kim et al., 2011). Assuming this were the case, then the significant white matter structure-function relationships reported in section 4.3 could principally reflect a role for those tracts in learning and memory rather than perception. This seems unlikely given that there were no statistically significant learning effects in the current tasks, but it remains a plausible possibility. A similar analysis was conducted in Chapter 5, but with behavioural data from a face/scene discrimination task that included trial-unique stimuli. In this case, the observed structure-behaviour effects provide more compelling evidence for category-sensitive contributions of the fornix/ILF to visual perception, because any incidental within-trial stimulus learning could not benefit performance in subsequent trials of the task. The evolution in the approach adopted here, provides a lesson for future studies of this kind that trial-unique stimuli should be employed as standard to avoid ambiguities over the role for a given structure in perception as well as learning/memory.

6.3.2. Focus on the fornix and the ILF

A limitation of the work presented in Chapters 3-5, is that the preferential role of white matter tracts in visual perception for particular visual categories was only investigated in the context of the fornix and the ILF. The principal reason for restricting the analysis to two tracts-of-interest was that this hypothesis-driven approach reduced the risk of reporting a) false-positive effects in regions for which we had no specific predictions and b) false-negative effects where true structure-function relationships are obscured due to corrections for large numbers of statistical comparisons. The fornix and the ILF were of particular interest as two tracts that may make differential contributions to scene and face perception, because whilst the former acts primarily as an input/output pathway for the HC (i.e. a key node within the putative 'spatial' processing stream), the latter is a prominent input pathway for the PRC (i.e. a key node within the putative 'non-spatial' processing stream). While such a sensible and restricted approach made sense in the context of the experiments proposed here, it is worth noting that I do not believe that the ILF and the fornix are the only white matter pathways that may play an important role in higher-level perception for faces and scenes, respectively. Indeed, this

seems unlikely given that category-sensitive brain regions are highly dispersed and are not connected via a single white matter pathway. In the case of scene processing, for example, the fornix does not connect the HC to other early posteromedial scene processing regions (e.g. TOS or posterior parietal cortex). One white matter pathway that may be more relevant in this context is the parahippocampal cingulum, which contains direct connections between early posterior parietal cortices (e.g. the posterior inferior parietal lobule) and both the PPA and the HC (Kravitz et al., 2011), and may therefore play an important role in the relay of information between these scene processing regions. Further, direct connections between the posterior HC and the TOS via the parahippocampal cingulum were reproduced in the probabilistic connectivity analysis reported here in Chapter 3 (section 3.3). Although these direct HC-TOS connections remain to be confirmed in the brain itself, they do suggest that the parahippocampal cingulum could be another interesting tract to investigate in the context of white matter pathways that may play a relatively greater role in visual processing for one category of stimuli (scenes) compared to another (faces).

A complementary and exploratory whole-brain Tract-Based Spatial Statistics (TBSS) analysis was, however, conducted for each of the white-matter structure-behaviour analyses that were reported in Chapters 3-5. These afforded investigations of any potential voxel-wise correlations between markers of visual discrimination and diffusion MRI measures of white matter micro-/macrostructure outside the main tracts-of-interest (i.e. the fornix and the ILF). The advantages of the preferred tract-reconstruction approach over such exploratory voxel-wise white matter structure-behaviour analysis techniques were outlined previously in the experimental Chapters themselves, but details of the voxel-wise analyses are, nevertheless, included in Appendix A for completeness.

6.3.3. Focus on the fornix/ILF at their broadest spatial scale

A related limitation of the current work is that in Chapters 3-5, the structural properties of the fornix and the ILF were collapsed along the entire length of the tracts prior to running the structure-function/behaviour analyses. Again, this design choice was partly driven by practical considerations related to statistical power. There were, however, also no *a priori* hypotheses to motivate a focus on distinct subsections of these tracts. Nevertheless, recent investigations have produced evidence that whilst a given white matter tract may, considered at its broadest spatial scale, contribute preferentially to

visual processing for a particular stimulus category, subsections of that tract may contribute to the processing of other stimulus categories. The ILF, for instance, is a large white matter fascicle (12cm; Gomez et al., 2015) which traverses the entire posterior-anterior extent of the extended VVS that culminates in the anterior temporal lobe (which includes PRC; Murray et al., 2007). It was therefore anticipated, here, that this pathway would be relatively specialised for the processing of non-spatial stimuli such as objects and faces, consistent with representational accounts. Nevertheless, along its medial aspect, the ILF also passes several scene processing cortices (e.g. lingual gyrus and PPA), and could therefore potentially carry some behaviourally-relevant shorter-range connections between scene processing regions. Indeed, Tavor et al., (2014) recently reported that performance in a face recognition task was associated with a diffusion MRI measure of white matter microstructure (FA) in the anterior sections of the ILF, whereas performance in a scene recognition task was associated with FA in posterior and intermediate sections of the ILF. Further, Gomez et al., (2015) recently used a functional localiser task to initiate tractography from face and scene-selective cortices corresponding to the FFA and PPA, respectively. The tracts propagated from the FFA were referred to as 'mFus-faces' and 'CoS-places'. FA in mFus-faces was found to correlate with face recognition scores, whereas CoS-places FA correlated with scene recognition scores. Gomez et al., (2015) concluded that properties of white matter local to category-sensitive functional ROIs can have a category-specific relationship to behaviour. Gomez and colleagues differentiate the mFus-faces and CoS-places fibers from those of the ILF, highlighting that both mFus-faces and CoS-places ran ventral to the ILF itself. Nevertheless, taken together with the findings of Tavor et al., (2014) their findings suggest that future studies may benefit from examining the relationship between behaviour and properties of white matter tracts at both broad and smaller spatial scales. This could afford investigations of whether the structural properties of different subsections of white matter fascicli are differentially predictive of performance in distinct conditions of visual processing tasks; comparisons could be made, not only across stimulus categories (e.g. face versus scene perception), but also within categories (e.g. face-part versus whole-face perception).

6.4. Outstanding questions

6.4.1. Multiple streams within the putative object-processing 'stream'?

The network-level representational framework outlined in section 1.6.2 proposed that a ventral-lateral processing stream culminating in the PRC supports higher-level perception for object-like stimuli. This proposition, in its simplest form, is agnostic with respect to whether all classes of object-like stimuli are processed in the same way along this visual stream. It has long been clear, however, that different categories of object-like stimuli are not treated the same by ventral-lateral EVC regions, which often respond preferentially to particular categories of stimuli (LOC = objects; FFA = faces; Downing et al., 2006; section 1.2). Indeed, in the regional functional analyses reported in section 2.3, both the FFA and the LOC were found to respond preferentially to images of both faces and artificial objects compared to scenes, but they each responded maximally to distinct object-like categories (FFA = faces; LOC = artificial objects). Further, for several stimulus categories, multiple EVC regions have previously been identified along the posterior-anterior extent of the classic VVS in which that category is 'preferred'. Taylor and Downing (2011) point out that there are at least two regions along the VVS that respond preferentially to images of faces (OFA and FFA), two that respond preferentially to objects (LOC and posterior fusiform), and even two that respond maximally to images of bodies (extrastriate body area [EBA] and fusiform body area). This prompts the question: Are there multiple pathways within the putative ventral-lateral processing stream that culminates in the PRC, each relatively specialised for a particular object-like stimulus category?

The functional connectivity analysis technique employed in Chapter 2 could have provided some traction on this issue because it is sensitive to context-dependent functional interactions with a given seed region. Thus, the analysis could have potentially detected the distinct patterns of inter-regional functional interactions with the EVC that support PRC contributions to higher-level perception for faces compared to artificial objects, and vice versa. Unfortunately, however, PRC activity was not sensitive to the present artificial object stimuli. Further, the only regions with which the PRC was found to increase its functional connectivity in a context-dependent manner was the FFA, and this was identified by contrasting functional connectivity with faces compared to both objects and scenes. I pointed out that these findings are in line with other studies showing that PRC damage is less consistently associated with visual

discrimination impairments for objects compared to faces (Lee et al., 2005a), and argued that the processing of face stimuli may be more dependent upon PRC representations than are objects, simply because faces inherently possess a higher degree of feature overlap/ambiguity than most classes of objects. It may therefore be important to employ task conditions that place greater demands on the ability to process the distinct sets of feature-conjunctions comprising individual exemplars, if the PRC is to be engaged by other categories of object-like stimuli. For instance, the PRC has been found to respond more to artificial object stimuli when they are presented from different compared to an identical viewpoint (Barense et al., 2010). Under such conditions, where the PRC itself is reliably engaged by more than one category of object-like stimuli, it may also be possible to demonstrate that there are various subdivisions of the ventral-lateral stream that eventually culminates in the PRC, each of which is relatively specialised for particular visual categories. In terms of how this finding would be reconciled with representational accounts, each 'sub-pathway' may simply support representations of particular kinds of visual features/conjunctions at a level of complexity that is *relatively* more useful in the context of processing some object-like stimuli compared to others.

In line with the work reviewed by Taylor and Downing (2011), I would anticipate that the PRC could be shown to interact in a stimulus category-dependent manner with face-sensitive EVC ROIs as already demonstrated here (i.e. the FFA), but also with object-sensitive EVC ROIs (e.g. LOC) and body-sensitive EVC ROI's (e.g. EBA).

6.4.2. Does the spatial stream terminate at the HC?

A key finding of the current Thesis was that inter-individual variation in fornix structural properties is predictive of discrimination accuracy for scenes but not faces. This finding was interpreted to indicate that HC contributions to higher-level scene perception are partly dependent on the ability of the HC to interact with other surrounding neo- and sub-cortical areas via the fornix. For instance, the fornix provides inputs to the HC from regions that influence theta rhythmicity in the HC, such as the medial septum (Saunders and Aggleton, 2007; Bland et al., 1995). Theta rhythmicity has been proposed to play a role in optimising synaptic plasticity in the HC (Burgess et al., 2002; Aggleton et al., 2010), and so these inputs via the fornix may be critical for the successful construction of spatial HC representations.

The fornix also contains HC *projections* to other brain regions in the medial diencephalon, however, such as the MBs and ATN. As noted previously, along with the HC and the fornix, these two regions have been proposed to form an extended HC-fornix-MBs-ATN network involved in the representation of complex visual scenes, and the arrangement of the objects within those scenes (Gaffan, 1994). Indeed, studies in rats confirm that damage to each of these gray/white matter structures results in impairments in the same tests of spatial learning (Aggleton and Nelson, 2015). Further, fornix transection leads to reduced activity – as indexed by the expression of the immediate-early gene c-*fos*; a marker of neural activity – across both the HC and ATN (and also the medial septum; see Vann and Brown, 2000).

It is possible that additional brain regions downstream from the HC, including the MBs and ATN, can also contribute to some aspects of higher-level scene perception. Studies in animals with focal MB/ATN lesions are unlikely to provide traction on this question because animals have to be trained extensively to perform visual tasks, thereby confounding perception measures with learning and memory. The small size and location of these structures also render brain imaging studies of these regions unfeasible (Vann, 2010). Human patient case studies may provide some insights because complex trial-unique perception tasks can be administered to patients without prior training. The interpretation of the data acquired from these prospective studies will, however, be complicated by the fact that damage to diencephalic structures is likely to be variable and incorporate other local brain regions that may have some functional relevance (Aggleton, 2008).

6.4.3. Temporal dynamics of information processing across two visual streams

Future studies should also aspire to determine how the complex conjunctive representations of the MTL interact with representations of lower-level feature-conjunctions in earlier EVC regions during complex object and scene perception tasks. For instance, what is the direction of information flow that best characterises the way in which the PRC contributes to object perception tasks? In the context of an object discrimination task, local differences in object features may be detected in early EVC regions prior to this information being sequentially propagated to the PRC, during the course of which these features are gradually integrated into highly distinct conjunctive representations of the different object stimuli under observation, which subsequently enables their discrimination. Alternatively, early EVC regions might rapidly propagate

visual information directly to the PRC – effectively bypassing intermediate EVC regions – to be bound into conjunctive representations that can then be projected back to intermediate and early EVC regions again to guide the visual search for local discrepant features.

The first proposal assumes that visual processing occurs in a largely feed-forward hierarchical manner, and is both intuitively plausible and consistent with evidence outlined in section 1.2 that cells in the anterior macaque inferotemporal cortex respond to more complex conjunctions of stimulus features than do cells in more posterior inferotemporal cortex (Tanaka et al., 1991). The second proposal, however, assumes that visual processing occurs in a recurrent manner across extended visual hierarchies. Indeed, as I noted in sections 3.1 and 3.4, the putative occipito-temporal object-processing pathway is actually a complex recurrent network that contains direct feedback as well as feed-forward connections, some of which bypass intermediate cortical regions, thereby allowing early and late regions of the hierarchy to interact with one another directly (see Kravitz et al., 2013). The PRC in monkeys, for instance, possesses direct connections with visual areas as early as area V1, bypassing intermediate occipito-temporal regions like areas TE and TEO (Clavagnier et al., 2004). The notion of a recurrent network with feedback as well as feedforward interactions is also supported by findings from backward-masking studies. In these studies, the presentation of a mask after a stimulus, often impairs both behavioural performance (e.g. in a scene categorization task; Bacon-Mace et al., 2005) and activity along occipitotemporal cortex in humans (Grill-Spector et al., 2000). This is relevant because, as explained by Kravitz et al., (2013, pp36): “In a purely feedforward system, there should be no effect of a mask presented after a stimulus evokes the initial neural response, yet the mask profoundly impairs both performance and awareness. Whether backward masking depends on the interruption of ongoing processing within a region,…or the disruption of feedback signals…, it clearly demonstrates the importance of recurrent connections and of processing beyond the initial neural response for even basic visual object perception.”

Similarly, whilst the posterior HC predominantly receives inputs from local structures like the PHC (Aggleton, 2012), tract tracer studies in monkeys show that it is also directly connected to early regions of parietal visual cortex whose function is important for spatial navigation (Kravitz et al., 2011; Clower et al., 2001), thereby bypassing the PHC and several other medial brain regions that are known to be involved in aspects of spatial processing (e.g. PPA; Epstein and Kanwisher, 1998). It is therefore perhaps

unsurprising that whilst the HC receives direct *inputs* from earlier scene processing regions, it has also been found to exert a top-down influence on activity in the PHC and even early visual cortex during a boundary extension paradigm (Chadwick et al., 2013).

It is, therefore, likely that the HC and PRC contribute to higher-level perception for scenes and object-like stimuli, respectively, via feedback as well as feedforward interactions with earlier visual regions in their respective visual streams. An understanding of the temporal dynamics of those interactions will help to constrain mechanistic models of PRC and HC contributions to perception, but given the short time spans under which these interactions are likely to occur, a technique with higher temporal resolution than fMRI is likely to be required. Magnetoencephalography (MEG) techniques enable investigation of the time course of task-related neural responses at an exquisite temporal resolution, and can now also offer a degree of cortical localisation, and may therefore be better suited to this purpose (Riggs et al., 2009).

6.5. Concluding remarks

I began this Thesis by pointing out that the ability to accurately perceive and respond to our visual environment is critical for optimising primate behaviour, and that understanding how the healthy brain supports visual perception is, therefore, a key goal for cognitive neuroscience. The experiments reported here used a combination of MRI techniques and behavioural paradigms in healthy participants to investigate the extended brain networks that subserve perception for scenes and other more object-like stimulus categories. These investigations, which were inspired by recent representational accounts of perception (Graham et al., 2010; Saksida and Bussey, 2010), provide evidence that a ventral-lateral processing stream culminating in PRC contributes more to perception for non-spatial stimulus categories like objects and faces, whereas a more medial stream culiminating in the posterior HC contributes more to perception for more spatial stimulus categories, including images of visual scenes. Further, the findings also suggest that inter-individual variation in the structural properties of the white-matter pathways providing inputs/outputs to the PRC or HC is an important factor underpinning the contributions of these MTL regions to successful higher-level perception. These novel findings highlight how successful higher-level perception for a complex visual stimulus is likely an emergent property of dynamic functional interactions between perceptual stimulus representations that are distributed

across both the EVC and the MTL, and connected to one another via white matter pathways (see also Behrmann and Plaut, 2013).

These insights are valuable in terms of our understanding of how perception for particular categories is supported by the brain, but also offer a challenge to the numerous contemporary 'memory system' accounts of MTL function, which assume that MTL regions like the PRC and HC are specialised to support specific memory 'processes' and do not contribute to higher-level perception (e.g. Squire et al., 2004; Aggleton et al., 2004; Diana et al., 2007); the latter being the presumed province of the EVC. Indeed, findings like those reported in this Thesis have now accumulated to the point where many more eminent memory researchers are re-considering the contributions of the MTL to cognitive functions beyond learning and memory (Yonelinas, 2013; Nadel and Peterson, 2013). This development demonstrates the impact that existing representational accounts of perception have already had in the field in terms of compelling us to revisit and reconsider long-held assumptions and concepts about how the brain supports various aspects of cognition in humans. Here, representational accounts afforded the generation of further novel and testable predictions about how the white and gray matter regions of the brain work in concert to support successful higher-level visual perception for different stimulus categories. It seems likely that representational perspectives will continue to play a welcome and vital role in generating new knowledge around how brain regions, and their key structural pathways, support higher-level perceptual discrimination, and in turn successful learning and memory.

References

Aggleton JP, Brown MW (1999) Episodic memory, amnesia, and the hippocampal-anterior thalamic axis. Behav Brain Sci 22:425–44; discussion 444–89.

Aggleton JP, McMackin D, Carpenter K, Hornak J, Kapur N, Halpin SF, Wiles CM, Kamel H, Brennan P, Carton S, Gaffan D (2000) Differential cognitive effects of colloid cysts in the third ventricle that spare or compromise the fornix. Brain 123:800-815.

Aggleton JP, Vann SD, Denby C, Dix S, Mayes AR, Roberts N, Yonelinas AP (2005) Sparing of the familiarity component of recognition memory in a patient with hippocampal pathology. Neuropsychologia 43:1810-1823.

Aggleton JP (2008) EPS mid-career award 2006. Understanding anterograde amnesia: disconnections and hidden lesions. Q J Exp Psychol 61:1441-1471.

Aggleton JP, Sanderson DJ, Pearce JM (2007) Structural learning and the hippocampus. Hippocampus 17:723-734.

Aggleton JP, O'Mara SM, Vann SD, Wright NF, Tsanov M, Erichsen JT (2010) Hippocampal-anterior thalamic pathways for memory: uncovering a network of direct and indirect actions. Eur J Neurosci 31:2292-2307.

Aggleton JP (2012) Multiple anatomical systems embedded within the primate medial temporal lobe: implications for hippocampal function. Neurosci Biobehav Rev 36:1579–96.

Aggleton JP, Nelson AJD (2015) Why do lesions in the rodent anterior thalamic nuclei cause such severe spatial deficits? Neurosci Biobehav Rev 54:131-144..

Aguirre GK, Zarahn E, D'Esposito M (1998) An area within human ventral cortex sensitive to "building" stimuli: Evidence and implications. Neuron 21:373–383.

Alonso-Ortiz E, Levesque IR, Pike GB (2014) MRI-based myelin water imaging: a technical review. Magn Reson Med 73:70-81.

Aly M, Knight RT, Yonelinas AP (2010) Faces are special but not too special: spared face recognition in amnesia is based on familiarity. Neuropsychologia 48:3941-3948.

Aly M, Yonelinas AP (2012) Bridging Consciousness and Cognition in Memory and Perception: Evidence for Both State and Strength Processes. PLoS ONE, 7:e30231.

Aly M, Ranganath C, Yonelinas AP (2013) Detecting Changes in Scenes: The Hippocampus Is Critical for Strength-Based Perception. Neuron, 78:1127-37.

Aly M, Wansard M, Segovia F, Yonelinas AP, Bastin C (2014a) Cortical and subcortical contributions to state- and strength-based perceptual judgements. Neuropsychologia 64:145-156.

Aly M, Ranganath C, Yonelinas AP (2014) Neural correlates of state- and strength-based perception. J Cogn Neurosci, 26:792-809.

Amaral DG (2002) The primate amygdala and the neurobiology of social behavior: implications for understanding social anxiety. Biol Psychiatry 51:11-17.

Avidan G, Hasson U, Malach R, Behrmann M (2005) Detailed exploration of face-related processing in congenital prosopagnosia: 2. Functional neuroimaging findings. J Cogn Neurosci 17:1150–1167.

Avidan G, Tanzer M, Hadj-Bouziane F, Liu N, Ungerleider LG, Behrmann M (2014) Selective dissociation between core and extended regions of the face processing network in congenital prosopagnosia. Cereb Cortex 24:1565–78.

Azadbakht H, Parkes LM, Haroon HA, Augath M, Logothetis NK, de Crespigny A, D'Arceuil HE,
Parker GJM (2015) Validation of high-resolution tractography against in vivo tracing in the macaque visual cortex. Cerebral Cortex doi: 10.1093/cercor/bhu326.

Bachevalier J, Saunders RC, Mishkin M (1985) Visual recognition in monkeys. Effects of transection of the fornix. Exper Brain Res, 57:547-53.

Bacon-Macé N, Macé MJ, Fabre-Thorpe M, Thorpe SJ (2005) The time course of visual processing: backward masking and natural scene categorisation. Vision Res 45:1459-69.

Baldassano C, Beck DM, Fei-Fei L (2013) Differential connectivity within the parahippocampal place area. Neuroimage 75:228-237.

Barense MD, Bussey TJ, Lee ACH, Rogers TT, Davies RR, Saksida LM, Murray EA, Graham KS (2005) Functional specialization in the human medial temporal lobe. J Neurosci 25:10239–10246.

Barense MD, Gaffan D, Graham KS (2007) The human medial temporal lobe processes online representations of complex objects. Neuropsychologia 45:2963-2974.

Barense MD, Henson RNA, Lee ACH, Graham KS (2010) Medial temporal lobe activity during complex visual discrimination of faces, objects and scenes: The effect of viewpoint. *Hippocampus 20*:389-401

Barense MD, Groen II, Lee AC, Yeung LK, Brady SM, Gregori M, Kapur N, Bussey TJ, Saksida LM, Henson RN (2012) Intact memory for irrelevant information impairs perception in amnesia. Neuron 75:157-167.

Bartko SJ, Winters BD, Cowell RA, Saksida LM, Bussey TJ (2007) Perirhinal cortex resolves feature ambiguity in configural object recognition and perceptual oddity tasks. Learn Mem 14:821-832.

Bartko SJ, Cowell RA, Winters BD, Bussey TJ, Saksida LM (2010) Heightened susceptibility to interference in an animal model of amnesia: impairment in encoding, storage, retrieval— or all three? Neuropsychologia 48: 2987–2997.

Barton JJ, Press DZ, Keenan JP, O'Connor M (2002) Lesions of the fusiform face area impair perception of facial configuration in prosopagnosia. Neurology 58:71-78.

Beaulieu, C (2002). The basis of anisotropic water diffusion in the nervous system—a technical review. NMR Biomed. 15; 435–455.

Beckmann C, Jenkinson M, Smith SM (2003) General multi-level linear modelling for group analysis in FMRI. NeuroImage 20:1052-1063.

Behrens TEJ, Woolrich MW, Jenkinson M, Johansen-Berg H, Nunes RG, Clare S, Matthews PM, Brady JM, Smith SM (2003) Characterization and propagation of uncertainty in diffusion-weighted MR imaging. Magn Reson Med 50:1077-1088.

Behrens TEJ, Johansen-Berg H., Jbabdi S., Rushworth M.F.S., Woolrich MW (2007) Probabilistic diffusion tractography with multiple fibre orientations. What can we gain? NeuroImage 23:144-155.

Behrmann M, Plaut DC (2013) Distributed circuits, not circumscribed centers, mediate visual recognition. Trends Cogn Sci 17**:**210–219.

Bennett IJ, Rypma B (2013) Advances in functional neuroanatomy: a review of combined DTI and fMRI studies in healthy younger and older adults. Neurosci Biobehav Rev 37:1201-1210.

Bettencourt KC, Xu Y (2013) The role of transverse occipital sulcus in scene perception and its relationship to object individuation in inferior intraparietal sulcus. J Cog Neurosci 25:1711-1722.

Bird CM, Shallice T, Cipolotti L (2007) Fractionation of memory in medial temporal lobe amnesia. Neuropsychologia 45:1160-1171.

Bird CM, Capponi C, King JA, Doeller CF, Burgess N (2010) Establishing the boundaries: the hippocampal contribution to imagining scenes. J Neurosci 30:11688–95.

Biswal B, Yetkin FZ, Haughton VM, Hyde JS (1995) Functional connectivity in the motor cortex of resting human brain using echo-planar MRI. Magn Reson Med 34:537–41.

Bland BH, Konopacki J, Kirk IJ, Oddie SD, Dickson CT (1995) Discharge patterns of hippocampal theta-related cells in the caudal diencephalon of the urethan-anesthetized rat. J Neurophysiol 74:322–333.

Bouvier SE, Engel SA (2006) Behavioral deficits and cortical damage loci in cerebral achromatopsia. Cereb Cortex 16:183-191.

Bowles B, Crupi C, Mirsattari SM, Pigott SE, Parrent AG, Pruessner JC, Yonelinas AP, Köhler S (2007) Impaired familiarity with preserved recollection after anterior temporal-lobe resection that spares the hippocampus. Proc Natl Acad Sci USA, 104:16382–16387.

Brown MW (1996) Neuronal responses and recognition memory. Semin Neurosci 8:23–32.

Brown MW, Warburton EC, Aggleton JP (2010) Recognition memory: Material, processes and substrates. Hippocampus, 20**:** 1228-1244.

Buckley MJ, Gaffan D (1997) Impairment of visual object-discrimination learning after perirhinal cortex ablation. Behav Neurosci 111:467–75.

Buckley MJ, Booth MC, Rolls ET, Gaffan D (2001) Selective perceptual impairments after perirhinal cortex ablation. J Neurosci 21:9824–36.

Buckley MJ, Charles DP, Browning PGF, Gaffan D (2004) Learning and retrieval of concurrently presented spatial discrimination tasks: role of the fornix. Behav Neurosci 118:138-149.

Burgess N, Maguire EA, O'Keefe, J (2002) The human hippocampus and spatial and episodic memory. Neuron 35:625-641.

Burwell RD (2000) The parahippocampal region: corticocortical connectivity. Ann NY Acad Sci 911:25–42.

Bussey TJ, Duck J, Muir JL, Aggleton JP (2000) Distinct patterns of behavioural impairments resulting from fornix transection or neurotoxic lesions of the perirhinal and postrhinal cortices in the rat. Behav Brain Res, 111:187-202.

Bussey TJ, Saksida LM, Murray EA. (2002) Perirhinal cortex resolves feature ambiguity in complex visual discriminations. Eur. J. Neurosci. 15:365–74

Bussey TJ, Saksida LM, Murray EA (2003) Impairments in visual discrimination after perirhinal cortex lesions: Testing 'declarative' vs. 'perceptual-mnemonic' views of perirhinal cortex function. Eur J Neurosci 17:649–660.

Bussey TJ, Saksida LM (2005) Object memory and perception in the medial temporal lobe: an alternative approach. Curr Opin Neurobiol 15:730-737.

Caeyenberghs K, Leemans A, Geurts M, Linden CV, Smits-Engelsman BC, Sunaert S, Swinnen SP (2011) Correlations between white matter integrity and motor function in traumatic brain injury patients. Neurorehabil Neural Repair 25:492-502.

Catani M*,* Howard RJ*,* Pajevic S*,* Jones DK *(*2002*)* Virtual *in vivo* interactive dissection of white matter fasciculi in the human brain*. NeuroImage* **17***:* 77–94*.*

Catani M, Jones DK, Donato R, Ffytche DH (2003) Occipito-temporal connections in the human brain. Brain 126:2093–2107.

Chadwick MJ, Mullaly SL, Maguire EA (2013) The hippocampus extrapolates beyond the view in scenes: an fMRI study of boundary extension. Cortex 49:2067-2079.

Chalfonte BL, Verfaellie M, Johnson MK, Reiss L (1996) Spatial location memory in amnesia; Binding item and location information under incidental and intentional encoding conditions. Memory 4:591-614.

Clarke A, Tyler LK (2014) Object-specific semantic coding in human perirhinal cortex. J Neurosci 34:4766-4775.

Clavagnier S, Falchier A, Kennedy H (2004) Long-distance feedback projections to area V1: implications for multisensory integration, spatial awareness, and visual consciousness. Cogn Affect Behav Neurosci 4:117-126.

Clelland CD, Choi M, Romberg C, Clemenson GD Jr, Fragniere A, Tyers P, Jessberger S, Saksida LM, Barker RA, Gage FH, Bussey TJ (2009) A functional role for adult hippocampal neurogenesis in spatial pattern separation. Science 325:210-213.

Clower DM, West RA, Lynch JC, Strick PL (2001) The inferior parietal lobule is the target of output from the superior colliculus, hippocampus, and cerebellum. J Neurosci 21:6283-6291.

Cressant A, Muller RU, Poucet B (1997) Failure of centrally placed objects to control the firing fields of hippocampal place cells. J Neurosci 17:2531-2542.

Croxson PL, Johansen-Berg H, Behrens TE, Robson MD, Pinsk MA, Gross CG, Richter W, Richter MC, Kastner S, Rushworth MF (2005) Quantitative investigation of connections of the prefrontal cortex in the human and macaque using probabilistic diffusion tractography. J Neurosci 25:8854-8866.

Daitz H (1953) Note on the fibre content of the fornix system in man. Brain 76:509–512.

Davachi L, Mitchell JP, Wagner AD (2003) Multiple routes to memory: distinct medial temporal lobe processes build item and source memories. Proc Natl Acad Sci USA 100:2157–2162.

Desikan RS, Ségonne F, Fischl B, Quinn BT, Dickerson BC, Blacker D, Buckner RL, Dale AM, Maguire RP, Hyman BT, Albert MS, Killiany RJ (2006) An automated labeling

system for subdividing the human cerebral cortex on MRI scans into gyral based regions of interest. NeuroImage 31:968-980.

Devlin JT, Price CJ (2007) Perirhinal Contributions to Human Visual Perception. Curr Biol 17:1484-1488.

Diana RA, Yonelinas AP, Ranganath C (2007) Imaging recollection and familiarity in the medial temporal lobe: a three-component model. Trends Cogn Sci 11:379–86.

Dilks DD, Julian JB, Paunov AM, Kanwisher N (2013) The occipital place area is causally and selectively involved in scene perception. J Neurosci 33:1331–1336.

Douglas RJ (1967) The hippocampus and behavior. Psychol Bull 67:416–22.

Downing PE, Chan AWY, Peelen MV, Dodds CM, Kanwisher N (2006) Domain specificity in visual cortex. Cereb Cortex 16:1453-1461.

Duncan K, Ketz N, Inati SJ, Davachi L (2012) Evidence for area CA1 as a match/mismatch detector: a high-resolution fMRI study of the human hippocampus. Hippocampus 22:389-398.

Duva CA, Floresco SB, Wunderlich GP, Lao TL, Pinel JPJ, Phillips AG (1997) Disruption of spatial but not object-recognition memory by neurotoxic lesions of the dorsal hippocampus in rats. Behav Neurosci 111:1184–96.

Eacott MJ, Gaffan D, Murray EA (1994) Preserved recognition memory for small sets, and impaired stimulus identification for large sets, following rhinal cortex ablations in monkeys. Eur J Neurosci 6:1466–78.

Eger E, Ashburner J, Haynes JD, Dolan RJ, Rees G (2008) FMRI activity patterns in human LOC carry information about object exemplars within category. J Cogn Neurosci 20:356–370.

Eickhoff SB, Jbabdi S, Caspers S, Laird AR, Fox PT, Zilles K, Behrens TE (2010) Anatomical and functional connectivity of cytoarchitectonic areas within the human parietal operculum. J Neurosci 30:6409-6421.

Elfman KW, Aly M, Yonelinas AP (2014) Neurocomputational account of memory and perception: thresholded and graded signals in the hippocampus. Hippocampus 24:1672-1686.

Ennaceur A, Aggleton JP (1997) The effects of neurotoxic lesions of the perirhinal cortex combined to fornix transection on object recognition memory in the rat. Behav Brain Res 88:181–93.

Ennaceur A, Neave N, Aggleton JP (1996) Neurotoxic lesions of the perirhinal cortex do not mimic the behavioural effects of fornix transection in the rat. Behav Brain Res 80:9–25.

Epstein R, Kanwisher N (1998) A cortical representation of the local visual environment. Nature, 392:598-601.

Epstein R, Harris A, Stanley D, Kanwisher N (1999) The parahippocampal place area: recognition, navigation, or encoding? Neuron 23:115–25.

Epstein R, Graham KS, Downing PE (2003) Viewpoint-Specific Scene Representations in Human Parahippocampal Cortex. Neuron 37:865–876.

Epstein RA, Higgins JS, Parker W, Aguirre GK, Cooperman S (2006) Cortical correlates of face and scene inversion: a comparison. Neuropsychologia 33:1145-1158.

Epstein RA (2014) Neural systems for visual scene recognition. In M. Bar & K. Keveraga (Eds.), Scene Vision. Cambridge MA: MIT Press, pp. 105-134.

Ewbank MP, Schluppeck D, Andrews TJ (2005) FMR-adaptation reveals a distributed representation of inanimate objects and places in human visual cortex. Neuroimage 28:268 –279.

Friston KJ, Harrison L, Penny W (2003) Dynamic causal modelling. Neuroimage, 19:1273–302.

Gaffan D (1994) Scene-specific memory for objects: a model of episodic memory impairment in monkeys with fornix transaction. J Cogn Neurosci 6:305-320.

Gaffan D (2001) What is a memory system? Horel's critique revisited. Behav Brain Res 127:5-11.

Gauthier I, Tarr MJ (1997) Becoming a "Greeble" expert: Exploring mechanisms for face recognition. Vision Res 37:1673–1682.

Gauthier I, Tarr MJ, Moylan J, Skudlarski P, Gore JC, Anderson AW (2000) The fusiform "face area" is part of a network that processes faces at the individual level. J Cogn Neurosci 12:495-504.

Goh JO, Siong SC, Park D, Gutchess A, Hebrank A, Chee MW (2004) Cortical areas involved in object, background, and object-background processing revealed with functional magnetic resonance adaptation. J Neurosci 24:10223-10228.

Gomez J, Pestilli F, Witthoft N, Golarai G, Liberman A, Poltoratski S, Yoon J, Grill-Spector K (2015) Functionally defined white matter reveals segregated pathways in human ventral temporal cortex associated with category-specific processing. Neuron 85:216-227.

Goodale MA, Milner AD (1992) Separate visual pathways for perception and action. Trends Neurosci 15:20-25.

Graham KS, Scahill VL, Hornberger M, Barense MD, Lee AC, Bussey TJ, Saksida LM (2006) Abnormal categorization and perceptual learning in patients with hippocampal damage. J Neurosci 26:7547-7554.

Graham KS, Barense MD, Lee ACH (2010) Going beyond LTM in the MTL: A synthesis of neuropsychological and neuroimaging findings on the role of the medial temporal lobe in memory and perception. Neuropsychologia 48:831-853.

Green DM, and Swets JA (1966) Signal Detection Theory and Psychophysics (New York: John Wiley and Sons).

Grill-Spector K, Kushnir T, Hendler T, Edelman S, Itzchak Y, Malach R (1998) A sequence of object processing stages revealed by fMRI in the human occipital lobe. Human Brain Mapp 6:316–328.

Grill-Spector K, Kushnir T, Hendler T, Malach R (2000) The dynamics of object-selective activation correlate with recognition performance in humans. Nat Neurosci 3:837-43.

Grill-Spector K, Kourtzi Z, Kanwisher N (2001a) The lateral occipital complex and its role in object recognition. Vision Res 41:1409-1422.

Grill-Spector K, Malach R (2001b) fMR-adaptation: A tool for studying the functional properties of human cortical neurons. Acta Psychol (Amst), 107:293–321.

Gschwind M, Pourtois G, Schwartz S, Van de Ville D, Vuilleumier P (2012) White-matter connectivity between face-responsive regions in the human brain. Cereb Cortex 22:1564-1576.

Hagmann P, Cammoun L, Martuzzi R, Maeder P, Clarke S, Thiran JP, Meuli R (2006) Hand preference and sex shape the architecture of language networks. Hum Brain Mapp 27:828-835.

Hampton RR (2005) Monkey perirhinal cortex is critical for visual memory, but not for visual perception: Reexamination of the behavioural evidence from monkeys. Quart J Exp Psychol B 58:283–299.

Hassabis D, Kumaran D, Maguire EA (2007a) Using imagination to understand the neural basis of episodic memory. J Neurosci 27:14365–74.

Hassabis D, Kumaran D, Vann SD, Maguire EA (2007b) Patients with hippocampal amnesia cannot imagine new experiences. Proc Natl Acad Sci USA 104:1726–1731.

Hasson U, Harel M, Levy I, Malach R (2003) Large-scale mirror-symmetry organization of human occipito-temporal object areas. Neuron 37:1027-1041.

Haxby JV, Hoffman EA, Gobbini MI (2000) The distributed human neural system for face perception. Trends Cogn Sci 4:223-233.

Haxby JV, Gobbini MI, Furey ML, Ishai A, Schouten JL, Pietrini P (2001) Distributed and overlapping representations of faces and objects in ventral temporal cortex. Science 293:2425-2430.

Hayward WG, Williams P (2000) Viewpoint dependence and object discriminability. Psychol Sci, 11:7-12.

Henderson JM, Larson CL, Zhu DC (2007) Cortical activation to indoor versus outdoor scenes: an fMRI study. Exp Brain Res 179:75– 84.

Hirshorn M, Grady C, Rosenbaum RS, WInocur G, Moscovitch M (2012) Brain regions involved in the retrieval of spatial and episodic details associated with a familiar environment: an fMRI study. Neuropsychologia 50:3094-3106.

Hofstetter S, Tavor I, Tzur MS, Assaf Y (2013) Short-term learning induces white matter plasticity in the fornix. J Neurosci 33:12844-50.

Hunsaker MR, Kesner RP (2009) Transecting the dorsal fornix results in novelty detection but not temporal ordering deficits in rats. Behav Brain Res 201:192-197.

Hyvarinen A (1999) Fast and robust fixed-point algorithms for independent component analysis. IEEE Transactions on Neural Networks 10:626–34.

Jankowski MM, Ronnqvist KC, Tsanov M, Vann SD, Wright NF, Erichsen JT, Aggleton JP, O'Mara SM (2013) Front Syst Neurosci 7:45.

Jenkinson M, Bannister P, Brady M, Smith S (2002) Improved optimization for the robust and accurate linear registration and motion correction of brain images. NeuroImage 17:825-841.

Jenkinson, M (2003) Fast, automated, N-dimensional phase-unwrapping algorithm. Mag Reson Med 49:193-197.

Jenkinson M, Beckmann CF, Behrens TE, Woolrich MW, Smith SM (2012) FSL. NeuroImage 62:782-90.

Jeurissen B, Leemans A, Jones DK, Tournier J-D, Sijbers J (2011) Probabilistic tractography using the residual bootstrap with constrained super-resolved spherical harmonic deconvolution. Hum Brain Mapp 32:461-79.

Jezzard P, Balaban RS (1995) Correction for geometric distortion in echo planar images from B(o) field variations. *Mag Reson Med:* 65-73.

Jones DK, Horsfield MA, Simmons A (1999) Optimal strategies for measuring diffusion in anisotropic systems by magnetic resonance imaging. Magnet Reson Med 42:515-525.

Jones DK, Catani M, Pierpaoli C, Reeves SJ, Shergill SS, O'Sullivan M, Maguire P, Horsfield MA, Simmons A, Williams SC, Howard RJ (2005) A diffusion tensor magnetic resonance imaging study of frontal cortex connections in very late-onset schizophrenia-like psychosis. Am J Geriat Psychiat 13:1092-1099.

Jones DK (2008) Studying connections in the living human brain with diffusion MRI. Cortex 44:936-952.

Jones DK (2010) Challenges and limitations of quantifying brain connectivity in vivo with diffusion MRI. Imaging Medicine 2:341-355.

Jones DK, Knosche TR, Turner R (2013) White matter integrity, fiber count, and other fallacies, the do's and don'ts of diffusion MRI. Neuroimage 73:239-254.

Kanwisher N, McDermott J, Chun MM (1997) The fusiform face area: a module in human extrastriate cortex specialized for face perception. J Neurosci 17:4302-4311.

Kanwisher N (2010) Functional specificity in the human brain: a window into the functional architecture of the mind. Proc Natl Acad Sci USA 107:11163-11170.

Karnath HO, Ruter J, Mandler A, Himmelbach M (2009) The anatomy of object recognition – visual form agnosia caused by medial occipitotemporal stroke. J Neurosci 29:5854-5862.

Keedwell PA, Chapman R, Christiansen K, Jones DK (2012) Cingulum white matter in young females at risk of depression: the effect of family history and anhedonia. Biol Psychiatry 72:296-302.

Kjelstrup KB, Solstad T, Brun VH, Hafting T, Leutgeb S, Witter MP, Moser EI, Moser MB (2008) Finite scale of spatial representation in the hippocampus. Science 321:140-143.

Kim S, Jeneson A, van der Horst AS, Frascino JC, Hopkins RO, Squire LR (2011) Memory, visual discrimination performance, and the human hippocampus. J Neurosci 31:2624-2629.

Kirwan CB, Wixted JT, Squire LR (2008) Activity in the medial temporal lobe predicts memory strength, whereas activity in the prefrontal cortex predicts recollection. J Neurosci 28:10541–10548.

Kivisaari SL, Tyler LK, Monsch AU, Taylor KI (2012) Medial perirhinal cortex disambiguates confusable objects. Brain 135:3757-3769.

Kondo H, Saleem KS, Price JL (2005) Differential connections of the perirhinal and parahippocampal cortex with the orbital and medial prefrontal networks in macaque monkeys. J Comp Neurol 493:479–509.

Korsnes MS, Wright AA, Gabrieli JD (2008) An fMRI analysis of object priming and workload in the precuneus complex. Neuropsychologia 46:1454-62.

Knowlton BJ, Squire LR (1993) The learning of categories: parallel brain systems for item memory and category knowledge. Science 262:1747–1749.

Knutson AR, Hopkins RO, Squire LR. (2012) Visual discrimination performance, memory, and medial temporal lobe function. Proc Natl Acad Sci 109: 13106–13111.

Kravitz DJ, Saleem KS, Baker CI, Mishkin M (2011) A new neural framework for visuospatial processing. Nat Rev Neurosci 12:217-230.

Kravitz DJ, Saleem KS, Baker CI, Ungerleider LG, Mishkin M (2013) The ventral visual pathway: an expanded neural framework for the processing of object quality. Trends Cog Sci 17:26-49.

Lawes IN, Barrick TR, Murugam V, Spierings N, Evans DR, Song M, Clark CA (2008) Atlas based segmentation of white matter tracts of the human brain using diffusion tensor tractography and comparison with classical dissection. Neuroimage 39:62-79.

Lebel C, Walker L, Leemans A, Phillips L, Beaulieu C (2008) Microstructural maturation of the human brain from childhood to adulthood. Neuroimage 40:1044-1055.

Lebel C, Beaulieu C (2011) Longitudinal development of human brain wiring continues from childhood into adulthood. J Neurosci 31:10937-10947.

Lee ACH, Bussey TJ, Murray EA, Saksida LM, Epstein RA, Kapur N, Hodges JR, Graham KS (2005a) Perceptual deficits in amnesia: Challenging the medial temporal lobe ‘mnemonic’ view. Neuropsychologia 43:1–11.

Lee ACH, Buckley MJ, Pegman SJ, Spiers H, Scahill VL, Gaffan D, Bussey TJ, Davies RR, Kapur N, Hodges JR, Graham KS (2005b) Specialization in the medial temporal lobe for processing of objects and scenes. Hippocampus 15:782–797.

Lee ACH, Scahill VL, Graham KS (2008) Activating the medial temporal lobe during oddity judgment for faces and scenes. Cereb Cortex 18:683–696.

Lee ACH, Rudebeck SR (2010) Investigating the interaction between spatial perception and working memory in the human medial temporal lobe. J Cogn Neurosci 22:2823–2835.

Lee AC, Yeung LK, Barense MD (2012) The hippocampus and visual perception. Front Hum Neurosci doi: 10.3389/fnhum.2012.00091.

Lee ACH, Brodersen KH, Rudebeck SR (2013) Disentangling spatial perception and spatial memory in the hippocampus: a univariate and multivariate pattern analysis fMRI study. J Cogn Neurosci 25:534–546.

Leemans A, Jeurissen B, Sijbers J, Jones DK (2009) ExploreDTI: A graphical toolbox for processing, analyzing, and visualizing diffusion MRI data. In: 17th Annual Meeting of the International Society for Magnetic Resonance in Medicine, Hawaii, USA, p. 3537.

Leutgeb JK, Leutgeb S, Moser MB, Moser EI (2007) Pattern separation in the dentate gyrus and CA3 of the hippocampus. Science 315:961-966.

Levy I, Hasson U, Harel M, Malach R (2004) Functional analysis of the periphery effect in human building related areas. Hum Brain Mapp 22:15–26.

Loui P, Li HC, Schlaug G (2011) White matter integrity in right hemisphere predicts pitch-related grammar learning. Neuroimage 55:500-507.

Maguire EA, Gadian DG, Johnsrude IS, Good CD, Ashburner J, Frackowiak RS, Frith CD (2000) Navigation-related structural change in the hippocampi of taxi drivers. Proc Natl Acad Sci USA 97:4398–4403.

Maguire EA, Mullaly SL (2013) The hippocampus: A manifesto for change. J Exp Psychol Gen. 142:1180-1189.

Malach R, Reppas JB, Benson RR, Kwong KK, Jiang H, Kennedy WA, Ledden PJ, Brady T J, Rosen BR, Tootell RB (1995) Object-related activity revealed by functional

magnetic resonance imaging in human occipital cortex. Proc Natl Acad Sci USA 92:8135–8139.

Malykhin NV, Lebel RM, Coupland NJ, Wilman AH, Carter R (2010) In vivo quantification of hippocampal subfields during 4.7T fast spin echo imaging. Neuroimage 49:1224-1230.

Martino J, da Silva-Freitas R, Caballero H, Marco de Lucas E, García-Porrero JA, Vazquez-Barguero A (2013) Fiber dissection and diffusion tensor imaging tractography study of the temporoparietal fiber intersection area. Neurosurgery 72:87-97.

Mazziotta J, Toga A, Evans A, Fox P, Lancaster J (1995) A probabilistic atlas of the human brain: theory and rationale for its development. Neuroimage 2:89-101.

McKenzie IA, Ohayon D, Li H, Paes de Faria J, Emery B, Tohyama K, Richardson WD (2014) Motor skill learning requires active central myelination. Science 346:318–322.

McLaren, DG, Ries, ML, Xu, G, Johnson, SC (2012) A Generalized Form of Context-Dependent Psychophysiological Interactions (gPPI): A Comparison to Standard Approaches. NeuroImage 61:1277-1286.

McTighe SM, Mar AC, Romberg C, Bussey TJ, Saksida LM (2009) A new touchscreen test of pattern separation: Effect of hippocampal lesions. Neuroreport 20:881–885.

McTighe SM, Cowell RA, Winters BD, Bussey TJ, Saksida LM (2010) Paradoxical false memory for objects after brain damage. Science 330:1408-1410

Mendez MF, Cherrier MM (2003) Agnosia for scenes in topographagnosia. Neuropsychologia 41:1387-1395.

Metzler-Baddeley C, Jones DK, Belaroussi B, Aggleton JP, O'Sullivan MJ (2011) Frontotemporal connections in episodic memory and aging: a diffusion MRI tractography study. J Neurosci 31:13236-13245.

Metzler-Baddeley C, O'Sullivan MJ, Bells S, Pasternak O, Jones DK (2012) How and how not to correct for CSF-contamination in diffusion MRI. Neuroimage 59:1394-1403.

Meunier M, Bachevalier J, Mishkin M, Murray EA (1993) Effects on visual recognition of combined and separate ablations of the entorhinal and perirhinal cortex in rhesus monkeys. J Neurosci 13:5418–5432.

Meunier M, Hadfield W, Bachevalier J, Murray EA (1996) Effects of rhinal cortex lesions combined with hippocampectomy on visual recognition memory in rhesus monkeys. J Neurophysiol 75:1190–1205.

Minear M, Park DC (2004) A lifespan database of adult facial stimuli. Behav Res Meth Instrum Comput 36:630-633.

Milner B (1962) Physiologie de l'hippocampe, P. Passouant, ed. (Paris: Centre National de la Recherche Scientifique), pp. 257–272.

Milner B, Corkin S, Teuber HL (1968) Further analysis of the hippocampal amnesic syndrome: 14-year follow-up study of H.M. Neuropsychologia 6:215–234.

Mishkin M, Ungerleider LG, Macko KA (1983) Object vision and spatial vision: two cortical pathways. Trends Neurosci 6:414-417.

Mori S, Zhang J (2006) Principles of diffusion tensor imaging and its applications to basic neuroscience research. Neuron 51:527-539.

Morris RGM (1981) Spatial localisation does not depend on the presence of local cues. Learn Motiv 12:239-260.

Moser MB, Moser EI (1998) Functional differentiation in the hippocampus. Hippocampus 8:608–619.

Mukherjee P, Chung SW, Berman JI, Hess CP, Henry RG (2008) Diffusion tensor MR imaging and fiber tractography: technical considerations. AJNR Am J Neuroradiol 29:843-52.

Mullin CR, Steeves JK (2011) TMS to the lateral occipital cortex disrupts object processing but facilitates scene processing. J Cogn Neurosci 23:4174-4184.

Mumby DG, Wood ER, Duva CA, Kornecook TJ, Pinel PJ, Phillips AG (1996) Ischemia-induced object-recognition deficits in rats are attenuated by hippocampal ablation before or soon after ischemia. Behav Neurosci 110:266–281.

Mundy ME, Downing PE, Graham KS (2012) Extrastriate cortex and medial temporal lobe regions respond differentially to visual feature overlap within preferred stimulus category. Neuropsychologia 50:3053-3061.

Mundy ME, Downing PE, Dwyer DM, Honey RC, Graham KS (2013) A critical role for the hippocampus and perirhinal cortex in perceptual learning of scenes and faces: Complementary findings from amnesia and fMRI. J Neurosci 33:10490-10502.

Murray EA, Mishkin M (1996) Forty-minute visual recognition memory in rhesus monkeys with hippocampal lesions. Soc Neurosci Abstr 22:281.

Murray EA, Bussey TJ (1999) Perceptual-mnemonic functions of the perirhinal cortex. Trends Cogn. Sci. 3:142–51.

Murray EA, Bussey TJ, Saksida LM (2007) Visual perception and memory: a new view of medial temporal lobe function in primates and rodents. Ann Rev Neurosci 30:99–122.

Murray EA, Wise SP (2012) Why is there a special issue on perirhinal cortex in a journal called hippocampus? The perirhinal cortex in historical perspective. Hippocampus 22:1941-1951.

Nadel L, Peterson MA (2013) The hippocampus: part of an interactive posterior representational system spanning perceptual and memorial systems. J Exp Psychol Gen 142:12421254.

Nasr S, Liu N, Devaney KJ, Yue X, Rajimehr R, Ungerleider LG, Tootell RBH (2011) Scene-selective cortical regions in human and nonhuman primates. J Neurosci 31:13771-13785.

Nasr S, Echavarria CE, Tootell RBH (2014) Thinking outside the box: Rectilinear shapes selectively activate scene-selective cortex. J Neurosci 34:6721-6735.

Nestor A, Plaut DC, Behrmann M (2011) Unraveling the distributed neural code of facial identity through spatiotemporal pattern analysis. *Proc Natl Acad Sci USA* 108:9998–10003.

O'Keefe J, Burgess N (1996) Geometric determinants of the place fields of hippocampal neurons. Nature, 381:425–428.

O'Keefe J, Dostrovsky J (1971) The hippocampus as a spatial map. Preliminary evidence from unit activity in the freely-moving rat. Brain Res 34:171–175.

O'Keefe J, Nadel L (1978) The hippocampus as a cognitive map. New York: Oxford University Press.

Olsen RK, Moses SN, Riggs L, Ryan JD (2012) The hippocampus supports multiple cognitive processes through relational binding and comparison. Front Hum Neurosci 146.

Op de Beeck HP, Haushofer J, Kanwisher NG (2008) Interpreting fMRI data: maps, modules, and dimensions. Nat Rev Neurosci 9:123-135.

O'Neil EB, Cate AD, Kohler S (2009) Perirhinal Cortex Contributes to Accuracy in Recognition Memory and Perceptual Discriminations. J Neurosci 29:8329-8334.

O'Neil EB, Barkley VA, Köhler S (2013) Representational demands modulate involvement of perirhinal cortex in face processing. Hippocampus 23:592–605.

O'Neil EB, Hutchison RM, McLean DA, Köhler S (2014) Resting-state fMRI reveals functional connectivity between face-selective perirhinal cortex and the fusiform face area related to face inversion. Neuroimage 92:349-355.

O'Reilly JX, Woolrich MW, Behrens TE, Smith SM, Johansen-Berg H (2012) Tools of the Trade: Psychophysiological Interactions and Functional Connectivity. Soc Cogn Affect Neurosci 7:604-609.

Orban GA (2008) Higher order visual processing in macaque extrastriate cortex. Physiol Rev 88:59-89.

Ortibus E, Verhoeven J, Sunaert S, Casteels I, De Cock P, Lagae L (2012) Integrity of the inferior longitudinal fasciculus and impaired object recognition in children: a diffusion tensor imaging study. Dev Med Child Neurol 54:1469-8749.

Osher DE, Saxe RR, Koldewyn K, Gabrieli JD, Kanwisher N, Saygin ZM (in press) Structural connectivity fingerprints predict cortical selectivity for multiple visual categories across cortex. Cereb Cortex. doi: 10.1093/cercor/bhu303.

Pasternak O, Sochen N, Gur Y, Intrator N, Assaf Y (2009) Free water elimination and mapping from diffusion MRI. Magnet Reson Med 62:717-730.

Peelen MV, Downing PE (2005) Within-subject reproducibility of category-specific visual activation with functional MRI. Hum Brain Mapp 25:402–408.

Peters A (2002) The effects of normal aging on myelin and nerve fibers: a review. J Neurocytol 31:581-593.

Pitcher D, Walsh V, Yovel G, Duchaine B (2007) TMS evidence for the involvement of the right occipital face area in early face processing. Curr Biol 17(18):1568–1573.

Pitcher D, Walsh V, Duchaine B (2011) The role of the occipital face area in the cortical face perception network. Exp Brain Res 209:481-493.

Poppenk J, Evensmoen HR, Moscovitch M, Nadel L (2013) Long-axis specialization of the human hippocampus. Trends Cogn Sci 17:230-240.

Postans M, Hodgetts CJ, Mundy ME, Jones DK, Lawrence AD, Graham KS (2014) Individual variation in fornix microstructure and macrostructure is related to visual discrimination accuracy for scenes but not faces. *J Neurosci*, 34:12121-12126.

Pourtois G, Schwartz S, Spiridon M, Martuzzi R, Vuilleumier P (2009) Object representations for multiple visual categories overlap in lateral occipital and medial fusiform cortex. Cereb Cortex 19:1806-1819.

Pyles JA, Verstynen TD, Schneider W, Tarr MJ (2013) Explicating the face perception network with white matter connectivity. PLoS ONE 8(4).

Rafal RD (2001) Balints syndrome. Handbook of Neuropsychology, 2nd Edition. 121-141. Elsevier Press.

Riggs L, Moses SN, Bardouille T, Herdman AT, Ross B, Ryan JD (2009) A complementary analytic approach to examining medial temporal lobe sources using magnetoencephalography. Neuroimage 45:627-42.

Rilling JK, Glasser MF, Preuss TM, Ma X, Zhao T, Hu X, Behrens TE (2008) The evolution of the arcuate fasciculus revealed with comparative DTI. Nat Neurosci 11:426-428.

Rochefort C, Lefort JM, Rondi-Reig L (2013) The cerebellum: a new key structure in the navigation system. Front Neural Circuits 7:35.

Rollins NK, Vachha B, Srinivasan P, Chia J, Pickering J, Hughes CW, Gimi B (2009) Simple developmental dyslexia in children: alterations in diffusion-tensor metrics of white matter tracts at 3 T. Radiology 251:882–891.

Rossion B, Dricot L, Devolder A, Bodart J-M, Crommelinck M, de Gelder B, Zoontjes R (2000) Hemispheric asymmetries for whole-based and parts-based face processing in the human fusiform gyrus. J Cogn Neurosci 12:793-802.

Rossion B (2008) Constraining the cortical face network by neuroimaging studies of acquired prosopagnosia. Neuroimage 40:423-426.

Rossion B, Hanseeuw B, & Dricot L (2012) Defining face perception areas in the human brain: A large-scale factorial fMRI face localizer analysis. Brain Cogn 79:138-157.

Rotshtein P, Richardson MP, Winston JS, Kiebel SJ, Vuilleumier P, Eimer M, Driver J, Dolan RJ (2010) Amygdala damage affects event related potentials for fearful faces at specific time windows. Hum Brain Mapp 31:1089-1105.

Rubin RD, Chesney SA, Cohen NJ, Gonsalves BD (2013) Using fMR-adaptation to track complex object representations in perirhinal cortex. Cognitive Neuroscience 4:107-114.

Rudebeck SR, Scholz J, Millington R, Rohenkohl G, Johansen-Berg H, Lee ACH (2009). Fornix microstructure correlates with recollection but not familiarity memory. J Neurosci 29:14987-14992.

Rugg MD, Vilberg KL, Mattson JT, Yu SS, Johnson JD, Suzuki M (2012) Item memory, context memory and the hippocampus: fMRI evidence. Neuropsychologia 50:3070-9.

Rushworth MF, Behrens TE, Johansen-Berg H (2006) Connection patterns distinguish 3 regions of human parietal cortex. Cereb Cortex 16 1418–1430.

Saksida LM, Bussey TJ, Buckmaster CA, Murray EA (2006) No effect of hippocampal lesions on perirhinal cortex-dependent feature-ambiguous visual discriminations. Hippocampus 16:421–430.

Saksida LM, Bussey TJ (2010) The representational-hierarchical view of amnesia: Translation from animal to human. Neuropsychologia 48:2370-2384.

Sang L, Qin W, Liu Y, Han W, Zhang Y, Jiang T, Yu C (2012) Resting-state functional connectivity of the vermal and hemispheric subregions of the cerebellum with both the cerebral cortical networks and subcortical structures. Neuroimage 61:1213-1225.

Saunders RC, Aggleton JP (2007) Origin and topography of fibers contributing to the fornix in macaque monkeys. Hippocampus 17:396-411.

Saygin ZM, Norton ES, Osher DE, Beach SD, Cyr AB, Ozernov-Palchik O, Yendiki A, Fischl B, Gaab N, Gabrieli JDE (2013) Tracking the roots of reading ability: white matter volume and integrity correlate with phonological awareness in prereading and early-reading kindergarten children. J Neurosci 33:13251-13258.

Scherf SK, Thomas C, Doyle J, Behrmann M (2014) Emerging structure-function relations in the developing face processing system. Cereb Cortex 24:2964-2980.

Scholz J, Klein MC, Behrens TE, Johansen-Berg H (2009) Training induces changes in white matter architecture. Nature Neuroscience. 12:1370–1371.

Scoville WB (1954) The limbic lobe in man. J Neurosurg, 11:64–66.

Scoville WB, Milner B (1957) Loss of recent memory after bilateral hippocampal lesions. J Neurol Neurosurg Psychiatry 20:11–21.

Shrager Y, Gold JJ, Hopkins RO, Squire LR (2006) Intact visual perception in memory-impaired patients with medial temporal lobe lesions. J Neurosci, 26:2235–2240.

Simpson DA (1952) The efferent fibres of the hippocampus in the monkey. J Neurol Neurosurg Psychiatry 15:79–92.

Skaggs WE, McNaughton BL, Wilson MA, Barnes CA (1996) Theta phase precession in hippocampal neuronal populations and the compression of temporal sequences. Hippocampus 6:149–172.

Smith S (2002) Fast Robust Automated Brain Extraction. Hum Brain Mapp 17:143-155.

Smith SM, Jenkinson M, Johansen-Berg H, Rueckert D, Nichols TE, Mackay CE, Watkins KE, Ciccarelli O, Cader MZ, Matthews PM, Behrens TE (2006) Tract-based spatial statistics: voxelwise analysis of multi-subject diffusion data. Neuroimage 31:1487-1505.

Smith SM, Nichols TE (2009) Threshold-free cluster enhancement: Addressing problems of smoothing, threshold dependence and localisation in cluster inference. Neuroimage 44:83–98.

Squire LR, Cave CB (1991) The hippocampus, memory, and space. Hippocampus, 1:269–271.

Squire LR, Zola-Morgan S (1991) The medial temporal lobe memory system. Science 253:1380–1386.

Squire LR (1992) Declarative and Nondeclarative Memory: Multiple Brain Systems Supporting Learning and Memory. J Cogn Neurosci 4:232–243

Squire LR, Stark CEL, Clark RE (2004) The medial temporal lobe. Annu Rev Neurosci 27:279-306.

Squire LR, Wixted JT, Clark RE (2007) Recognition memory and the medial temporal lobe: a new perspective. Nat Rev Neurosci 8:872–883.

Stieltjes B, Kaufmann WE, van Zijl PCM, Fredericksen K, Pearlson GD, Mori S (2001) Diffusion tensor imaging and axonal tracking in the human brainstem. Neuroimage 14: 723–735.

Suzuki WA (2009) Perception and the medial temporal lobe: evaluating the current evidence. Neuron 61, 657–666.

Suzuki WA, Amaral DG (1994) Topographic organization of the reciprocal connections between the monkey entorhinal cortex and the perirhinal and parahippocampal cortices. J Neurosci 14:1856-1877.

Tanaka K, Saito H, Fukada Y, Moriya (1991) Coding visual images of objects in the inferotemporal cortex of the macaque monkey. J Neurophysiol 66: 170–189.

Tavor I, Yablonski M, Mezer A, Rom S, Assaf Y, Yovel G. (2014) Separate parts of occipito-temporal white matter fibers are associated with recognition of faces and places. Neuroimage 86:123-130.

Taylor KJ, Henson RNA, Graham KS (2007) Recognition memory for faces and scenes in amnesia: dissociable roles of medial temporal lobe structures. Neuropsychologia, 45:2428–38.

Taylor JC, Downing PE (2011) Division of labor between lateral and ventral extrastriate representations of faces, bodies, and objects. J Cogn Neurosci 23:4122-4137.

Thomas C, Avidan G, Humphreys K, Jung K, Fuqiang G, Behrmann M (2009) Reduced structural connectivity in ventral visual cortex in congenital prosopagnosia. Nat Neurosci 12:29-31.

Toosy AT, Ciccarelli O, Parker GJ, Wheeler-Kingshott CA, Miller DH, Thompson AJ (2004) Characterizing function-structure relationships in the human visual system with functional MRI and diffusion tensor imaging. Neuroimage 21:1452-1463.

Tootell RB, Mendola JD, Hadjikhani NK, Ledden PJ, Liu AK, Reppas JB, Sereno MI, Dale AM (1997) Functional analysis of V3A and related areas in human visual cortex. J Neurosci 17:7060 –7078.

Tournier JD, Yeh CH, Calamante F, Cho KH, Connelly A, Lin CP (2008) Resolving crossing fibres using constrained spherical deconvolution: validation using diffusion-weighted imaging phantom data. Neuroimage 42:617– 625.

Tsivilis D, Vann SD, Denby C, Roberts N, Mayes AR, Montaldi D, Aggleton JP (2008) A disproportionate role for the fornix and mammillary bodies in recall versus recognition memory. Nat Neurosci 11:834-842.

Tulving E (1985) Memory and consciousness. Can Psych 26:1-12.

Tusa RJ, Ungerleider LG (1985) The inferior longitudinal fasciculus: A reexamination in humans and monkeys. Ann Neurol 18:583–591.

Ungerleider LG, Gaffan D, Pelak VS (1989) Projections from inferior temporal cortex to prefrontal cortex via the uncinate fascicle in rhesus monkeys. Exp Brain Res 76:473–484.

Ungerleider LG, and Haxby JV (1994) 'What' and 'Where' in the human brain. Curr Opin Neurobiol 4:157-165.

Van Essen DC, Anderson CH, Felleman DJ. Information processing in the primate visual system: an integrated systems perspective. Science 255: 419–423.

Vann S, Brown M (2000) Using fos imaging in the rat to reveal the anatomical extent of the disruptive effects of fornix lesions. J Neurosci 20:8144–8152.

Vann SD, Denby C, Love S, Montaldi D, Renowden S, Coakham HB (2008) Memory loss resulting from fornix and septal damage: impaired supra-span recall but preserved recognition over a 24-hour delay. Neuropsychology 22:658-668.

Vann SD, Tsivilis D, Denby CE, Quamme JR, Yonelinas AP, Aggleton JP, Montaldi D, Mayes AR (2009) Impaired recollection but spared familiarity in patients with extended hippocampal system damage revealed by 3 convergent methods. Proc Nat Acad Sci 106:5442-5447.

Vann SD (2010) Re-evaluating the role of the mammillary bodies in memory. Neuropsychologia 48:2316-2327.

Vann SD, Erichsen JT, O'Mara SM, Aggleton JP (2011) Selective disconnection of the hippocampal formation projections to the mammillary bodies produces only mild deficits on spatial memory tasks: Implications for fornix function. Hippocampus, 21:945-957.

Vuilleumier P, Richardson MP, Armony JL, Driver J, Dolan RJ (2004) Distant influences of amygdala lesion on visual cortical activation during emotional face processing. Nat Neurosci 7:1271-1278.

Vuilleumier P (2005) How brains beware: neural mechanisms of emotional attention. Trends Cogn Sci 9:585-594.

Wakana S, Caprihan A, Panzenboeck MM, Fallon JH, Perry M, Gollub RL, Hua K, Zhang J, Jiang H, Dubey P, Blitz A, van Zijl P, Mori S (2007) Reproducibility of quantitative tractography methods applied to cerebral white matter. Neuroimage 36:630-644.

Wang Q, Sporns O, Burkhalter A (2012) Network analysis of corticocortical connections reveals ventral and dorsal processing streams in mouse visual cortex. J Neurosci 32:4386-4399.

Watson HC, Wilding EL, Graham KS (2012) A role for perirhinal cortex in memory for novel object-context associations. J Neurosci 32:4473-4481.

Weiskopf N, Hutton C, Josephs O, Deichmann R (2006) Optimal EPI parameters for reduction of susceptibility-induced BOLD sensitivity losses: A whole-brain analysis at 3 T and 1.5 T. NeuroImage 33:493-504.

Williams P (1997) Prototypes, exemplars, and object recognition. Yale University. New Haven, CT.

Williams P, Simons DJ (2000) Detecting changes in novel, complex three-dimensional objects. Visual Cognition 7:297-322.

Wilson CRE, Charles DP, Buckley MJ, Gaffan D (2007) Fornix transection impairs learning of randomly changing object discriminations. J Neurosci 27:12868-12873.

Woolrich MW (2008) Robust Group Analysis Using Outlier Inference. NeuroImage 41:286-301.

Yassa MA, Stark CEL (2011) Pattern separation in the hippocampus. Trends Neurosci 34:514-525.

Yonelinas AP (1994) Receiver-operating characteristics in recognition memory: Evidence for a dual-process model. J Exp Psychol Learn Mem Cogn 20:1341–1354.

Yonelinas AP, Aly M, Wang WC, Koen JD (2010). Recollection and familiarity: examining controversial assumptions and new directions. *Hippocampus*, 20 (11), 1178-94.

Yonelinas AP (2013) The hippocampus supports high-resolution binding in the service of perception, working memory and long-term memory. Behav Brain Res 254:34-44.

Zachariou V, Klatzky R, Behrmann M (2013) Ventral and dorsal visual stream contributions to the perception of object shape and object location. J Cog Neurosci 26:189-209.

Zeidman P, Mullaly SL, Maguire EA (2014) Constructing, perceiving, and maintaining scenes: Hippocampal activity and connectivity. Cereb Cortex, doi:10.1093/cercor/bhu266.

Zola-Morgan S, Squire LR, Mishkin M (1982) The neuroanatomy of amnesia: Amygdala-hippocampus vs. temporal stem. Science, 218:1337-1339.

Zola-Morgan S, Squire LR (1984) Preserved learning in monkeys with medial temporal lesions: sparing of motor and cognitive skills. J Neurosci 4:1072-1085.

Zola-Morgan S, Squire LR, Amaral DG (1989a) Lesions of the amygdala that spare adjacent cortical regions do not impair memory or exacerbate the impairment following lesions of the hippocampal formation. J Neurosci 9:1922–1936.

Zola-Morgan S, Squire LR, Amaral DG, Suzuki WA (1989b) Lesions of perirhinal and parahippocampal cortex that spare the amygdala and hippocampal formation produce severe memory impairment. J Neurosci 9:4355–4370.

Appendix A –Tract-Based Spatial Statistics (TBSS) Analyses

For each of the tractography-based white matter structure-behaviour analyses that were reported in this Thesis, I also conducted an exploratory whole-brain TBSS analysis with threshold-free cluster enhancement (TFCE; for details see Smith et al., 2006; Smith & Nichols, 2009). Briefly, for each analysis, all subjects' DTI data (FA, MD and TVF) was non-linearly projected onto a skeletonised mean-FA white matter mask (thresholded at FA ≥ 0.2), before voxel-wise cross-subject statistics were computed. This afforded investigation of any potential voxel-wise correlations between markers of visual discrimination and diffusion MRI measures of white matter micro-/macrostructure outside the main tracts-of-interest (i.e. the fornix and the ILF). Details of each of these analyses is reported sequentially below.

Chapter 4 – Visual Discrimination Tasks

To complement the tractography-based white matter structure-behaviour analyses reported in Chapter 4, general linear models and contrasts-of-interest were implemented to identify regions within the skeletonised mean-FA mask in which a given diffusion-MRI metric was more predictive of overall scene versus face discrimination accuracy, and vice versa. These analyses were performed separately for Tasks A and B, with a significance threshold of $p \leq 0.001$ uncorrected, cluster size ≥ 10 voxels, as per Rudebeck et al., (2009). Briefly, this whole-brain TBSS analysis revealed that, for MD and *f*, there were no regions that predicted scene discrimination accuracy to a greater extent than faces (and vice versa). For FA, however, there were clusters in the white matter of the cerebellum, in which FA was more predictive of discrimination accuracy for scenes than faces. This was true for both Task A and Task B (see Tables A1 and A2, respectively). The opposite contrast (i.e. Face accuracy > Scene accuracy) revealed no significant clusters for either Task A or B.

Table A1. Table of coordinates for the whole brain TBSS analysis performed using the behavioural data acquired for Task A in Chapter 4. Significant cluster peaks are reported for mean FA. All reported coordinates are in MNI 152 space.

Metric	Contrast	Area	Voxels	*t*-max	*x*	*y*	*z*
FA	Scenes > Faces Accuracy	Right cerebellum	12	2.27	34	-52	-43

Table A2. Table of coordinates for the whole brain TBSS analysis performed using the behavioural data acquired for Task A in Chapter 4. Significant cluster peaks are reported for mean FA. All reported coordinates are in MNI 152 space.

Metric	Contrast	Area	Voxels	*t*-max	*x*	*y*	*z*
FA	Scenes > Faces	Right cerebellum	11	3.17	26	-63	-22
	Accuracy	Right cerebellum	11	2.35	4	-59	-32
		Right cerebellum	10	3.74	38	-58	-36

Chapter 5 - Change detection task

The same contrasts were conducted using the discrimination accuracy measures acquired from the change-detection task reported in Chapter 5. These contrasts revealed no significant clusters in which inter-individual variation in a given DTI metric (FA, MD, or *f*) was more predictive of discrimination accuracy for scenes versus faces, or vice versa. For this change-detection task, however, ROC markers of perception were also available for each stimulus category. Contrasts were, therefore, also established to identify regions within the skeletonised mean-FA mask in which a given diffusion-MRI metric was more predictive of: 1) Pd for scenes compared to faces and *vice versa*, 2) K for scenes compared to faces and vice versa. Again, a significance threshold of $p \leq 0.001$ uncorrected, cluster size ≥ 10 voxels was adopted, as per Rudebeck et al., (2009). The results of this analysis are reported in Table A3 below. Briefly, these analyses revealed a cluster in the corpus callosum in which MD was

more predictive of Pd for faces compared to scenes. There was also a cluster in the corpus callosum in which MD was more predictive of K for faces compared to scenes. No other contrasts returned significant clusters.

Table A3. Table of coordinates for the whole brain TBSS analysis performed using the behavioural data acquired for the change-detection task in Chapter 5. Significant cluster peaks are reported for mean MD. All reported coordinates are in MNI 152 space. Abbreviations: CC = Corpus Callosum.

Metric	Contrast	Area	Voxels	*t*-max	*x*	*y*	*z*
MD	Faces Pd > Scenes Pd	Left CC	19	4.32	-27	-55	24
	Faces K > Scenes K	Left CC	18	4.37	-27	-52	24

Contrasts were also established to identify regions in which a given DTI metric was more predictive of: 1) Pd compared to K for scenes and vice versa, 2) Pd compared to K for faces and vice versa. Again, a significance threshold of $p \leq 0.001$ uncorrected, cluster size ≥ 10 voxels was adopted, as per Rudebeck et al., (2009). The results of this analysis are reported in Table A4 below. Briefly, these analyses revealed a cluster in the right superior longitudinal fasciculus (SLF) in which FA was more predictive of K compared to Pd for scenes. There was also a cluster in the right SLF in which MD was more predictive of Pd compared to K for scenes. Finally, there was a cluster in the right ILF in which *f* was more predictive of Pd compared to K for faces. No other contrasts returned significant clusters.

Table A4. Table of coordinates for the whole brain TBSS analysis performed using the behavioural data acquired for the change-detection task in Chapter 5. Significant cluster peaks are reported for mean FA, MD and *f*. All reported coordinates are in MNI 152 space. Abbreviations: SLF = Superior Longitudinal Fasciculus; ILF = Inferior Longitudinal Fasciculus.

Metric	Contrast	Area	Voxels	*t*-max	*x*	*y*	*z*
FA	Scenes K > Scenes Pd	Right SLF	12	5.04	46	-65	25
MD	Scenes Pd > Scenes K	Right SLF	19	5.16	44	-18	23
F	Faces Pd > Faces K	Right ILF	12	2.16	28	-5	-14